# Synthesis and Characterization of Heterocyclic Polymers as Polymer Electrolytes for Fuel Cells and other Applications

A thesis submitted to the

## UNIVERSITY OF PUNE

For the degree of

## DOCTOR OF PHILOSOPHY

in

## CHEMISTRY

by

## Mahesh P. Kulkarni

Polymer Science and Engineering Division
National Chemical Laboratory
PUNE 411 008

**March 2009**

# DECLARATION

I hereby declare that all the experiments embodied in this thesis entitled **"Synthesis and Characterization of Heterocyclic Polymers as Polymer Electrolytes for Fuel Cells and other Applications"**, submitted for the degree of Doctor of Philosophy in Chemistry, to the University of Pune has been carried out by me at the Polymer Science and Engineering Division, National Chemical Laboratory, Pune, 411008, India, under the supervision of Dr. S. P. Vernekar. The work is original and has not been submitted in part or full by me, for any degree or diploma to this or to any other University.

March, 2009

Pune

**Mahesh P. Kulkarni**

Senior Research Fellow

Polymer Science and Engineering Division

National Chemical Laboratory

Pune – 411 008

राष्ट्रीय रासायनिक प्रयोगशाला

(वैज्ञानिक तथा औद्योगिक अनुसंधान परिषद)

डॉ. होमी भाभा मार्ग पुणे – 411 008. भारत

# NATIONAL CHEMICAL LABORATORY

(Council of Scientific & Industrial Research)

Dr. Homi Bhabha Road, Pune - 411 008. India.

## Certificate of the Guide

**Certified** that the work incorporated in the thesis entitled: **"Synthesis and Characterization of Heterocyclic Polymers as Polymer Electrolytes for Fuel Cells and other Applications"**, submitted by **Mr. Mahesh P. Kulkarni** was carried out by the candidate under my supervision/ guidance. Such material as has been obtained from other sources has been duly acknowledged in the thesis.

March, 2009
Pune

**Dr. S. P. Vernekar**
(Research Guide)

**Dr. K. Vijayamohanan**
(Research Co-Guide)

Dedicated to my

*F*amily
&
*F*riends

# Acknowledgement

I would first like to thank my research guide, Dr. S. P. Vernekar, for his guidance and support over the past years. I am deeply impressed by his breadth and depth of knowledge, his continuous devotion to his students, and his sincerity and patience both as a teacher and a scholar. I especially enjoyed his style of mentoring students from which I have benefited tremendously in my personal and professional growth. I would also like to thank my research co-guide, Dr. K. Vijayamohanan for his time and suggestions for developing this thesis. Their comments and insightful suggestions have substantially improved the quality of my work.

I would like to thanks Dr. A. J. Varma and Dr. P. P. Wadgaonkar for giving me chance to enter in the research world in NCL.

I am very much grateful to Dr. M. G. Kulkarni, Head, PSE division, for providing the infrastructure and facilities for my research work and allowing me access to the facilities in the division.

I would like to thank Council of Scientific and Industrial Research, New Delhi for the award of Research fellowship and Director, NCL for allowing me to carry out my research work in this prestigious institute.

I owe a special thanks to Dr. R. A. Kulkarni, Mr. A. S. Patil and Dr. (Mrs.) A. N. Bote for their advice and valuable help rendered to me during my stay in lab. I am also thankful to NMR, elemental analysis, glass blowing and workshop groups for technical support. I also wish to thank Library, administrative and other supporting staff of NCL for their co-operation.

I sincerely acknowledge Dr. R. S. Khisti, Dr. S. S. Mahajan, Dr. M. B. Sabne, Dr. A. A. Gunari, Dr. S.D. Patil, Dr. B. M. Shinde, Dr. T. P. Mohandas, Dr. C. Ramesh, Dr. C. V. Avadhani, Dr. B. B. Idage, Dr.Mrs. S.B. Idage, Dr. (Mrs.) Garnaik, Mr. K. G. Raut, Mr. S. Menon, Dr. U. K. Kharul, Dr. S. Ponrathnam, Dr. C. Rajan, Dr. N. N.Chavan, , Mrs. D. A. Dhoble, Dr. B. D. Sarawde, Dr. P. G. Sukhla, Dr. C. Baskar, Dr. A. K. Lele, Mr. Harshwardhan Pol, Mr. K. D. Deshpande, Dr. R. P. Singh, Dr. U. Natarajan and Mr. Kiran Pandare for their valuable help and cooperation during my research stay in NCL. I am greatful to Siddeshwar, Mahesh Rote, Bashir, Sathe, Zine, Shelar and More for their cooperation.

I also wish to thank my seniors and more over my friends Dr. Omprakash Yemul, Dr. (Mrs.) Jinu Mathew, Dr. Anuj Mittal, Dr. Mrs. Smita Nayar, Dr. Gnyaneshwar Dr. Bhoje Gowda and Dr. Rahul Shingte for their helpful hand and sympathetic ear. I would like to thank all other members of polymer chemistry division, for a friendly and cheerful working atmosphere.

Special thanks to Fuel Cell Group members, Dr. A. Sudlai, Dr. I. S. Mulla, Dr. Sreekumar, and Mr. Ganesh Kale. I also thanks to my fuel Cell Group friends, Kannan, Srikuttan, Nirajan, Bhalchandra, Bhaskar, Mukta, Trupti, Deepali, Mahima, Mandar, Mira, Jadab, Satish, Rupali and Shalaka.

I also wish to express my gratitude to my earlier and present lab-mates Supriya, Padmaja, Vinod, Kokane Madam, Prerana, Sandeep, Ravi Potrekar, Ravi Sonawane, Wasif, Panjab, Deepak, Nilakshi, Mugdha, Parimal, Yogita and Pankaj.

I would like to express my deep felt gratitude to my colleagues and friends Arvind, Arun, Sony, Anjana, Prakash, Sharad, Biyani, Savita, Vijay, Nana, Kailash, Dilip, Pratheep, Mukesh, Ashutosh, Ravi Shukla, Mallikarjun, Sunil, Rakesh, Hamid, Sarika, Shailesh, Vipin, Santosh, Shubhangi, Tanveer, Pinak, Rajkiran, Rajeshwari, Vivek and many in NCL who are not named in person, for their valuable friendship and helping hand.

I specially thanks to my friend Girish for sharing his Scientific knowledge and Software skills with me, which were useful for my Thesis work and for my Future Life.

With immense pleasure I thank my brother Ganesh and his wife Madhuri, for their lavish support, love, and patience beyond limits. The completion of this thesis would have been a difficult task without their help and cooperation.

No thanks can be enough to acknowledge the encouragement, love, support, and patience beyond limits of my wouldbe Swati Yewalkar.

This may also be the place to remember my dear sister and brother-in –law (Jiju) who saw me past every hurdle, big and small with love and understanding. I also remember my father and mother, whose endless patience and constant encouragement have been a source of motivation through out these years. I will be forever grateful to them for providing me the opportunity and inspiration to seek higher education.

With great pleasure I dedicate this work to my Family and my Friends.

**Mahesh Kulkarni**

# Table of contents

| | |
|---|---|
| **Chapter 2** | **Amino & Nitro group based Polybenzimidazole Copolymers for Proton Exchange Membrane Fuel Cell- Synthesis and Characterization** |

| Chapter 3 | Hydroxyl group based Polybenzimidazole Copolymers for Proton Exchange Membrane Fuel Cell- Synthesis and Characterization |
|---|---|

**Chapter 4**     **Benzimidazole group based Polybenzimidazole Copolymers for Proton Exchange Membrane Fuel Cell - Synthesis and Characterization**

---

**Chapter 5**      **Blends of Polybenzimidazole with Sulfonated-PEEK and commercial PVOH for Proton Exchange Membrane Fuel Cell - Preparation and Characterization**

---

| | |
|---|---|
| **Chapter 6** | **Carboxylic and Sulfonic acid group based Polyimide Copolymers for Proton Exchange Membrane Fuel Cell - Synthesis and Characterization** |

**Chapter 7**      **Summary and Conclusions**

# <u>Abstract</u>

The proton exchange membrane fuel cell (PEMFC) is one of the most promising electrochemical power sources for electricity generation and electric vehicle applications. Fuel cells represent a clean and efficient conversion technology and it is alternate energy source for the vehicles to control vehicular pollution for clean environment. However, high cost is the obstacle in commercialization of PEMFC. One of major component, which decides cost of fuel cell, is the cost of polymer electrolytes. Presently Nafion is used as polymer electrolyte which has very high cost about 700 US $/m^2$. There is dire need to develop alternate cost effective efficient polymer electrolytes for fuel cells and hence there has been a consistent effort to develop comparatively less expensive alternate membrane material for PEFC having properties comparable to Nafion.

A good polymer electrolyte is desired to have good thermal stability, high proton conductivity, good $N_2$ and $O_2$ barrier properties, good oxidative and chemical resistance, high current density and long service life with least change in efficiency with time even at high operational temperature. Cost is another important factor, which controls the application of a polymer electrolyte for fuel cell. Significant work is being carried out to replace expensive Nafion membrane with cheap material. Polybenzimidazoles (PBI) are good polymer electrolytes after acid doping as they are thermally very stable and have longer service life at high temperature. PBI are stable in stronger acidic medium, as they are basic polymers. N-H of benzimidazole ring forms a complex with acid molecule and shows good proton conductivity when doped with $H_3PO_4$. However, proton conductivity of PBI, compared to Nafion is low and requires enhancement. Moreover, efficiency of PBI decreases with time due to leaching out of $H_3PO_4$ by water or MeOH. Various methods including structural variations, blends and others are being tried to overcome drawbacks in PBI. The present work is a step towards this and it describes synthesis and characterization of new PBI containing functional groups, new sulfonated polyimides and blends to possible application of these polymers as polymer electrolytes for PEMFC.

**Chapter 1** gives a comprehensive literature review on heterocyclic polymers, with special emphasis on polybenzimidazoles and Sulfonated polyimides and their Fuel cell application. It also includes the blends of heterocyclic polymer with other Sulfonated and commercial polymers used as PEM in fuel cells. This chapter also discusses the scope and objective of the thesis in detail.

**Chapter 2** presents a synthesis and characterization of two diacid monomers having nitro and amino functional groups, namely, 5-(4-nitrophenoxy) isophthalic acid and 5-(4-aminophenoxy) isophthalic acid hydrochloride. It also describes synthesis of new polybenzimidazoles and a series of copolybenzimidazoles containing functional groups and characterization of these polymers by IR spectroscopy, inherent viscosity, elemental analysis, solubility tests, X-ray diffraction studies, differential scanning calorimetry and thermogravimetric analysis, tensile properties study. These polymers show good oxidative stability in Fenton's reagent. The fuel cell characterization such as acid doping study, proton conductivity measurements and actual fuel cell performance in single fuel cell stack was also conducted to explore possible application of these polymers as polymer electrolyte for fuel cell.

**Chapter 3** presents synthesis and characterization new polybenzimidazole and a series of copolybenzimidazoles from the 5 hydroxy isophthalic acid and 3,3',4,4,'-tetra amino biphenyl (TAB). The new hydroxyl group containing PBIs were characterized by the tests mentioned in chapter 2. As these polymers contain hydroxyl groups, the conductivity of these polymers on doping with 6M KOH was also determined.

**Chapter 4** presents a synthesis and characterization of a new diacid monomer having benzimidazole functional groups. The diacid synthesized were i) 5-(1H-benzo[d]imidazol-2-yl) isophthalic acid. New polybenzimidazole and a series of copolybenzimidazoles from the new diacid having benzimidazole functional groups were synthesized and characterized. The fuel cell characterization such as acid doping study, proton conductivity measurements and actual fuel cell performance in single fuel cell stack was also done.

**Chapter 5** presents a preparation and characterization of i) acid-Base blends of amino group containing PBI and sulfonated-PEEK and ii) commercial PBI and Polyvinyl alcohol in different Wt%. The blends were characterized by SEM, IR, and DSC, TGA. These blends show good mechanical properties. All fuel cell characterization was done as mentioned in chapter 2.

**Chapter 6** presents a synthesis and characterization of two diamine monomers having carboxyl and sulfonic acid functional groups. The diamines synthesized were i) 4-(2, 4-diaminophenoxy) benzoic acid ii) 3-(3, 5-diaminobenzoyl) benzenesulfonic acid. New polyimides and copolyimides from the new diamines having functional groups were synthesized and characterized by methods mentioned in chapter 2. The fuel cell characterization, such as water uptake study, proton conductivity measurements and actual fuel cell performance in single fuel cell stack is also described.

**Chapter 7** summarizes the salient conclusions of the work.

# List of Tables

# List of Schemes

# List of Figures

# Chapter **1**

## Introduction and Literature Review

## 1.1 Introduction

Much of the humanity's progress has been marked by dramatic improvements in the materials, structures and mechanics that chemists and engineers have developed, from the 'Stone Age' to the 'Iron Age' to the 'Bronze Age' and now to the "Polymer Age". The development of polymers is perhaps the biggest achievement chemistry has made and it has a significant effect on every day life. "Polymer" is not a household word. Polymers are big molecules, the materials that constitute most of our natural and synthetic environment. The world would have appeared totally different without artificial fibers, plastics, elastomers, etc. and as cheaper, better and stronger synthetic materials are developed, their use will undoubtedly increase further.

Polymeric materials, as they are constantly being modified, improved and fine-tuned for current and additional needs, and more readily accepted by the public, will have an ever-expanding influence on everyday life. Today polymers are used as replacements for woods, glass and metals and for wide variety of applications in industries such as packaging, automobiles, building and construction, electronics, aerospace, electric equipments etc. In the high technology microelectronics area, many opportunities exist for polymers to serve as improved dielectrics, improved plasma etch resistance barriers, improved lithographic resists, etc.

Polymers are materials for the future and are versatile substances that can be tailored in an almost infinite number of ways to meet evolving needs. It is not surprising that much of the high technology in future, from biotechnology to microelectronics, will depend on our ability to synthesize and manipulate polymers. Syntheses of new polymers with special functionalities are greatly needed to fine-tune existing polymers for specific tasks. The raw materials cost, market size, energy needs, and health and environmental concerns have been the important factors especially for discovery and introduction of new polymers. There have been always constant quest for new polymers that can be used for specialty applications. In this context, the synthesis of polymers that can be used as polymer electrolytes for fuel cells has attracted considerable attention of research workers throughout the world. Electricity is the fastest growing form of energy. Although it is being used more efficiently, and despite

progress having been made in switching to fuels other than oil, the electricity industry still faces a number of challenges, one of most important is environmental impact of electricity generation and use. The other principle contributor to urban pollution is road transport. Fuel cells will contribute to reducing the demands for fossil fuel and nuclear-derived energy both in power generation sector and road transport sector.

Fuel cells represent a clean and efficient conversion technology and it is alternate energy source for vehicles to control vehicular pollution for clean environment. Today various kinds of fuel cells containing different types of electrolytes are used in various applications. The proton exchange membrane fuel cell (PEMFC) is one of the most promising electrochemical power sources for electricity generation, electronic appliances and transportation.

Today there has been increasing interest to develop proton exchange membrane fuel cell (PEMFC) [1-3] due to its advantage as compared to other fuel cell systems particularly for portable electronic devices and vehicular transportation applications. One of the important components of PEMFC is polymer electrolyte. It is an ionomer capable of conducting protons. Presently, Nafion [4-5] is used as polymer electrolyte which has very high cost about 700 US $/m$^2$. There is a direct need to develop alternate cost effective efficient polymer electrolytes for fuel cells and hence there has been consistent effort to develop comparatively less expensive alternate membrane material for PEMFC having properties comparable to Nafion. Thus, polymers as polymer electrolytes have assumed significant importance in fuel cell technology also.

Before entering into the subject of polymer electrolytes in detail, a background of fuel cell, in general, is given below.

## 1.2 General background of fuel cells and polymer electrolyte membranes

### 1.2.1   Introduction to fuel cells

According to William Grove who discovered the basic principal of a fuel cell in 1839, [6] a fuel cell is "an electrochemical device that continuously converts chemical energy into electrical energy (and some heat) as long as fuel and oxidant are supplied". Unlike internal combustion engines, fuel cells are not thermodynamically limited by the Carnot efficiency. Fuel cell operates quietly, and when the hydrogen is used as a fuel, generates only power, product water and heat. Thus, it is commonly called a zero emission engine.

A typical fuel cell is composed of three active components: an anode electrode, a cathode electrode and an electrolyte sandwiched between them. At the anode of an acid electrolyte fuel cell, the hydrogen gas ionizes, releasing electrons and creating $H^+$ ions (protons). At the cathode, oxygen reacts with electrons taken from the anode electrode, and protons from the electrolytes to form product water.

The chemical equations for these reactions are shown below:

$$Anode: 2H_2 \rightarrow 4H^+ + 4e^-$$
$$Cathode: O_2 + 4e^- + 4H^+ \rightarrow 2H_2O$$
$$Overall: 2H_2 + O_2 \rightarrow 2H_2O$$
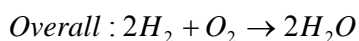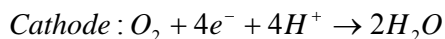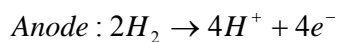
In an alkaline electrolyte fuel cell, the overall reaction is same as reaction takes place in an acid electrolyte fuel cell, but the reactions at each electrode are different because hydroxyl ($OH^-$) ions are available and mobile in an alkali electrolyte. At the anode, OH- ions react with hydrogen, releasing electrons, and producing water. At the cathode, oxygen reacts with electrons taken from the anode electrode, and water in the electrolyte, forming new OH- ions.  In either case, the electrons that flow through the external circuit form to perform useful work.

$$Anode: 2H_2 + 4OH^- \rightarrow 4H_2O + 4e^-$$
$$Cathode: O_2 + 4e^- + 2H_2O \rightarrow 4OH^-$$
$$Overall: 2H_2 + O_2 \rightarrow 2H_2O$$
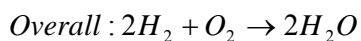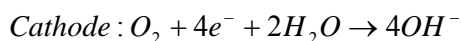
Types of electrolyte, types of ions transferred through the electrolyte, types of reactants, and operating temperature can classify fuel cells. The most widely used classification is by types of electrolytes. Six categories of fuel cells classified by their electrolyte

are summarized in Table 1.1[7].

**Table 1.1** Types of fuel cells.

| Type of Fuel Cell | Electrolyte | Operating Temperature | Efficiency | Electric Power | Possible Applications |
|---|---|---|---|---|---|
| Alkaline (AFC) | Potassium Hydroxide | 60-90 °C | 45-60% | Up to 20 kW | Submarines, Spacecraft |
| Molten Carbonate (MCFC) | Immobilized Liquid Molten Carbonate | 650 °C | 45-60% | > 1 MW | Power Stations |
| Solid Oxide (SOFC) | Ceramic | 1000 °C | 50-65% | > 200 kW | Power Stations |
| Phosphoric Acid (PAFC) | Immobilized Liquid Phosphoric Acid | 200 °C | 35-40% | > 50 kW | Power Stations |
| Proton Exchange Membrane (PEMFC) | Ion Exchange Membrane | 60-130 °C | 40-60% | Up to 250 kW | Vehicles, Stationary |
| Direct Methanol (DMFC) | Ion Exchange Membrane | 60-130 °C | 40% | < 10 kW | Portable Applications |

Each type of fuel cell has its own advantages and drawbacks and may be useful in different applications. While phosphoric acid fuel cells (PAFC), molten carbonate fuel cells (MCFC), solid oxide fuel cells (SOFC) are used for large power units, alkaline fuel cells (AFC) and proton exchange membrane fuel cells (PEMFC) are being used in relatively small power units. AFCs, PEMFCs, DMFCs and PAFCs are classified as low temperature fuel cells, while MCFCs and SOFCs are classified as high temperature fuel cells.

As mentioned earlier, currently, proton exchange membrane fuel cells (PEMFC) have attracted significant attention due to their portable applications in electronic devices and transportation.

### 1.2.2    Polymer electrolyte or proton exchange membrane fuel cells (PEMFCs)

The polymer electrolyte membrane fuel cell (PEMFC), also known as proton exchange membrane fuel cell or solid polymer electrolyte fuel cell was first developed by General Electric using sulfonated polystyrene in the 1960s for NASA. Recently, PEMFCs have become the most promising candidates for new power sources in transportation, stationary co-generation and portable applications due to their weight, volume, cost and wide power range from few watts for portable electronic devices to hundreds of kilowatts for urban transit buses and passenger cars.
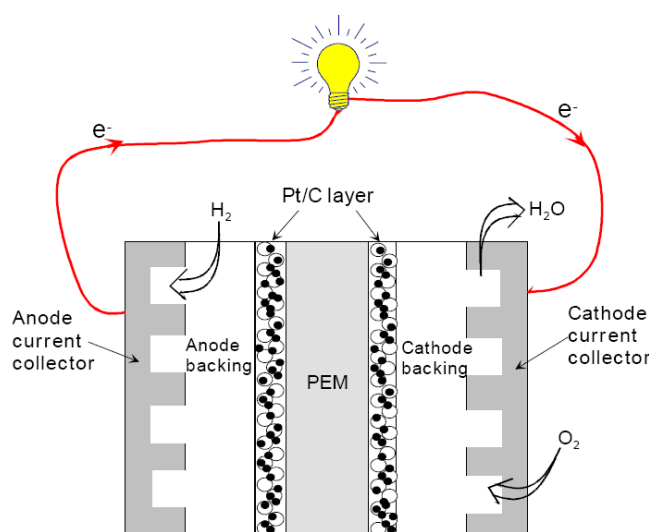


**Figure 1.1** Schematic diagram of a proton exchange membrane fuel cell.

A schematic diagram showing the basic operation of a PEMFC is shown in Figure 1.1[8]. In the polymer electrolyte membrane (PEM) fuel cells, a catalyst at the anode ionizes hydrogen molecules into protons and electrons. The membrane in the center transports the protons to the cathode, leaving electrons behind. The electrons flow through an external circuit to the cathode, forming an electric current to do useful work. At the cathode, another catalyst layer helps the electrons, protons and oxygen from air to combine to form water. When input is pure hydrogen, the exhaust consists of water vapor and of course, only water and heat are exhausted from the fuel cell. The basic parts of the cell are the proton exchange membrane having catalysts on both the anode and cathode sides (membrane electrode assembly, MEA), gas diffusion layers for uniform gas distribution and gas flow channels and mechanical support.

In PEMFCs systems, Polymer electrolyte membranes serve multiple roles in addition to transporting the protons from the anode to cathode. Hence, polymer electrolyte membranes need to meet the following requirements:

- Low cost

- Good film-formation

- Capable of fabrication into MEAs

- High proton conductivity (especially at low relative humidity)

- Electronically insulator

- Water retention above 100 °C

- Thermal, oxidative and hydrolytic stability

- Effective reactant separator(low permeability for fuel and oxident)

- Mechanical durability at high temperature (80-200 °C) for long times

### 1.2.3    Polymer electrolyte membranes

The polymer electrolytes are ionomers, capable of conducting protons. Various types of polymer ionomers have been reported as polymer electrolytes, which can be classified as Sulfonated polymers and Acid doped heterocyclic polymers which are used as polymer electrolyte membranes for fuel cells.  These materials broadly grouped mainly in three categories. 1) Fluorinated polymers such as Nafion or Sulfonated trifluoro vinyl styrene's. 2) Non-fluorinated polymers such as Sulfonated polystyrenes, polyphenylene oxides (PPO) [9], polyphenylene sulphides [10] polyether ether ketone (PEEK) [11] block copolymers of styrene-ethylene-butylenes. [12] 3) Heterocyclic polymers such as polybenzimidazoles [13] polyimides, [14] polyquinoxalines, [15] etc. Apart from these three classes of polymers, grafted polymers [16] are also reported.

The most widely used polymer electrolyte membranes are a class of perfluorosulfonic acid (PFSA) membranes such as Nafion˚ which were developed by DuPont in the 1960s for use in the chloro-alkali industry. The chemical structure of Nafion˚ is shown in Figure 1.2

It has PTFE-like (polymerized tetrafluoroethylene, DuPont trade name Teflon˚) backbone with pendant perfluorovinyl ether side chains having sulfonic acid groups. The Dow Chemical company introduced perfluorosulfonic acid membranes, having shorter side chains,

lower equivalent weights and high proton exchange capacity or acidity (defined as the mass of polymer per active sulfonic acid group) compared to Nafion˙.
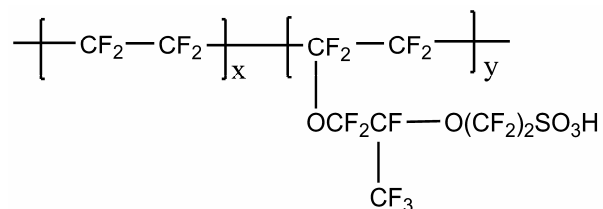


**Figure 1.2** Chemical structure of Nafion˙.

The most successful membrane is the Nafion˙ membrane (Figure 1.2), which has several advantages. This membrane offers quite good performance below 90 °C under fully hydrated conditions. Although the content of sulfonic group is low (ion exchange capacity (IEC) =0.9), it has high conductivity (>0.05 S/cm at room temperature and 100% relative humidity (RH)). In addition to above advantages, it has good chemical and mechanical stability due to the perfluorinated main chain.

However, it has some disadvantages like the proton conductivity of Nafion˙ is dependent on the presence of water to solvate the proton of the sulfonic acid groups. Consequently, the operational temperature is limited to below 100 °C, typically 50~90 °C, at ambient pressure. The gases (typically, hydrogen and oxygen) need to be well humidified before entering the fuel cell. During the operation of the fuel cell, water is produced at the cathode from the reduction of oxygen. Water also migrates with proton from the anode to the cathode. The excess water at cathode diffuses back to anode. Accumulation of excess water at the cathode side results in flooding at the cathode, preventing oxygen from approaching the catalyst and causing mass transfer resistance, meanwhile starvation of water at anode side due to migration of water with protons results in the decrease of conductivity. This is called "issue of water management", which influences the performance of the fuel cell significantly. Furthermore, the barrier properties of the membrane are usually insufficient when methanol is used as fuel, i.e. methanol crossover is large, which decreases the potential of the cell due to mixed potential and lower fuel efficiency. Moreover, the cost of this membrane is high (Approx. US$ 600/m$^2$) [17] considering the high cost of PFSA, various aromatic sulfonated

polymers were studied for possible application as polymer electrolyte but they show inferior properties as compared to the PSFA membranes.

One of the major disadvantage of PFSA and other sulfonated polymers is low operational temperature. The performance of the fuel cell is determined by its current at a given voltage. In case of the fuel cell the higher the current (or current density) at a given voltage, the better the performance. For a galvanic cell, where the power output (power = current x voltage) is the key parameter, performance is increased by maximizing the voltage at which a given current density can be obtained.

The theoretical open circuit voltage of these cells is 1.23 volts at room temperature. Deviations from this theoretical value are caused by several factors including the resistance of cell, the rate of the reaction at the cathode surface and the change in concentration of the reactant in the electrolyte around the electrode surface. All of these factors are termed as over-potentials. The resistance of the cell is termed as ohmic over-potential, the loss due to electrode kinetics is termed as activation over-potential and the effect of changes in concentration of the reactant is known as concentration over-potential [18]. Each of these factors can be reduced by operating the cell at a higher temperature. The cell resistance will be lower at higher temperature due to the more rapid transport of protons through the membrane.

The kinetics of the electrode reaction will also be improved since higher temperature helps to overcome the activation barrier associated with this step. The rate of diffusion of the reactant to the electrode will also increase with temperature. In addition, higher temperature avoids the catalyst poisoning which offers the possibility of using $H_2$ from reformats which contains 1-3% of CO which could lead to cost savings. Therefore, higher temperature, from a kinetic standpoint, will improve the performance of fuel cells and may also reduce their cost.

Since the temperature at which these cells can be run is limited by the thermal stability of the electrolyte membranes, the development of highly thermally stable PEMs is an important endeavour.

Considering the disadvantages of sulfonated polymers and advantages of polymer electrolyte capable of operating at high temperature, the research was focused on the
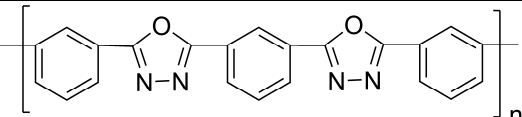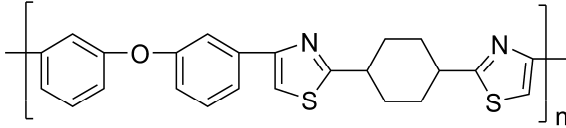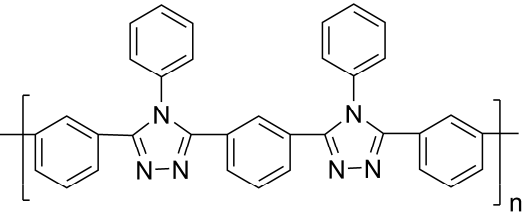
development of high temperature stable polymer ionomers capable of transporting protons without water in presence of high boiling proton vehicles. As a result, heterocyclic polymers which have higher thermal stability emerged as material of choice for proton conduction.

### 1.2.4 Heterocyclic Polymers
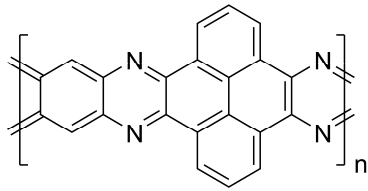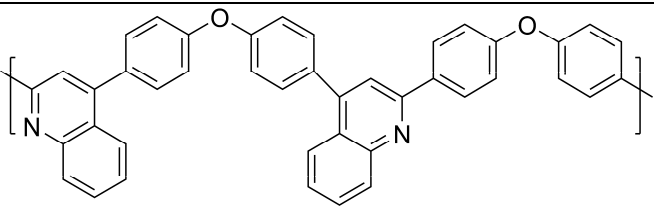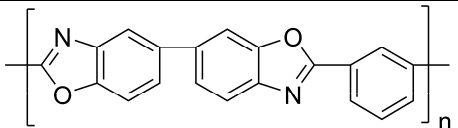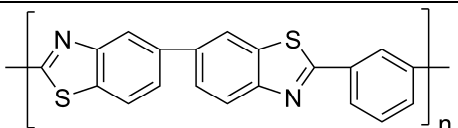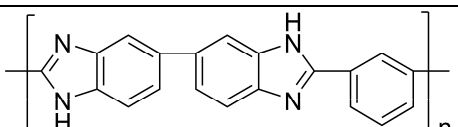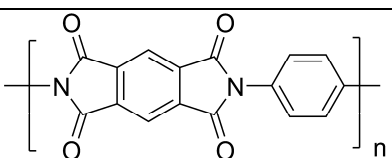
Aromatic heterocyclic polymers constitute important class of thermally stable polymers. They are condensation polymers incorporating the hetero atoms such as (O, S, and N) in their repeating units as rings and are generally derived from the reaction of organic tetraamines, bis(aminophenol)s, bis(aminothiol)s and diamines with organic aromatic dicarboxylic acids or their derivatives and tetracarboxylic acids or their dianhydrides. Aromatic heterocyclic polymers are of genuine interest from a practical viewpoint and will be discussed in short.

Aromatic heterocyclic polymers can be classified according to hetero atoms present in the heterocyclic ring and where the ring formation has taken place. We can classify the heterocyclic polymers as following given in the Table 1.2

**Table 1.2** Name and structure of heterocyclic polymers.

| | Name of Heterocyclic polymer | Structure of Heterocyclic polymer | Ref |
|---|---|---|---|
| 1 | Polyoxadiazole |  | [19] |
| 2 | polythiazole |  | [20] |
| 3 | polytriazole |  | [21] |

| 4 | polyquinoxaline | | [22] |
|---|---|---|---|
| 5 | polyquinoline | | [23] |
| 6 | Polybenzoxazole | | [24] |
| 7 | polybenzothiazole | | [25] |
| 8 | Polybenzimidazole | | [26] |
| 9 | polyimide | | [27] |

Of all these heterocyclic polymers, polybenzimidazoles as a class has been considered as potential candidate of future high temperature polymer electrolyte for fuel cell. Significant research work is expended to improve the electrochemical properties of polybenzimidazole to replace Nafion. Similarly, sulfonated polyimides are also being widely investigated as polymer electrolytes for fuel cell. Present work is focused on these two types of polymers and more details of these two types of polymers are presented below.

### 1.3 Polybenzimidazoles

Polybenzimidazoles (PBIs) is a class of high performance heterocyclic polymers, which after doping with strong acids constitute another important class of thermally stable polymer electrolytes. They are condensation polymers incorporating the benzimidazole moiety as a part of the repeating unit in the polymer backbone generally derived from a condensation reaction of aromatic bis-o-diamines and dicarboxylates or dicarboxylic acids. Poly [2,2`-(m-phenylene)-5,5`-bibenzimidazole] shown in Figure 1.3 is the only commercially available PBI and will be called PBI in the present thesis.
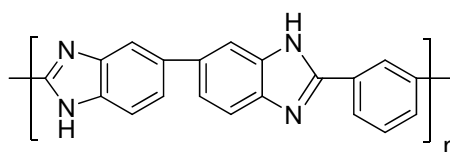


Polybenzimidazole (PBI)

**Figure 1.3** Chemical structure of commercially available polybenzimidazole.

The first aromatic polybenzimidazole [28-29] was synthesized by H. Vogel and C. S. Marvel in 1961. The polymer is well known for its excellent thermal and chemical stability and mechanical properties. It has a glass transition temperature of about 450 °C and melting point of >600 °C because of its rigid aromatic structure. In 1983, Hoechst –Celanese corporation commercialized polybenzimidazole fibers for use in fabrics for fire protection clothing [30]. These polymers synthesized by different routes as described in the following.

### 1.3.1    Synthetic methods for the preparation of polybenzimidazoles

The earlier attempts to prepare polybenzimidazoles were made by Brinker and Robinson [31] who discovered that the reaction of bis-o-diaminophenyl compounds, with aliphatic dicarboxylic acids could be employed to form linear condensation polymers. Following this, Vogel and Marvel [28] in 1961 reported the first aromatic polybenzimidazole by the reaction of an aromatic diester, with bis-o-diamine like 3,3',4,4'-tetraminobiphenyl (TAB) or 1,2,4,5-tetraaminobenzene by heating to temperatures in excess of 270 °C. Intractable polybenzimidazole powders resulted from the aromatic diesters, with bis-o-diamines. Thereafter, considerable research work had been expended to explore the different

routes for the synthesis of polybenzimidazole and now, a number of synthetic methods are available. The main routes for the synthesis of polybenzimidazoles are melt polymerization and solution polymerization.

### 1.3.1.1 Melt polycondensation of bis-o-diamines and aromatic diesters or diacids

Many aromatic polybenzimidazoles syntheses have been reported by this method. The method involves polycondensation of 3,3',4,4'-tetraminobiphenyl (TAB) with aromatic dicarboxylic acid derivatives or diacids. The polycondensation were carried out generally in two stages, i.e. a combination of melt polymerization of TAB with diphenyl isophthalate (DPIP), [28, 32-33] isophthalic acid (IPA), dimethyl isophthalate, followed by a second-stage solid-state polymerization at an elevated temperature. A single-stage melt polymerization of TAB with DPIP [34] and IPA [35] are also reported.

> ➤ **Two- stage melt polycondensation**

A two-stage melt-solid polymerization is used to produce commercial-grade PBI from TAB and diphenylisophthalate (DPIP) as described in Scheme 1.1. In two-stage melt polymerization TAB, diphenylisophthalate (DPIP), and a specified amount of catalyst (dichlorophenylphosphine) are placed in a three-necked flask equipped with a nitrogen inlet and outlet, a mechanical stirrer, and a condenser. The flask is degassed and then filled with nitrogen. The degassing is repeated at least three times. Then mixture is heated rapidly with stirring to 225 °C. The stirring is stopped and temperature of the reaction mixture is raised upto 270 °C and held at that temperature for the next 1.5 h. The resulting prepolymer is cooled to room temperature and then it is pulverized. The pulverized prepolymer is placed in a flask, and degassing steps are repeated, then the prepolymer is heated at 360 °C for 1 h. The resulting PBI exhibited an inherent viscosity upto 1.0 dL/g, when measured in a concentration of 0.4% of PBI in 100 mL of 97% sulfuric acid.

In the two-stage polymerization, voluminous foam created by the evolution of the water and phenol byproducts, limits the degree of polymerization. Thus a second-stage is required to increase molecular weight of PBI. Choe developed a single-stage process as shown in scheme 1.2 which reduced the foaming phenomenon and the raw materials cost.
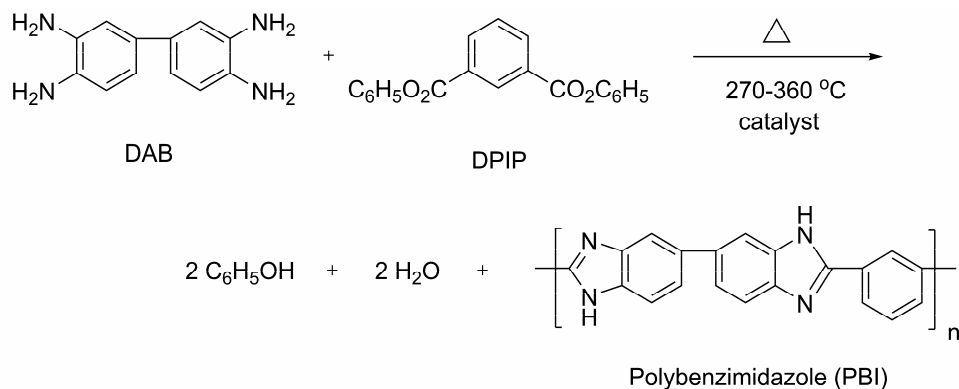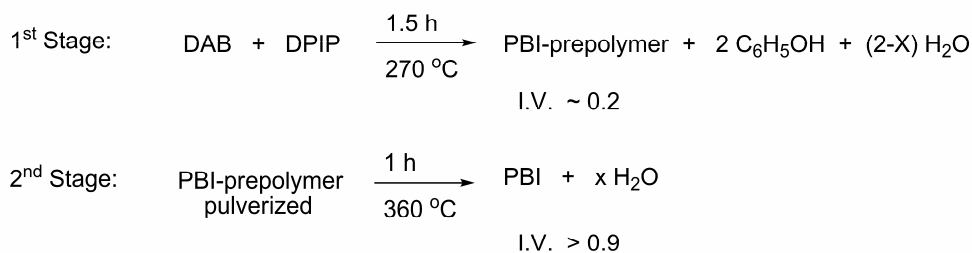
**Scheme 1.1** Two-stage melt-polycondensation reaction of commercial PBI.

➤ **Single stage melt polycondensation**

In single stage melt polymerization 3,3',4,4'-tetraminobiphenyl (TAB), isophthalic acid (IPA) and a specified amount of catalyst are placed in three-necked flask equipped with a nitrogen inlet and outlet, a mechanical stirrer, and a condenser. The flask is degassed and then filled with nitrogen. The degassing is repeated at least three times. The mixture is heated rapidly from 200 to 310 °C with stirring for a period of 15 min. The rate of stirring is reduced from 200 rpm at about 250 °C to 0 rpm at 310 °C.
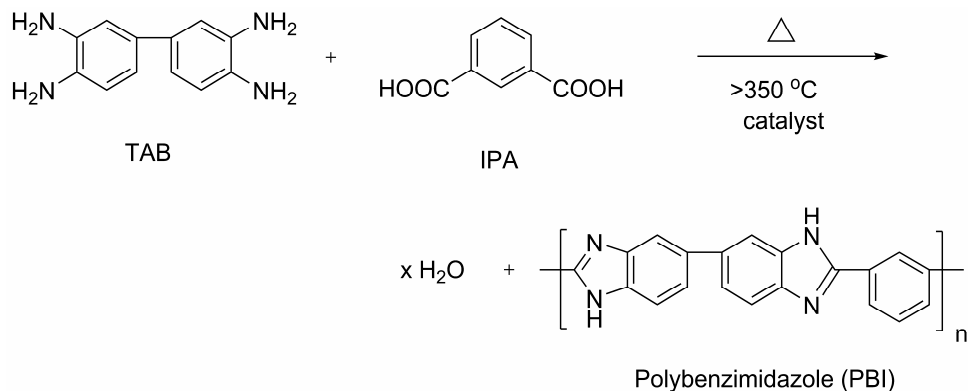
**Scheme 1.2** Single-stage melt-polycondensation reaction of PBI.

The resulting polymer is heated for a period of 45 min to an elevated temperature (i.e.415 °C) as designated in the specific runs. A quantitative amount of water is collected. The temperature of the reaction mixture is maintained at the elevated temperature (i.e. 415 °C) for another hour. The resulting product is cooled to room temperature to provide a quantitative yield of the PBI. The PBI exhibited an inherent viscosity upto 0.8 dL/g when measured in a concentration of 0.4 g of the PBI in 100 mL of 97% sulfuric acid. The polymer is completely soluble in dimethylacetamide containing 2% lithium chloride.

### 1.3.1.2 Mechanism of polybenzimidazole formation

The mechanism of the melt condensation process was believed to involve straightforward aminolysis of the phenyl ester in the first step, resulting in poly(aminoamide) formation (Figure 1.4) with loss of phenol.
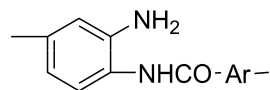


**Figure 1.4** Structure of poly(aminoamide).
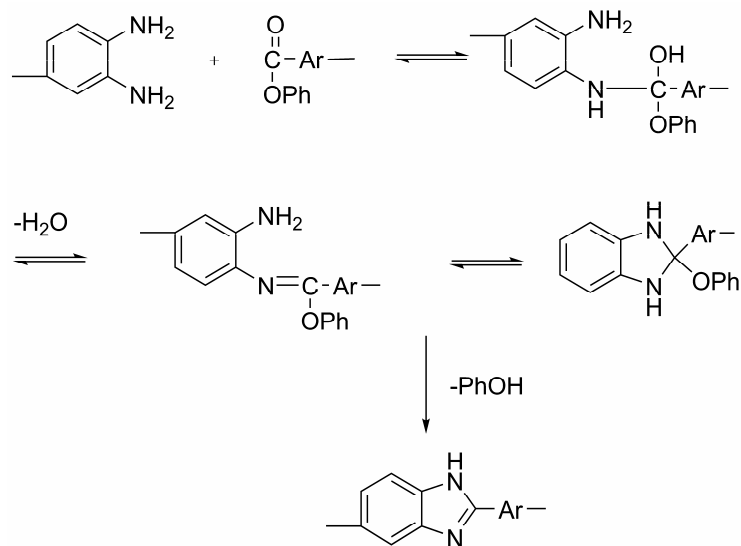


**Scheme 1.3** Mechanism of polybenzimidazole formation by melt polymerization of bis(o-diamine) with aromatic bis(phenoxycarbonyl) reactant.

The second step represents a simple cyclodehydration to the imidazole system. However, an elaborate kinetic study conducted by Levine et.al. [36] provided results

contradictory to this premise. By monitoring, the consumption of tetraamine and evolution of both water and phenol for the polycondensation of bis(o-diamine) with aromatic bis(phenoxycarbonyl) reactant determined that water generation precede the expulsion of phenol. Thus, an alternative mechanism was proposed (Scheme 1.3).

The addition of an amine nucleophile to the ester carbonyl occurs in the first stage with the elimination of water. The C-phenoxy-substituted azomethine polymer was formed in equilibrium with the cyclised benzimidazoline tautomer, which eliminates phenol in the second stage to produce the polybenzimidazole [37].

### 1.3.1.3 Solution polycondensation of bis-o-diamines and aromatic diacids or diesters

Recognizing the shortcomings such as maintaining high temperature, stepwise heating in the melt condensation approach, numerous research groups directed their attention to the task of finding alternative preparative methods in solution form. Some of the features of solution polycondensation are described below.

> **Solution polycondensation in polyphosphoric acid**

In 1964, Iwakura et.al. [38] introduced a method for the polybenzimidazole synthesis in poly(phosphoric acid) where poly(phosphoric acid) acts as solvent as well as condensation agent for imidazole cyclisation. Iwakura's technique offers an advantage of using the tetraamine monomers in hydrochloride form which are stable and easy-to-handle in place of the extremely air-sensitive free bases. In addition, the method permits the use of the free dicarboxylic acids as monomers, most of which are too sensitive to survive the high temperatures of the classical process without undergoing major degradative decarboxylation. General method for the synthesis of PBI by solution polycondensation is described below.

▪ **General method for solution polycondensation**

In a solution polymerization 3,3',4,4'-tetraminobiphenyl (TAB) isophthalic acid (IPA) , and a specified amount of PPA are placed in three-necked flask equipped with a nitrogen inlet and outlet, a mechanical stirrer, and a condenser. The mixture is heated to 140 °C with stirring under a stream of nitrogen. After the complete dissolution of TAB, a specified amount of isophthalic acid (IPA) is added slowly with stirring and the temperature of the

reaction mixture is raised to 170 °C. The diacid dissolves in half hour giving homogeneous solution. The solution is then heated to 200 °C and maintained at this temperature for 12 h. The resulting viscous solution is cooled and poured into water to precipitate the polymer as fiber. The polymer is filtered, washed repeatedly with water and stirred in 10% aqueous $Na_2CO_3$ solution overnight to eliminate residual phosphoric acid. The polymer is washed again with water repeatedly to neutrality and heated further in boiling water for 6 h, three times. The polymer is dried at 100 °C for 24 h and at 150 °C for another 24 h. A brown fibrous polymer is obtained. Yield of the polymer is quantitative. The inherent viscosity of this polymer at 0.5 g.dL$^{-1}$ concentrations, measured in $H_2SO_4$ at 30 °C is upto 2-3 dL.g$^{-1}$.

The resultant benzimidazole polymers are identical with and possess the same properties as the corresponding products of Marvel's melt condensation process. Many novel polybenzimidazoles are synthesized in poly(phosphoric acid), such as polymers containing an aromatic imide group [39], the thermostable phenoxathin [40] or quinazolinedione [38] units, the flame retarding phosphine oxide function [41] or the cobalticenium cation [42] in the chain. Widely used solvent for the synthesis of PBI by solution condensation is PPA.

Though the poly(phosphoric acid) solution polycondensation method presents a convenient means of synthesizing polybenzimidazoles of high molecular weight, it is not amenable to prepolymer isolation and processing. It is, therefore, restricted in its usefulness to such cases where the ultimate products are utilized, in spinning or film casting. Another drawback of poly(phosphoric acid) solvent is its propensity for promoting the self-condensation of amines; Marvel's group has shown that 1,2,4,5-tetraaminobenzene and other bis(o-diamine)s undergo rather smooth polycondensation when heated in poly(phosphoric acid), giving highly fused aromatic polymer structures containing dihydrophenazine groupings in the chain [43]. Furthermore, poly(phosphoric acid) tends to be incorporated into, or strongly adsorbed to, polar polymeric compounds, thereby creating phosphorus contents in the product [44]. Poly(phosphoric acid) also known to attack glass at elevated temperatures [45], which may lead to the incorporation of silica into the polymer, adversely affecting elemental analysis results. Poly (phosphoric acid) is unsuitable for polymerization of monomers unstable in a hot acidic environment [42]. But for the use of PBI in fuel cells as a

$H_3PO_4$ doped polyelectrolyte membrane, poly(phosphoric acid) solution polycondensation method presents a convenient way for synthesizing acid doped polybenzimidazoles. However, other high boiling solvents can also be used for the synthesis of PBI.

➤ **Solution polycondensation in high boiling solvents**

F. L. Hedberg and C. S. Marvel [46] reported new method for synthesis of polybenzimidazole in high boiling solvents. They used the sulfolan solvents for polymerization of bis(o-diamine)s and bis(phenyl ester)s at the solvent's boiling temperatures under nitrogen. They got linear polybenzimidazoles of high molecular mass without cross-linking. Some of the advantages of the sulfolan polymerization are, (1) it is a one step reaction, (2) the solution or suspension of monomers is easier to deaerate than a mixture of solids, (3) transition states of intermediates are well solvated by the polar sulfonyl group of the solvent which lowers the energy of activation and in turn, permits a lower temperature and shorter time for the reaction with less consequent chance of cross-linking, (4) constant mixing is possible throughout the course of reaction, permitting reactive end groups to find one another more easily; (5) the by-products, water and phenol, are driven out of the reaction by the boiling solvent.

Many polybenzimidazoles with structural variations have been synthesized. Some of the reported PBIs are listed below in Figure 4.5
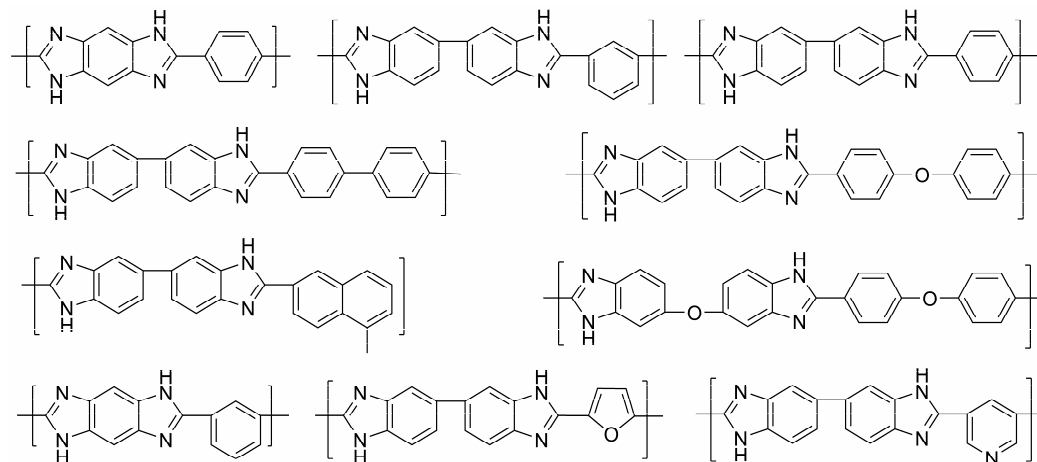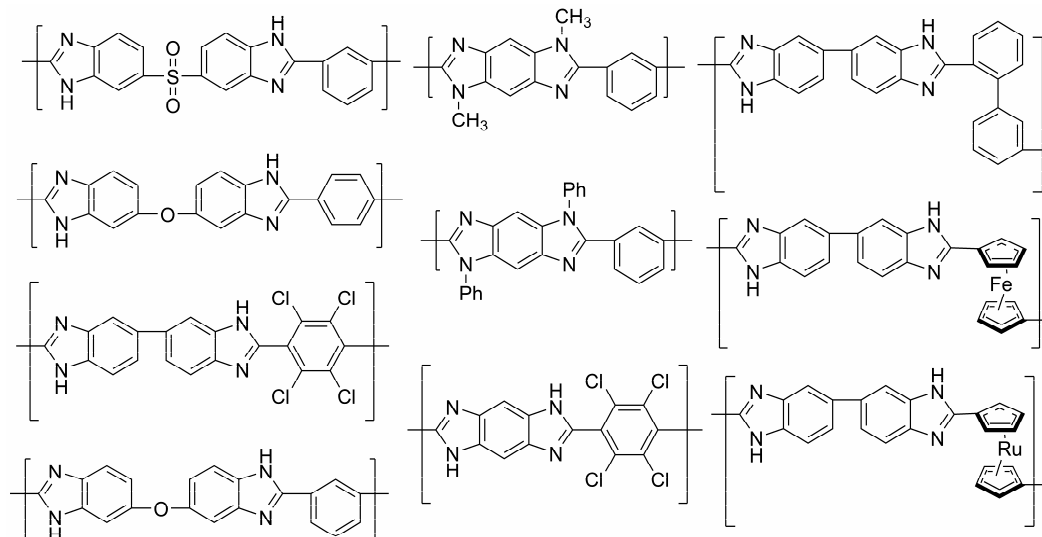
**Figure 1.5** Polybenzimidazoles synthesized with structural variations.

### 1.3.2    Properties and applications of polybenzimidazoles

Polybenzimidazoles show excellent thermal stability, heat resistance and non-flammability, high chemical stability and good mechanical, dielectric, adhesive, and fiber-forming properties. Aromatic polybenzimidazoles represent an outstanding class of engineering materials for use in a variety of applications over a wide temperature span.

The $T_g$ of commercial PBI is reported as ~ 430 °C and can be increased to 500 °C by annealing in nitrogen at 500 °C for 200 minutes due completion of ring closure and cross-linking. PBI is used as thermo-insulators in form of foams or loosely textured mats [47] as these materials possess excellent mechanical properties at low and high temperatures in addition to showing exceptionally low flame spread, self-ignition, and smoke generation characteristics. PBI-Foams with low-density are the excellent materials for fire and thermal insulation in automotive, aircraft and aerospace vehicles [48-50].

PBI shows 3.48 ε relative permittivity and $6.5 \times 10^{-3}$ δ loss tangent at room temperature, while 3.80 ε and $8.8 \times 10^{-3}$ δ at 538 °C. This indicates the good retention of dielectric properties in a high-temperature environment, which is coupled with good corrosion resistance in contact with certain reactive chemicals, suggests excellent applications of polybenzimidazole in electrical insulation and other dielectric applications at high operating temperatures and/or in aggressive chemical environments. Typical applications are

found in special cable and wire insulation, in the manufacture of circuit boards and radomes for supersonic aircraft, as battery and electrolytic cell separators and as fuel cell frame structural materials [51-53].

The strength retention of PBI fibers in inorganic acids and bases is excellent. It shows ~90-100 % strength retention after immersing in inorganic acids and bases for 150 hours. Compared to other high performance fibers such as Nomex, PBI shows outstanding chemical stability. PBI fibers also exhibit outstanding hydrolytic stability in severe environments. The fibers retain 96% of their strength after exposure to 149 °C for 72 h in a 67 psi steam atmosphere and lost little or no strength after 16 h at 182 °C and 140 psi steam atmosphere. [54]. The moisture regain of PBI fabrics can be as high as 15%, while other synthetic fibers such as nylon and Nomex can have water contents of 4.5% and 5% respectively. The high moisture regain of PBI fabrics contributes to their perceived comfort as wearable garments. Due to the good spinning characteristics, high thermal stability and moisture regain, PBI are used in special fire-fighting suits and in flight crew clothing for military and space missions [55].

The exceptionally high moisture regain observed with polybenzimidazole fibers find the utility of polybenzimidazole films as semi-permeable membranes [56] for reverse osmosis processes, such as sea water desalination. The polybenzimidazole film performance increases with increase in temperature, the flux increases from 693 L m $^{-2}$ day $^{-1}$ at 49 °C to 1019 L m $^{-2}$ at 90 °C. When, PBI in the form in hollow filaments, bundled and co-aligned in a suitable tube module, presents a higher specific operating surface and tolerate a higher pressure than a membrane. The hollow-filament approach offers a considerable economic advantage over the membrane technique [57]. Both, membrane and hollow filament material demonstrate the superiority of polybenzimidazoles in high-temperature reverse osmosis [58-60]. The excellent bonding characteristics of PBI adhesives in metal joining at high temperature and low temperature makes PBI as top structural adhesive [44] in aircraft and space design-oriented organizations. At temperatures as low as -196 °C, the PBI does not embrittle and a PBI adhesive exhibits tensile shear strengths of 39.3 MPa (5700 psi) at -225 °C [61]. PBI adhesives are not accepted by industrial processors due to its high cost and the requirement of hot melt

processing. The use of polybenzimidazole materials as adhesives is, therefore, largely restricted to military and aircraft component design.

Pure PBI is an electronic and ionic insulator, which becomes a very good ionic conductor on doping by acids under proper conditions. The benzimidazole group has a pKa of about 5.5, which facilitates its absorption of acid as a plasticizer. In 1995, Savinell et.al. [62] proposed PBI doped with phosphoric acid as a promising electrolyte for high temperature PEM fuel cells. It has been shown that phosphoric acid doped PBI exhibits good proton conductivity, [63-64] low methanol permeability [65], almost zero water electro-osmotic drag coefficient for water and methanol [66], excellent oxidative and thermal stability [67] and good mechanical flexibility at elevated temperature [68-69].

As a polymer electrolyte for high temperature PEM fuel cell, phosphoric acid doped PBI have been extensively studied. Additional studies have focused on properties and proton conductivities of acid and base doped PBI membranes, modified and sulfonated PBI and their performance in fuel cells, polymer blends of PBI with other polymers and their use as polyelectrolyte membranes. The following sections will present recent developments of PBI membranes as polymer electrolytes.

## 1.4 Application of polybenzimidazoles to PEM fuel cells

Various parameters such as structure of polymer, technique used for the preparation of membranes, thickness of membrane, method used for doping, doping level, moisture content, temperature, water electro-osmotic drag coefficient, thermal, hydrolytic and oxidative stability of membrane, catalyst loading and MEA fabrication have influence on the performance of PEM. Extensive study has been done to understand the effect of various parameters on the performance of PEM. Though, PBI has been doped with various strong acids, PBI/$H_3PO_4$ system has been found to be the most suitable as polymer electrolyte for fuel cell at high temperature and as such, the system has been extensively studied. Some of this work is summarized below.

**1.4.1   Phosphoric acid doped PBI membranes**

**1.4.1.1 Preparation methods of acid doped PBI membranes**

Phosphoric acid doped PBI membranes are prepared by several methods (1) Cast from a solution of polymer in NaOH/ethanol solution under $N_2$ environment, and washed by water until pH 7, then doped by immersion in phosphoric acid solution [69] (2) The conventional way of casting from a solution of PBI in DMAc, then doping the membrane in phosphoric acid bath [63, 67] (3) Direct casting of phosphoric acid doped membranes from trifluoroacetic acid/$H_3PO_4$ solution [70]. (4) Synthesizing the polymer in polyphosphoric acid (PPA) and casting the film to hydrolyze the PPA to phosphoric acid [71].

In the DMAc method, the 3~5 wt% of PBI is dissolved in DMAc with 1~2 wt% LiCl by heating upto 240 °C under pressure for several hours and then filtered. The obtained solution is concentrated to 20 wt% by solvent evaporation. The concentrated solution is cast on a clean, level glass plate using a Gardner knife, and heated in an air oven at 120 °C for at least four h. The films are washed by immersing in boiling water to remove the LiCl, dried in a vacuum oven for 24 h at 150°C and then doped by immersion in phosphoric acid solution. The final acid loading is calculated from the weight difference of the membranes before and after the immersion. Most of the PBI membranes reported in the literatures were prepared by the DMAc method [72-76, 62].

The direct casting method from TFA/acid solution is an easy way to prepare acid doped PBI membranes, which have well controlled acid doping level. Even though the doping levels are similar, the properties of films formed by the various methods are substantially different. Films cast using the DMAc method are normally stronger and tougher than those cast from TFA. The TFA films require a polymer of higher inherent viscosity (I.V.) in order to generate films of reasonable strength [68]. Commercial PBI powder can be extracted with DMAc to increase average molecular weight for better mechanical properties. The TFA cast film has comparably much more crystallinity than a DMAc cast film, and the surface texture is different. The TFA films are more rubbery and softer, and the conductivity of TFA cast film is higher. Following the similar methods, (i.e. the acid soaking method and direct acid casting method) Asensio et.al. [77] prepared phosphoric acid doped ABPBI membranes with a

different solvent (i.e. methanesulfonic acid, DMAc) With the same doping level, the direct acid casting ABPBI membrane has higher crystallinity but lower conductivity and higher activation energy compared to the acid soaking ABPBI membranes, which was ascribed to the dehydration of the phosphoric acid during MSA evaporation at 150~200 °C [78].

Synthesis of PBIs in PPA followed by film casting and hydrolysis of PPA to phosphoric acid was reported by Benicewicz et.al. [71] High molecular weight PBIs were synthesized from TAB and various pyridine-containing diacids in PPA at 190 °C. The viscous polymer solutions were cast and the PPA was hydrolyzed over a period of 24 h at 25 °C and about 40% relative humidity, which has been termed a sol-gel process. Using this method, large amounts of phosphoric acid were incorporated in the membranes, resulting in very high conductivity at low humidity and high temperatures (~0.2 S/cm at 160-180 °C, 0% RH).

### 1.4.2    Properties of phosphoric acid doped PBI membranes

The phosphoric acid doped PBI shows many characteristic properties, such as good thermo-oxidative stability, moisture regain, low methanol permeability, zero water electro-osmotic drag coefficient and good proton conductivities at high temperature.

The thermo-oxidative degradation of pristine PBI in dry air occurs after heating at 350 °C for 10 h [79]. while the PBI/phosphoric acid system, as shown by Samms et.al. [67]  are stable below 600 °C under simulated fuel cell conditions, where they show loss of only absorbed water and water produced from acid dehydration. Phosphoric acid stabilizes the PBI membrane. Linkous [80] compared the thermo-hydrolytic stability of PBI (pristine PBI, phosphate-PBI and annealed PBI) as well as a number of other high-temperature polymers under harsh conditions. The samples were tested under steam (0.5atm $H_2O$)/$H_2$ and steam (0.5atm $H_2O$)/$O_2$ for 24 h separately. The phosphoric acid doped PBI (phosphate-PBI) gained weight at 200 °C, indicating the capability to retain moisture at high temperatures. However, at 300 °C, pristine PBI, phosphoric acid doped PBI and annealed-PBI all showed severe decomposition, especially under oxidative conditions, which was explained on the basis of hydrolysis of some part of the imidazole ring. Methanol crossover rates through $H_3PO_4$ doped PBI membranes have been determined by direct measurement of the methanol permeability

[63], by a methanol sorption technique, and by real-time analysis of the cathode exhaust stream of an operating fuel cell using mass spectrometry [65]. Each of these measurements yielded crossover rates in order of the 10 mA/cm$^2$ for 3 mil thick films.

Of all PBI systems, phosphoric acid doped PBI membrane has been studied in detail for proton transport, proton transfer mechanism and proton conductivities. Wasmus et.al. [73] used solid-state NMR characterization of $H_3PO_4$ doped PBI to show that the phosphoric acid absorbed by the PBI membrane was relatively immobile as compared to free phosphoric acid, and revealed that there was an interaction between imidazole groups of PBI and phosphoric acid. Glipa et.al. [74] with IR spectroscopy, confirmed proton transfer from $H_3PO_4$ to the imino groups of PBI and the presence of un-dissociated $H_3PO_4$ at high doping levels.

Li et.al. [75] measured conductivity as a function of temperature and a wide range of acid doping levels (x =3.0-16.0, where x is acid molecules per polymer repeat unit) at R.H. between ~80-85%. They obtained a conductivity of $4.6 \times 10^{-2}$ S/cm at 165 °C. They suggested a useful $H_3PO_4$ doping level between 3.5-7.5 moles/repeat unit, considering both conductivity and mechanical strength. Kawahara et.al. [81] prepared $H_3PO_4$ doped PBI membranes by immersing the PBI membranes into a mixed solution of acid and methanol. The highest doping level observed was 2.9 moles $H_3PO_4$/repeat unit. Based on FTIR data, they concluded that $H_3PO_4$ did not protonate the imidazole groups of PBI but interacted by hydrogen bonding between the OH and =N- groups. The presence of $HPO_4^{2-}$ and $H_2PO_4^{-}$ anions, based on FTIR, implied that the proton conduction occurred according to the Grotthus mechanism. The conductivity of the anhydrous PBI·2.9$H_3PO_4$ complex reached $10^{-4}$ S/cm at 160 °C.

Fontanella et.al. [64] measured the isobaric conductivity data of PBI·6 $H_3PO_4$ membrane at temperatures of 25, 50 and 75 °C. Based on the activation volume values (4-7 cm$^3$/mol), they proposed that proton transport in the acid doped PBI was mediated by segmental motions of the polymer. Bouchet et.al. [82] proposed an activated mechanism (Grotthus mechanism) for the proton migration from conductivity data as a function of temperature (30-90°C) and isostatic pressure (1-4000 bars), and determined the activation volume $\Delta V^*$ (4-10 cm$^3$/mol), $\Delta H^*$ (0.6-1.1eV) and $\Delta S^*$ (40-190 J/(mol·K)) from isobaric and isothermal conductivity data. Based on IR spectroscopic study of PBI-acid complexes a

microscopic model was developed, suggesting proton transfer from one imidazole site to another, in which the anionic species participate by the Grotthus mechanism. The nitrogen of the imidazole was protonated by the acids. The anions were linked to the polymer by rather strong hydrogen bonding.

Pu et.al. [83] proposed that proton transport in phosphoric acid blended PBI was the consequences of the two contributions: one was based on rapid proton exchange (hopping) via hydrogen bonds between solvent molecules, which could be the phosphate, N-heterocycles of PBI and water molecules; and the other was based on the self-diffusion of phosphate moieties and water molecules (vehicle mechanism). They studied the temperature and pressure dependence of the conductivity of PBI·xH$_3$PO$_4$ membranes (x=1.8-3.8) (activation volume of 3.8-6 cm$^3$/mol). From their conductivity data, the activation energy (70-85 kJ/mol), obtained using the Arrhenius equation, was approximately independent of acid concentration. Although the proton conduction mechanisms proposed by the various authors discussed here are different, the values of the activation volume reported are consistent. They all showed that activation volume decreased with increasing temperature.

Fontanella et.al. [64] at 75 °C, even obtained a negative activation volume for 85% phosphoric acid. This result suggested that only a small charge carrier, a solvent free proton, transported through the membrane. The results of Hittorf measurements by Weng [84] to measure the transference number of PBI·5H$_3$PO$_4$ at 150 °C were also compatible with the above results. They obtained an anion (H$_2$PO$_4^-$) transference number of 0.01-0.02, and a proton transference number of 0.98-0.99, indicating that the vast majority of the charge was carried by the proton in the acid doped PBI membranes.

Mecerreyes et.al. [85] prepared porous PBI membranes doped with phosphoric acid, where very high doping level up to x =14.6 could be obtained. The porous structure was formed by leaching out a low-molecular-weight porogen (such as phthalates or triphenyl phosphate) using a selective solvent of the porogen from polymer/porogen mixtures, and the morphology of the porous films strongly depended on the porogen/PBI ratio and the chemical nature of the porogen. The proton conductivity of these acid doped porous membranes with

high doping levels was up to $10^{-2}$ S/cm at 140 °C and 0% RH. However, the mechanical properties are questionable due to the large porosity of the membranes (up to 70%).

Based on observation of various researchers following mechanism (Grotthus) for proton transport in $H_3PO_4$ doped PBI membranes has been proposed as shown in Figure 1.6



A) H3PO4  protonated PBI                                B) Proton transfer along acid-PBI-acid



C) Proton transfer along acid -acid                    D) Proton transfer along acid-H2O
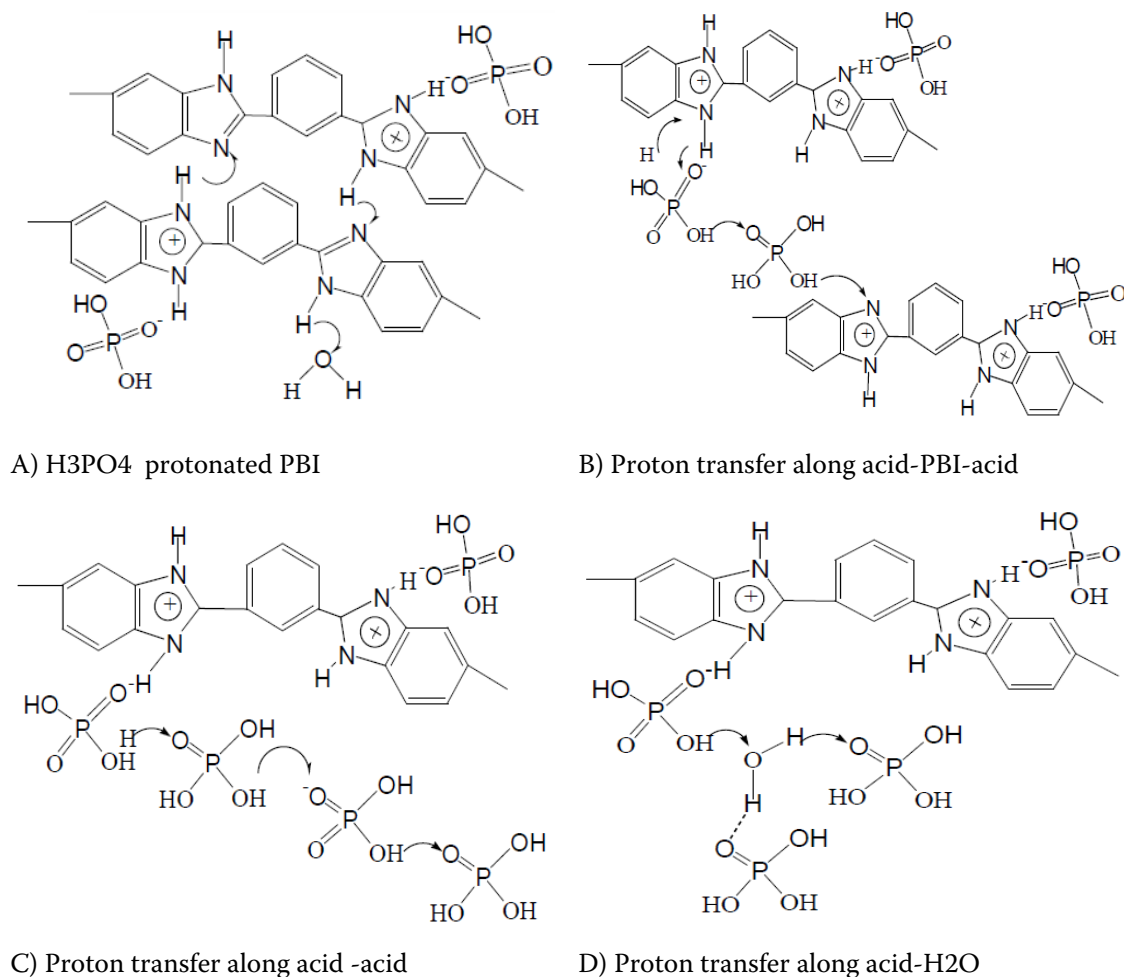
**Figure 1.6** Schematic plot for proton transfer in phosphoric acid doped PBI membrane [86].

Asensio et.al. [78] prepared phosphoric acid doped ABPBI membranes by casting DMA/ABPBI membranes followed by acid bath doping procedure, and direct acid casting procedure. They found that ABPBI·$3H_3PO_4$ membrane with the latter procedure had a conductivity of $1.5 \times 10^{-2}$ S/cm at 180 °C in dry conditions compared to a conductivity of $2.5 \times 10^{-2}$ S/cm at the same condition from ABPBI·$2.7H_3PO_4$ membrane with the former procedure.

Thus, PBI membrane doped with $H_3PO_4$ has good thermo-oxidative stability, good mechanical strength when doped with appropriate doping level, zero water electro-osmotic

drag, good proton conductivity at high temperature even in absence of water, and good tolerance to CO at high temperature suitable for application as PEM for fuel cells.

### 1.4.3    Polybenzimidazoles in $H_2/O_2$ fuel cells

The application of $H_3PO_4$ doped PBI in $H_2/O_2$ fuel cells has been investigated extensively. Wang et.al. [87] first demonstrated the use of $H_3PO_4$ doped PBI membranes in high temperature $H_2/O_2$ fuel cells. They used E-Tek electrodes with a platinum (pt) loading of 0.5 mg/cm$^2$ on carbon as electrodes. The results showed no membrane deterioration after a 200 h test at 150°C. The maximum power was 0.25 W/cm$^2$ at 700 mA/cm$^2$ current with $H_2$ and $O_2$ gas feed at atmospheric pressure and room temperature humidification.

Recent $H_2/O_2$ fuel cell results presented by Samms [88] using lower Pt loadings (0.35mg Pt/cm$^2$ on each electrode) and TFA-cast films (3 mil, 0.0075 cm thick), evaluate the effects of temperature and anode feed gas composition $H_2$/25% $CO_2$/1% CO) at atmospheric pressure and without humidification. The maximum power density reported was *ca.* 0.4W/cm$^2$ at 0.5V. The power output rose with temperature, reaching a broad plateau between 175 and 225 °C. The addition of 1% CO to the hydrogen stream decreased the cell potential by 17 mV at 600 mA/cm$^2$ at 200 °C.

Savadogo and Xing [89] have reported $H_2/O_2$ fuel cell results between 50-185 °C at atmospheric pressure with non-humidified gases using sulfuric and phosphoric acid doped PBI membranes. A maximum power output of 0.65 W/cm$^2$ was reported. They found that the addition of 3% CO to the hydrogen feed had no effect on the polarization curves at 185 °C.

Li et.al. [90] reported a power density of nearly 0.5 W/cm$^2$ (at ca. 0.5V), on a $H_2/O_2$ fuel cell based on PBI·6.5$H_3PO_4$ membrane operating at 190 °C with $H_2$ and $O_2$ stream at atmospheric pressure**.** The power output increased substantially as the temperature was increased from 55 to 190 °C. Furthermore, Li et.al. [91] studied the effects of temperature on CO poisoning in PEMFC based on PBI·5.3 $H_3PO_4$ membrane operating at temperatures from 125 to 200 °C. By defining CO tolerance as a voltage loss less than 10 mV, it was found that 3% CO in hydrogen could be tolerated at current densities up to 0.8 A/cm$^2$ at 200 °C, compared to the tolerance of only 0.0025% CO (25 ppm) at 80 °C at current densities up to 0.2 A/cm$^2$.

Uchida et.al. [92] reported the $H_2/O_2$ fuel cell performance of ABPBI·1.0 $H_3PO_4$ membrane, which was operated at 120°C and ambient pressure with $H_2$ and $O_2$ humidified at room temperature. The performances were not satisfactory with low open circuit potential.

Asensio et.al. [93] investigated $H_2/O_2$ fuel cell using ABPBI·2.8$H_3PO_4$ membrane as electrolyte, which was prepared by casting membranes from (DMAc) solution followed by $H_3PO_4$ acid bath doping. The fuel cell showed the best performance at 130 °C with the maximum power densities of 175 mW/cm$^2$ with humidified gases at room temperature, which was comparable to the maximum power density of 185 mW/cm$^2$ from PBI·6.4$H_3PO_4$ membranes obtained at the same conditions. The fuel cell operating at higher temperatures up to 180 °C showed a small decrease in the maximum power density.

Xiao et.al. [94] reported $H_2/O_2$ fuel cell using pyridine-based PBI (PPBI) membrane as electrolyte, which was prepared by casting membranes directly from PPA polymerization solution followed by hydrolysis of PPA to PA by atmospheric moisture. The fuel cell showed the best performance at 160 °C with the maximum power density 500 mW/cm$^2$ without any humidification or external pressure.

Seland et.al. [95] describe the testing of the gas-diffusion electrodes for polymer electrolyte membrane fuel cells utilizing phosphoric acid doped polybenzimidazole (PBI) electrolyte, which allows for an operating temperature as high as 200 °C. In order to determine the optimum structure of anodes and cathodes, they varied the platinum content in the Pt/C catalyst and catalyst loading, as well as the loading of the PBI electrolyte dispersed in the catalyst layer. They tested different MEAs in terms of their performance by recording polarization curves using pure oxygen and hydrogen. It was found that a high platinum content and a thin catalyst layer on both anode and cathode, gave the overall best performance. They attributed it to the different catalyst surface areas, the location of the catalyst in relation to the electrolyte membrane and particularly the amount of PBI dispersed in the catalyst layer. The best performance they obtained was 250 mW/cm$^2$ at 125 °C and 550 mW/cm$^2$ at 175 °C of power densities using a catalyst of 50% Pt/C and a relative high PBI loading in the catalyst layer on both anode (0.4 mg cm$^{-2}$ Pt, 0.36 mg cm$^{-2}$ PBI) and cathode (0.6 mg cm$^{-2}$ Pt, 0.6 mg cm$^{-2}$ PBI), respectively.

### 1.4.4    Polybenzimidazoles in direct methanol fuel cells (DMFC)

A DMFC using phosphoric acid doped PBI membrane (DMAc cast membrane) was reported by Wang et.al. [72] This fuel cell demonstrated a maximum power density of about 0.1 W/cm$^2$ in the current density range of 275-500 mA/cm$^2$ at 200 °C with atmospheric pressure feed of a 1:2 methanol: water mixture and oxygen. Using air instead of the pure oxygen resulted in an approximately 120 mV voltage loss within the current density range of 200-400 mA/cm$^2$. Wainright et.al. [96] reported DMFC data, which employed TFA-cast membranes as polymer electrolyte, and Pt black and Pt/Ru as catalysts for O$_2$ reduction and methanol oxidation, respectively. The measurements were performed at 200 °C and atmospheric pressure, with an anode feed of water and methanol mixture, mole ratio of 2:1; the maximum power density obtained was 0.2 W/cm$^2$ at 0.4 V. The effects of temperature (150-200 °C) and varying water to methanol ratios (1:1 to 4:1) in the anode feed were also evaluated.

PBI based polymer electrolyte has low proton conductivity compared to Nafion, particularly, below 100 °C. In attempts to enhance proton conductivity of PBI based polymer electrolytes various methods have been used, which are summarized below.

## 1.5 Sulfonated polybenzimidazoles

Considering the high proton conductivity of sulfonated polymers, considerable efforts were made to introduce sulfonic acid groups in PBI. The ways to introduce the sulfonic acid groups in PBI includes post sulfonation, post-modification by grafting of sulfonated molecule and the direct polycondensation of sulfonated diacids with tetraamines.

### 1.5.1    Post sulfonation of polybenzimidazoles

The post-sulfonation of PBI fiber was initially reported for flame stabilization. [97] PBIs can be post-sulfonated using common sulfonating agents such as sulfuric acid. In this process, PBI membrane is immersed in dilute sulfuric acid solution, the sulfuric acid protonates the imidazole group of the PBI molecule, forming a sulfate ionic salt. On heating, the ionic bond of the salt is converted to a permanent, covalent C-S bond [98]. The presence of covalent C-S bonds in sulfonated PBI was shown by Ariza et.al. [99] After washing

sulfonated PBI with boiling water for 3-4 h, the sulfonated PBI membrane (24% of the PBI units were sulfonated) showed low but stable proton conductivity ($10^{-6}$ S/cm at 20 °C and 100%RH), poor solubility in dimethylsulfoxide (while PBI membrane is soluble) and decreasing thermal stability.

The conductivity of post-sulfonated PBIs is generally low, approaching only 7.5 x $10^{-5}$ S/cm (160 °C, 100% RH). This can be attributed to protonation of the benzimidazole ring by the acid groups, which lowers the proton mobility. It is believed that the resulting "hydrogen bridge" causes the acidified polymer to be insoluble in common aprotic solvents [100].

### 1.5.2    Post modification of polybenzimidazoles

Post-modification of PBIs has been accomplished by first deprotonating the N-H group on the polymer backbone with lithium hydride, followed by reaction with an appropriate sulfonated molecule, such as sodium (4-bromomethyl) benzene sulfonate [101-102], 1, 3-propane sultone [103] or 1,4-butane sultone [104].  The degree of sulfonation can be controlled by varying the amount of either LiH or sulfonated reagent, and is usually measured by elemental analysis. Increased solubility of PBIs in polar aprotic solvents has been observed after sulfonation. Although, the conductivity of sulfonated PBIs is much more lower than Nafion at low temperatures (<100 °C), there are some reports that PBI maintains its conductivity as the temperature is increased above 100 °C, while Nafion decreases significantly. When complexed with base (sodium hydroxide), the sodium sulfonate form of PBI has demonstrated ionic conductivity as high as $10^{-2}$ S/cm (25 °C, 100% RH) [101].

Hongting et.al. [105] modified PBI by chemical grafting of benzylsulfonate groups on the imidazole nitrogen atoms. They found that sulfonated PBI forms strong inter-chain hydrogen bonding with phosphoric acid, which reduces the proton mobilities of PEMs. The proton conductivity of sPBI in the hydrated state was $4.69 \times 10^{-4}$ Scm$^{-1}$ at room temperature. The methanol permeability in sPBI is high and increases with increasing methanol concentration, although this trend is reverse for PBI. The methanol permeability in both sPBI and PBI also increases with increasing temperature, with the permeability of sPBI being less sensitive to temperature than that of PBI.

### 1.5.3    Direct polycondensation of sulfonated monomer

The direct polycondensation of sulfonated diacids with tetra-amines is general route to synthesize sulfonated PBI. Sulfonated isophthalic and terephthalic acids have also been used to produce PBIs with sulfonic acid groups directly attached on the polymer backbone [106-107]. Sulfonated polybenzimidazoles have also been synthesized by direct copolymerization of a benzimidazole-containing bisphenol with a sulfonated and non-sulfonated dihalide [108]. The water uptake of sulfonated copolymers increased with the degree of sulfonation, but the proton conductivity actually decreased with the introduction of increasing number of sulfonic acid sites. This trend led to the conclusion that the proton conduction was due mostly to the imidazole moieties, which became tied up in strong interactions with sulfonic acid groups as the amount of sulfonic acid groups was increased.

Yan et.al. [109] reported a novel sulfonated aromatic diacid, 3,3`-disulfonyl-4,4`-dicarboxyldiphenylsulfone (DSDCDPS), and successfully synthesized a series of sulfonated polybenzimidazoles (sPBI-SS)  by solution polycondensation of DSDCDPS and TAB with varying sulfonation degrees in poly(phosphoric acid). The membranes presented good thermal stabilities (5% weight loss temperatures higher than 430 °C), and the thermal degradation activation energies of the sulfonic group of sPBI-SS having 40% sulfonation evaluated under $N_2$ by both Ozawa and Kissinger methods were 266.06 and 264.79 kJ/mol, respectively. The membranes also exhibited high storage moduli, glass transition temperatures (above 238 °C) and tensile strengths (~80 MPa), in addition to water uptakes (22.3–25.2%) and low swelling degrees (<14.0%)

### 1.6 Blends of PBI with other commercial polymer

Blending of PBI with other polymers is another method used for modification of properties of PBI. Blends of PBI with basic and acidic polymers have been studied as polymer electrolyte for fuel cells. Miscibility of polymers is important for the formation of homogeneous blends. Miscible blends of aromatic PBI with the polyimides have been reported by Macknight et.al. [110-111] The miscibility of these polymers was demonstrated by single composition dependent *Tg's* intermediate between those of the component

polymers and single tan δ dynamic mechanical relaxation peaks. In the composition-dependent IR study, number of miscible PBI/PI blends show spectral shifts of up to 55 cm$^{-2}$ for the N-H stretching band and 6 cm$^{-2}$ for the carbonyl stretching bands which suggest that PBI/PI blend miscibility is related to inter-macromolecular interactions involving the carbonyl and >NH groups in which PBI is the sole source of >NH groups and PI is the sole source of carbonyl groups [112].

Musto et.al. [113] studied the PBI/ polyetherimide blends with the FTIR spectroscopy at various temperatures ranging from 25-400 °C and observe the hydrogen bonding dissociation and correlate this phenomenon with the onset of large-scale molecular mobility with the occurrence of phase separation for various investigated compositions. Musto further studied the thermo-oxidative degradations of a PBI/Ultem 1000 blend using FTIR spectroscopy and found that the two components undergo thermo-oxidative degradation without interacting chemically with each other [114].

PBI/PI binary polymer mixture forms homogeneous dilute solutions in DMAc, and on the removal of the solvent, it forms non-equilibrium, single-phase structure. Phase separation is prevented by kinetic factors such as low segmental mobility in the glassy state but above the glass transition, the segmental mobility is high enough to result phase separation. Thus, preparation conditions especially solvent removal, drying and annealing play an important role in determining the properties of the solvent cast blend films [115].

Choe et.al. [116] cast the blend films of solutions of PBI with poly(amic-acids) (PAA's) synthesized from BTDA (3,3',4,4'-tetracarboxybenzophenone dianhydride) and DSDA (3,3`,4,4`-tetracarboxydiphenyl sulfone dianhydride) in DMAc solvent and transformed into PBI/polyimide (PI) blends by curing at higher temperatures than the $T_g$'s of the blends. They studied the strength of intermolecular interaction between PBI and various polyimides by means of DSC, DMTA, FTIR, and showed that the strengths of hydrogen bonding in the BTDA-based blends are relatively higher than the DSDA systems due to the difference of the electron affinity between benzophenone carbonyl in BTDA and symmetric sulfone in DSDA.

Acid-base blends of PBI with polyaryl polymers containing sulfonic acid group is another type of blend investigated widely as polymer electrolyte for fuel cell. The ionic

interactions between basic and acidic groups render these blends miscible. The miscibility of polymer blends of PBI with sulfonated polysulfone (SPSF) for fuel cells was demonstrated by Hasiotis and Li et.al. [117] the miscibility depended on the PBI to SPSF ratio and the sulfonation degree of the SPSF. Based on FTIR and FT-Raman spectral results, a specific interaction between the N-H bonds of PBI and sulfonic acid and/ or sulfone groups of the SPSF in the polymer blend was suggested. They also studied the dependence of conductivity [118] of $H_3PO_4$ doped PBI/SPSF blends on temperature, acid doping level, and sulfonation degree of SPSF, RH, and blend composition.  The proton conductivity of the blends was found to be higher than that of pure PBI under the same doping conditions. They obtained conductivity up to $10^{-1}$ S/cm with $H_3PO_4$ doping level of x =5, at 160 °C and 80% RH for 75%PBI-25%SPSF (70% degree of sulfonation) as compared to $2.7 \times 10^{-2}$ S/cm for a PBI-5$H_3PO_4$ at 150 °C and 80% RH. [119] At high temperature such as 150 °C, the mechanical properties were improved for the blend membranes. A $H_2/O_2$ fuel cell [120] using a polymer blend (75% PBI-25% SPSF (sulfonation degree 36%) + 5$H_3PO_4$) as electrolyte and Pt/C at loading of 0.45 mg/cm$^2$ as electrodes gave a current of 670 mA/cm$^2$ at 0.6V and the maximum power density of 540 mW/cm$^2$ under atmospheric pressure at 200 °C.

Kerres et.al. [121-123] prepared covalently and ionically cross-linked blend membranes by mixing acidic polyaryl membranes such as sulfonated polysulfone (PSU), sulfonated polyetheretherketones (sPEEK), and sulfonated polyetherketone (sPEK), with basic polymers such as PBI as well as P4VP, PEI, and ortho-sulfone aminated PSU. They investigated the strong interactions between acidic and basic components indirectly via ion-exchange capacity of the blend membranes and FTIR spectroscopy [124-125]. Since, covalently crosslinked membranes have the disadvantage of brittleness when drying due to the inflexibility of covalent networks, acid-base ionically crosslinked blend membranes are more promising due to their high mechanical flexibility even in dry state at temperatures of up to 80-100 °C. This is due to the hydrophilicity of ionic cross-links which also involve hydrogen bonds from the ionic cross-links to the membrane-water. It is notable that, based on the ion exchange capacity (IEC), the strong acid-base ionic bonding in the ionically crosslinked membranes containing sulfonated polyaryl ionomers (90-95wt%) and PBI (5-

10wt%) is not broken by the HCl post-treatment (10% HCl at 80 °C) due to the strong basicity of PBI [124]. The conductivity of the blend membranes depends on the composition and IEC of the membranes. Furthermore, they used these membranes in $H_2$ fuel cells and DMFC and concluded that the low methanol-permeability made these membranes suitable for DMFC even at 110 °C. None of these blend membranes was doped with $H_3PO_4$ or any other acids since the fraction of PBI was small (5wt%-20wt%) and the sulfonic acid groups dominated the conductivity.

Another PBI/SPSF blend polymer (PBI/SPSF=2/8), studied by Manea et.al. [127] reported a lower degree of swelling in aqueous methanol solution and showed that one order of magnitude lower methanol permeability useful for DMFC. However, no DMFC performance has been reported based on this blend membrane by this group. Polymer blends composed of 76wt%, 19wt%, and 5wt% of s-PEEK (83% sulfonation), PBI, and PAN (polyacrylonitrile), respectively, were tested at 120 °C and 24-psig pressure [128].

Kosmala et.al. [129] prepared an acid-base polymer blend films by mixing DMAc solutions of PBI and sulfonated poly (2,6-dimethyl-1, 4-phenylene oxide) (SPPO) in the ammonium salt form, and treating the films with aqueous hydrochloric acid. The performance in a $H_2/O_2$ fuel cell using this membrane at room temperature increased with the increase in the content of SPPO sulfonic acid groups in the blend with an optimum ratio of both components.

Considering miscibility of PBI and P4VP polymers, due to strong hydrogen bonding between PBI's NH groups and P4VP's N= groups, and ability of both the polymers for acid doping, Pu et.al. [130] studied the blends of PBI/P4VP doped with $H_3PO_4$. The thermal stabilities of the blends are lower than that of PBI. The mechanical stability of the blends at high temperatures is questionable. No fuel cell performance based on these membranes has been shown.

Zaidi et.al. [131] reported the composite membranes prepared from acid–base polymer blend and solid inorganic proton conductive boron phosphate ($BPO_4$). The blends are composed of sulfonated polyetheretherketone (SPEEK) as the acidic component and PBI as the basic component. The contents of solid boron phosphate ($BPO_4$) in the composite

membrane varied from 10 to 40 wt%. The conductivity of the composite membranes was measured by impedance spectroscopy at room temperature. The conductivity of the composite membranes was found to increase with the incorporation of $BPO_4$ particles into blend membranes. The highest conductivity of $6 \times 10^{-3}$ S/cm was observed for composite membrane at room temperature

Proton conducting membranes based on blends of PBI with aromatic polyethers containing pyridine units were prepared by Daletou et.al.[132] in order to improve the acid uptake and conductivity values. They found that the membranes with high PBI content retained their flexibility and good mechanical properties after the treatment with $H_2O_2$, indicating the high oxidative stability of the system. Doping with phosphoric acid upto the doping level of 220 wt% and relative humidity 30%, they found the conductivity of $1.0 \times 10^{-2}$ S/cm at 25 °C and $7.0 \times 10^{-3}$ S/cm at 150 °C.

PBI/polyimide (PI) and PBI/polyvinylpyrrolidone (PVP) blends were prepared by Hongting et.al. [133] they studied the temperature dependence of proton conductivity of acid doped PBI/PI and PBI/PVP blends. They found that, proton conductivity of $H_3PO_4$ doped PBI/PVP and PBI/PI blends increases with increase in temperature, while proton conductivity of $H_3PO_4$ doped PBI/PVP and PBI/PI blends decreases with increase in content of PI or PVP in the blend. Methanol permeability in a PBI/PI, PI, and PBI membrane decreases with increasing methanol concentration.

Wycisk et.al. [134] reported the proton conducting membranes for a direct methanol fuel cell (DMFC) fabricated from blends of Nafion® and polybenzimidazole (PBI) by solution casting. Prior to dissolution in the casting solvent, the sulfonic acid groups of the Nafion® component of the blend were partially exchanged with sodium ions. The dependence of membrane proton conductivity and methanol permeability on the extent of proton substitution of Nafion® during blending and on the PBI content of the final membrane was studied. It was found that membrane selectivity (the ratio of proton conductivity to methanol permeability) was the highest (four times that of Nafion 117) when fully protonated Nafion® was used during blending and when the PBI content was 8%. DMFC performance of Nafion®–

PBI membranes (approximately 60 μm in thickness) was found to be superior to that of Nafion 117 at 1.0 and 5.0 M methanol feeds.

Brandell et.al. [135] prepared the Nafion®–PBI composites by diffusing synthesized PBI from solution phase into Nafion® membranes, using different concentrations and drying temperatures. In some cases, they treated Nafion® with diethyl amine to screen the $-SO_3H$ groups and thereby avoiding the strong acid–base interactions between the polymers during diffusion. The presence of PBI in the membranes was characterized with FTIR spectroscopy. The performance of the membranes was studied by in-plane conductivity and methanol permeability. The performance ratio between conductivity and methanol permeability compared to Nafion® increased by up to 50% for the composite membranes compared to Nafion®.

Kerres et.al. [136] prepared the statistical (ABAC type) co-poly(arylene ether sulfone)s and sulfonated them by fuming sulfuric acid (65% sulfur trioxide) and used for acid–base blending with PBI. The comparison of these PBI blend membranes among one another and with those of the corresponding homo-polymers (x = 0, 1.0) revealed that the water uptake and proton conductivity of the PBI blend membranes can be controlled by the ratio of the two different bisphenol monomers (BHPHFP/BHPS), whereof the specific resistance decreases and the water uptake increases with increasing content of BHPS.

Lee et.al. [137] also reported proton exchange membranes prepared from blends of PBI and sulfonated poly(arylene thioether)s and investigated in terms of water uptake, swelling, proton conductivity and oxidative chemical stability. PBI-sulfonated polymer blend membranes had a room temperature proton conductivity in the range 0.12–0.22 S/cm and exhibited lower water uptakes and better chemical stability against hydrogen peroxide treatment as compared to that of pure sulfonated polymer membranes. The membrane prepared from the blend of sulfonated poly(arylene thiosulfone)s and PBI showed excellent oxidative stability, displaying no weight loss for 45 h in 5 wt% hydrogen peroxide solution at 60 °C.

Thus, polymer blends of PBI with other polymers exhibit various properties, depending on the choice of the polymers and the composition of the blends. Polymer blends

with high fraction of PBI still need to be doped with phosphoric acid to obtain high proton conductivity while polymer blends with low fraction of PBI do not need acid as dopant but exhibit higher dependence on humidity. It is hard to find a polymer that can satisfy all fuel cell conditions.

## 1.7 Sulfonated polyimides

Sulfonated polyimides constitute another important class of thermally stable heterocyclic polymer electrolytes. They are condensation polymers incorporating the imide group in their repeating units as rings and are generally derived from the reaction of organic sulfonated diamines with organic tetracarboxylic acids or their dianhydrides. However, only polyimides containing six member imide rings based on naphthalic anhydride polyimides are of genuine interest from a practical viewpoint of fuel cell due to their high hydrolytic stability compared to five member imide groups containing PIs and will be discussed in detail.

The first reference to a polynaphthalimide was dated back to 1994, a work done by Rusanov [138]. Five-membered ring polyimides are high performance thermally stable materials that have been investigated for many years [139]. However, when sulfonated five membered ring (phthalic) polyimides are used for proton exchange membranes in fuel cells, they quickly degrade and become brittle, whereas six-membered ring (naphthalenic) polyimides do not. It is likely that hydrolysis of the phthalimide structure under strong acid conditions quickly leads to chain scission and causes the membrane to become brittle [140]. Since, the six-membered ring of the naphthalenic polyimide is much more stable to hydrolysis, this membrane is better suited for fuel cell applications. It was reported that a sulfonated six-membered ring polyimide was stable for over 3000 hours at 60 °C and that its performance is comparable with that of Nafion 117 under fuel cell conditions [141].

Mercier et.al. [142] and group reported a synthetic method to produce random and block (segmented) sulfonated copolyimides based on 1,4,5,8 naphthalene tetracarboxylic dianhydride (NTDA) with a diamine monomer containing two sulfonic acid groups, the 4,4'-diaminobiphenyl 2,2' disulfonic acid (BDSA) and proton conductivity of these polymers.
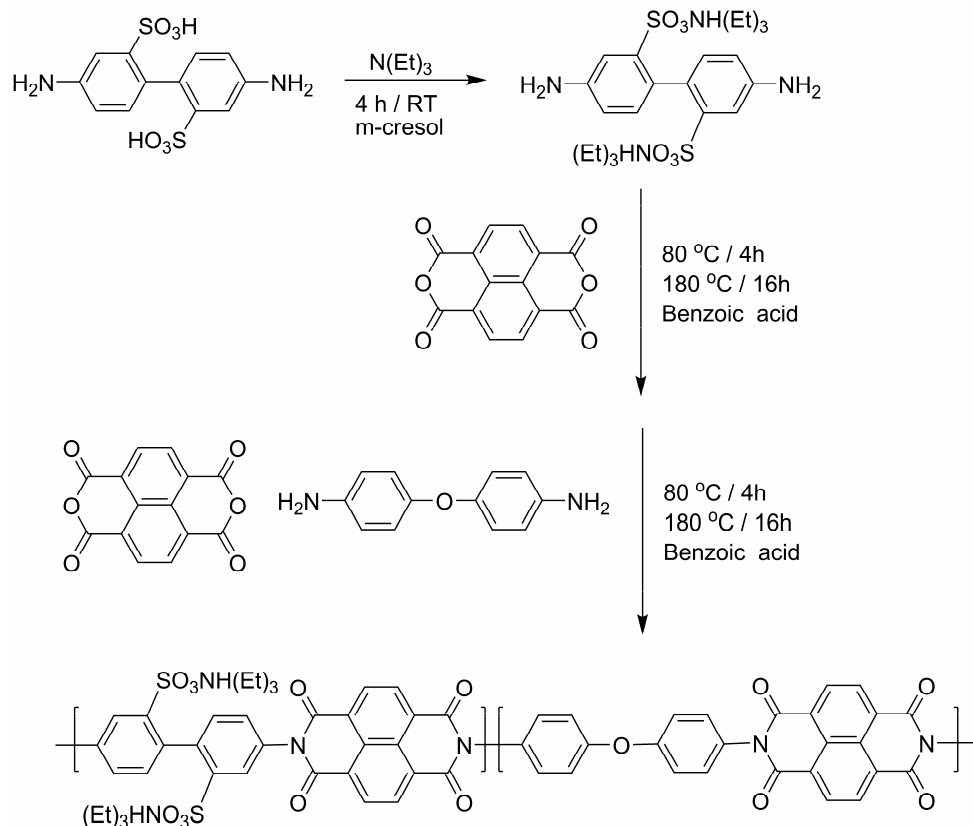
**Scheme 1.4**   Synthesis of SPI, a sulfonated six-membered ring polyimide based on BDA, ODA, and NTDA.

The synthetic procedure is shown in Scheme 1.4 for their most studied copolymer, sPI. The first step involves preparation of short sequences of BDA condensed with NTDA. An adjusted ratio of these two monomers allows one to create different block lengths of the sulfonated sequence. In the second step, the degree of sulfonation can be precisely controlled by regulating the molar ratio of BDA and the nonsulfonated diamine, 4,4'-oxydianiline (ODA), in sPI. It is well known that control of the degree of sulfonation is very important because, a high degree of sulfonation generally leads to high swelling or even dissolution of the polyimide membrane. If a statistically random copolymer is needed, all the monomers can be added at the beginning of the reaction. It was found that a block length of three sulfonated repeat units yields the highest proton conductivity [143].

BDA is an available disulfonated diamine having two sulfonic acid groups, so it is a logical choice for polyimide synthesis for PEMs. In addition, it is the most studied

sulfonated diamine used in the preparation of polyimides for fuel cell applications. Several groups have reported copolymers using this diamine [144].

Miyatake et.al. [145] reported a series of novel sulfonated polyimides containing 10–70 mol % 1,5-naphthylene moieties by polycondensation of NTDA, 4,4'-diamino-2,2'-biphenyldisulfonic acid, and 1,5-diaminonaphthalene. The polyimide containing 20 mol % 1,5-naphthylene moieties showed higher proton conductivity (0.3 S/cm) at 120 °C and 100% relative humidity than perfluorosulfonic acid polymers. Same author synthesized sulfonated polyimides containing fluorenyl groups which showed good thermal and oxidative stability as well as a high proton conductivity of 1.67 S /cm at 120 °C and 100% RH [146].

To date, the synthesis of sulfonated six-membered ring polyimide copolymers has been done by the direct copolymerization procedure. This approach requires that a sulfonated monomer is used in the copolymerization, since sulfonation is difficult in the parent polymer. Stoichiometric amounts of sulfonated diamine relative to nonsulfonated diamine, and NTDA as the dianhydride, have been used for sulfonated copolyimide synthesis. A 1:1 stiochiometric ratio of total diamine to dianhydride was used to obtain high molecular weight polymer. The degree of sulfonation could be varied by changing the ratio of sulfonated to non-sulfonated diamines.

The copolymerizations were always a one-step high temperature polycondensation in *m*-cresol; however, the catalysts employed have been varied. In all cases, the triethylammonium salt form of the sulfonated diamine is used to synthesize high molecular weight polyimides. The acid and sodium sulfonate forms of most diamines are insoluble in *m*-cresol. By adding triethylamine to a sulfonated diamine in m-cresol at room temperature for about 4 h, the triethylammonium salt form of the sulfonated diamine was formed, which was soluble in the reaction medium. Also, the free un-complexed aromatic amine will be more reactive. Benzoic acid and isoquinoline are used as catalysts for imide formation. The reasons for using these catalysts will be discussed further in a subsequent section.

Mercier et.al. [140] did not use isoquinoline in their reactions, yet FTIR of their products showed a characteristic imide absorption band which indicates complete

imidization. This observation suggests that isoquinoline may not be necessary due to the use of another base, triethylamine, in the first step of the reaction.

### 1.7.1 Synthetic methods for the preparation of polyimides

Polycondensation of diamine and dianhydrides is the most widely used method for the synthesis of polyimides. The polymerization of diamines and dianhydrides can be carried out in two different ways

a. Two-step method via poly(amic acid)s

b. One-step method

### 1.7.1.1 Two step method *via* poly (amic acid)s from dianhydrides and diamines

A successful route to the synthesis of high molecular weight polyimide was described first by Endrey [147] in 1965 by two stage method via polyamic acid intermediate.

A soluble poly(amic acid) was prepared in polar sovent, which was then converted to the desired polyimide (Scheme 1.7).
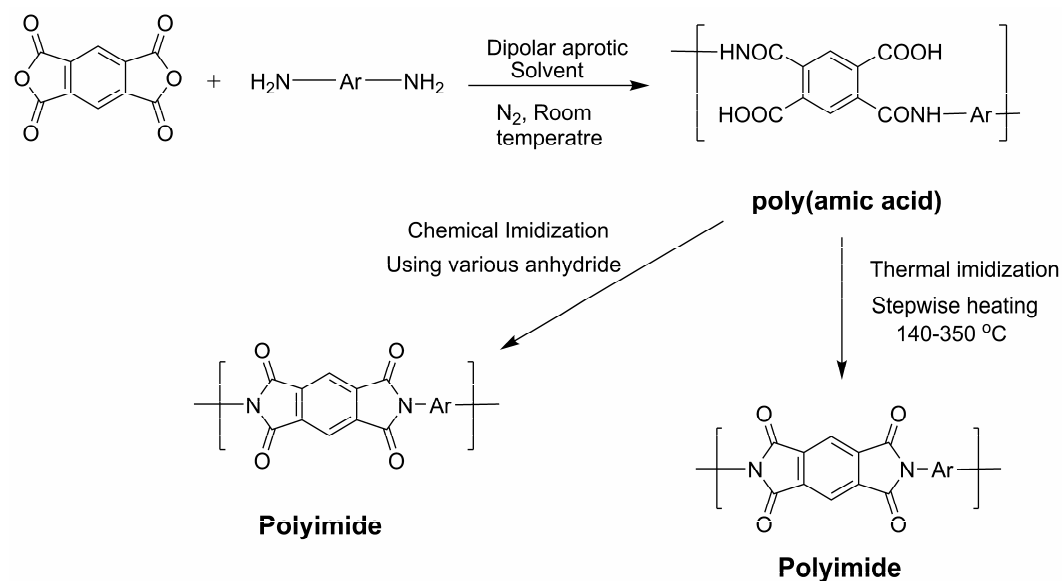


**Scheme 1.5** Two step synthesis of polyimides.

This method is, particularly, useful for the synthesis of polyimides having poor solvent solubility even at high temperature. The first step is crucial to attain high molecular weight chains and the second one has a great influence on the final nature of the polymer since a quantitative conversion in the cyclodehydration process has to be there to obtain fully

cyclized polyimide. This two-step reaction initiated enormous research and industrial activity in the field of polyimides. Thus, this highly elegant process made it possible to bring the first significant commercial polyimide products into the market and it is still the method of choice in majority of applications. This process involves several elementary reactions interrelated in a complex scheme, which are discussed in the following section.

**(i) Formation of poly (amic acid)s**

When a diamine and a dianhydride are added into a dipolar aprotic solvent such as N,N'-dimethylacetamide (DMAC), N,N'-dimethylformamide (DMF), or N-methylpyrrolidone (NMP), poly(amic acid) is rapidly formed at ambient temperatures. The reaction mechanism involves the nucleophilic attack of the amine group on the carbonyl carbon of anhydride group, followed by opening of the anhydride ring to form the amic acid group. This reaction is an equilibrium reaction, where the forward reaction is favored by the high concentration of monomers. Formation of high molecular weight polyamic acid is dependant upon the purity of monomers, reactivity of monomers, strict stoichiometric balance, and rigorous exclusion of moisture, choice of solvents and low to moderate temperatures [148]. Since the acylation of amine is a highly exothermic reaction, the equilibrium is usually favored at lower temperatures.

The progress of polycondensation reactions largely depends on the nature of the monomers. Since the poly(amic acid) formation is a nucleophilic substitution reaction it is expected that the reaction rate is governed by the electrophilicity of the carbonyl groups of the anhydride and the nucleophilicity of the amine nitrogen atom of the diamine. In general, high value of amine basicity and electronic affinity of dianhydride will favor the reaction resulting in a higher reaction rate. Soviet researchers [149] have studied the acid/ base relationships of some dianhydrides and diamines used in the synthesis of poly(amic acid)s. Solvents used in the formation of poly (amic acid)s also plays an important role. Most commonly used solvents are dipolar aprotic solvents such as DMF, DMAc, NMP and tetramethyl urea (TMU). Solvents like hexamethyl phosphoramide (HMPA), dimethylsulphoxide (DMSO), pyridine and m-cresol can also be used alone or in combination with other solvents such as benzene, dioxane, toluene, cyclohexane, xylene etc.

More recently Woo et.al. [150] used a solvent mixture (NMP + DMSO) in synthesizing the poly(amic acid), because BDSA with triethylammoniumsulfate (BDSA–Et₃HN) is hardly soluble in a common solvent. However, lower thermal stability and difficulty in removing the solvent in the process of imidization stands against its use. Best solvents are dipolar aprotic amide solvents since they are 'Lewis bases'. The orthoamic acid formed in the reaction medium is a strong carboxylic acid and the interaction between the amide solvent and the amic acid is a major cause for the formation of exotherm in the reaction and is one of the most important driving forces. Therefore, the rate of poly (amic acid) formation is faster in more polar and more basic solvents. However, the rate is even faster in acidic solvents like m-cresol than in DMAc at high temperature, indicating that the acylation of amine is catalyzed by the acid.

In order to obtain a successful polymerization, a fixed mode of monomer addition has been suggested. Thus, the addition of the dianhydride (preferably as a solid) to the diamine solution has been recommended as the right mode of addition to ensure high molecular weight polyimides [151]. Poly (amic acid)s are known to undergo hydrolytic degradation even at ambient temperatures. In presence of water, the anhydride groups can hydrolyze to form ortho dicarboxylic groups. The ortho dicarboxylic acid groups thus formed remain as one of the end groups of the poly(amic acid) and does not revert to the anhydride. The effect of water on the molecular weight of the already polymerized poly(amic acid)s in solution is well documented [152].

**(ii) Conversion of poly (amic acid)s to polyimides**

Conversion of poly (amic acid)s to polyimides is generally carried out by thermal or chemical imidization methods

➢     **Thermal imidization of poly(amic acid)**

The conversion of poly (amic acid)s to the corresponding polyimides is usually performed thermally in solid state. The films cast from the poly (amic acid) solutions are dried and gradually heated up to 250-350 °C, depending upon the stability and glass transition temperature of the polymer. The imidization process may be followed by a variety of means

and has been studied on poly (amic acid)s, as well as in molecular models by IR [153] and NMR [154] spectroscopy.

Thermal imidization reaction does not take place in a true solid state but rather in a very concentrated viscous solution, and therefore, the presence of residual solvents play an important role. The imidization proceeds faster in the presence of dipolar aprotic solvents. This may be due to the specific solvation, which allows the favorable conformation of the amic acid group to cyclized [155]. It may also be explained by the plasticizing effect of the solvent, which helps to increase the mobility of the reacting functional groups. The basicity of the amide solvent, which helps it to accept proton may also be responsible for this effect. The imidization proceeds rapidly at the initial stage and slows down in later stages. The initial rapid stage imidization is attributed to the ring closure of the amic acid in the favorable conformation (a) as shown in Scheme 1.8. The lower rate in the later stage is attributed to the unfavorable conformation (b), which has to rearrange to conformation (a) before the ring closure.

➢ **Chemical imidization of poly (amic acid)**

The cyclodehydration of the poly (amic acid)s to polyimides can be readily achieved by means of chemical dehydration at ambient temperature. Commonly used reagents are acid dianhydrides in dipolar aprotic solvents or in the presence of tertiary amines. Among the dehydrating agents commonly used were acetic anhydride, propionic anhydride, n-butyric anhydride, benzoic anhydride, and others. Among the amine catalysts used were pyridine, methylpyridines, lutidine, N-methylmorpholine, trialkylamines, and others. The cyclizing agent was most effective when an optimum ratio of acetic anhydride/pyridine (4:3.5 moles per repeat unit of polyamic acid) was employed. Vinogradova et.al. [156] showed that the pKa value of the base has a significant effect on the conversion of poly (amic acid) to polyimide. In the presence of trialkylamines with pKa >10.65, high molecular weight polyimides were obtained.

**1.7.1.2 One step method**

The polycondensation of an aromatic dianhydride and a diamine is the traditional method employed in the synthesis of polyimides and is shown in Scheme 1.6.

A single-stage homogeneous solution polymerization technique can be employed for polyimides, which are soluble in organic solvents at polymerization temperatures. In this process, a stoichiometric mixture of monomers is heated in a high boiling solvent or a mixture of solvents in a temperature range of 140-250 °C where the imidization reaction proceeds rapidly. This method is also used in the case of sterically hindered monomers having lower reactivity that cannot be polymerized to high molecular weight polyimides by the two step method.
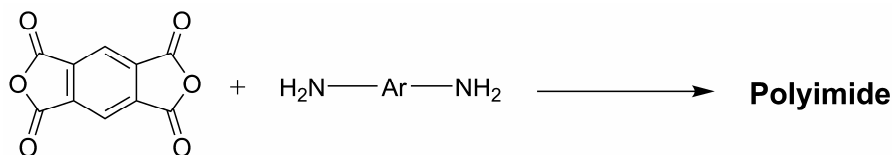


**Scheme 1.6** Condensation of dianhydride with diamine.

Commonly used solvents are nitrobenzene, benzonitrile, o-chloronaphthalene, trichlorobenzenes and phenolic solvents such as m-cresol and chlorophenols in addition to dipolar aprotic amide solvents. Toluene is often used as a co- solvent to facilitate the removal of water of condensation. Gerashchenko et.al. [157] studied one-step solution polymerization in nitrobenzene employing a soluble polyimide system based on 9,9-bis(4-aminophenyl)fluorene with pyromellitic dianhydride (PMDA) or 4,4'-oxydiphthalic anhydride (ODPA). Vinogradova et.al. [156] and Lavrov et.al. [158] studied the imidization of a model compound N-phenylphthalamic acid to N-phenylphthalimide and showed that the rates were lower in basic aprotic amide solvents and faster in acidic solvents like m-cresol.

In general, imidization reaction has been shown to be catalyzed by acid (benzoic acid). [158-159] High temperature solution polymerization in m-cresol is often performed in the presence of high boiling tertiary amines such as quinoline as catalyst. Dialkylaminopyridines and other tertiary amines were effective catalysts in neutral solvents like nitrobenzene. [160] Alkali metal and zinc salts of carboxylic acids, [161] and salts of

certain organophosphorus compounds were also found to be efficient catalysts in one step polycondensation of polyimides.

### 1.7.2  Properties and applications of Polyimides

Aromatic polyimides are extensively used in microelectronics and aerospace industries for their excellent mechanical properties, high thermal stability, high glass transition temperatures, good chemical resistance and low dielectric constants. The final properties such as tensile strength, toughness, and modulus and upper-use temperature depend on the selection of the starting monomers. These aromatic-based polyimide materials generally display high glass transition temperatures in the range of 200- 400 °C or higher, which greatly depend on the stiffness of the backbone chain. In addition, fully imidized aromatic polyimides, due to their highly conjugated, rigid-rod-like chemical structures, are insoluble in most organic solvents. Consequently, direct processing of polyimides becomes impossible in their imidized forms.
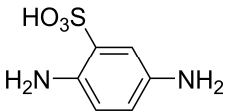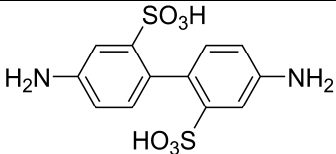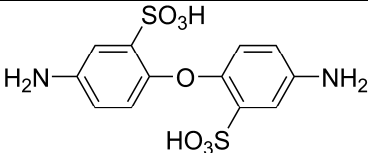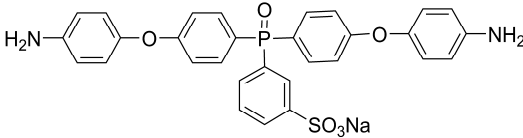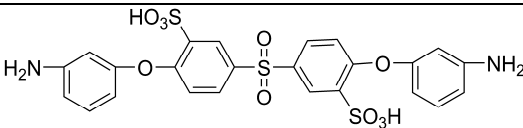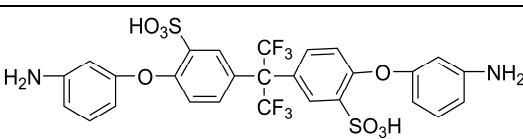
Of the various alternatives to design novel process-able polyimides, some general approaches have been universally adopted. Introduction of aliphatic or another kind of flexible segment, which reduces chain stiffness [162-163], introduction of bulky side chain substituent [164-165], which help in the separation of polymer chains and hinder molecular packing and crystallization enhancing solvent solubility; use of enlarged monomers containing angular bonds, which suppress coplanar structures [166] use of 1,3-substituted instead of 1,4-substituted monomers, and/or asymmetric monomers that lower regularity and molecular ordering and preparation of co-polyimides from two or more dianhydrides or diamines, are some of the methods used for modifying the properties of PIs. However, factors leading to better solubility or lower $T_g$ or melting temperatures ($T_m$) in a polymer often conflict with other important requirements, such as mechanical properties, thermal resistance or chemical resistance. Therefore, an adjusted degree of modification should be applied to optimize the balance of properties.
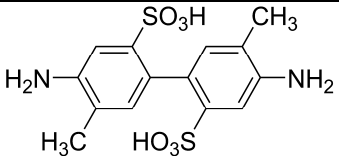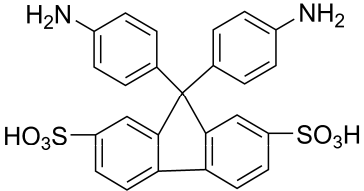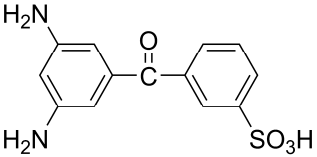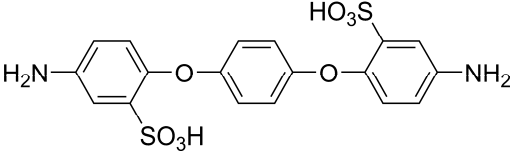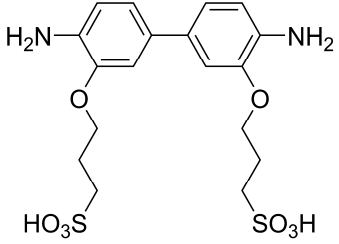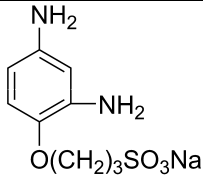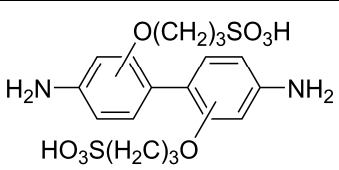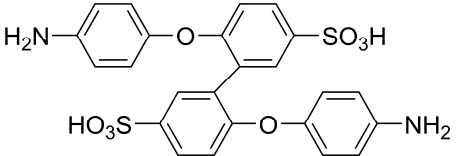
One of the recent applications of PI is as polymer electrolyte for PEMFC. Membranes of sulfonated PI (sPI) have been found to exhibit, good thermal stability, high water uptake and good proton conductivity suitable for fuel cell applications. These polymers are generally
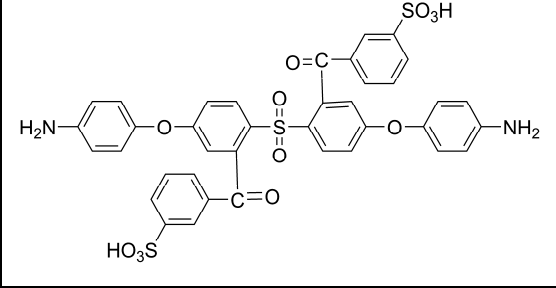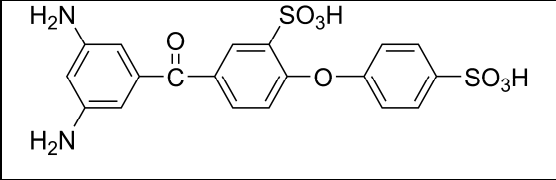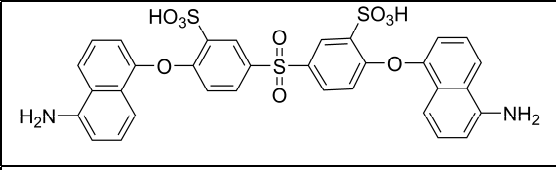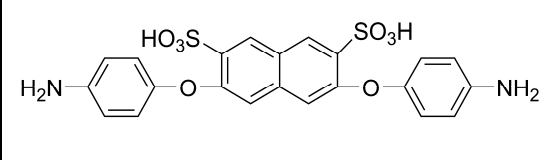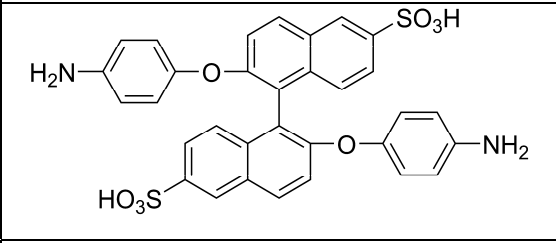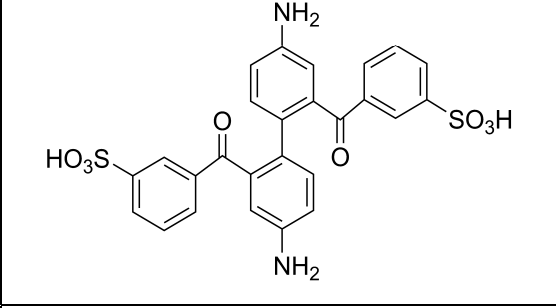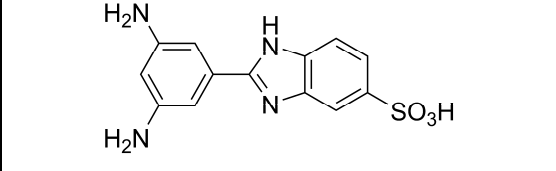
synthesized by polycondensation of a diamine containing sulfonic acid and a dianhydride. Several sPIs have been synthesized by on step method in phenolic solvents. A list of sulfonated diamine used for the preparation of sPIs is given below.

Several sulfonated diamines which have been used for sulfonated copolymer synthesis for PEMs are shown in Table 1.3. The first three, 2,5-diaminobenzenesulfonic acid (DAB), 4,4'-diamino-2,2'-biphenyl disulfonic acid (BDA), and 4,4'-diamino-5,5'- dimethyl-2,2'-biphenyl disulfonic acid (6TS) are commercially available, while the rest were synthesized by the investigators.

**Table 1.3** List of sulfonated diamines used for sulfonated copolymer synthesis for PEMs.

| Structure of Sulfonated diamine | Name of Sulfonated diamine | Abbreviation | Ref. |
|---|---|---|---|
|  | 2,5-Diaminobenzene-sulfonic acid | DAB | [144] |
|  | 4,4'-Diamino-2,2'-biphenyl disulfonic acid | BDA | [167] |
|  | 4,4'-Diaminodiphenyl ether-2,2'-disulfonic acid | ODADS | [168] |
|  | 3-Sulfo-4',4''-bis(3-aminophenoxy) triphenyl phosphine oxide sodium salt | SBAPPO | [169] |
|  | 3,3'-Disulfonate-bis[4-(3-aminophenoxy) phenyl]sulfone | SA-DADPS | [170] |
|  | 2,2-Bis[4-(4-aminophenoxy)phenyl] hexafluoropropane disulfonic acid | BAHFDS | [171] |

| Structure | Name | Abbreviation | Ref |
|---|---|---|---|
| | 4,4'-Diamino-5,5'-dimethyl-2,2'-biphenyl disulfonic acid | 6TS | [172] |
| | 9,9'-Bis(4-aminophenyl)fluorine-2,7-disulfonic acid | BAPFDS | [173] |
| | 3-(3,5-diaminobenzoyl) benzenesulfonic acid | DABBSA | Chap 6 |
| | 1,4-bis(4-amino-2-sulfonic acid-phenoxy)-benzene | DSBAPB | [174] |
| | 3,3'-Bis(sulfopropoxy)-4,4'-diaminobiphenyl | BSPA | [175] |
| | 3-(2',4'-diaminophenoxy) propane sulfonic acid | DAPPS | [176] |
| | 2,2'-bis(3-sulfopropoxy)benzidine /3,3'-bis(3-sulfopropoxy)benzidine | (2,2'-BSPB) /(3,3'-BSPB) | [177] |
| | 2,2_-bis(4-aminophenoxy) biphenyl-5,5-disulfonic acid | (*o*BAPBDS) | [178] |

| Structure | Name | Abbreviation | Ref |
|---|---|---|---|
|  | bis[4-(4-amino phenoxy)-2-(3-sulfobenzoyl)]phenyl sulfone | BAPSBPS | [179] |
|  | 3,5-Diamino-3'-sulfo-4'-(4-sulfophenoxy) Benzophenone | DASSPB | [180] |
|  | 3,3(-disulfonic acidbis[4-(5-amino-1-naphthoxy)phenyl] sulfone | DANPS | [181] |
|  | 1,4-bis(4-aminophenoxy)-naphthyl-2,7-disulfonic acid | BAPNDS | [182] |
|  | 2,2'-bis(p-amino phenoxy)-1,10-binaphthyl-6,6'-disulfonic acid | BNDADS | [182] |
|  | 2,2'-bis(3-sulfobenzoyl)benzidine | 2,2'-BSBB | [183] |
|  | 2-(3,5-Diaminophenyl) benzimidazole-5-sulfonic Acid | sDABI | [184] |

### 1.7.3    Novel sulfonated diamines

Generally diamines are sulfonated by sulfuric acid and fuming sulfuric acid (30-60% SO₃). A diamine is dissolved in 95% $H_2SO_4$ at low temperature (0 °C), fuming sulfuric acid (30-60% SO₃) is added to the solution slowly at low temperature and the solution is heated at 60 °C for 2-4 h. The sulfonated diamine monomer is precipitated in sodium salt form from the solution of sulfuric acid by 'salting out' procedure using sodium chloride. Gunduj et.al. [170] reported the synthesis of 3,3'-disulfonate-bis[4-(3-aminophenoxy) phenyl]sulfone (S-DADPS) using this method.

The sulfonated monomer from the solution of sulfuric acid can be isolated by adding the solution to ice water, neutralizing it by alkali followed by acidification. Sulfonated diamines are usually insoluble in water. Okamoto's group took advantage of this fact and reported three novel sulfonated diamines, 4,4'-diaminodiphenylether-2,2'-disulfonic acid (ODADS), 9,9'-Bis(4-aminophenyl)fluorene-2,7-disulfonic acid (BAPFDS), and 2,2-bis[4-(4-aminophenoxy)phenyl] hexafluoropropane disulfonic acid (BAHFDS) [171] and copolymers of ODADS and BAPFDS diamines. [173] The sulfonated monomer precipitated from solution was filtered and washed with methanol. No recrystallization step to purify the monomers is discussed before polymerization of either diamine. Since the protonated amine group of ODA is a strong electron-withdrawing group, the sulfonation reaction mainly occurs at the position meta to the amine group. The ether bond para to the amine group also supports the meta-position substitution.

Shobha et.al. [169] described the sulfonation of 4,4'-difluoro-triphenylphosphine oxide (BFPPO) to SBFPPO and reported sulfonated diamine, SBAPPO, which was synthesized through a nucleophilic substitution reaction of *m*-aminophenol and SBFPPO. Polymers having sulfonic acid groups bonded to the side chains have different properties from the main chain type ones. The polymers having sulfonic acid groups in polymer backbone have the homogenous morphology, which is different than the Nafion's morphology, Nafion® have microphase-separated structure which gave rise to the hydrophobic main chain polymer backbone and hydrophilic side chain due to ion-rich domains which form channels favorable for proton conduction. Many researchers introduced sulfonic acid group in polyimides by using sulfonated diamine having sulfonic acid group in side chain through aliphatic chain.

Okomoto group [176] reported the three sulfonated diamine 3-(2',4'-diaminophenoxy)propane sulfonic acid (DAPPS) and 2,2'-bis(3-sulfopropoxy)benzidine / 3,3'-bis(3-sulfopropoxy)benzidine and (2,2'-BSPB) /(3,3'-BSPB) [177]. Watanabe et.al. [175] also reported the synthesis of 3,3'-Bis(sulfopropoxy)-4,4'-diaminobiphenyl (BSPA). Polyimides containing sulfonic acid group in the side chain showed better proton conductivity comparable to Nafion, good hydrolytic stability due to the microphase-separated structure.

### 1.7.4   Membrane Preparation

The method used for the preparation of membrane has significant effect on the performance of the membrane. Various research groups used their own methods for the preparation of membranes which makes it difficult to compare performance. It is difficult to compare the performance of sulfonated six-member ring polyimide systems due to the difference in method used for the preparation of membranes. Films of the s-polyimides made by Mercier et.al. [185] were cast directly from the reaction solution. The membranes were dried under a heat lamp at 60 °C for several days to evaporate the solvent. At this point the membranes still have some residual m-cresol, so they were boiled in methanol for two hours. Although this process eliminates any remaining m-cresol and catalysts, it creates pores in the membrane. The porosity is dependent upon the degree of sulfonation and ionic block length [186]. Okamoto's and McGrath's groups isolate the polymers first by precipitating them in an appropriate solvent, [178, 187] and extracted the copolymer further with methanol to remove any remaining catalysts and m-cresol. Finally, the copolymer was redissolved in DMAc, NMP, or m-cresol, depending on its solubility, to cast a film. The water uptake of the sPI is directly dependant on the degree of sulfonation irrespective of methods used for membrane preparation.

### 1.7.5   Membrane Properties

The candidature of sulfonated polyimides as a promising polymer electrolyte membrane for fuel cells depends on many characteristic properties, such as degree of sulfonation, water uptake, moisture regain, hydrolytic stability, ion exchange capacity and proton conductivity.

Several methods have been used to determine the degree of sulfonation in the sulfonated polyimide membranes. Non-aqueous potentiometric titration, infrared spectroscopy (IR) and thermogravimetry (TGA) confirm the introduction of sulfonic acid sites. A loss in weight at around 100 °C in TGA was attributed to the absorbed water in the membrane, and a loss at about 200 °C was due to desulfonation of the polyimide film. This evidence was further supported by the evolution of sulfur monoxide and sulfur dioxide. The successful introduction of sulfonic acid groups can be confirmed by FTIR spectroscopy. Strong characteristic absorption peaks around 1030 and 1090 cm$^{-1}$ were assigned to symmetric and asymmetric stretching of the sulfonic acid groups. Titration is a good method to determine quantitatively the number of sulfonic acid sites in the polymer backbone. This number is generally stated as the ion-exchange capacity (IEC), which is the milli-equivalents of sulfonic acid per gram of polymer, and is essentially the reciprocal of the equivalent weight.

The research conducted by Okamoto and co-workers has shown that the flexibility and basicity of the diamines have a distinct effect on the hydrolytic stability of the resulting naphthalenic polyimides [168]. They have shown that sulfonated polyimides incorporating 4,4'-diaminodiphenyl ether-2,2'-disulfonic acid had superior hydrolytic stability compared to those based on 4,4'-diamino-biphenyl-2,2'-disulfonic acid due to the flexible ether linkages. Although the hydrolytic stability was improved, data up to only 200 h in liquid water at 80 °C has been reported.

In contrast, when the sulfonated diamine was 2,2'-bis(4-aminophenoxy)biphenyl-5,5'-disulfonic acid (*ortho* linkages instead of *para*), the stability in water was greatly decreased. This is possibly due to much large water uptake values for the kinked structures. [178] When 9,9-bis(4-aminophenyl)fluorene-2,7-disulfonic acid was used as the sulfonated diamine, the polymers did not last more than 27 h under the same conditions [173]. A very flexible sulfonated diamine with *meta*-linkages, ether bonds, and a sulfone moiety was synthesized and used to create sulfonated polyimides with controlled degrees of sulfonation that were soluble in polar aprotic solvents. Two different non-sulfonated diamines (4,4'-oxydianiline and bis[4-(3-aminophenoxy)phenyl] sulfone) were used in this work and the dianhydride, NTDA, was kept constant to form polyimides with 6-member imide rings [170].

Due to the 6-member imide ring, these copolyimides exhibited better hydrolytic stability than traditional 5-member ring polyimides.

The copolymers made from bis[4-(3-aminophenoxy)phenyl] sulfone [188] as a non-sulfonated diamine showed better hydrolytic stability than those made from 4,4'-oxydianiline, due to the increased content of flexible ether and sulfone linkages. The copolymers presented in this study showed significantly lower methanol permeability compared to Nafion, but the DMFC performance was similar to Nafion due to the lower conductivity of the polyimide membranes.

Highly sulfonated six-member-ring polyimides based on NTDA, 4,4'-diamino-5,5'-dimethyl-2,2'-biphenyl disulfonic acid, and 4,4'-(9-fluorenylidene)dianiline exhibited very high proton conductivity (0.31 S/cm at 50 °C and 100% RH). After cross-linking however, the proton conductivity decreased to 0.14 S/cm (50 °C, 100% RH) [172]. The side-chain sulfonated diamine monomers (2,2'-bis(3-sulfopropoxy)benzidine and 3,3'-bis(3-sulfopropoxy) benzidine) have several advantages. Due to possible aggregation of the sulfonic acid groups, the conductivity is very promising (0.1 S/cm at 35 °C and 80% RH). The copolymers synthesized from 2,2'-bis(3-sulfopropoxy)benzidine survived over six months in liquid water at 80 °C with no loss in mechanical properties, which the researchers attribute to increased basicity of the diamine. Those made from 3,3'-bis(3-sulfopropoxy)benzidine lasted only 1000 h [189].

Although there is only one sulfonic acid group per repeat unit in polyimides made from 3-(2',4'-diaminophenoxy)propane sulfonic acid, the homopolymer (100% sulfonated) display exceptional proton conductivity of 0.12 S/cm at 35 °C (liquid water), and this value increases to 0.35 S/cm at 90 °C (liquid water). Despite its high level of sulfonation, the methanol permeability of this polyimide was still 25% with respect to Nafion® [176]. Due to the rigidity and liquid crystalline behavior of some six-member-ring polyimides, a small amount of a bulky or bent unit, especially the spacing between the chains can significantly affect the properties. This increased free space between the chains could possibly allow room for the aggregation of sulfonic acid groups, creating ion channels. These ion channels can take up greater amounts of water and increase the conductivity at low relative humidity.

In a preliminary report, one group of researchers has found that the incorporation of a small amount of bulky groups into sulfonated rigid naphthalenic polyimides increased the conductivity at low relative humidity; probably due to an increase in inter chain separation, as measured by X-ray diffraction. The angled and bulky comonomers used in this study include 4,4'-(9-fluorenylidene) dianiline, 4,4'-oxydianiline, 2,2'-dibenzoyl benzidine and 1,4-bis(4-aminophenyl)-2,3,5,6-tetraphenyl benzene[190]. The proton conductivity at 15% relative humidity was $1.4 \times 10^{-3}$ S/cm for the polyimide copolymer. Even though this is still very low, Nafion displayed a conductivity of only $5 \times 10^{-5}$ S/cm under the same conditions [191].

In addition to the effects on inter chain spacing, bulky or flexible groups have also been used to increase the solubility of six-member-ring polyimides. Polyimides with meta-linkages exhibited greater solubility in organic solvents than those with para- linkages. This study also suggested that random copolyimides had better stability than both homopolymer (nonsulfonated) and blocky (sequenced) structures [178]. However, this is debatable, and it has been suggested that block copolymers in which the sulfonated block does not contain any polyimide units may possess greater stability.

Sequenced copolyimides exhibit modestly higher conductivity than their random counterparts at similar IECs. For example, a random copolyimide with 30 mole% of disulfonated monomer exhibited a conductivity of $0.91 \times 10^{-3}$ S/cm (room temperature, liquid water). When the block length was increased to five while the IEC remained constant, the conductivity increased to $1.3 \times 10^{-3}$ S/cm (same conditions). The number of water molecules per sulfonic acid group also increased. The sequenced copolyimide membrane with 30 mole% disulfonated monomer maintained mechanical integrity for 200 h in water at 80 °C [185].

The sequence length also has a definite effect on the membrane morphology, which often influences other membrane properties, such as conductivity and water content [192]. In porous polyimide membranes, the volume increase, on wetting, has been found to be less than the weight increase. While the number of water molecules per sulfonic acid group (λ) remains constant, the water uptake of such membranes increases with IEC, This suggests that there is no swelling of the hydrophobic phase, and that the porosity is mainly located within the sulfonated domains. Sequenced structures offer some advantages, although large-scale phase

separation occurred when the block length reached nine or more units, resulting in opaque films [167]. Due to a higher amount of porosity, the water uptake increased as the block length increased. However, the decrease in conductivity is observed under such conditions. The authors concluded that the excess water contained in the pores of the membrane does not participate in proton conduction [186].

Electron spin resonance spectroscopy (ESR) was also used to evaluate the water in sulfonated polyimide membranes. These studies revealed the presence of water clusters in sulfonated polyimide membranes, but with a smaller diameter than those present in Nafion. The authors commented that the water was in a "glassy" state. More detailed studies on the effect of "free" water in sulfonated PEMs for fuel cells have since been published, which illustrate the importance of the three "states of water" [193].

Branched and cross-linked sulfonated polyimides have been prepared by electron beam radiation (with minimal chemical degradation) as well as by the addition of a small amount of trifunctional amine (melamine) during the polymerization process. These have lower water uptake than their linear counterparts at the same IEC. They also last approximately twice as long in the so-called Fenton's reagent at 80 °C, and the conductivity is maintained at high temperatures [194].

The permeability of reactant gases is important for hydrogen-air fuel cell membranes, and the membrane must effectively separate the reactants. The permeability of certain sulfonated polyimides to hydrogen and oxygen has been reported. These reports suggest that the gas transport in such membranes occurs through the nonsulfonated domains; therefore, highly sulfonated polyimide membranes show extremely low permeability to reactant gases [195]. The relative humidity was also found to have an effect on the gas permeability. In the range of 0 to 70% relative humidity, the gas permeability decreased as the relative humidity increased. However, at higher levels of hydration, an increase in the gas flux across the membrane was observed. The researchers hypothesized that the hydrophobic domains control the gas flux at low water content, while the hydrophilic domains take over at high levels of hydration [196].

Miyatake et.al. [145] have successfully demonstrated that partially disulfonated copolyimides can be synthesized from monomers that are all commercially available. A copolymer of NTDA, 4,4'-diamino-2,2'-biphenyldisulfonic acid (80%), and 1,5-diaminonaphthalene (20%) had excellent proton conductivity (0.12 S/cm at 27 °C and 100% RH), which did not decrease at elevated temperatures, as does Nafion. In fact, the conductivity of these copolyimides increased to 0.3 S/cm at 120 °C (100% RH) under pressure. However, the stability of this copolymer in water was not reported, and is likely not very good.

Bis[4-(3-aminophenoxy)phenyl]sulfone-3,3'-disulfonate salt has been used in combination with various non-sulfonated diamines and NTDA to synthesize naphthalenic polyimides with a wide range of IECs. These copolymers display promising fuel cell performance under DMFC conditions at 80 °C [197]. To improve the oxidative stability of sulfonated polyimide membranes, trifluoromethyl groups have been incorporated.101 Although, the applicability of Fenton's reagent is highly debated, the stability of these partially fluorinated systems was superior to other sulfonated polyimides in Fenton's reagent. In fact, these maintained mechanical stability for over nine hours in Fenton's reagent at 80 °C. However, the copolymers did exhibit a decrease in proton conductivity above 100 °C due to poor water retention, which some believe could be remedied by addition of a small amount of bulky comonomer [198]. Sulfonated dianhydride monomers are an alternative route to sulfonated polyimides. 3,4,9,10-Perylenetetracarboxylic dianhydride has been sulfonated and employed in the synthesis of polyimides [199].

Hydrolytic stability is still a very important issue for six-member-ring polyimides. The suggested explanation of the relative instability of most polyimides is that the aromatic imide linkage can undergo acid-catalyzed hydrolysis by water molecules, resulting in chain scission. It has been suggested that increasing the electron density of the imide nitrogen can increase the stability of the polymers by preventing this attack [200].

This corresponds to the increased basicity of the diamine, addressed by Okamoto and co-workers. [177-180] To show that the electron density of the nitrogen was more important to the hydrolytic stability than the aromatic character of the backbone, an aliphatic non-sulfonated diamine was used in the synthesis of disulfonated copolyimides along with a

sulfonated diamine containing electron-donating groups. The stability of this membrane was tested at 140 °C and 100% RH.

While other sulfonated polyimides lasted less than one day, the partially aliphatic membrane remained relatively unchanged after one week. The stability in Fenton's reagent was similar to wholly aromatic sulfonated polyimides. Although the proton conductivity of this membrane was lower than Nafion at temperatures below 100 °C [200]. the values for the two membranes converged above 100 °C. Although great improvements have been made in the hydrolytic stability of sulfonated polyimides, many researchers believe that it will not be applicable for PEM fuel cells because of their inherent instability. However, novel approaches to increasing the stability could still be successful. It is important to keep in mind the long-term operation requirements for commercialization of any fuel cell membrane.

## 1.8 Scope and objectives

From the foregoing discussions it is understood that aromatic polybenzimidazoles and sulfonated polyimides constitute a major class of thermally stable polymer electrolytes having excellent thermal, mechanical and electrical properties over a wide range of temperature. However these polymers possess lower proton conductivity as compared to Nafion which limits their commercialization in fuel cell application areas. Thus, the enhancement of proton conductivity of these polymers without sacrificing their excellent properties became the object of wide spread study.

Literature reports many attempts to improve the proton conductivity of these polymers by making use of structurally modified monomers. Various approaches have been suggested to improve the proton conductivity of these polybenzimidazoles and sulfonated polyimides. These include (1) introduction of functional groups, which will increase the protonation of phosphoric acid and water in the polymer chains, (2) introduction of bulky side substituent, which help in the separation of polymer chains and absorbing more phosphoric acid and water in the polymer matrix, (3) blending these polymer with commercially available cheap polymers, (4) preparation of copolyimides from two or more diamines.

Various monomers synthesized based on these approaches, have been discussed in detail in the previous sections. The aim of the present work is to make use of one or more of these structural modifications together to have a combined effect on the properties of the resulting polymer. With this objective in mind we decided to synthesize substituted monomers having pendant functional groups like amine, nitro, hydroxyl, carboxyl, sulfonic acid and benzimidazole group along with polar linking groups like ether and ketone. Even though functional groups are known to improve solubility, they reduce the thermal stability of the resulting polymer to some extent. But such functional group containing polymers can be used in a fuel cell application as polymer electrolyte membrane where the thermal stability upto 200-250 °C is sufficient.

Incorporation of pendant functional groups in a rigid polymer, like PBI tends to disrupt the chain interactions and chain distance in this polymers resulting in increase, in free volume which helps in imbibing more acid or water in polymer matrix. Extra pendant basic functional group, like amine, in PBI is expected to enhance proton conductivity due to extra protonating sites generated by the amine groups by the interaction with acid dopant. Thus, incorporation of appropriate functional groups in PBI and PI is expected to enhance solvent solubility, water and acid uptake and proton conductivity.

There has been a consistent effort from various research groups to modify the properties of polybenzimidazole and polyimides by structural modifications to enhance properties of these polymers, necessary for the commercial application as polymer electrolytes for fuel cells. However, except sulfonic acid groups, much information is not available on the effect of functional groups on electrochemical properties of these polymers. Hence, objective of the present work is synthesize polybenzimidazoles containing functional groups such as, amino, nitro, hydroxyl group to study the effect of these groups on electrochemical and other properties of these polymers.

Infact, polybenzimidazole containing some of these groups can be prepared by introducing these groups on preformed polymer by appropriate reactions. However, exact composition of these polymers is not possible to know with certainty, which makes correlation between functional groups and properties difficult. The composition of the

polymer synthesized by the condensation of monomers containing desired functional groups can be determined by the feed ratio of monomers. Moreover, polymer with desired functional group content and structural variations can also be prepared by selecting appropriate monomer ratio with different monomers having different structures, by this method.

Polybenzimidazole is synthesized by the condensation of a diacid with a tetraamine and desired functional group in the polymer can be introduced by selecting either a diacid or a tetraamine containing these groups. But, such monomers are not available in the market and one has to synthesize such monomers. Weighing the steps and difficulties involved in the synthesis of both tetraamine and diacid monomers containing these functional groups, choice was made to synthesize diacids containing these functional groups and three new diacid monomers were synthesized. Similarly two diamine monomers containing carboxyl and sulfonic acid groups were synthesized for the synthesis of polyimide.

Thus, the present work involves

- Synthesis and characterization of new m-phenylene diacids containing pendant nitro and amino phenyl groups linked to diacid via ether group and  m-phenylene diacid containing benzimidazole pendant group as shown below (Figure 1.7).
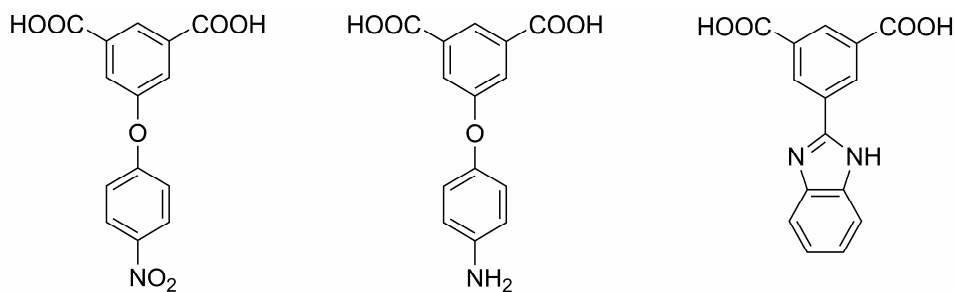


**Figure 1.7**  Diacids synthesized

- Synthesis and characterization of polybenzimidazoles and copolybenzimidazoles based on these diacids  and also polybenzimidazole polymers containing phenolic hydroxyl  groups based on 5-hydroxy, isophthalic acid, to study the effect of these groups on physical properties such as acid uptake, water uptake and proton

conducting properties of these polymers and their performance in fuel cell. (Figure 1.8).
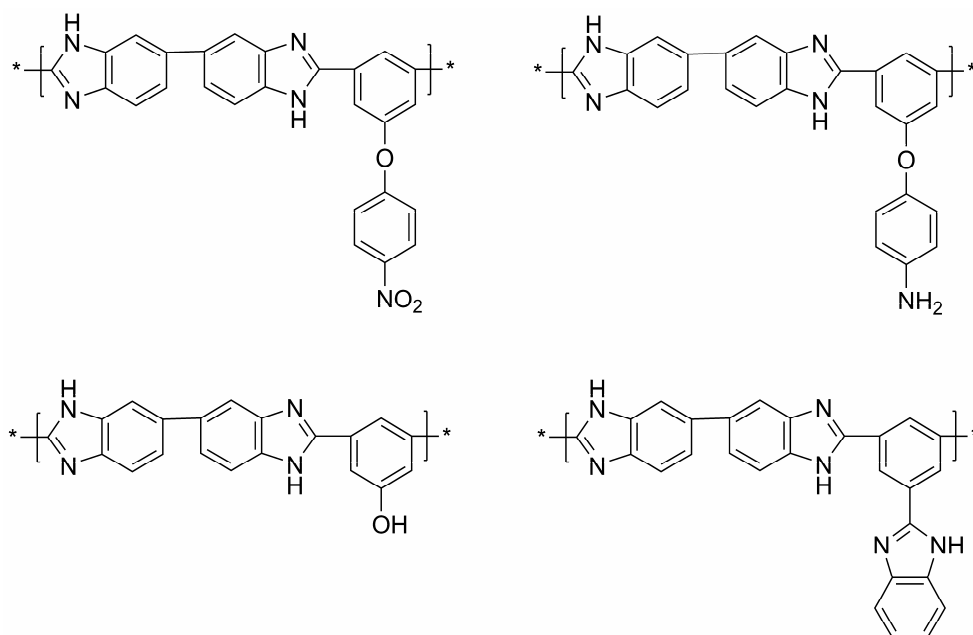


**Figure 1.8** Polybenzimidazoles synthesized

- Preparation and characterization of blends of polybenzimidazoles with commercially available polymers such as PVOH and SPEEK, to study the effect of these blending on physical properties such as acid uptake, water uptake and proton conducting properties of these polymers and their performance in fuel cell. (Figure 1.6).

- Synthesis and characterization of new m-phenylene diamines containing pendant phenyl carboxyl and phenyl sulfonic acid groups linked to diamine via ether and keto group respectively (Figure 1.9).
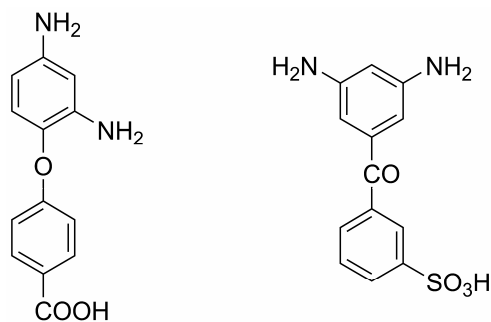


**Figure 1.9** Diamines synthesized

- Synthesis and characterization of polyimides and copolyimides based on these diamines having pendant functional groups and to study the effect of these groups on the water uptake and hydrolytic stability, proton conducting properties of polymers and their performance in fuel cell.
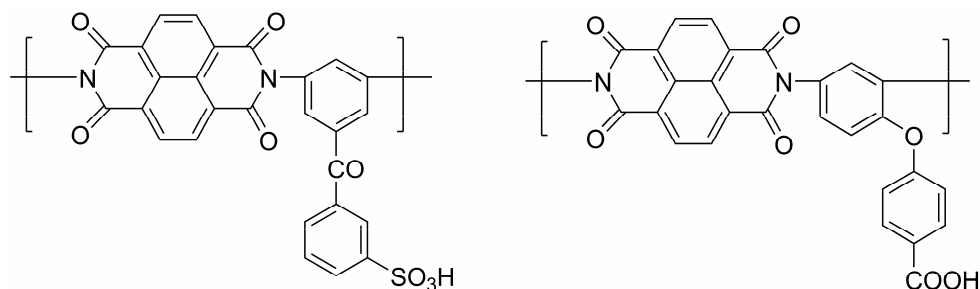


**Figure 1.10** Polyimides Synthesized

## References

1. Ticianelli, E.A.; Deroucin, C.R.; Srinivasan, S. *J. Electroanal. Chem.* **1988**, 251, 275.

2. Patil, P.G. *J. Power Sources* **1992,** 37, 171.

3. Haggin, J. *Chem Eng. News* **1995,** 28, 28.

4. Grot, W.G. Perfluorinated ion exchange polymers and theiruse in research and industry, *Macromol. Symposia* **1994**, 82, 161-172.

5. Vaughan, D.J. *Du Pont innovation* **1973**, 4,10.

6. *Fuel cell technology handbook*; Eds Hoogers, G. Ed. CRC Press LLC, 2003.

7. *Fuel Cell Today*, Johnson Matthey Public Limited Company. www.fuelcelltoday.com.

8. Winter, M.; Brodd, R.J. *Chem. Rev.* **2004**, *104*, 4245-4270.

9. Chalk, A.J.; Hay, A S. *Journal of Polymer Science Part A* **1968**, 7, 691.

10. Qi, Z.; Lefebvre M.C.; Pickup, P.G. *J Electroanal Chem* **1998**, 459, 9.

11. Kobayashi, H.; Tomita, H.; Moriyama, H. *Journal of American Chemical Society* **1994**, 116, 3153-3154.

12. Makrini, A.; Acosta, J.L. *Polymer* **2001**, 42, 9-15.

13. Wainright, J.S.; Wang, J.-T.; Weng, D.; Savinell R.F.; Litt, M.H. In *Proceedings of the Intersociety Energy Conversion Engineering Conference*; IEEE: Washington, DC, USA, 1996; Vol. 2, p 1107-1111.

14. Faure, S.; Pineri, M.; Aldebert, P.; Mercier, R.; Sillion, B. PCT Int.Appl. WO 9742253A1 13 Nov 1997, 51 pp.

15. Steck, A.; Stone, C. Montreal, Canada, 1997, pp. 792-807.

16.    Scherer, G.G. Polymer membrane for fuel cells. Ber. Bunsenges. *Phys. Chem.* **1990**, 94, 1008-1014.

17.    *DuPont Fuel Cells*, Information on *Nafion* membranes from www.fuelcells.dupont.com.

18.    Kordesch, K.; Simader, G. *Fuel Cells and Their Applications*, VCH, P.72 (1996)

19.    Masaki, Hasegawa.; Terunobu, Unish. *Polymer Letters* **1964**, 2, 237-239.

20.    Sheehan, W. C.; Cole, T. B.; Picklesimer, L. G. *Journal of Polymer Science Part A:* **3,** 1443 (1965).

21.    Holsten, J. R.; Lilyquist, M. R. *Journal of Polymer Science Part A:* **1965, 3**, 3905.

22.    Paul, M. Hergenrother.; Harold, H. Levine. *Journal of Polymer Science Part A-I: Polymer Chem.* **1967,6** 1453.

23.    Imai, Y.; Johnson, E. F.; Katto, T.; Kurihara, M.; Stille, J. K. *Journal of Polymer Science Part A-I: Polymer Chem* ,**13**, 2233 (1975).

24.    Moyer, W. W.; Carl Cole, T.; Anyos. *Journal of Polymer Science Part A:* **1965, 3**, 2107.

25.    Paul, M. Hergenrother.; Wolfgang, Wrasidlo.; Harold, H. Levine. *Journal of Polymer Science Part A:* **1965,** 3, 1665.

26.    Herward, Vogel.; Marvel, C. S. Polybenzimidazoles. II. *Journal of Polymer Science Part A: General Papers* **1963**, *1*, 1531-1541.

27.    Mittal, K. L. "*Polyimides. Synthesis, Characterization and Applicatons*", Dekker, New York (**1984**).

28.    Herward Vogel.; Marvel, C. S. *Journal of Polymer Science* **1961**, *50*, 511-539.

29.    Hedberg, F. L.; Marvel, C. S. *Journal of Polymer Science: Polymer Chemistry Edition* **1974**, *12*, 1823-1828.

30.    Powers, E. J.; Serad, G. A. eds. *History and Development of Polybenzimidazoles,High perfomance polymers: their orgin and development*, Elsevier, Amsterdam, 1986.

31.    Brinker, K. C.; Robinson, J. M. *U. S. Pat.* 2,895,948 **(1959)**.

32.    Marvel, C. S.; Vogel, H. *U.S. Patent* 3,174,947 (Mar-*1965).*

33.    Chenevey, E.; Conciatori, A. B. *U.S. Patent* 3,433,772(Mar. **1969**).

34.    Prince, A. E. *U.S. Patent,* 3,509,108 (Apr. **1970**).

35.    Choe, E.-W. Catalysts for the preparation of polybenzimidazoles. *Journal of Applied Polymer Science* **1994,** 53, 497-506.

36.    Wolfgang Wrasidlo.; Levine, H. H. *Journal of Polymer Science Part A: General Papers* **1964,** 2, 4795-4808.

37.    Neuse, E. Aromatic polybenzimidazoles. Syntheses, properties, and applications. In *Synthesis and Degradation Rheology and Extrusion*, **1982**; pp 1-42.

38.    Iwakura, Y.; Uno, K.; Chau, N. *Makromol. Chem.* **1975**, 176, 23.

39.    Korshak, V. V. *Vysokomol. Soedin., Ser.* **1980**, A *22,* 1209.

40. Srinivasan, P. R.; Mahadevan, V.; Srinivasan, M. *Makromol. Chem.* **1979,**180, 1845.

41. Sivriev, H.; Borissov, G.; *European Polymer Journal* **1977,**13, 25.

42. Neuse, E. W.; Horlbeck, G. *Polym. Eng. Sci.* **1977,** *17,* 821.

43. Banihashemi, A.; Fabro, D.; Marvel, C. S.; *Journal of Polymer Science Part A-1: Polymer Chemistry* **1969,** 7, 2293.

44. Levine, H. H.: *Encycl. Polym. Sci. Tech.* **1969,** 11, 188.

45. Marvel, C. S. *Techn. Rep.* ML-TDR-64-39, Part I (**1964**).

46. Hedberg, F. L.; Marvel, C. S. *Journal of Polymer Science: Polymer Chemistry Edition* **1974,** 12 (8), 1823.

47. Marks, B. S.; Shoff, L. E.; Watsey, G. W. Techn. Rep. NASA CR-1723 (1971) Levine, H. H.: *Encycl. Polym. Sci. Tech.* **1969,**11, 188.

48. Kourtides, D. A.; Parker, J. A. *Polym. Eng. Sci.* **1975,** 15, 415.

49. Dunay, M. US Pat. 3,775,213 (1973); *Chem. Abstr.: 80,* 71793 (1974).

50. Sheratte, M. B.: US Pat. 4,154,919 (1979*); Chem. Abstr.: 91,* 92439 (1979).

51. Verzwyvelt, S. A.: Fr. Dem. 2440084 (1978); *Chem. Abstr. 94,* 124660 (1981).

52. Martin, R. E. *Technical Rep.* NASA-CR-159653, FCR-1017 (1978).

53. Yaffe, M. R.; Murray, J. N. Proc. DOE *Chem./Hydrogen Energy Syst.* Contract. Rev. (CONF-781142), 37 (1978; publ. 1979); *Chem.Abstr. 94,* 22105 (1981).

54. Coffin, D. R.; Serad, G. A.; Hicks, H. L.; Montgomery, R. T. Text. Res. J. **1982**, 52, 466.

55. Tesoro, G.; Moussa, A.: Fire Retard., Proc. Eur. Conf. Flammability, Fire Retard., 2nd, 159(1978; pub. 1980); *Chem. Abstr. 92,* 182415 (1980).Defosse, T. C., Welch, I. H.: Mod. Text. *52,* 65 (1971).

56. Model, F. S.; Lee, L. A.: *Polybenzimidazole Reverse Osmosis Membranes, in: Reverse Osmosis Membrane Research,* Lonsdale, H. K. and Podall, H. E. Eds., Plenum Publishing Co., New York **1972**.

57. Belohlav, L. R. *Angew. Makromol. Chem.* **1974,** 40/41, 465.

58. Tan, M.; Davis, H. J.: *Techn. Rep.* W 79-07571, OWRT-7527(1) (1978); *Chem. Abstr. 92,*99356 (t980).

59. Goldsmith, R. L. et.al.: *Technical Rep.* W 79-09314, OWRT-7509(1) (1979); *Chem. Abstr. 92,* 203270 (1980).

60. Senoo, M.; Moil, K.; Taketani, Y.: *Ger. Pat.* 2,559,931(1979); *Chem. Abstr. 92,* 111507 (1980).

61. Gosnell, R. B.; Levine, H. H.: *J. Macromol. Sci. Chem.* **1969**, 3, 1381.

62. Savinell, R. F et.al.., A H2/O2 fuel cell using acid doped polybenzimidazole as polymer electrolyte. *Electrochimica Acta* **1996**, *41*, 193-197.

63. Wainright, J. S.; Wang, J. T.; Weng, D.; Savinell, R. F.; Litt, M. *Journal of The Electrochemical Society* **1995**, *142*, L121-L123.

64.  Fontanella, J. J.; Wintersgill, M. C.; Wainright, J. S.; Savinell, R. F.; Litt, M. *Electrochimica Acta* **1998**, *43*, 1289-1294.

65.  Wang, J. T.; Wasmus, S.; Savinell, R. F. *Journal of the Electrochemical Society* **1996**, *143*, 1233-1239.

66.  Weng, D.; Wainright, J. S.; Landau, U.; Savinell, R. F. *Journal of the Electrochemical Society* **1996**, *143*, 1260-1263.

67.  Samms, S. R.; Wasmus, S.; Savinell, R. F. *Journal of the Electrochemical Society* **1996**, *143*, 1225-1232.

68.  R. Ameri, *Polybenzimidazole film containing phosphoric acid as proton exchange membrane (PEM)*,PhD, Case Western Reserve University, Cleveland, 1997.

69.  Litt, M.; Ameri, R.; Wang, Y.; Savinell, R.; Wainright, J. *Materials Research Society symposium Proceedings,* **1999**, 548, 313.

70.  Savinell, R. F.; Litt, M. *WO patent* 973796.

71.  Xiao, L.; Zhang, H.; Choe, E.-W.; Scanlon, E.; Ramanathan, L. S.; Benicewicz, B. C. *ACS Fuel Chemistry Division Preprints* **2003**, *48*, 447-448.

72.  Wang, J. T.; Wainright, J. S.; Savinell, R. F.; Litt, M. *Journal of Applied Electrochemistry* **1996**, *26*, 751-756.

73.  Wasmus, S.; Dauch, B. A.; Moaddel, H.; Rinaldi, P. L.; Litt, M.; H. Rogers, C.; Valeriu, A.; Mateescu, G. D.; Savinell, R. F. In *Solid-state NMR characterization of H3PO4-doped polybenzimidazole polymer electrolyte fuel cell membranes*, Electrochemical Society Meeting, Reno, NV, May 21-26, **1995**; p 716.

74.  Glipa, X.; Bonnet, B.; Mula, B.; Jones, D. J.; Roziere, J. *Journal of Materials Chemistry* **1999**, *9*, 3045-3049.

75.  Li, Q. F.; Hjuler, H. A.; Bjerrum, N. J. *Journal of Applied Electrochemistry* **2001**, *31*, 773-779.

76.  Bouchet, R.; Siebert, E. *Solid State Ionics* **1999**, *118*, 287-299.

77.  Asensio, J. A.; Borros, S.; Gomez-Romero, P. *Journal of The Electrochemical Society* **2004**, *151*, A304-A310.

78.  Asensio, J. A.; Gómez-Romero, P. *Fuel Cells* **2005**, *5*, 336-343.

79.  Musto, P.; Karasz, F. E.; Macknight, W. J. *Polymer* **1993**, *34*, 2934-2945.

80.  Linkous, C. A. *International Journal Hydrogen Energy* **1993**, 18, (8), 641.

81.  Kawahara, M.; Morita, J.; Rikukawa, M.; Sanui, K.; Ogata, N. *Electrochimica Acta* **2000**, 45, 1395-1398.

82.  Bouchet, R.; Miller, S.; Duclot, M.; Souquet, J. L. *Solid State Ionics* **2001**, 145, 69-78.

83.  Pu, H. T.; Meyer, W. H.; Wegner, G. *Journal of Polymer Science Part B: Polymer Physics* **2002**, 40, 663-669.

84.  Weng, D. *Water and methanol transport through polymer electrolytes in elevated temperature fuel cells*, PhD, Case Western Reserve University, Cleveland, 1996.

85.   Mecerreyes, D.; Gre, H.; Miguel, O.; Ochoteco, E.; Marcilla, R.; Cantero. I. *Chemistry of Materials* **2004**, 16, 604-607.

86.   Ma, Y. L.; Wainright, J. S.; Litt, M. H.; Savinell, R. F. *Journal of the Electrochemical Society* **2004**, 151, A8-A16.

87.   Wang, J. T.; Savinell, R. F.; Wainright, J.; Litt, M.; Yu, H. *Electrochimica Acta* **1996**, 41, 193-197.

88.   Samms, S. *Kinetics in an Internal Reforming Fuel Cell, High Temperature PEM Fuel Cell Performance, and a Fundamentals Based Impedance Model*, PhD, Case Western Reserve University, Cleveland, OH, 2001.

89.   Savadogo, O.; Xing, B. *Journal of New Materials for Electrochemical Systems* **2000**, *3*, 343-347.

90.   Li, Q. F.; Hjuler, H. A.; Bjerrum, N. J. *Electrochimica Acta* **2000**, *45*, 4219-4226.

91.   Li, Q. F.; He, R. H.; Gao, J. A.; Jensen, J. O.; Bjerrum N. J. *Journal of The Electrochemical Society* **2003**, *150*, A1599-A1605.

92.   Uchida, H.; Yamada, Y.; Asano, N.; Watanabe, M.; Litt, M. *Electrochemistry* **2002**, *70*, 943-945.

93.   Asensio, J. A.; Borros, S.; Gomez-Romero, P. *Journal of The Electrochemical Society* **2004**, *151*, A304-A310.

94.   Xiao, L.; Zhang, H.; Jana, T.; Scanlon E.; Chen, R.; Choe, E. W.; Ramanathan L. S.; Yu S.; Benicewicz, B. C. *Fuel Cells* **2005**, *5*, 287-295.

95.   Seland, F.;Berning, T.; Børresen, B.; Tunold, R. *Journal of Power Sources* **2006**, *160*, 27-36.

96.   Wainright, J. S.; Litt, M.; Savinell, R. F. eds., High-temperature membranes, Handbook of Fuel Cell, Fundamentals, Technology, and Application, Vol. 3, John Wiley & Sons, **2003**.

97.   Powers, E. J.; Serad G. A. eds., History and Development of Polybenzimidazoles, High perfomance polymers: their orgin and development, Elsevier, Amsterdam, **1986**.

98.   Kuder, J. E.; Chen. J. C. *US Patent* 4,634,530, **1987.**

99.   Ariza M. J.; Jones, D. J.; Roziere, J. *Desalination* **2002**, *147*, 183-189.

100.  Staiti, P.; Lufrano, F.; Arico, A. S.; Passalacqua, E.; Antonucci, V. *Journal of Membrane Science* **2001**, *188*, 71-78.

101.  Jones, D. J.; Roziere, J. *Journal of Membrane Science* **2001**, *185*, 41-58.

102.  Glipa, X.; El Haddad, M.; Jones, D. J.; Roziere, J. *Solid State Ionics* **1997**, *97*, 323-331.

103.  Gieselman, M. B.; Reynolds, J. R. *Macromolecules* **1992**, *25*, 4832-4834.

104.  Bae, J.-M.; Honma, I.; Murata, M.; Yamamoto, T.; Rikukawa, M.; Ogata, N. *Solid State Ionics* **2002**, 147, 189-194.

105.  Hongting, Pu.; Qizhi, Liu. *Polymer International* **2004**, *53*, 1512-1516.

106.  Reynolds, J. R.; Lee, Y.; Kim, S.; Bartling, R. L.; Gieselman, M. B.; Savage, C. S. *American Chemical Society, Polymer Preprints, Division of Polymer Chemistry* **1993**, 34(1), 1065-1066.

107. Uno, K.; Niume, K.; Iwata, Y.; Toda, F.; Iwakura, Y. *Journal of Polymer Science: Polymer Chemistry Edition* **1977**, *15*, 1309-1318.

108. Einsla, B.R.; Hill, M.L.; Harrison, W.L.; Tchatchoua, C.N.; McGrath, J.E. *Proceedings of the 204th Electrochemical Society International Meeting* **2005**.

109. Shengbo, Qing.; Wei Huang, Deyue Yan. *Journal of Polymer Science Part A: Polymer Chemistry* **2005**, 43(19), 4363.

110. Bung, L.; Williams, D. J.; Karasz, F. E.; MacKnight, W. J. *Polym. Bd.* **1986**, 16,457.

111. Gaetano Guerra,; David J. Williams.; Frank E. Karasz.; William J. MacKnight. *Journal of Polymer Science Part B: Polymer Physics* **1988**, *26*, 301-313.

112. Guerra, G.; Choe, S.; Williams, D. J.; Karasz, F. E.; MacKnight, W. J. *Macromolecules* **1988**, *21*, 231-234.

113. Musto, P.; Karasz, F. E.; MacKnight, W. J. *Macromolecules* **1991**, *24*, 4762-4769.

114. Musto, P.; Karasz, F. E.; MacKnight, W. J. *Polymer* **1993**, 34, 2934-2945.

115. Kuiming, Liang.; György Bánhegyi, Frank.; E. Karasz.; William J. MacKnight. *Journal of Polymer Science Part B: Polymer Physics* **1991**, *29*, 649-657.

116. Ahn, T. K.; Kim, M.; Choe, S. *Macromolecules* **1997**, *30*, 3369-3374.

117. Deimede, V.; Voyiatzis, G. A.; Kallitsis, J. K.; Qingfeng, L.; Bjerrum, N. J. *Macromolecules* **2000**, *33*, 7609-7617.

118. Hasiotis, C.; Qingfend, L.; Deimede, V.; Kallitsis J. K.; Kontoyannis, C. G.; Bjerrum, N. J. *Journal of the Electrochemical Society* **2001**, 148, (5), A513.

119. Hasiotis, C.; Deimede, V.; Kontoyannis, C. *Electrochimica Acta* **2001**, *46*, 2401-2406.

120. Li, Q. F.; Hjuler, H. A.; Hasiotis, C.; Kallitsis, J. K.; Kontoyannis, C. G.; Bjerrum, N. J. *Electrochem. Solid State Lett.* **2002**, 5, (6), A125.

121. Kerres, J.; Ullrich, A.; Haring, T. the 3rd *International Symposium* on New Materials for Electrochemical Systems, Montreal, Canada, 4-8 July, 1999, pp 231.

122. Jorissen, L.; Gogel, V.; Kerres, J.; Garche J., *Journal of Power Sources* **2002**, *105*, 267-273.

123. Kerres, J.; Zhang, W.; Jorissen, L.; Gogel, V. *Journal of New Materials for Electrochemical Systems* **2002**, *5*, 97-107.

124. Kerres, J.; Ullrich, A.; Haring, T.; Baldauf, M.; Gebhardt, U.; Preidel, W. *Journal of New Materials for Electrochemical Systems* **2000**, *3*, 229-239.

125. Kerres, J. A. *Journal of Membrane Science* **2001**, *185*, 3-27.

126. Kerres, J.; Ullrich, A.; Meier, F.; Haring, T. *Solid State Ionics* **1999**, *125*, 243-249.

127. Manea, C.; Mulder, M. *Desalination* **2002**, 147(1-3), 179.

128. Lakshmanan, B.; Huang, W.; Olmeijer, D.; Weidner, J. W. *Electrochem. Solid State Lett.* **2003**,*6*, (12), A282.

129. Kosmala, B.; Schauer, J. *Journal of Polymer Science* **2002**, 85, 1118.

130.   Hongting, Pu. *Polymer International* **2003**, *52*, 1540-1545.

131.   Zaidi, S. M. Javaid. *Electrochimica Acta* **2005,** 50, 4771-4777**.**

132.   Daletou, M. K.; Gourdoupi, N.; Kallitsis, J. K. *Journal of Membrane Science* **2005**, 252, 115.

133.   Pu, H.; Liu, Q.; Qiao, L.; Yang, Z. *Polymer Engineering and Science* **2005**, *45*, 1395-1400 .

134.   Wycisk, R.; Chisholm, J.; Lee, J.; Lin, J.; Pintauro, P. N. *Journal of Power Sources* **2006**, *163*, 9-17.

135.   Ainla, Alar.; Brandell, Daniel. *Solid State Ionics* **2007**, 178 (7-10), 581.

136.   Schönberger, F.; Hein, M.; Kerres, J. *Solid State Ionics* **2007**, *178*, 547-554.

137.   Lee, J. K.; Kerres, J. *Journal of Membrane Science* **2007**, 294 (1-2), 75.

138.   Rusanov, A.L. *Adv. Polym. Sci.* **1994**, *111*, 115-175.

139.   Feger, C.; McGrath, J.E.; Khojasteh, M.M. *Polyimides: Materials, Chemistry and Characterization.* Elsevier: New York, **1988**.

140.   Genies, C.; Mercier, R.; Sillion, B.; Petiaud, R.; Cornet, N.; Gebel, G.; Pineri, M. *Polymer* **2001**, *42*, 5097-5105.

141.   Savadago, O. *J. New Mat. Electrochem. Systems* **1998**, *1*, 47-66.

142.   Faure; R. Mercier; P. Aldebert; M. Pineri and B. Sillion, *French patent* 96 05707 (**1996**).

143.   Cornet, N.; Diat, O.; Gebel, G.; Jousse, F.; Marsacq, D.; Mercier, R.; Pineri, M. *J. New Mat. Electrochem. Systems* **2000**, *3*, 33-42.

144.   Gunduz, N. Synthesis and Characterization of Sulfonated Polyimides as Proton Exchange Membranes for Fuel Cells. *Ph.D. Dissertation*, Virginia Tech, Blacksburg, VA, *2001*.

145.   Miyatake, E.; Asano, N.; Watanabe, M. *Journal of Polymer Science, Part A: Polymer Chemistry* **2003**, 41, (24), 3901-3907.

146.   Miyatake, K.; Zhou, H.; Uchida, H.; Watanabe, M. *Chemical Communications* **2003,** 9, (3), 368-369.

147.   Sroog, C.E.; Endrey, A.L.; Abramo, S.V.; Berr, C.E.; Edwards, W.M.; Olivier, K.L. *Journal of Polymer Science, Part A: Gen. Papers* **1965**, *3*, 1373-1390.

148.   Cassidey, P. E.; Fawcett, N. C. "*Kirk-Othmer Encyclo. Chem. Technol.",* John Wiley and Sons, New York, **18,** 704 (**1982**).

149.   Pebalk, D. V. et.al.., *Reports from the Soviet Acadamy of Sciences*, **6,** 236 (1977).

150.   Woo, Y.; Oh, S. Y.; Kang, Y. S.; Jung, B. *Journal of Membrane Science* **2003,** 220, (1-2), 31-45.

151.   Kumar, D. *Journal of Polymer Science, Polym. Chem. Ed.*, **1981,** 19**,** 795.

152.   Bessonov, M. I.; Koton, M. M.; Kudryavtsev, V. V.; Laius, A. "*Polyimides: Thermally Stable Polymers"*, Plenum, New York (**1987**).

153.   Yanagishita, H.; Kitamoto, D.; Haraya, K.; Nakane, T.; Okada, T.; Matsuda, H.; Idemoto, Y.; Koura, N. *Journal of Membrane Science* **2001**,188, 165.

154.  Seshadri, K. S.; Antonoplos, P. A.; Heilman, W. J. *Journal of Polymer Science., Part*-A-1, **1980**, 18**,** 2649.

155.  Harris, F. W. "*Polyimides*", Blackie,Chapman and Hall, New York (**1990**).

156.  Vinogradova, S. V.; Vygodskii, Ya. S.; Vorob'ev, V. D.; Churochkina, N. A.; Chudina, L. I.; Spirina, T. N.; Korshak, V. V. *Vysokomol. Soyed.*, **1974**, A16**,** 506.

157.  Gerashchenko, A. V.; Vygodskii,Ya. S.; Slonimskii, G. L.; Klimova, A. A.; Sherman, F. B.; Korshak,V.V. *Vysokomol. Soyed.,* **1973**, A15**,** 1718.

158.  Lavrov, S. V.; Ardashnikov, A. Ya.; Kardash, I. Ye; Pravednikov, A. N. *Polym. Sci., USSR*, 1977, 19**,** 1212.

159.  Solomin, V. A.; Kardash, I. E.; Snagovskii, Yu. S.; Masserle, P. E.; Zhubanov, B. A.; Pravendnikov, A. N. *Dokl. Akad. Nauk SSSR*, **1977**, 236**,** 139.

160.  White, D. M. *U. S. Pat. 4324884* (1982), to General Electric Co.

161.  Takekoshi, T.; Klopfer, H. J. *U. S. Pat. 4293683* (1981), to General Electric Co.

162.  Sroog, C.E. *Journal of Polymer Science, Part C:* **1967**, *16*, 1191-1198.

163.  Imai, Y.; Maldar, N.N.; Kakimoto, M. *Journal of Polymer Science, Part A: Polymer Chemistry* **1984**, *22*, 2189-2196.

164.  Keller, U.; Eiselt, P.; Schmidt, H.-W. *Journal of Polymer Science, Part A: Polymer Chemistry* **1993**, *31*, 141-151.

165.  Lozano, A.E.; de la Campa, J.G.; de Abajo, J.; Preston, J. *Journal of Polymer Science, Part A: Polymer Chemistry* **1994**, *35*, 873-880.

166.  Kaneda, T.; Katsura, T.; Nakagawa, K.; Makino, H. *Journal of Applied Polymer Science* **1986**, *32*, 3151-3176.

167.  Cornet, N.; Diat, O.; Gebel, G.; Jousse, F.; Marsacq, D.; Mercier, R.; Pineri, M. *J. New Mat. Electrochem. Systems* **2000**, *3*, 33-42.

168.  Fang, J.; Guo, X.; Harada, S.; Watari, T.; Tanaka, K.; Kita, H.; Okamoto, K,-I. *Macromolecules* **2002**, *35 (24)*, 9022-9028.

169.  Shobha, H.K.; Sankarapandian, M.; Glass, T.E.; McGrath, J.E. *American Chemical Society, Polymer Preprints, Division of Polymer Chemistry* **2000**, *41(2)*, 1298-1299.

170.  Einsla, B.R.; Hong, Y.T.; Kim, Y.S.; Wang, F.; Gunduz, N.; McGrath, J.E. *Journal of Polymer Science, Part A: Polymer Chemistry* **2004**, *42*, 862-874.

171.  Zhou, W.; Watari, T.; Kita, H.; Okamoto, K,-I.. *Chem. Lett.* **2002**, 534-535.

172.  Watari, T.; Fang, J.; Tanaka, K.; Kita, H.; Okamoto, K. *ACS Polym. Mat.: Sci. & Eng. (PMSE)* **2001**, *85*, 334.

173.  Guo, X.; Fang, J.; Watari, T.; Tanaka, K.; Kita, H.; Okamoto, K,-I. *Macromolecules* **2002**, *35(17)*, 6707-6713.

174.  Shang, Y.; Xie, X.; Jin, H.; Guo, J.; Wang, Y.; Feng, S.; Wang, S.; Xu, J. *European Polymer Journal* **2006,** 42, (11), 2987-2993.

175. Asano, N.; Aoki, M.; Suzuki, S.; Miyatake, K.; Uchida, H.; Watanabe, M. *Journal of the American Chemical Society* **2006,** 128, (5), 1762-1769.

176. Yin, Y.; Fanga, J.; Cui, Y.; Tanaka, K.; Kita, H.; Okamoto, K. I. *Polymer* **2003,** 44, (16), 4509-4518.

177. Yin, Y.; Fang, J.; Watari, T.; Tanaka, K.; Kita, H.; Okamoto, K. I. *Journal of Materials Chemistry* **2004,** 14, (6), 1062-1070.

178. Guo, X.; Fang, J.; Tanaka, K.; Kita, H.; Okamoto, K. I. *Journal of Polymer Science, Part A: Polymer Chemistry* **2004,** 42, (6), 1432-1440.

179. Chen, S.; Yin, Y.; Tanaka, K.; Kita, H.; Okamoto, K. i. *Polymer* **2006,** 47, (8), 2660-2669.

180. Zhaoxia, H. U.; Yin, Y.; Chen, S.; Yamada, O.; Tanaka, K.; Kita, H.; Okamoto, K. I. *Journal of Polymer Science, Part A: Polymer Chemistry* **2006,** 44, (9), 2862-2872.

181. Rabiee, A.; Mehdipour-Ataei, S.; Banihashemi, A.; Yeganeh, H. *Polymers for Advanced Technologies* **2008,** 19, (5), 361-370.

182. Li, Y.; Jin, R.; Cui, Z.; Wang, Z.; Xing, W.; Qiu, X.; Ji, X.; Gao, L. *Polymer* **2007,** 48, (8), 2280-2287.

183. Li, N.; Cui, Z.; Zhang, S.; Xing, W. *Journal of Membrane Science* **2007,** 295, (1-2), 148-158.

184. Alvarez-Gallego, Y.; Nunes, S. P.; Lozano, A. E.; De La Campa, J. G.; De Abajo, J. *Macromolecular Rapid Communications* **2007,** 28, (5), 616-622.

185. Genies, C.; Mercier, R.; Sillion, B.; Cornet, N.; Gebel, G.; Pineri, M. *Polymer* **2001**, 42, 359-373.

186. Cornet, N.; Beaudoing, G.; Gebel, G. *Sep. Purif. Technol.* **2001**, 22-23, 681-687.

187. Hong, Y.T.; Einsla, B.; Kim, Y.S.; McGrath, J.E. *American Chemical Society, Polymer Preprints, Division of Polymer Chemistry* **2002**, 43(1), 666-667.

188. Einsla, B.R.; Kim, Y.S.; Hickner, M.A.; Hong, Y.-T.; Hill, M.L.; Pivovar, B.S.; McGrath, J.E. *Journal of Membrane Science* **2005**, *255*, 141-148.

189. Watari, T.; Fang, J.; Tanaka, K.; Kita, H.; Okamoto, K.; Hirano, T. *Journal of Membrane Science.* **2004**, *230*, 111-120.

190. Zhang, Y.; Litf, M.; Savinell, R. F.; Wainright, J. S. *American Chemical Society, Polymer Preprints, Division of Polymer Chemistry* **1999**, *40*, 480-481.

191. Zhang, Y.; Lilf, M.; Savinell, R. F.; Wainright, J. S.; Vendramini, J. In *American Chemical Society, Polymer Preprints, Division of Polymer Chemistry*, **2000**; 41, 1561-1562.

192. Essafi, W.; Gebel, G.; Mercier, R. *Macromolecules* **2004**, *37*, 1431-1440.

193. Kim, Y. S.; Dong, L.; Hickner, M. A.; Glass, T. E.; Webb, V.; McGrath, J. E. *Macromolecules* **2003**, *36*, 6281-6285.

194. Miyatake, K.; Zhou, H.; Watanabe, M. *Macromolecules* **2004**, *37*, 4956-4960.

195. Piroux, F.; Espuche, E.; Mercier, R.; Pineri, M.. *Desalination* **2002**, 145, 371-374.

196. Piroux, F.; Espuche, E.; Mercier, R. *Journal of Membrane Science.* **2004**, 232, 115-122.

197.   Einsla, B. R.; Hill, M. L.; Kim, Y.S.; Pivovar, B.; McGrath, J. E. *Abstracts of the 205th Meeting of the Electrochemical Society* **2004**, 24.

198.   Miyatake, K.; Zhou, H.; Matsuo, T.; Uchida, H.; Watanabe, M. *Macromolecules* **2004**, *37*, 4961-4966.

199.   Lyapunov, V. V.; Lyakh, E. N.; Solomin, V. A.; Zhubanov, B. A. *Doklady Akademii Nauk* **1992**, *326*, 106-108.

200.   Asano, N; Miyatake, K.; Watanabe, M. *Chemistry of Materials* **2004**, *16*, 2841-2843.

# Chapter 2

Amino & Nitro Group based Polybenzimidazole Copolymers for Proton Exchange Membrane Fuel Cell- Synthesis and Characterization

### 2.1 Introduction

Aromatic polybenzimidazoles (PBIs) are heterocyclic high performance polymers having high thermal stability, good flame resistance, excellent chemical resistance and high mechanical properties [1] offering an attractive combination of chemical, physical and mechanical properties for various applications, with capacity to withstand extreme conditions. The major applications of these materials include fire resistant garments, high temperature stable adhesives [2] and coatings for aerospace, desalination, and membrane separation. Presently, PBIs have received considerable attention in the view of development of material for high temperature polymer electrolyte membrane for proton exchange membrane fuel cell PEMFC) (and direct methanol fuel cell (DMFC) applications. However, high melting points and poor solvent solubility make them intractable and hence hinder the development of new applications. Commercial PBI, a condensation product of isophthalic acid (IPA) and 3,3',4,4,'-tetra amino biphenyl (TAB), is a rigid polymer having poor tractability. Persistent efforts are being made to improve processability or to modify the properties of PBIs by introducing flexibilizing groups, pendant bulky units in main chain or side chain to suit desired applications.

Thus, PBIs containing ether group [3], aliphatic groups [4-5], sulfone linkages [6], alicyclic structures [7], azo groups [8], dibenzothiophene and dioxodibenzothiophene units [9] adamantine units [10], pyridine and imidazole groups [11], thiaxanthone groups[12], cardo (florene) groups [13], benzofuro-benzofuran structures [14], amide groups [15] and phenoxaphosphine [16] have been reported. However, in most of the cases the modifying units are in main chain of PBIs. Functional group containing PBIs have also been reported in literature. Junhan Cho et.al. [17] describe the synthesis of PBI containing nitro groups in which preformed PBI polymer is nitrated with nitric acid to enhance solvent solubility. Sulfonated PBI have been synthesized by condensing sulfonated isophthalic acid with TAB [18-19]. Replacing hydrogen of imidazole ring with a suitable functional group containing substituent to produce substituted PBI is another route to modify PBI. Thus, PBI containing N-phenyl group [20] to enhance thermal and oxidative stability, aromatic nitro and cyano groups [21], aromatic nitro group for non linear optical properties[22], hydroxyl group [23] to

impart hydrophilicity, N-substituted alkyl acid and ester groups [24] for ultrafilters and cation exchange resins and sulfonic acid groups [25-26] for polymer electrolyte for fuel cell have been synthesized. These functional groups are introduced in preformed high molecular weight PBIs. It is difficult to obtain well defined polymers by opting introduction of functional groups on preformed PBIs, since extent of substitution is difficult to control on a preformed polymer.

PBI is considered to be promising future membrane material for high temperature polymer electrolyte for PEMFC and DMFC. However, it has low proton conductivity compared to Nafion particularly below 80 °C. Moreover, proton conductivity of PBI is dependent on extent of doping level of phosphoric acid and poses threat of leaching out of unbound phosphoric acid by water and methanol at high doping level resulting in the loss of efficiency with time. To circumvent these shortcomings of commercial PBIs, strategies to develop modified PBIs, focused on incorporation of functional groups in side chain capable of interacting with free phosphoric acid of doped PBI, may help to reduce phosphoric acid loss by leaching out with water even at high doping level.

Though, PBIs containing sulfonic acid groups as polymer electrolytes are known, the effect of pendant functional group other than sulfonic acid group in side chain on proton conductivity and other properties of PBI have not been reported so far. With this perspective, we initiated a work to develop PBIs containing functional group in side chain capable of interacting with phosphoric acid. A bulky pendant group in side chain has definite advantages. It improves solvent solubility by disrupting rigid structure of polymer, increases free volume to increase acid uptake and modifies other properties of a polymer depending on the chemical structure of the pendant group.

As a part of this chapter, we developed PBIs containing pendant nitrophenoxy and phenoxy amine groups by using diacids having nitro and amino functional group in side chain, which leaves imidazole group of PBI intact without affecting phosphoric acid uptake property of resultant polybenzimidazole. A reactive functional group in side chain of a polymer offers wide scope for further reactions such as cross-linking, linking other functional units for specific applications and improving miscibility with other polymers.

The present work is intended to study the effect of two pendant functional groups, capable of interacting with phosphoric acid, namely, nitro (anhydride of an acid) and amino (basic group) on proton conductivity and other properties of these polymers. Thus, this chapter describes synthesis and characterization of new diacids containing nitro and amino groups, namely, 5-(4-nitrophenoxy) isophthalic acid (NEDA) and 5-(4-aminophenoxy) isophthalic acid (AEDA), condensation of this diacid and varying mixture of this acid and isophthalic acid and other commercial diacids in different ratio with 3,3',4,4,'-tetra amino biphenyl (TAB) in polyphosphoric acid at high temperature to obtain novel homo and co-polybenzimidazoles containing pendant nitrophenoxy and phenoxyamine groups in the side chain and investigation of these polymers as potential candidate for fuel cell applications.

## 2.2  Experimental

### 2.2.1  Materials

4-nitrochorobenzene (Fluka, Switzerland) was recrystallized from ethanol. 3,3',4,4,'-tetra amino biphenyl (TAB) (Aldrich Chemicals, USA) was recrystallized from water. Isophthalic acid (IPA) (Fluka, Switzerland), adipic acid and sebacic acid (Aldrich Chemicals, USA) were purified by recrystallization from methanol. Terephthalic acid (Aldrich Chemicals, USA) was purified by sublimation and pyridine 2, 6-dicarboxylic acid (Aldrich Chemicals, USA) was recrystallized from 1:1 water/HCl. Dimethylformamide (DMF) was dried over $CaH_2$ and vacuum distilled. N-methyl-2-pyrollidinone (NMP) and N,N-dimethylacetamide (DMAc) (S. D. Fine Chem., India) were dried over phosphorus pentoxide and vacuum distilled. 3,5 dimethyl phenol (Aldrich Chemicals, USA), 5% and 10% Pd/C (Aldrich, USA), ethyl acetate (Merck, India) were used as received. Potassium carbonate (S. D. Fine Chem., India) was dried at 120 °C prior to use. Petroleum ether (60-80 °C), petroleum ether (40-60 ° C), methanol, 3,5-dinitro benzoic acid, potassium permanganate, pyridine, hydrochloric acid, sodium bicarbonate, ortho phosphoric acid (85%) and phosphorus pentoxide ( all from S. D. Fine Chem., India) were used as received. Polyphosphoric acid (PPA) was prepared by heating 1:1.8 weight ratio of ortho phosphoric acid (85%) and phosphorus pentoxide for 6h at 100 °C.

**2.2.2    Analytical methods**

The elemental analysis was carried out by CHNS-O, EA 1108-Elemental Analyzer of Carlo-Erba Instruments, Italy. The IR spectra were recorded on a Perkin Elmer 16 PC FT-IR spectrophotometer. The $^1$H NMR and $^{13}$C NMR spectra were recorded on Bruker NMR instrument AC-200 and AC-400 respectively. Solvent solubility was determined by dissolving 4 mg of polymer in 0.5 mL solvents. Inherent viscosity of polymers was determined at 0.5-g/dL concentrations at 30 °C using an Ubbelhode viscometer. Films were prepared by casting the 2.5-wt % homogeneous solution of polymer on a glass plate and evaporating solvent in a leveled oven at 80 °C for 15 h.

**Thermal study-** The Thermo gravimetric analysis (TGA) was performed on Perkin Elmer TGA-7 in $N_2$ atmosphere at heating rate of 10 °C min$^{-1}$. Glass transition temperature ($T_g$) was measured using DSC Q-10 (TA) in $N_2$ atmosphere at heating rate of 20 °C min$^{-1}$.

**XRD-** The wide-angle x-ray diffraction spectra (WAXD) were obtained using Rigaku Dmax 2500 diffractometer with Cu-K $\alpha$ radiation source. Tensile properties of polymer films were determined on Instron tensile tester series IX using film strip of size 1.5 x 7 cm at shear rate of 5mm/min.

**Oxidative stability-** Oxidative stability was evaluated by the Fenton test. Three weighed pieces of membranes of 2 cm × 2 cm were immersed in 3% $H_2O_2$ containing 4 ppm of $Fe^{2+}$ (Mohr's salt, $(NH_4)_2Fe(SO_4)_2 \cdot 6H_2O$) at 70 °C. The samples were withdrawn from the solution after 24 h or desired time period, washed thoroughly with distilled water, dried at 120 °C for 6 h and weighed. The Fenton's solution was replaced by freshly prepared solution after every 24 h.  Stability was evaluated in terms of weight loss after Fenton test.

**Phosphoric acid uptake-** To determine the $H_3PO_4$ uptake, the weighed samples of membrane was immersed in the different molar concentrations of $H_3PO_4$ for various time intervals at room temperature. For determining the acid uptake by membranes, the membranes after doping for desired time were withdrawn from acid; the adhered phosphoric

acid was wiped out by tissue paper and dried at 100 °C under vacuum until an unchanged weight was obtained. The acid uptake in wt % was determined by using the equation,

$$\mathrm{H_3PO_4} \text{ uptake } [\mathrm{Wt\,\%}] = \frac{\mathrm{W_{wet} - W_{dry}}}{\mathrm{W_{dry}}} \times 100$$

Where, $\mathrm{W_{dry}}$ is the weight of the dried sample before immersing in $\mathrm{H_3PO_4}$ and $\mathrm{W_{wet}}$ the weight of the dried doped membrane samples respectively.

**Proton conductivity measurements-** The proton conductivity of $\mathrm{H_3PO_4}$ doped membranes was determined by a two probe electrochemical impedance spectroscopy (EIS) method using an impedance analyzer (Autolab PGSTAT 30 with FRA software) recorded between 1 MHz and 0.1 Hz with 10 points per decade at maximum perturbation amplitude of 10 mV. To measure the temperature dependence of the conductivity, the cell was placed in a sealed, tempered glass vessel and the temperature recorded in close proximity to the membrane with a K-type thermocouple. Measurements were carried out in a conductivity cell at temperatures ranging from 25 to 175 °C without humidification. The conductivity (σ) was calculated by the

formula:           $\sigma = \dfrac{L}{RA}$

Where, R and L are the measured resistance and thickness and *A* is cross-sectional area of the membrane, respectively.

**Fuel cell performance tests-** Platinum catalysts (20% Pt) supported on carbon black (Vulcan XC-72R, Cabot) was purchased from Arora matthey Ltd. and electrodes were prepared as per Lee's procedure. [27] A wet-proofed carbon cloth (Electrochem Inc.) was coated with PTFE/C layer and catalyst ink, prepared by using Nafion solution, was applied on PTFE/C layer by a brushing technique. Membrane electrode assemblies (MEAs) using the acid-doped polymer membranes and electrodes were prepared by means of hot press at 120 °C. A single test cell (9 cm$^2$) with gas manifolds on both cathode and anode sides was fabricated using graphite plates and two gold coated end plates with attached heaters to clamp the graphite plates and for current collectors. Fuel and oxidant gases were supplied by means of mass flow controllers and performance curves were obtained by using an Arbin Fuel cell test Station.

### 2.2.3     Synthesis of new substituted aromatic diacid monomers

### 2.2.3.1 Synthesis of 5-(4-nitrophenoxy) isophthalic acid (NEDA)

This diacid was synthesized in two steps, by nucleophilic substitution reaction of 3,5-dimethylphenol with 4-nitrochlorobenzene in the presence of an acid acceptor, potassium carbonate, followed by oxidation of resultant 1,3-dimethyl-5-(4-nitrophenoxy)benzene to the corresponding diacid using potassium permanganate in pyridine. Various steps involved in this synthesis are outlined in Scheme 2.1

**(i) Synthesis of 1,3-dimethyl-5-(4-nitrophenoxy)benzene (I)**

To a 250 mL three necked round bottom flask equipped with a magnetic stirrer, reflux condenser, thermo-well, nitrogen inlet and calcium chloride guard tube was added 13.662g (111.81 mmol) of 3, 5-dimethyl phenol, 17.625g (111.81 mmol) of 1-chloro-4-nitrobenzene, 16.56g (120.0 mmol) of $K_2CO_3$ and 120 mL DMF at room temperature under a stream of nitrogen. The reaction mixture was then heated to 140 °C with stirring and the reaction continued for 12 h at this temperature. After completion of the reaction, the reaction mixture was cooled to room temperature and poured into excess water to precipitate the product. The crude product was filtered, washed with large excess of water, dried and recrystallized from pet ether/ethyl acetate (8:2)

 Yield: 25.5 g (93%)      Melting Point: 82-84 °C

FTIR: IR (KBr, cm$^{-1}$): 1517, 1344 (-NO$_2$ stretching); 1232, 1100 (-C-O-C- stretching); 846 (-C-N stretching); 1581, 1487 (aromatic) (Figure 2.1).

$^1$H NMR [200 MHz, CDCl$_3$, δ ppm] showed signals of different protons at δ values of 8.21 (d, 2H, H$_a$); 7.03 (d, 2H, H$_b$); 6.89 (s, 1H, H$_c$); 6.70 (s, 2H, H$_d$ ); 2.33 (s, 6H, H$_e$) (Figure 2.2).

$^{13}$C NMR [400 MHz, CDCl$_3$,δ, ppm ] showed values at 163.63, 154.66, 142.45, 140.45, 127.10, 125.86, 118.11, 117.03 and 21.26 (Figure 2.3).

| **Elemental analysis:** | C% | H% | N% |
|---|---|---|---|
| **C$_{14}$H$_{13}$NO$_3$** | | | |
| Calculated: | 69.12% | 5.39% | 5.76% |
| Observed: | 68.95% | 5.35% | 5.64% |
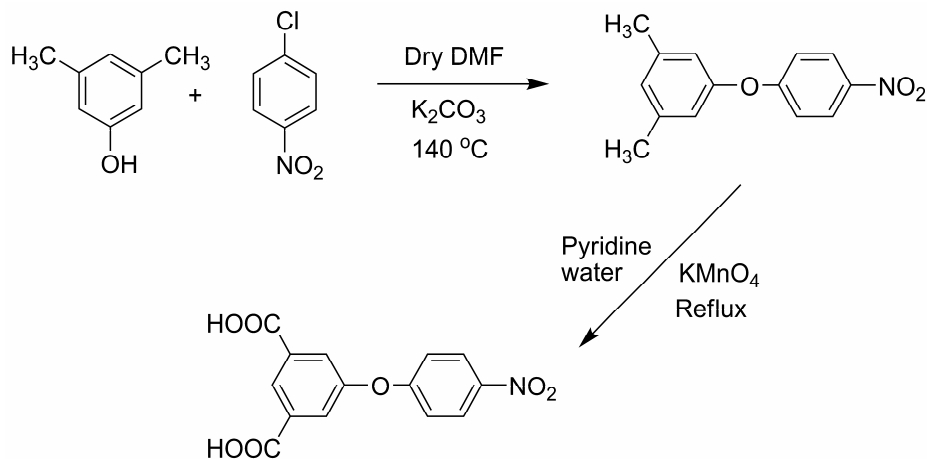
**Scheme 2.1** Synthesis of 5-(4-nitrophenoxy) isophthalic acid.

### (ii) Synthesis of 5-(4-nitrophenoxy) isophthalic acid (NEDA)

To a 500 mL three necked round bottom flask equipped with a thermo-well, a reflux condenser and a mechanical stirrer was added 20.0 g (82.20 mmol) 1,3-dimethyl-5-(4-nitrophenoxy)benzene, 65 mL water and 140 mL pyridine and the solution was heated to reflux. To this solution 85 g (552.5 mmol) solid $KMnO_4$ was added at a slow rate with stirring to maintain a slow reflux. Water was added occasionally to replace the loss by evaporation and to wash down the permanganate. The solution was then refluxed for 12 h. After the refluxing, 85 mL of methanol was added to the reaction mixture to destroy excess permanganate. The $MnO_2$ was suction filtered while hot and washed with boiling water. Filtrate and washings were combined and the pyridine was removed by vacuum distillation. After cooling, the solution was acidified with concentrated HCl and the precipitate obtained was filtered and washed with water several times. The diacid obtained was again dissolved in aqueous sodium carbonate solution, treated with charcoal, filtered and acidified with HCl. The precipitated solid was dried at 80 °C under vacuum and recrystallized from acetic acid.

Yield: 21.2 g (85%)    Melting Point: 258 – 260 °C.

FT-IR (KBr, cm$^{-1}$): 1689 (C=O); 1520, 1349 (-NO$_2$ stretching); 1234, 1102 (-C-O-C-stretching); 1583, 1487 (aromatic) (Figure 2.4).

$^1$H NMR [200 MHz, DMSO-d$_6$, $\delta$ ppm] showed signals of different protons at $\delta$ values of 8.35 (T, 1H, H$_a$); 8.30 (d, 2H, H$_b$); 7.86 (d, 2H, H$_c$); 7.28 (d, 2H, H$_d$) (Figure 2.5).

$^{13}$C NMR [400 MHz, DMSO-d$_6$,δ, ppm] showed values at 166.16, 162.19, 155.30, 143.44, 134.06, 126.86, 126.62, 124.81 and 118.80 (Figure 2.6).

| Elemental analysis: | C% | H% | N% |
|---|---|---|---|
| C$_{14}$H$_9$NO$_7$ | | | |
| Calculated: | 55.45% | 2.99% | 4.61% |
| Observed: | 55.05% | 2.77% | 4.55% |

**2.2.3.2 Synthesis of 5-(4-aminophenoxy) isophthalic acid hydrochloride (AEDA)**

A solution of 10 g (32.97 mmol) 5-(4-nitrophenoxy) isophthalic acid in 100 mL methanol in a Parr autoclave was stirred with 0.2g of 5 % Pd/C catalyst at 70 °C under 800 psi hydrogen pressure for 5h. When the absorption of hydrogen was complete, the solution was filtered to remove the catalyst and the product was recovered by removing methanol completely under vacuum. The product was dissolved in 150 mL boiling 1:1 water/HCl, treated with activated charcoal and the solution was filtered. 50 mL of concentrated HCl was added to the filtrate and kept overnight at room temperature. White color crystals formed were filtered and dried at 90 °C under vacuum for 12 h.

Yield: 7.2 g (70 %)   Melting Point: above 300 °C (decompose)
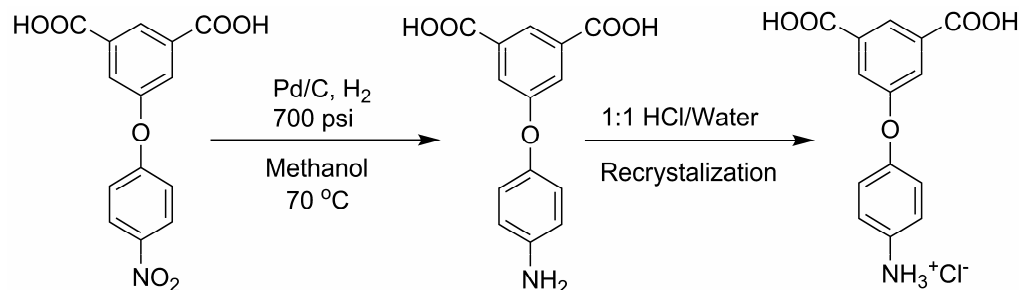


**Scheme 2.2** Synthesis of 5-(4-aminophenoxy) isophthalic acid hydrochloride.

FT-IR (KBr, cm$^{-1}$): 1692 (C=O); 3395 (N–H stretching); 1609 (N–H deformation); 1225, 1100(-C-O-C- stretching); 1584, 1498 (aromatic) (Figure 2.7).

$^1$H NMR [200 MHz, DMSO-d$_6$, δ ppm] showed signals of different protons at δ values of 8.24 (t, 1H, H$_a$); 7.69 (d, 2H, H$_b$); 7.50 (d, 2H, H$_c$); 7.29(d, 2H, H$_d$) (Figure 2.8).

$^{13}$C NMR [400 MHz, DMSO-d$_6$,δ, ppm] showed values at 165.83, 157.16, 154.80, 133.14, 128.19, 125.30, 124.72, 122.70 and 120.77. (Figure 2.9)

| Elemental analysis: | C% | H% | N% |
|---|---|---|---|
| C$_{14}$H$_{12}$ClNO$_5$ | | | |
| Calculated: | 54.29% | 3.91% | 4.52%. |
| Observed: | 53.91% | 3.71% | 4.16% |

### 2.2.4 Synthesis of model compound, 4-(3,5-di(1H-benzo[dimidazol-2- yl]phenoxy) aniline

To a 50 mL three necked round bottom flask equipped with a mechanical stirrer, nitrogen gas inlet and a guard tube was added 0.572 g (4.53 mmol) ortho phenylene diamine and 20 g of polyphosphoric acid and the mixture was heated to 140 °C with stirring under a stream of nitrogen. After the complete dissolution of ortho phenylene diamine, 0.700 g (2.265 mmol) of 5-(4-aminophenoxy) isophthalic acid hydrochloride was added slowly with stirring and the temperature of reaction mixture was raised to 160 °C. The diacid dissolved in 2 h giving homogeneous solution. The solution was then heated to 200 °C and maintained at this temperature for 6 h.
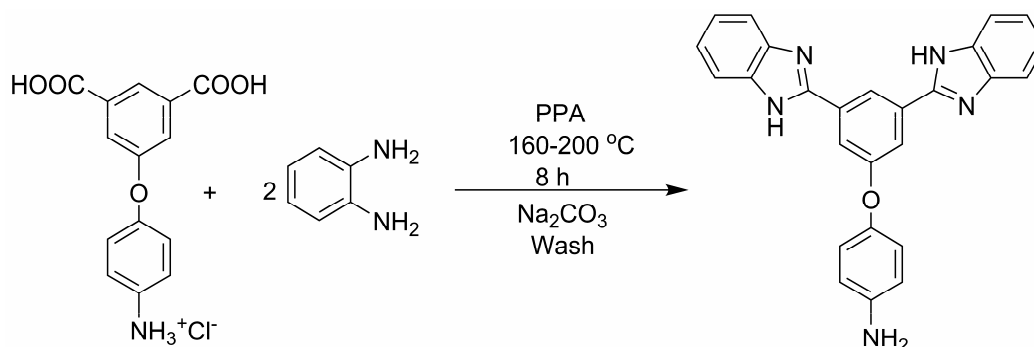


**Scheme 2.3** Synthesis of model compound 4-(3,5-di(1H-benzo[d]imidazol-2-yl)phenoxy) aniline.

The resulting viscous solution was cooled and poured into 200 mL water to precipitate the compound. The compound was filtered, washed repeatedly with water and stirred in 10% Na$_2$CO$_3$ solution for 2 h to eliminate residual phosphoric acid. The compound was filtered and again washed with water to neutrality and dried. It was recrystallized from methanol, filtered and dried at 100 °C for 24 h. A yellowish compound was obtained.

Yield: 0.910 g (95 %), Melting Point: sublime above 300 °**C**.

FT-IR (KBr, cm$^{-1}$): 1618 (C=N); 3395 (N–H stretching); 1609 (N–H deformation); 1225-1109 (-C-O-C stretching); 1584, 1498 (aromatic) (Figure 2.10).

^{1}H NMR [200 MHz, DMSO-d[6], δ ppm] showed signals of different protons at δ values of 13.16 (s, 2H,Ha); 8.73 (s, 1H, H[b]); 7.81 (d, 2H, H[c]); 7.70 (d, 2H, H[d]); 7.55 (d, 2H,H[e]); 7.26 (m, 4H, H[f]); 6.94 (d, 2H, H[g]); 6.72 (d, 2H, H[h]); 5.16 (s, 2H, H[i]); 3.39 (s, 4H, H[j]) (Figure 2.11).

^{13}C NMR [400 MHz, DMSO-d[6], δ ppm] showed values at 160.08, 150.57, 145.95, 145.12, 132.44, 122.42, 121.28, 118.30, 115.35 and 115.14 (Figure 2.12).

| **Elemental analysis:** | C% | H% | N% |
|---|---|---|---|
| **C$_{26}$H$_{19}$N$_5$O** | | | |
| Calculated: | 68.86% | 5.11% | 15.40 |
| Observed: | 68.47% | 4.86% | 15.43% |

### 2.2.5    Synthesis of new substituted homo and co-polybenzimidazoles

Polybenzimidazoles containing nitrophenoxy and amino phenoxy groups were synthesized by condensing 3,3',4,4,'-tetra amino biphenyl (TAB) with NEDA and AEDA (Scheme 2.4 and 2.6). Co-polybenzimidazoles having nitro group were synthesized by condensing TAB with a mixture of NEDA **a**nd other diacids namely 1) isophthalic acid 2) adipic acid 3) sebacic acid 4) 2,5-pyridine dicarboxylic acid and 5) terephthalic acid (scheme 2.5). Similarly co-polybenzimidazoles having amino groups were synthesized by condensing TAB with a mixture of AEDA and other diacids mentioned above (scheme 2.7) by using high temperature solution polycondensation technique in polyphosphoric acid. A typical procedure for high temperature solution polycondensation is described below.

### 2.2.5.1 Synthesis of polybenzimidazole having pendant nitro groups

A 100 mL three necked round bottom flask, equipped with a mechanical stirrer, nitrogen gas inlet and a guard tube, was charged with 2.0 g (9.334 mmol) of TAB and 80 g of PPA and the mixture was heated to 140 °C with stirring under a stream of nitrogen. After the complete dissolution of TAB, 2.830 g (9.334 mmol) of 5-(4-nitrophenoxy) isophthalic acid (NEDA) was added slowly with stirring and the temperature of the reaction mixture was raised to 170 °C. The diacid dissolved in 5 h giving homogeneous solution. The solution was then heated to 190 °C and maintained at this temperature for 4 h. The resulting viscous solution was cooled and poured into 500 mL water to precipitate the polymer as fiber. The

polymer was filtered, washed repeatedly with water and stirred in 10% aqueous $Na_2CO_3$ solution overnight to eliminate residual phosphoric acid.
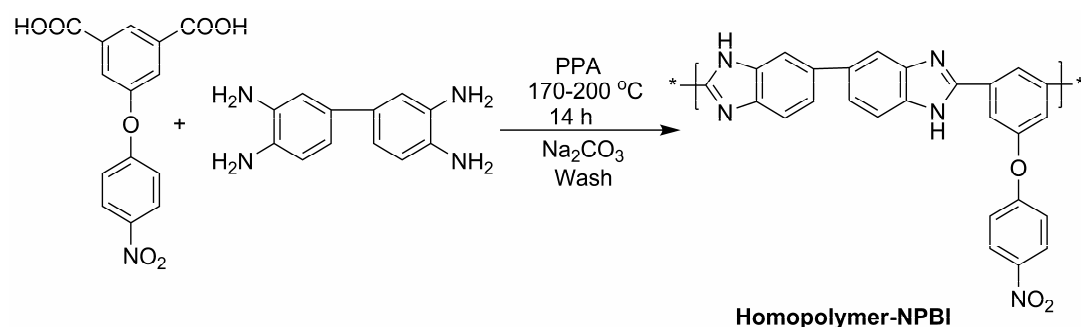


**Scheme 2.4** Synthesis of polybenzimidazole from 5-(4-nitrophenoxy) isophthalic acid.

The polymer was washed again with water repeatedly to neutrality and heated in boiling water for 6 h, three times. The polymer was dried at 100 °C for 24 h and 150 °C for another 24 h in vacuum oven. A brown fibrous polymer was obtained. Yield of the polymer was 96%. The inherent viscosity of this polymer at 0.5 g.dL$^{-1}$ conc. measured in DMAc at 30 °C was 0.75 dL.g$^{-1}$.

FT-IR (film, cm$^{-1}$): 1618 (C=N); 3395 (N–H stretching); 1609 (N–H deformation); 1520, 1349 (-NO$_2$ stretching); 1220, 1110 (-C-O-C- stretching); 1584, 1498 (aromatic) (Figure 2.13).

$^1$H NMR [400 MHz, DMSO-d$_6$, δppm] showed signals of different protons at δ values of 13.16 (s, 2H, H$_a$); 8.81 (s, 1H, H$_b$); 8.04-7.66 (m, 8H, H$_{c-f}$); 7.01 (d, 2H, H$_g$); 6.74 (d, 2H, H$_h$); 5.18 (s, 2H, H$_i$) (Figure 2.17)

| **Elemental analysis:** | C% | H% | N% |
|---|---|---|---|
| **C$_{26}$H$_{15}$N$_5$O$_3$** | | | |
| Calculated: | 70.11% | 3.39% | 15.72% |
| Observed: | 69.30% | 3.17% | 15.06% |

**2.2.5.2 Synthesis of co-polybenzimidazoles having pendant nitro groups with different diacids**

➢ **Synthesis of copolybenzimidazole NPBI-1 (NEDA 90%: IPA 10%)**

A 100 mL three necked round bottom flask, equipped with a mechanical stirrer, nitrogen gas inlet and a guard tube, was charged with 2.0 g (9.334 mmol) TAB and 80 g of polyphosphoric acid and the mixture was heated to 140 °C with stirring under a stream of nitrogen. After the complete dissolution of TAB, 2.547 g (8.400 mmol) of 5-(4-nitrophenoxy) isophthalic acid (NEDA) and 0.155 g (0.934 mmol) isophthalic acid was added slowly with stirring. A homogeneous solution was obtained after 5 h, when the reaction mixture temperature was raised to 170 °C. Afterwards the solution was heated to 200 °C and maintained at this temperature for 5 h. The resulting viscous solution was then cooled and poured into 500 mL water to precipitate the polymer as fiber. The polymer was filtered, washed repeatedly with water and stirred with 10% aqueous $Na_2CO_3$ solution overnight to eliminate residual phosphoric acid. The polymer was again washed with water repeatedly to neutrality and heated in boiling water for 6 h, three times. The polymer was dried at 100 °C for 24 h and 150 °C for another 24 h in vacuum oven. A brown fibrous polymer was obtained. Yield of the polymer was 98%. The inherent viscosity of this polymer, at 0.5 g.dL$^{-1}$ concentration, measured in DMAc at 30 °C, was 0.95 dL.g$^{-1}$. The ratio of 5-(4-nitrophenoxy) isophthalic acid (NEDA) and isophthalic acid (IPA) in this co-polybenzimidazole is 90:10 mol%.

Following co-polybenzimidazoles of NEDA and other diacids in different ratio (mentioned in bracket) with TAB were prepared following similar procedure.

**NPBI-2** was synthesized as a reddish brown fiber in 96% yield by condensing 70:30 mole ratio of NEDA and isophthalic acid with TAB ($\eta_{inh}$ – 1.10 dL.g$^{-1}$ in DMAc).

**NPBI-3** was synthesized as a yellowish brown fiber in 98% yield by condensing 50:50 mole ratio of NEDA and isophthalic acid with TAB ($\eta_{inh}$ – 0.99 dL.g$^{-1}$ in DMAc).

**NPBI-4** was synthesized as a yellowish fiber in 97% yield by condensing 30:70 mole ratio of NEDA and isophthalic acid with TAB ($\eta_{inh}$ – 1.40 dL.g$^{-1}$ in DMAc).

**NPBI-5** was synthesized as a yellowish fiber in 98% yield by reacting 10:90 mole ratio of NEDA and isophthalic acid with TAB ($\eta_{inh}$ – 1.01 dL.g$^{-1}$ in DMAc).

**NPBI-6** was synthesized as a blackish brown fiber in 90% yield by condensing 50:50 mole ratio of NEDA and adipic acid with TAB (gives insoluble polymer).

**NPBI-7** was synthesized as a brown fiber in 92% yield by condensing 50:50 mole ratio of NEDA and sebacic acid with TAB (gives insoluble polymer).

**NPBI-8** was synthesized as a yellowish fiber in 95% yield by condensing 50:50 mole ratio NEDA and pyridine-2, 6-dicarboxylic acid with TAB ($\eta_{inh}$ – 0.82 dL.g.$^{-1}$ in DMAc).

**NPBI-9** was synthesized as a brown fiber in 98% yield by condensing 50:50 mole ratio of NEDA and terephthalic acid with TAB ($\eta_{inh}$ – 1.15 dL.g.$^{-1}$ in DMAc).
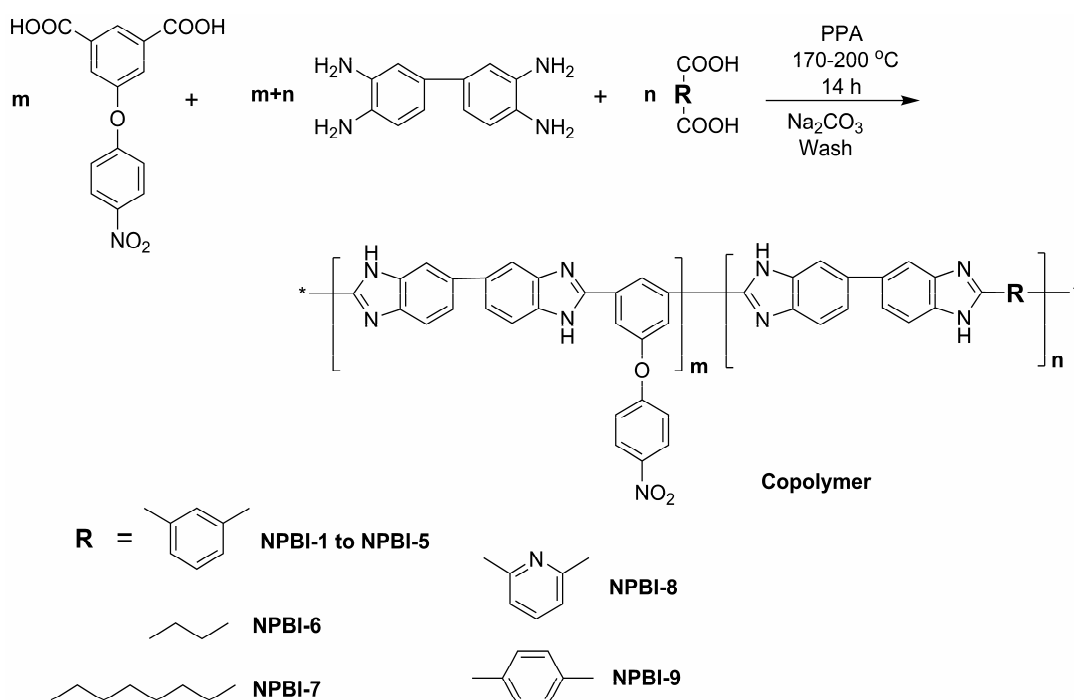


**Scheme 2.5** Synthesis of Co-polybenzimidazoles from 5-(4-nitrophenoxy) isophthalic acid and other diacids.

### 2.2.5.3 Synthesis of polybenzimidazole having free amino groups

A 100 mL three necked round bottom flask, equipped with a mechanical stirrer, nitrogen gas inlet and a guard tube, was charged with 2.5 g (11.667 mmol) 3,3',4,4,'-tetra amino biphenyl (TAB) and 100 g of polyphosphoric acid and the mixture was heated to 140

°C with stirring under a stream of nitrogen. After the complete dissolution of TAB, 3.603 g (11.667 mmol) of 5-(4-aminophenoxy) isophthalic acid hydrochloride (AEDA) was added slowly with stirring and the temperature of the reaction mixture was raised to 170 °C. The diacid dissolved in 2 h giving homogeneous solution. The solution was then heated to 200 °C and maintained at this temperature for 12 h. The resulting viscous solution was then cooled and poured into 500 mL water to precipitate the polymer as fiber. The polymer was then filtered, washed repeatedly with water and stirred in 10% aqueous $Na_2CO_3$ solution overnight to eliminate residual phosphoric acid. The polymer was washed repeatedly with water to neutrality and heated in boiling water for 6 h, three times. The polymer was dried at 100 °C for 24 h and 150 °C for another 24 h in vacuum oven. A brown fibrous polymer was obtained. Yield of the polymer was 97%. The inherent viscosity of this polymer at 0.5 g.dL$^{-1}$ conc. measured in DMAc at 30 °C was 1.2dL.g$^{-1}$.



**Scheme 2.6** Synthesis of polybenzimidazole from 5-(4-aminophenoxy) isophthalic acid hydrochloride.

FT-IR (film, cm$^{-1}$): 1618 (C=N); 3395 (N–H stretching); 1609 (N–H deformation); 1222-1010 (-C-O-C- stretching); 1584, 1498 (aromatic) (Figure 2.28).

$^1$H NMR [400 MHz, DMSO-d$_6$, δ ppm] showed signals of different protons at δ values of 13.16 (s, 2H, Ha); 8.81 (s, 1H, H$_b$); 8.04-7.66 (m, 8H, H$_{c-f}$); 7.01 (d, 2H, H$_g$); 6.74 (d, 2H, H$_h$); 5.18 (s, 2H, H$_i$) (Figure 2.31).

| **Elemental analysis**: | C% | H% | N% |
|---|---|---|---|
| **C$_{26}$H$_{17}$N$_5$O** | | | |
| Calculated: | 75.16% | 4.91% | 16.23% |
| Observed: | 73.91% | 5.17% | 15.66% |

**2.2.5.4 Synthesis of copolybenzimidazole having free amino groups with different diacids**

  ➢ **Synthesis of copolybenzimidazoles APBI-1 (AEDA 90%: IPA 10%)**

A 100 mL three necked round bottom flask, equipped with a mechanical stirrer, nitrogen gas inlet and a guard tube, was charged with 2.5 g (11.67 mmol) TAB and 100 g of polyphosphoric acid and the mixture was heated at 140 ℃ with stirring under a stream of nitrogen. After the complete dissolution of TAB, 3.242 g (10.50 mmol) of 5-(4-aminophenoxy) isophthalic acid hydrochloride (AEDA) and 0.193 g (1.167 mmol) IPA were added slowly with stirring. A homogeneous solution was obtained after 5 h, when the temperature of reaction mixture was raised to 170 °C. The solution was heated to 200 ℃ and maintained at this temperature for 12 h. The resulting viscous solution was then cooled and poured into 500 mL water to precipitate the polymer as fiber. The polymer was then filtered, washed repeatedly with water and stirred with 10% aqueous $Na_2CO_3$ solution overnight to eliminate residual phosphoric acid. The polymer was washed repeatedly with water to neutrality and heated in boiling water for 6 h, three times. The purified polymer was dried at 100 ℃ for 24 h and 150 ℃ for another 24 h in vacuum oven. A brown fibrous polymer was obtained. Yield of the polymer was 97%. The inherent viscosity of this polymer, at 0.5 g.dL$^{-1}$ concentrations, measured in DMAc at 30 ℃, was 1.12dL.g$^{-1}$. The ratio of AEDA and IPA in this co-polybenzimidazole is 90:10 mol%.

Following co-polybenzimidazoles of AEDA and other diacids in different ratio with TAB were prepared following similar procedure.

**APBI-2** was synthesized as a reddish brown fiber in 96% yield by condensing 70:30 mole ratio of AEDA and IPA with TAB ($\eta_{inh}$ – 1.29 dL.g$^{-1}$ in DMAc).

**APBI-3** was synthesized as a yellowish brown fiber in 98% yield by condensing 50:50 mole ratio of AEDA and IPA with TAB ($\eta_{inh}$ -1.36 dL.g$^{-1}$ in DMAc).

**APBI-4** was synthesized as a yellowish fiber in 97% yield by condensing 30:70 mole ratio of AEDA and IPA with TAB ($\eta_{inh}$ – 1.23 dL.g$^{-1}$ in DMAc).

**APBI-5** was synthesized as a yellowish fiber in 98% yield by condensing 10:90 mole ratio of AEDA and IPA with TAB ($\eta_{inh}$ – 1.49 dL.g$^{-1}$ in DMAc).

**APBI-6** was synthesized as a blackish brown fiber in 90% yield by condensing 50:50 mole ratio of AEDA and adipic acid with TAB ($\eta_{inh}$ – 0.62 dL.g$^{-1}$ in DMAc).
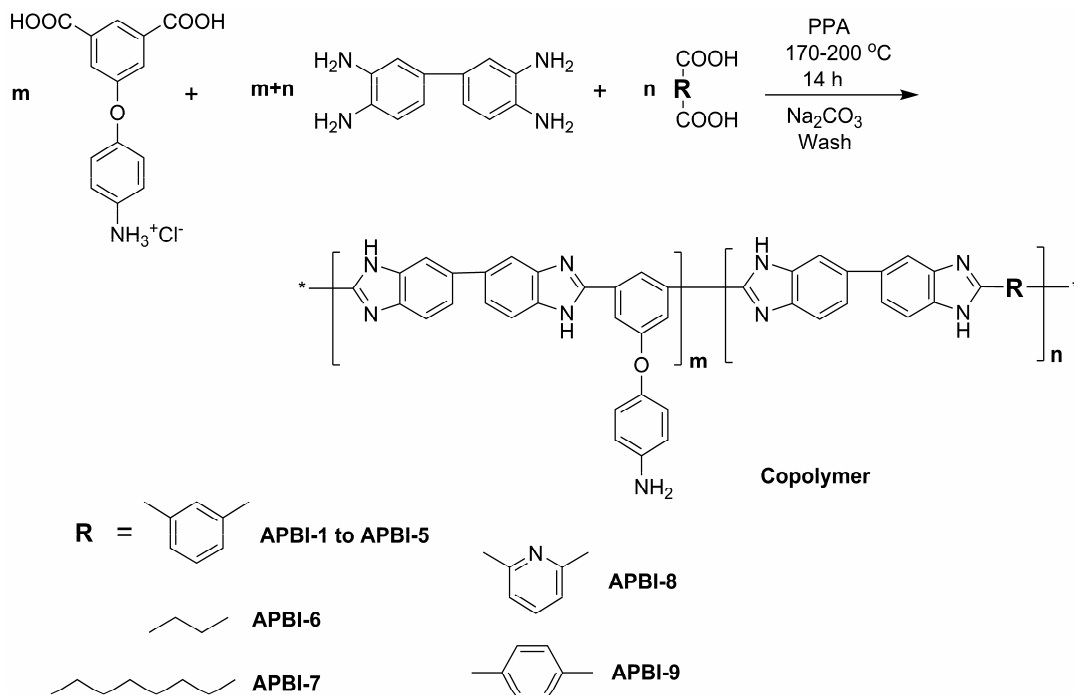


**Scheme 2.7** Synthesis of Co-polybenzimidazoles from 5-(4-aminophenoxy) isophthalic acid hydrochloride and other diacids.

**APBI-7** was synthesized as a brown fiber in 92% yield by condensing 50:50 mole ratio of AEDA and sebacic acid with TAB ($\eta_{inh}$ – 0.72 dL.g$^{-1}$ in DMAc).

**APBI-8** was synthesized as a yellowish fiber in 95% yield by condensing 50:50 mole ratio of AEDA and pyridine-2, 6-dicarboxylic acid with TAB ($\eta_{inh}$ – 0.82 dL.g.$^{-1}$ in DMAc).

**APBI-9** was synthesized as a brown fiber in 98% yield by condensing 50:50 mole ratio of AEDA and terephthalic acid with TAB ($\eta_{inh}$ –1.52 dL.g.$^{-1}$ in DMAc).

### 2.2.5.5 Membrane preparation

Polymer membranes of 90-100 μm thickness, used for mechanical properties study, proton conductivity measurement and fuel cell studies were obtained by solution casting method. Three percent solution of polymer was prepared in DMAc and the solution was filtered through a 10 μm filter to remove any particulates. The clear polymer solution was poured into a clean Petri dish (diameter 7.5 cm). The DMAc was evaporated slowly in a

leveled oven at 80 °C for 15 h. The films were removed and were heated in boiling distilled water for 6 h to remove the traces of DMAc solvent and subsequently dried at 150 °C for two days under reduced pressure.

## 2.3  Results and discussion

### 2.3.1    Synthesis and characterization of monomers
### 2.3.1.1 Synthesis and characterization of 5-(4-nitrophenoxy) isophthalic acid (NEDA)

A detailed procedure for the synthesis and purification of NEDA and intermediate compound, 1,3 dimethyl-5-(-4 nitro phenoxy)benzene, is described in experimental part. This diacid was synthesized from 3,5 dimethyl phenol and 1-chloro 4-nitrobenzene in two steps (Scheme 2.1). In the first step 1,3 dimethyl-5-(-4 nitro phenoxy)benzene was synthesized by the reaction of 3,5 dimethyl phenol with 1-chloro-4-nitrobenzene in dimethyl formamide (DMF) at 120 °C for 12 h using $K_2CO_3$ as acid acceptor. The product obtained was purified by recrystallization from petroleum ether and ethyl acetate in ratio 8:2. The chemical structure of intermediates and final compounds was confirmed by elemental analysis, FT-IR, ^{1}H NMR and ^{13}C NMR spectroscopy. The elemental analysis values were found to be in good agreement with the calculated values.
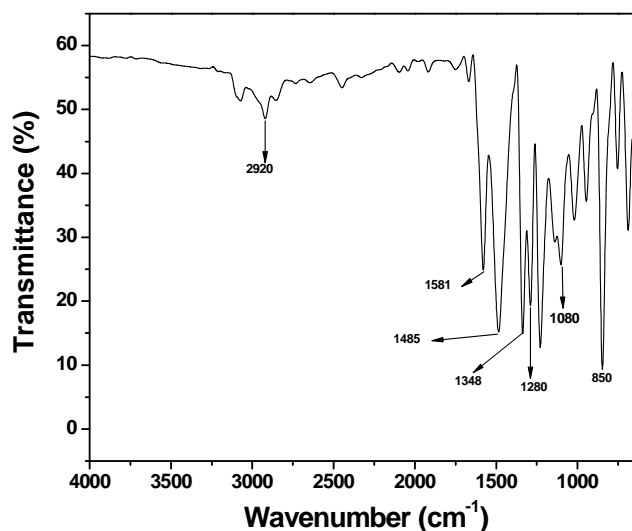


**Figure 2.1**  FTIR spectrum of 1,3 dimethyl-5-(-4 nitro phenoxy)benzene.

FT-IR spectrum of 1,3 dimethyl-5-(-4 nitro phenoxy)benzene (Figure 2.1) showed absorption bands at 1532 and 1344 cm$^{-1}$ due to asymmetric and symmetric $-NO_2$ stretching

vibrations. The bands at 1280 and 1070 cm$^{-1}$ are due to –C-O-C- asymmetric and symmetric stretching vibrations. The band at 850 cm$^{-1}$ is due to the aromatic –C-N stretching vibration.

$^1$H NMR spectrum of 1,3 dimethyl-5-(-4 nitro phenoxy)benzene (Figure 2.2) showed signal at 2.64 δ ppm corresponding to the six protons of –CH$_3$, attached to the aromatic ring, in addition to signals corresponding to aromatic protons in the region 6.87-8.93 δ ppm with expected multiplicity and integration equivalent to seven protons.
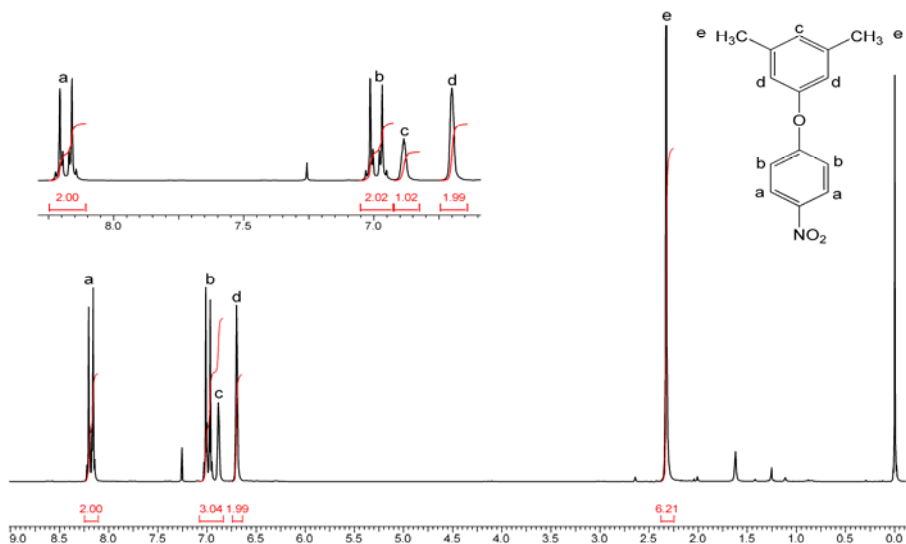


**Figure 2.2** $^1$H NMR spectrum of 1,3 dimethyl-5-(-4 nitro phenoxy)benzene.
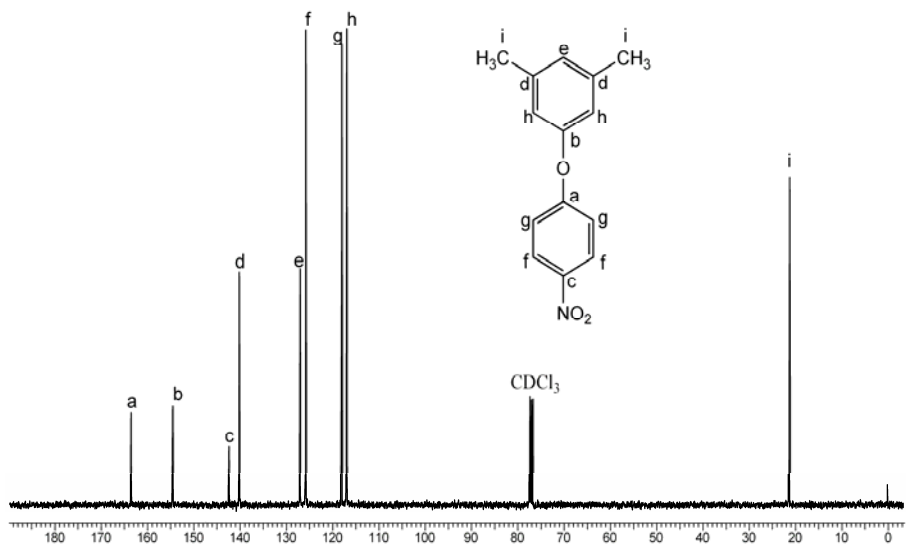


**Figure 2.3** $^{13}$C NMR spectrum of 1,3 dimethyl-5-(-4 nitro phenoxy)benzene.

The $^{13}$C NMR spectrum of 1,3 dimethyl-5-(-4 nitro phenoxy)benzene showed δ ppm values corresponding to 13 carbon atoms and were in good agreement with the proposed structure. Aromatic carbons in the range of 117–163 δ ppm and two carbons of methyl groups appear at 21.26 δ ppm (Figure 2.3).       Thus, elemental and spectral analysis confirm the structure of 1,3 dimethyl-5-(-4 nitro phenoxy)benzene.

In the second step, 5-(4-nitrophenoxy) isophthalic acid was synthesized by the oxidation of 1,3 dimethyl-5-(-4 nitro phenoxy) benzene using aqueous KMnO$_4$-pyridine. In the oxidation step, excess KMnO$_4$ was added to ensure complete oxidation of the methyl groups (upto the point till the color of the solution did not fade on refluxing). This helped in improving the yield and purity of diacid, which in turn helped in increasing the molecular weight of polymer. The compound, 5-(4-nitrophenoxy) isophthalic acid, was purified by crystallization from acetic acid. The chemical structure of the compound was confirmed by means of elemental analysis, FT-IR, $^1$H NMR and $^{13}$C NMR spectroscopy.
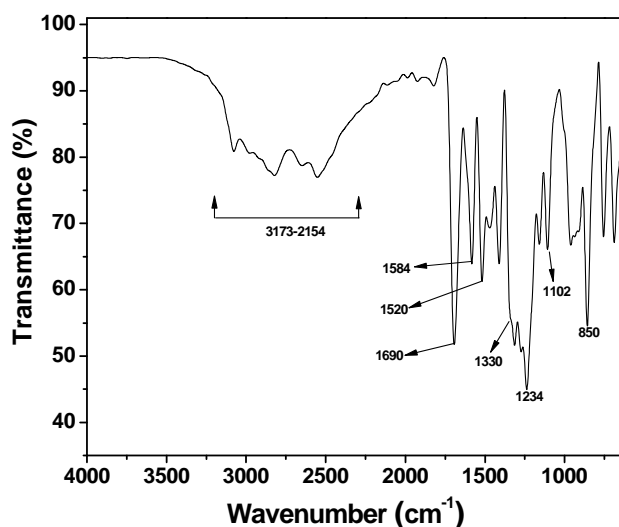


**Figure 2.4**  FTIR spectrum of 5-(4-nitrophenoxy) isophthalic acid.

FT-IR spectrum of 5-(4-nitrophenoxy) isophthalic acid (Figure 2.4) showed new broad absorption bands in the region 2524-3017 cm$^{-1}$ due to hydrogen bonded –OH of carboxyl groups and at 1690 cm$^{-1}$ due to C=O of carboxyl group along with the bands at 1520 and 1330 cm$^{-1}$ due to asymmetric and symmetric –NO$_2$ stretching vibrations. The bands at 1250 and 1090 cm$^{-1}$ are due to –C-O-C- asymmetric and symmetric stretching vibrations. The band at 850 cm$^{-1}$ is due to the aromatic –C-N stretching vibration.
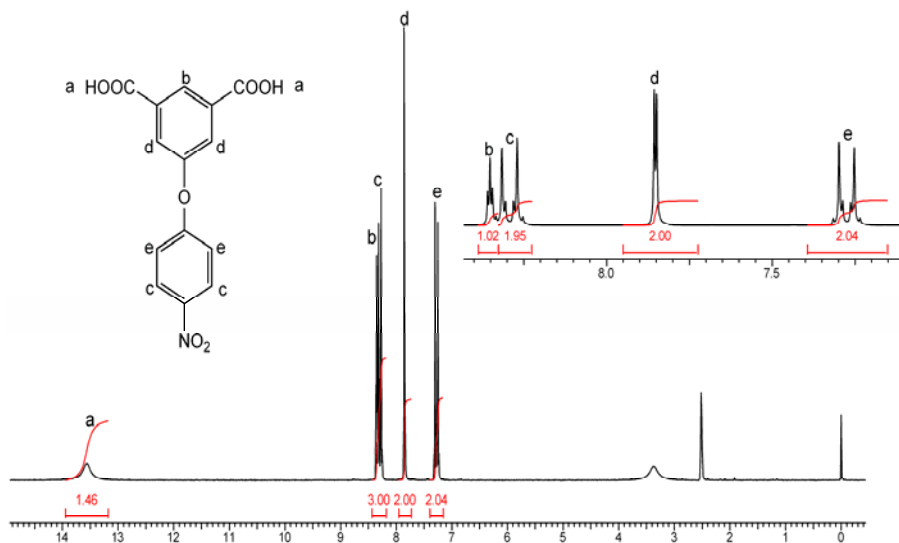
**Figure 2.5** $^1$H NMR spectrum of 5-(4-nitrophenoxy) isophthalic acid.

$^1$H NMR spectrum of 5-(4-nitrophenoxy) isophthalic acid (Figure 2.5) shows aromatic protons in the region of 7.25–8.35 δ ppm with expected multiples and integration and absence of methyl protons. $^{13}$C NMR spectrum of 5-(4-nitrophenoxy) isophthalic acid (Figure 2.6) shows aromatic carbons at 118–167 δ ppm as expected and methyl carbons at 21.26 δ ppm disappear and carbons of carboxyl group appeared as a single peak at 166.16 δ ppm.

Thus, elemental and spectral analyses confirm the structure of 5-(4-nitrophenoxy) isophthalic acid.
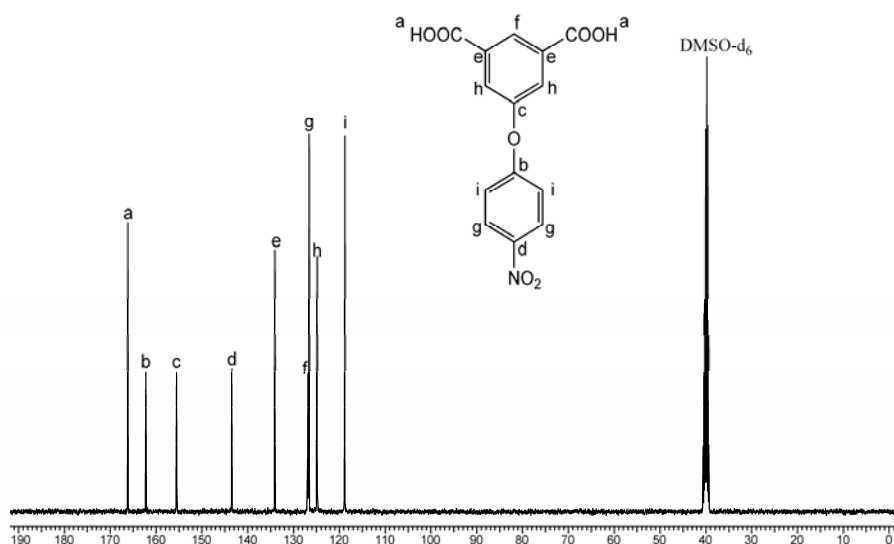


**Figure 2.6** $^{13}$C NMR spectrum of 5-(4-nitrophenoxy) isophthalic acid.

**2.3.1.2 Synthesis of 5-(4-aminophenoxy) isophthalic acid hydrochloride (AEDA)**

The 5-(4-aminophenoxy) isophthalic acid was synthesized by catalytic hydrogenation of 5-(4-nitrophenoxy) isophthalic acid in methanol using Pd/C and hydrogen in Parr pressure reactor as described in experimental part. The resulting diacid was crystallized from 1:1 water/HCl mixture. It was observed that, the crystallization from methanol, failed to give high molecular weight PBI on condensation with TAB, probably, due to oxidation of amino group. The amine group in this compound is prone to oxidation and hence it was recrystallized as hydrochloride from 1:1 water/HCl mixture.

The FT-IR spectrum of 5-(4-aminophenoxy) isophthalic acid hydrochloride (Figure 2.7) showed absorptions bands in the region 2524-3017 due to hydrogen bonded –OH of carboxyl group and a strong band at 1700 cm$^{-1}$ due to C=O of carboxyl group. A new absorption bands at 3395 cm$^{-1}$ due to N–H stretching is observed and the bands at 1520 and 1349 cm$^{-1}$ of $NO_2$ group of NEDA disappeared. An absorption band at 1225 cm$^{-1}$ is due to ether linkage present in the compound.
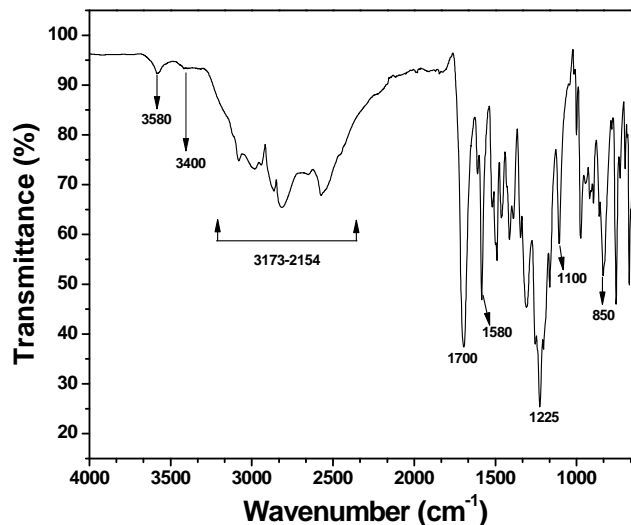


**Figure 2.7** FT-IR spectrum of 5-(4-aminophenoxy) isophthalic acid hydrochloride.
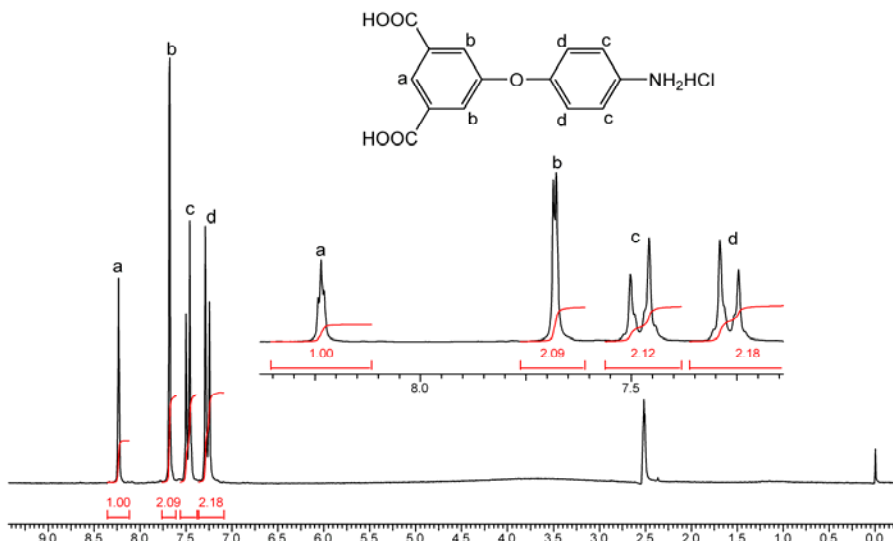
**Figure 2.8** $^1$H NMR spectrum of 5-(4-aminophenoxy) isophthalic acid hydrochloride.

In $^1$H NMR, the aromatic protons of 5-(4-aminophenoxy) isophthalic acid hydrochloride shifted to downfield since it is in hydrochloride form. Aromatic protons in the region 7.25–8.25 δ ppm showed the expected multiplicity and integration values as shown (Figure 2.8) $^{13}$C NMR spectrum of 5-(4-aminophenoxy) isophthalic acid hydrochloride has δ-values close to that of nitro diacid compound since it is in hydrochloride form. Aromatic carbons observed in the region 120–166 δ showed the expected values as shown in (Figure 2.9). Thus, elemental and spectral analyses confirm the structure of 5-(4-aminophenoxy) isophthalic acid hydrochloride.
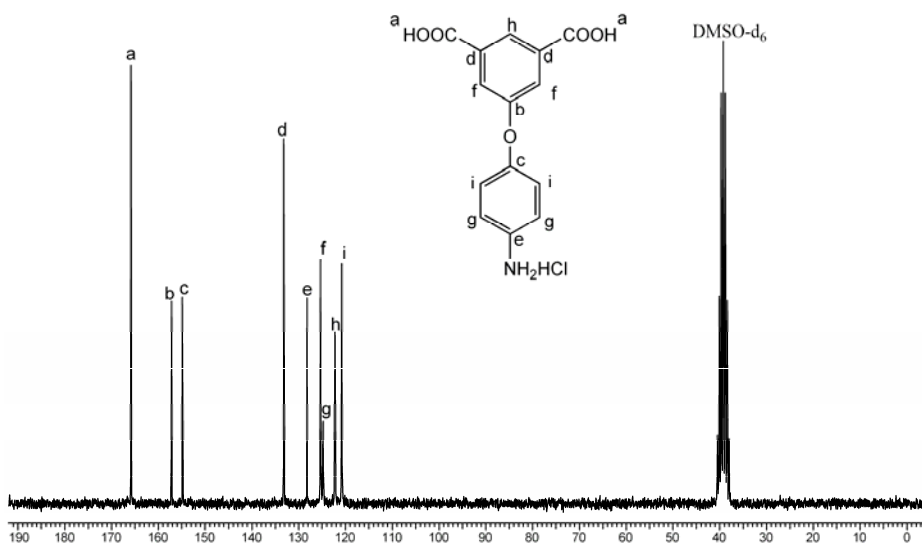


**Figure 2.9** $^{13}$C NMR spectrum of 5-(4-aminophenoxy) isophthalic acid hydrochloride.

**2.3.1.3 Synthesis and characterization of model compound of 5-(4-aminophenoxy) isophthalic acid with O- phenylene diamine**

The fate of formation of high molecular weight PBI of 5-(4-aminophenoxy) isophthalic acid hydrochloride with 3,3',4,4,'-tetra amino biphenyl without cross-linking depends on the reactivity of amino group in 5-(4-aminophenoxy) isophthalic acid hydrochloride with carboxyl groups. High reactivity of this amino group with carboxyl group comparable to amino groups in TAB during polymerization leads to cross-linked polymer.

Expected linear high molecular weight polymer can be obtained only if amino group in 5-(4-aminophenoxy) isophthalic acid hydrochloride does not react with carboxyl group during polymerization. The reactivity of amino group in 5-(4-aminophenoxy) isophthalic acid hydrochloride is expected to be low due to the presence of the electron withdrawing two-carboxyl groups in the molecule. To verify that the amino group in 3,5-(4-aminophenoxy) isophthalic acid hydrochloride does not take part during the reaction with TAB, a model compound namely, 4-(3,5-di(1H-benzo[d]imidazol-2-yl)phenoxy)aniline of 5-(4-aminophenoxy) isophthalic acid hydrochloride with O-phenylene diamine, was synthesized (Scheme 2.3) as described in the experimental part. The chemical structure of the model compound was established by elemental analysis, FT-IR, ^{1}H NMR and ^{13}C NMR.
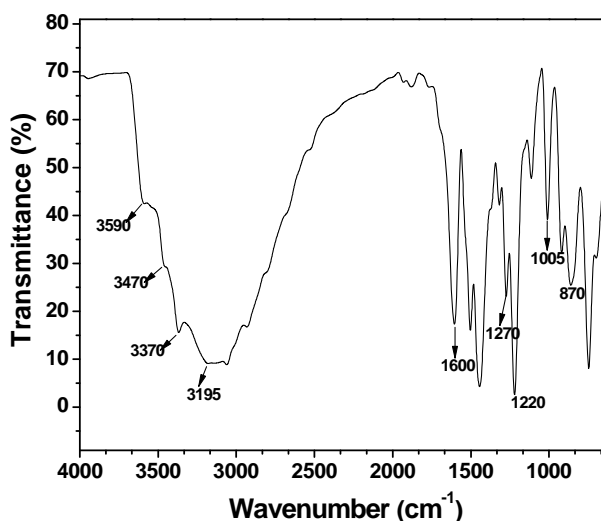


**Figure 2.10** FT-IR of model compound 4-(3,5-di(1H-benzo[d]imidazol-2-yl)phenoxy) aniline.

The C, H and N values of elemental analysis of the model compound match well with theoretical values as given in experimental part. The FT-IR spectrum of model compound

shows absorption bands at 3465 cm$^{-1}$ & 3376 cm$^{-1}$ due to N-H stretching which confirms the

presence of free NH$_2$ group, while band at 3585 cm$^{-1}$ indicates the NH group of imidazole ring

(Figure 2.10) The band due to breathing mode of imidazole ring, generally occurs at 1284 cm$^{-1}$

in polymer, is observed at 1277 cm$^{-1}$. Absorption at 1220 cm$^{-1}$ is due to ether linkage.
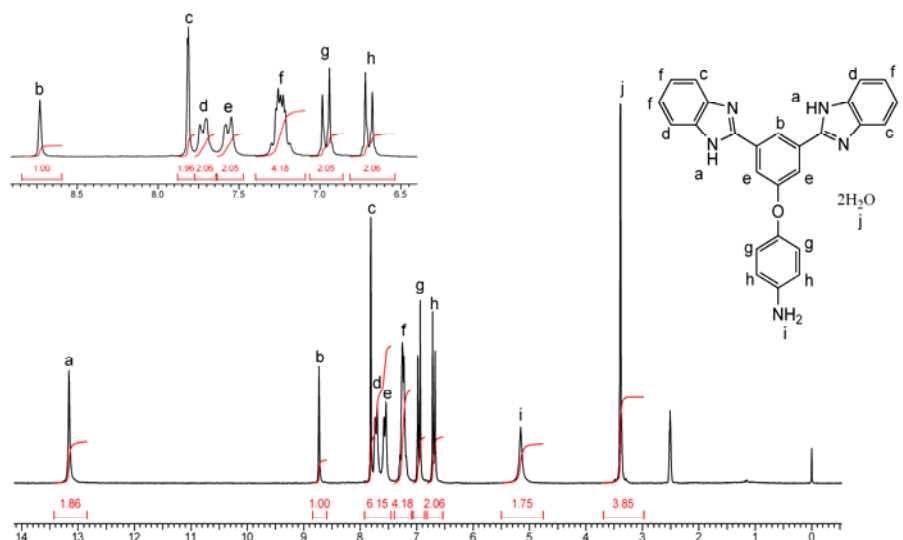


**Figure 2.11**  $^1$H NMR of model compound 4-(3,5-di(1H-benzo[d]imidazol-2-yl)phenoxy)
aniline.

$^1$H NMR confirmed the presence of free amino group and imidazole ring formation in

model compound. Two protons observed as a singlet at 13.16 δ and two protons at 5.16 δ

ppm are assigned to hydrogen's of N-H group of imidazole ring and hydrogen atoms of

aromatic amine respectively. Other aromatic protons appeared with expected multiplicities

and integration in the region at 6.6–8.8 δ ppm (Figure 2.11) and were consistent with the

expected chemical structure of the compound. The presence of four protons at 3.9 δ ppm was

due to the two molecules of water that may be taken by imidazole rings as water of

crystallization. The $^{13}$C NMR spectrum of model compound showed aromatic carbons in the

region at 115-161 δ ppm with expected values (Figure 2.12).

Thus, elemental analysis, FT-IR, $^1$H NMR, and $^{13}$C NMR fully substantiate the

expected chemical structure of benzimidazole derivative of 5-(4-aminophenoxy) isophthalic

acid, which has free amino group and imidazole rings.  Having confirmed that the carboxyl

groups in 5-(4-aminophenoxy) isophthalic acid react preferentially with amino groups of

ortho-phenylene diamine over amino group in the diacid, work was undertaken to synthesize

new polybenzimidazole and co-polybenzimidazoles containing pendant phenoxyamine groups by reacting AEDA with TAB.
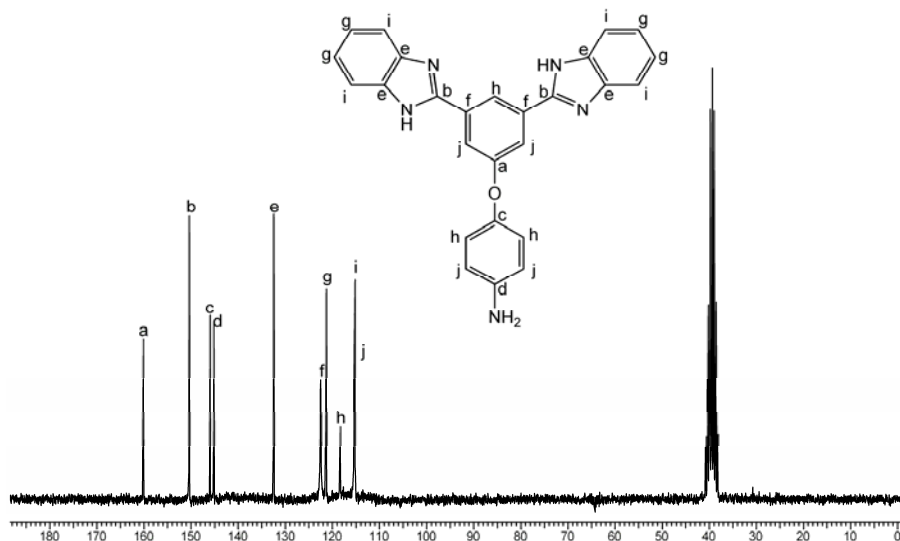


**Figure 2.12** $^{13}$C NMR of model compound 4-(3,5-di(1H-benzo[d]imidazol-2-yl)phenoxy)aniline.

### 2.3.2   Synthesis and structural characterization of polybenzimidazole and co-polybenzimidazole having pendant nitro groups

PBIs are generally synthesized by two methods (i) solid state polymerization at high temperature [28] or (ii) solution polymerization in polyphosphoric acid [29]. In the present work, solution polymerization method in polyphosphoric acid is adopted to synthesize PBIs. Homopolymer of 5-(4-nitrophenoxy) isophthalic acid (NEDA) with conventional TAB ( Scheme 2.4) and copolymers of TAB with a mixture of different mole ratios (90:10, 70:30, 50:50, 30:70 and 10:90) of NEDA and isophthalic acid were synthesized as detailed in experimental part, in order to study the effect of pendant nitrophenoxy content on properties of PBIs (Scheme-2.5).

To study structure-property relationships, few more new co-polybenzimidazoles containing nitrophenoxy pendant groups with structural variations were synthesized, by condensing TAB with a mixture of 5-(4-nitrophenoxy) isophthalic acid and commercially available aromatic diacids such as terephthalic acid, pyridine 2,6 dicarboxylic acid, adipic acid, and sebacic acid in 50:50 mole ratio. During the synthesis of homopolymer of NEDA, we observed that heating above 200 °C accelerates polymerization reaction rate forming a

rubbery material, which stops mechanical stirring within half an hour. The polymer obtained is insoluble in all solvents including $H_2SO_4$. To avoid this problem, the polymerization was conducted at 190-200 °C for 4 h. However, long time heating at this temperature also results in the insolubility of a polymer in the common organic solvents. Low molecular weight polymer is obtained below 190 °C. Therefore, it was concluded that, approximately 12 h stepwise heating is essential to form high molecular weight polymers. All co-polymers remained soluble in polyphosphoric acid without precipitation forming a viscous solution, which on pouring in water formed strong thread like structure. All these polymers have film-forming properties and they form transparent, tough film on casting from DMAc solution.

Inherent viscosity was determined in DMAc (0.5 g.dL$^{-1}$ concentration at 30 °C) using Ubbelhode viscometer. The inherent viscosities of these polymers were in the range of 0.75-1.4 dL.g$^{-1}$ (Table-2.1) indicating the polymers are of reasonably high molecular weights. All these polymers form tough and flexible films.

**Table 2.1** Inherent viscosity and film nature of nitro group containing   Polybenzimidazoles.

| Polymer Code | Diacids used (mole ratio %) | Inherent viscosity $\eta_{inh}$ (dL/g) | Film Color | Film Nature |
|---|---|---|---|---|
| **NPBI** | NEDA **100%** | 0.75 | Pale yellow | Flexible |
| **NPBI-1** | NEDA / IPA **90:10** | 0.95 | Light brown | Flexible |
| **NPBI-2** | NEDA / IPA **70:30** | 1.10 | Light brown | Flexible |
| **NPBI-3** | NEDA / IPA **50:50** | 0.99 | Yellowish | Flexible |
| **NPBI-4** | NEDA / IPA **30:70** | 1.40 | Yellowish | Flexible |
| **NPBI-5** | NEDA / IPA **10:90** | 1.01 | Yellowish | Flexible |
| **NPBI-6** | NEDA / AA **50:50** | ND | -- | -- |
| **NPBI-7** | NEDA / SA **50:50** | ND | -- | -- |
| **NPBI-8** | NEDA / PDA **50:50** | 0.82 | Yellowish | Flexible |
| **NPBI-9** | NEDA / TPA **50:50** | 1.15 | Light reddish | Flexible |

**NEDA:** 5-(4-nitrophenoxy) isophthalic acid, **IPA:** Isophthalic acid, **AA:** Adipic acid, **SA:** Sebacic acid, **PDA:** Pyridine dicarboxylic acid, **TPA:** Terephthalic acid, **ND:** not determined

The polymers, thus obtained, were characterized by FTIR and $^1$H NMR spectroscopy. IR spectra of all the polymers were scanned using thin films. The FT-IR spectra of NPBI, NPBI-1, NPBI-2, NPBI-3, NPBI-4, NPBI-5, and NPBI-8 & NPBI-9 were shown in Figure 2.13, 2.14 & Fig 2.15.
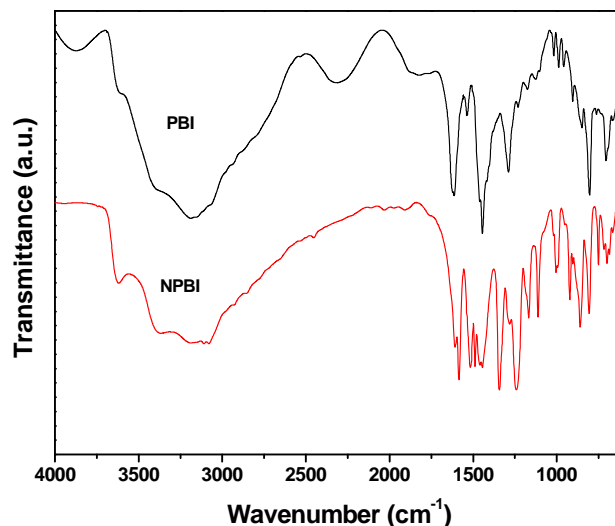
**Figure 2.13** FTIR spectrum of nitro group containing Polybenzimidazole compared with PBI.

The formation of polybenzimidazole ring was confirmed by the characteristic absorption band in the region at 1610-1623 cm$^{-1}$ due to C=N stretching of imidazole ring and another characteristic band in the range of 1284 -1288 cm$^{-1}$ of breathing mode of imidazole ring. Due to structural variations of these polymers these bands appear at different wavelength in the range mentioned above. The absorption at 1585 is due to the C-H of phenyl ring in the NEDA, which is present only in NPBIs and absent in PBI. Absorption band at 1340 & 1520 cm$^{-1}$ are due to free NO$_2$ groups. It is observed that, the intensity of bands at 1340 & 1520 cm$^{-1}$ (Figure 2.14) due to free nitro group decreases as percentage of NEDA in co-PBI series of IPA decreases from 100 to 10%. Absorption band at 860 cm$^{-1}$ corresponds to aromatic C–N stretching vibration of C–NO$_2$ group.
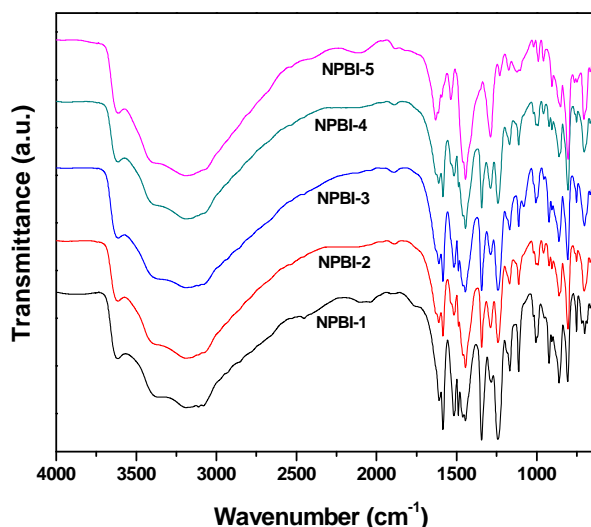


**Figure 2.14** FTIR spectrum of nitro group containing co-polybenzimidazoles of IPA.
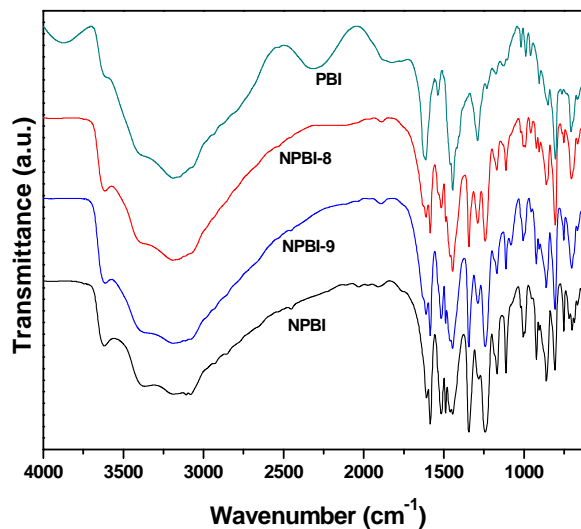
**Figure 2.15** FTIR spectrum of nitro group containing co-polybenzimidazoles compared with PBI.

Intensity of absorption band at 1240 cm$^{-1}$ due to C-O-C linkage was observed to decrease, as NEDA content in co-polymer decreased. Polybenzimidazole shows broad peak at 3395 – 3180 cm$^{-1}$ due to N-H groups which is assigned to self-associated N-H interaction of PBI chains. The absorption bands in this region due to the N-H groups could be distinctly seen in NPBI polymer (Figure 2.14).
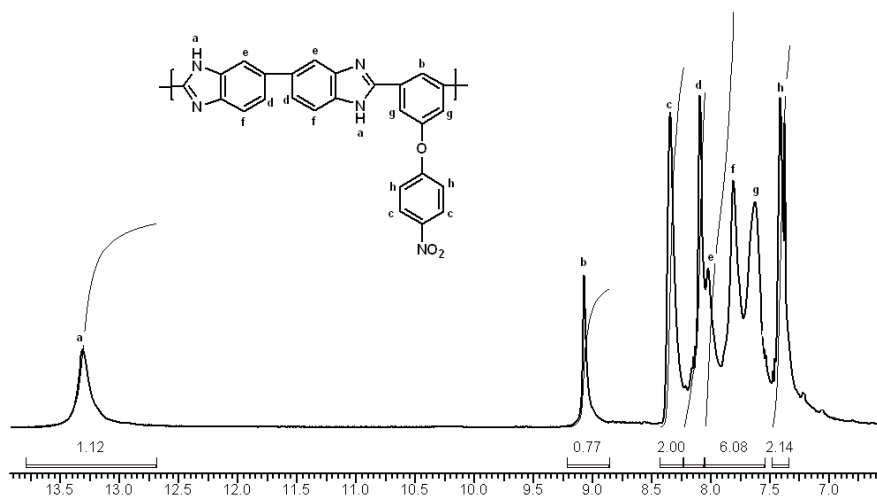


**Figure 2.16** $^1$H NMR spectrum of nitro group containing Polybenzimidazole (NPBI).

The presence of benzimidazole groups and free nitro group in NPBI was further confirmed by $^1$H NMR spectrum (Fig 2.16). The proton at 13.30 δ ppm assigned to hydrogen of N-H group of imidazole ring and the aromatic protons at 7.2–9.2 δ ppm with expected

multiplicity and integration substantiate the formation of polybenzimidazole with free nitro groups. Thus, the formation of desired polymers was confirmed by spectral analysis.

### 2.3.3 Properties of NPBIs

The properties of NPBIs were evaluated by solubility measurements, X-ray diffraction, DSC, TGA and mechanical property study.

### 2.3.3.1 Solubility measurements

PBIs are rigid polymers with high softening point and polymer solubility plays a major role for applications. Solubility behavior of newly synthesized polymers was studied by dissolving 4.0 mg of polymers in 0.5 mL solvent. Commercial PBIs is soluble only in aprotic solvents such as DMAc, after heating at high temperature for several hours in presence of lithium chloride. The NPBI polymers in the present study, displayed good solubility pattern compared to commercial PBI. They are soluble in polar aprotic solvents such as DMAc, NMP, DMSO, (Table 2.2) at ambient temperature.

**Table 2.2** Solubility behaviors of nitro group containing polybenzimidazoles.

| Polymer Code | Solvents | | | | | | | | |
|---|---|---|---|---|---|---|---|---|---|
| | TFA | MSA | HCOOH | $H_2SO_4$ | DMF | DMSO | DMAc | NMP | THF |
| NPBI | + + | + + | + | + + | + | + + | + + | + + | - - |
| NPBI-1 | + + | + + | + + | + + | - - | + + | + + | + + | - - |
| NPBI-2 | + + | + + | + + | + + | - - | + + | + + | + + | - - |
| NPBI-3 | + + | + + | + + | + + | + | + | + + | + + | - - |
| NPBI-4 | + | + + | + + | + + | + + | + + | + + | + + | - - |
| NPBI-5 | + + | + + | + + | + + | + + | + + | + + | + + | - - |
| NPBI-6 | - - | - - | - - | - - | - - | - - | - - | - - | - - |
| NPBI-7 | - - | - - | - - | - - | - - | - - | - - | - - | - - |
| NPBI-8 | + + | + + | + + | + + | + + | + + | + + | + + | - - |
| NPBI-9 | + + | + + | + + | + + | + + | + + | + + | + + | - - |
| PBI | + + | + | + + | + + | + | + | + | + | - - |

+ +**:** Soluble at room temperature: +: soluble on heating, and - -: insoluble on heating.

**TFA:** Trifluro acetic acid, **MSA:** Methane sulfonic acid **H₂SO₄:** Conc. sulfuric acid, **DMF:** N, N-dimethylformamide**, DMAc**: N, N-dimethyl acetamide, **DMSO:** Dimethyl sulfoxide, **NMP:** N-methyl-2-pyrrolidone, **THF:** Tetrhydrofuran, **HCOOH:** Formic acid.

They are readily soluble in strong acids such as $H_2SO_4$, trifluroacetic acid (TFA), formic acid, methane sulfonic acid etc. However, these polymers are not soluble in common organic solvents such as chloroform, toluene, tetrahydrofuran, dioxane & acetic acid due to

their polar nature. The presence of flexible nitrophenoxy group in side chain of these polymers enhance the solvent solubility. Incorporation of aliphatic chains using adipic and sebacic acid renders these polymers insoluble in any solvents.

### 2.3.3.2 Crystallinity

Crystalline nature of these polymer specimens in film form was studied by X-ray diffraction (Figure 2.17). No sharp peak for crystalline nature was observed. The amorphous nature of polybenzimidazoles could be attributed to their unsymmetrical structural units and the bulky nitrophenoxy groups, which reduced the intra and inter polymer chain interactions, resulting in loose polymer chain packaging and aggregates.
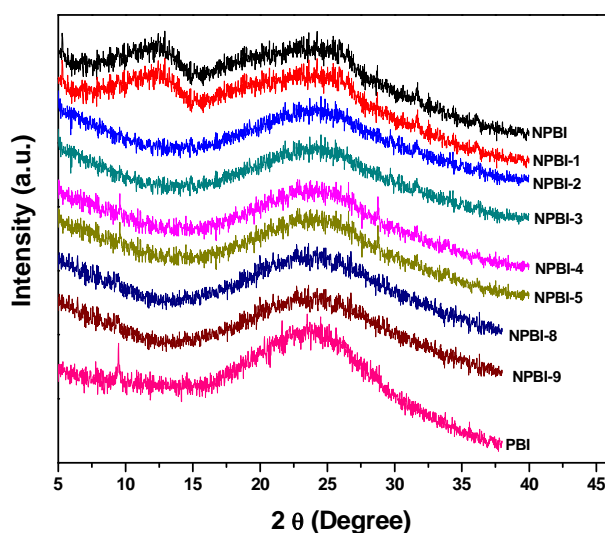


**Figure 2.17** Wide-angle X-ray diffraction patterns, of the nitro group containing polybenzimidazoles with IPA and other acids compared with PBI.

### 2.3.3.3 Thermal properties of polymers
➢ **Thermo gravimetric analysis**

The thermal behavior of the nitro group containing PBIs, and conventional PBI was analyzed by thermo gravimetric analysis at a heating rate of 10 °C /min in nitrogen atmosphere. The initial weight loss observed upto 200 °C in some cases is probably due to loss of absorbed moisture. All PBIs containing nitro groups exhibited a two-step degradation pattern (Figure 2.18 and 2.19). The first step of degradation was observed between 300-400 °C due to the decomposition of nitro groups. [30] Also, the percentage of weight loss in the first step due to the elimination of nitro groups in the region 300-400 °C increases with

increase in nitro group content. This also proves that the first step decomposition is due to loss of nitro group. The second step decomposition occurs at 520-620 °C due to the decomposition of polymer main chain.

Low values of initial decomposition temperature (IDT) (380-415 °C), $T_5$ (410-550 °C) and $T_{10}$ (500 – 680 °C) compared to PBI indicate that the nitro phenoxy group lowers thermal stability of PBI. However, thermal stability of these polymers is high enough for applications such as polymer electrolyte membranes for fuel cell or membrane separation at high temperature.

**Table 2.3** Thermal properties of nitro group containing polybenzimidazoles.

| Polymer Code | IDT (ºC) | SDT (ºC) | $T_5$ (ºC) | $T_{10}$ (ºC) | $T_{max}^1$(ºC) | $T_{max}^2$(ºC) | Residue (wt %) |
|---|---|---|---|---|---|---|---|
| NPBI | 400 | 577 | 424 | 501 | 440 | 635 | 67 |
| NPBI-1 | 394 | 560 | 418 | 530 | 430 | 685 | 73 |
| NPBI-2 | 402 | 546 | 420 | 500 | 431 | 732 | 71 |
| NPBI-3 | 385 | 582 | 419 | 589 | 410 | 726 | 74 |
| NPBI-4 | 380 | 614 | 526 | 671 | 430 | 744 | 79 |
| NPBI-5 | 416 | 527 | 548 | 680 | 542 | 721 | 80 |
| NPBI-8 | 412 | 580 | 450 | 630 | 441 | 728 | 73 |
| NPBI-9 | 350 | 540 | 407 | 595 | 408 | 723 | 72 |
| PBI | 603 | -- | 679 | 760 | 751 | -- | 84.5 |

**IDT**: Initial decomposition temperature due to $NO_2$ group, **SDT**: Second decomposition temperature due to decomposition of polymer backbone **$T_5$, $T_{10}$**, : Temperature at which 5%, 10% weight loss of polymer takes place, **$T_{max}^1$, $T_{max}^2$** : Temperatures at which maximum weight loss of polymer takes place in first and second step decomposition respectively,
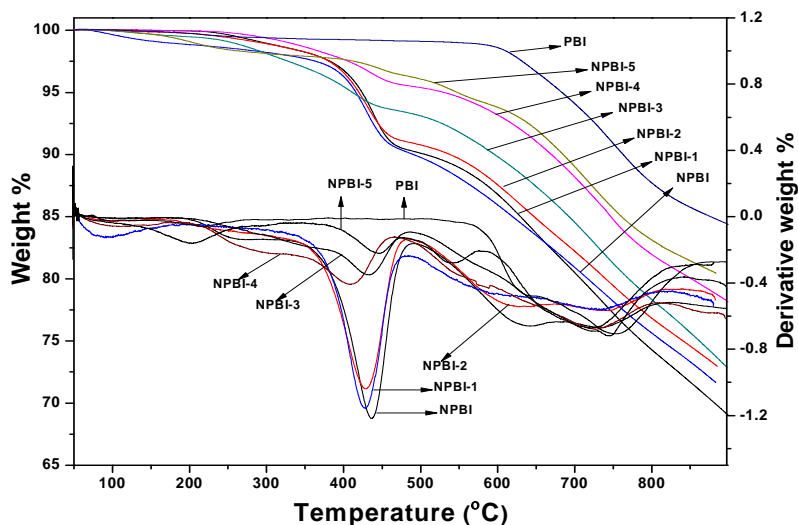


**Figure 2.18** TGA thermograms of nitro group containing Polybenzimidazoles compared with PBI in $N_2$ at heating rate 10 °C min$^{-1}$.
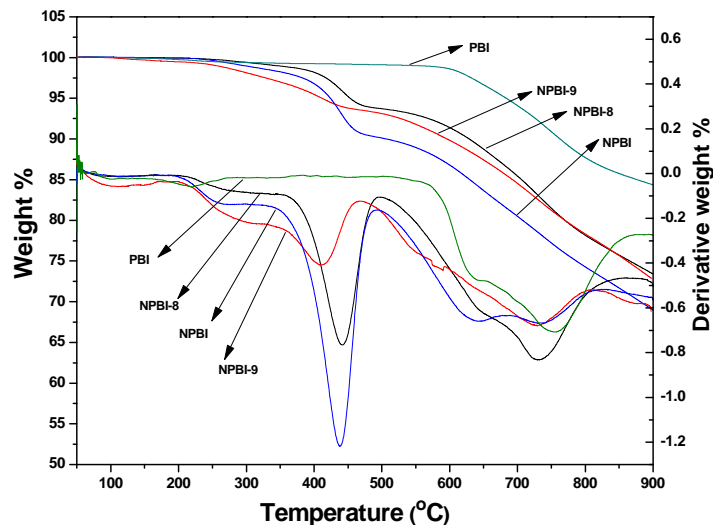
**Figure 2.19** TGA thermograms of nitro group containing Polybenzimidazoles compared with PBI in $N_2$ at heating rate 10 °C min$^{-1}$.

> **Glass transition temperature ($T_g$)**

PBI, due to rigid structure, show high glass transition temperature. Incorporation of flexible groups in side chain is expected to lower $T_g$. NEDA based PBIs were subjected to differential scanning calorimetry (DSC) analysis in nitrogen atmosphere at a heating rate of 20 °C /min to determine glass transition temperature and the DSC thermograms of these polymers are shown in Figure 2.20. $T_g$ of all these polymers could not be detected in DSC curves. From the curves in figure-7 we can clearly see the exothermic reaction occurring above 300 °C, probably due to decomposition of nitro group which may be interfering in the detection of $T_g$. [31]

It appears that the $T_g$ of nitro group containing PBI is not below 300 °C, which is sufficiently high for applications in polymer electrolyte for fuel cell or membranes for separation technology at high temperature. These polymers also showed remarkable thermal stability for high temperature applications.
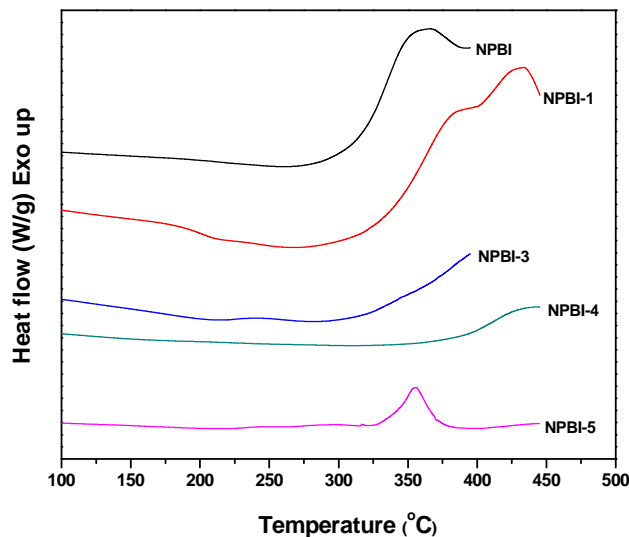
**Figure 2.20** DSC thermograms of nitro group containing Polybenzimidazoles in $N_2$ at heating rate 20 °C min$^{-1}$.

### 2.3.3.4 Mechanical properties of polymers

Polymer membranes when served as a material for applications such as polymer electrolyte for fuel cell or separation technology are expected to have good strength. Commercial PBI has superior mechanical properties due to rigid structure and any structural change is expected to affect mechanical properties. Commercial PBI has meta substituted phenyl rings in main chain where as, NEDA based PBIs also has meta substituted phenyl ring in main chain and in addition, nitrophenoxy pendant group attached to the phenyl ring. In the present study, it is observed that the pendant nitrophenoxy groups reduce the tensile strength of PBI from 151 MPa (PBI) to 62 MPa (NPBI) (Table-2.4), probably due to disruption of rigid polymer structure by flexible bulky pendant group increasing free volume of the polymer. Tensile properties of co-PBIs of NEDA and IPA in Fig 2.21 reveal that the addition of different mole % IPA to NEDA does not improve the tensile strength above 65 MPa, probably due to disruption of regular polymer structure of PBI. Similar trend is observed in case of modulus.

Thus, modulus of polybenzimidazole of NEDA (NPBI) is 2949 MPa whereas, modulus of co-polybenzimidazole containing different mole % of NEDA decreases up to 2069 MPa. Compared to NPBI, the toughness of all copolybenzimidazoles of NEDA and IPA is higher. Highest toughness of 29.9 MPa is shown by NPBI-5.

**Table 2.4** Mechanical properties of nitro group containing polybenzimidazoles.

| Polymer Code | diacid used (mole ratio %) | Tensile Stress (MPa) | Modulus (MPa) | Toughness (MPa) | Elongation at Break (%) |
|---|---|---|---|---|---|
| NPBI | NEDA 100 | 62 | 2949 | 3.26 | 3.64 |
| NPBI-1 | NEDA / IPA 90:10 | 61 | 2508 | 5.03 | 5.21 |
| NPBI-2 | NEDA / IPA 70:30 | 57 | 2585 | 2.69 | 3.29 |
| NPBI-3 | NEDA / IPA 50:50 | 63 | 2577 | 6.22 | 6.15 |
| NPBI-4 | NEDA / IPA 30:70 | 56 | 2069 | 12.05 | 12.03 |
| NPBI-5 | NEDA / IPA 10:90 | 65 | 2158 | 29.9 | 24.65 |
| NPBI-8 | NEDA / PDA 50:50 | 52.62 | 2570 | 3.69 | 4.56 |
| NPBI-9 | NEDA / TPA 50:50 | 61.46 | 2670 | 5.69 | 6.13 |
| PBI | IPA 100 | 151 | 3771 | 5.77 | 6.28 |

**NEDA:** 5-(4-nitrophenoxy) isophthalic acid, **IPA:** Isophthalic acid.

Similar trend was observed for elongation at break (Figure 2.21). High elongation at break of ~24.65% is shown by NPBI-5. Mechanical properties of co-polybenzimidazoles containing 50-mole % of NEDA and 50-mole % of different acids (NPBI-3, NPBI-8 and NPBI-9) are shown in Table 2.4. Monomer composition of NPBI-3 and NPBI-9 is similar except the nature of linking. (Isophthalic acid is Meta linking where as, terephthalic acid is para linking). However, NPBI-3 has near about same tensile properties, modulus, toughness and elongation at break when compared to NPBI-9. Comparatively low mechanical properties were exhibited by NPBI-8 containing pyridine moiety. These results indicate that the ratio of diacid monomers has significant effect on mechanical properties of copolymers.
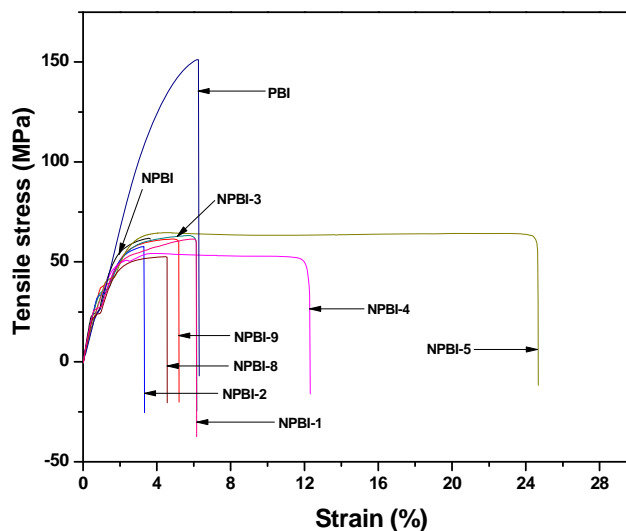


**Figure 2.21** Tensile stress versus strain graph of nitro group containing polybenzimidazoles compared with PBI.

Though, polybenzimidazole containing pendant nitrophenoxy groups has low tensile strength and modulus compared to commercial PBI, the observed strength is good enough for applications such as high temperature membrane materials for polymer electrolytes for fuel cell, separation technology and others.

### 2.3.4    Fuel cell characterization of pendant nitrophenoxy group containing PEM

### 2.3.4.1 Oxidative stability study

PBI membranes undergo degradation by .OH radicals formed by the decomposition of hydrogen peroxide generated at cathode under operational conditions of fuel cells, resulting in overall reduction in life time of the membrane. [32] The oxidative stability is measured by Fenton test described in experimental part.
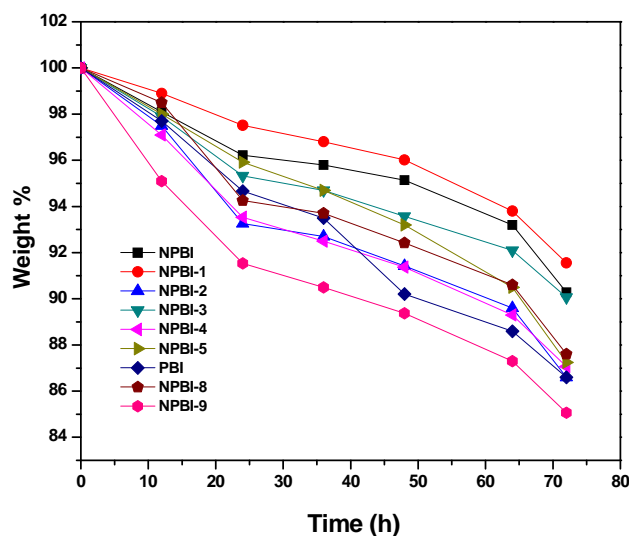


**Figure 2.22** Oxidative stability expressed  as weight loss in Fenton's test of nitro group containing polybenzimidazoles compared with PBI.

Fenton reagent test was carried out with NPBIs containing nitro group and commercial PBI to examine the radical oxidative stability of these membranes (Fig 2.22). The membranes (thickness: 90–100 µm) were immersed in 3% $H_2O_2$ containing 4 ppm of $Fe^{2+}$ (Mohr's salt, $(NH_4)_2Fe (SO_4)_2 \cdot 6H_2O$) at 70 °C for 12 h and the stability was correlated to the weight loss of the samples. Same samples were immersed further in fresh solutions of Fenton reagent and the samples were tested for 72 h after changing the Fenton reagent every 12 h.

As shown in Figure 2.22, NPBI, NPBI-1, NPBI-3 containing nitro group showed 9-10 % weight loss after 72 h in Fenton reagent test, NPBI-2, 4, 5 and commercial PBI showed 12-14 % weight loss after the 72 h, while NPBI-8, 9 showed 13-14 % weight loss after the same period. Thus, compared to NPBI, weight loss of conventional PBI is much higher. The membrane samples of NPBIs were still very tough indicating good oxidative stability of these membranes.

### 2.3.4.2 Phosphoric acid doping study

The doping level of phosphoric acid in PBI has profound effect on proton conductivity. Proton conductivity increases with increase in the doping level. The doping level of PBI depends on concentration of the phosphoric acid, time and temperature of doping and the structure of the polymer. The acid uptake capacity of newly synthesized polymers was determined by doping membranes of NPBIs and commercial PBI for comparison in 2-14 molar $H_3PO_4$ solutions for 24 h at room temperature. The time dependant doping study of NPBIs and PBI was also conducted in 85% $H_3PO_4$ at room temperature for 36 h to study the effect of time on doping level.

The doping level is expressed as the wt% of $H_3PO_4$ of the polymer or copolymers. Compared to PBI, NPBIs show low acid uptake (wt%) in all concentration of acid as shown in Figure 2.23 The acid uptake is slow upto 8 M $H_3PO_4$ solution in comparison with PBI, although a steady increase in acid uptake with increase in concentration is observed. In-fact, the acid uptake in NPBI, should have been faster than that for PBI, because of expected enhancement of free volume due to bulky nitro-phenoxy group in side chain, which should facilitate diffusion of phosphoric acid into matrix faster compared to rigid PBI. However, the phosphoric acid uptake of NPBIs upto 8 molar is slow compared to PBI (Figure 2.23). Upto 8 molar phosphoric acid, the percent of water (v/v) is more than that of phosphoric acid and it appears, that the nitro phenyl group being hydrophobic in nature does not support uptake of acid fast from the acid solution of low concentration. However, acid uptake is faster above 10 molar acid solution (Figure 2.23), because above 10 molar solution content of phosphoric acid is more than water. Thus, phosphoric acid uptake of NPBI in 12 and 14 molar phosphoric

acid increases faster and acid uptake of NPBI is 268 wt % compared to 250 wt% for PBI in 14

molar phosphoric acid.
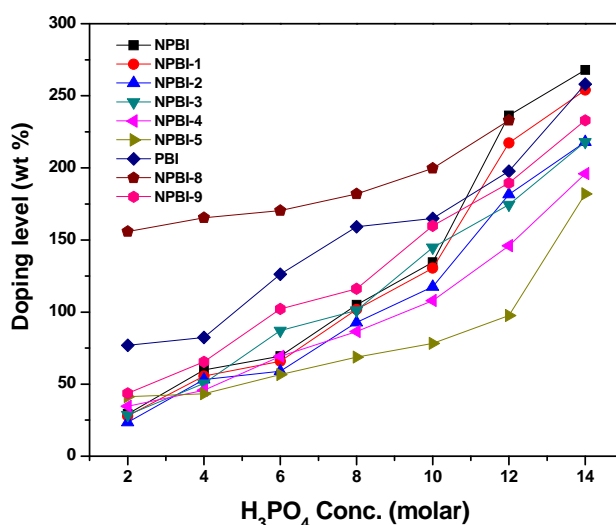


**Figure 2.23**  Doping level of phosphoric acid (wt% of $H_3PO_4$) in polymers as a function of
the $H_3PO_4$ concentration for nitro group containing Polybenzimidazoles
compared with PBI.

This is further substantiated by the time dependant acid uptake study in 85% $H_3PO_4$

solution (Figure 2.24). In case of PBI, a steady increase in acid uptake with time upto 24-27 h

and thereafter saturation is observed, whereas acid uptake in NPBIs is comparatively fast and

saturation point is reached within 12-15 h. This is, probably, due to the nature of N-H group

bonding in these polymers. The rigidity of PBI, due to the presence of high self associated H-

N---H hydrogen bonding between inter-chain imidazole groups, resists penetration of

phosphoric acid into polymer matrix, whereas NPBIs, having  more un-bonded free N-H

groups compared to PBI, as evidenced by the IR-study, gives access for easy penetration of

phosphoric acid in polymer matrix.

Thus, acid uptake in copolymers increases with increase in NEDA content in

polymer. Interestingly, the membranes of NPBIs have good strength and flexibility suitable for

preparation of PEM even after high acid uptake. After confirming the stability of membranes

of NPBIs in 85% phosphoric acid, the membranes for the proton conductivity study were

doped with 85% phosphoric acid for 24 h.
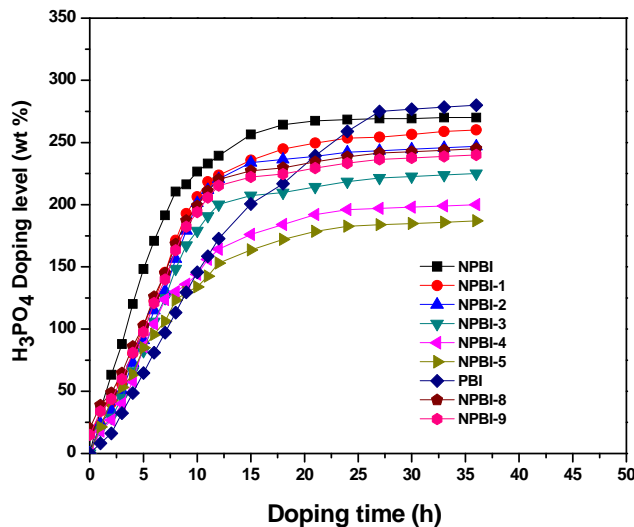
**Figure 2.24**   Time dependant doping level of nitro group containing Polybenzimidazoles compared with PBI in 85% $H_3PO_4$ at room temperature.

### 2.3.4.3 Proton conductivity measurement

Proton conductivity of PBI, NPBI and copolymers, NPBI-1-5, doped with 85% phosphoric acid for 24 h was determined by AC impedance method at different temperature in the range of 25-175 °C as described in experimental part. As expected, proton conductivity of all polymer membranes increases with increase in temperature (Figure 2.25). In case of PBI, proton conductivity increases from $3.96 \times 10^{-3}$ S/cm at 25 °C to $3.30 \times 10^{-2}$ S/cm at 175 °C, where as the proton conductivity of NPBI membrane is $6.84 \times 10^{-3}$ S/cm at 25 °C and $4.59 \times 10^{-2}$ S/cm at 175 °C (Figure 2.25).

High proton conductivity of NPBI is, probably, due to high phosphoric acid doping level. Though, apparently it appears that the doping level of NPBI (260 wt%) is lower than doping level of PBI ( 280 wt%), the doping level in mole/repeat unit for PBI is 8.8 moles compared to NPBI 11.8 moles/repeat unit (Table.2.5), because  the molecular weight of repeat unit of polybenzimidazole in PBI is 308, whereas that of NPBI is 445. Thus, free phosphoric acid after bonding with imidazole groups is more in NPBI which explains observed high proton conductivity in NPBI. Interestingly, copolymer NPBI-1 shows highest conductivity of $1.91 \times 10^{-2}$ S/cm at 25 °C and $5.15 \times 10^{-2}$ S/cm at 175 °C, probably, due to high doping level (10.85 mole/repeat unit). Thus, incorporation of nitrophenoxy groups in PBI enhances proton conductivity significantly.

**Table 2.5** Proton conductivity and Doping level in wt% and mol/repeat unit of PBI and NPBIs at 175 °C.

| Polymer Code | Doping level of $H_3PO_4$ (wt %) | Doping level of $H_3PO_4$ (moles) | $\sigma_{max}$ (S cm$^{-1}$) |
|:---:|:---:|:---:|:---:|
| NPBI | 260 | 11.5 | $4.6 \times 10^{-2}$ |
| NPBI-1 | 250 | 10.85 | $5.1 \times 10^{-2}$ |
| NPBI-2 | 240 | 9.79 | $4.4 \times 10^{-2}$ |
| NPBI-3 | 220 | 8.16 | $4.9 \times 10^{-2}$ |
| NPBI-4 | 190 | 6.57 | $3.9 \times 10^{-2}$ |
| NPBI-5 | 180 | 6.08 | $3.6 \times 10^{-2}$ |
| NPBI-8 | 220 | 8.16 | $4.7 \times 10^{-2}$ |
| NPBI-9 | 225 | 8.34 | $4.8 \times 10^{-2}$ |
| PBI | 280 | 8.92 | $3.3 \times 10^{-2}$ |
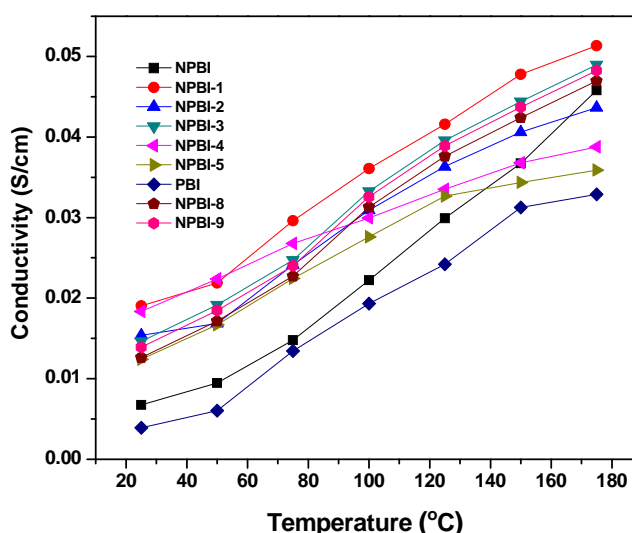


**Figure 2.25** Proton conductivities of nitro group containing Polybenzimidazoles compared with PBI at different temperature.

### 2.3.4.4 Membrane electrode assembly fabrication

The electrode was composed of a gas diffusion layer and a catalyst layer. The gas diffusion layer was prepared on wet-proofed carbon cloth with PTFE. The mixture of carbon powder (Vulcan XC-72, Cabot Co.), 60 wt% of PTFE and cyclohexane was mechanically mixed in an ultrasonic mixer and deposited by brushing method. The carbon and PTFE loading were maintained at a fixed ratio of 10:1.5. The viscous mixture was deposited by brushing on to the wet-proofed carbon cloth and the PTFE/C loading was 4.5 mg/cm$^2$. Then

gas diffusion layer on carbon cloth was dried by using hot air gun and cold-pressed for 3 minutes at 70 atm. After that it was sintered for 30 minutes at 350 °C in oven.

The method used to fabricate the catalyst layer on the gas diffusion layer is same as used for fabricating gas diffusion layer on the wet-proofed carbon cloth. The catalyst ink was prepared using commercial Pt/C (20 wt %, Arora Matthey Ltd.). The Pt/C, Nafion solution, and isopropyl alcohol was mechanically mixed in an ultrasonic mixer and deposited by brushing method on the gas diffusion layer. The Pt and Nafion loading were fixed at 0.5 mg/cm$^2$ and 0.6 mg/cm$^2$ respectively. After that the 2 wt% PBI solution in DMAc was coated on the catalyst layer by brushing.

Polymer electrolyte membranes, NPBI (80 µm) and PBI (90 µm), were doped in 85 wt% H$_3$PO$_4$ for 24 were wiped out by tissue paper and dried at 100 °C under vacuum. The membrane and electrode assemblies (MEAs) were made by hot-pressing the pretreated electrodes (9 cm$^2$) and the membrane under the conditions of 120 °C, 130 atm for 3 min.

### 2.3.4.5 Polarization study

Figure 2.26 and 2.27 show a comparison of the fuel cell performance of NPBI and PBI membranes in terms of polarization plots of MEAs fabricated using 20% Pt/C for both anode and cathode in a single cell experiment , at 100, 125 and 150 °C with a dry H$_2$/O$_2$ gas flow rate of 0.4 slpm (standard liters per minute). NPBI membrane shows better performance than that of the PBI membrane. The open-circuit voltage (OCV) obtained with the NPBI membrane is 0.95 V at 150 °C, whereas for PBI it is 0.92 V. However, the activation loss and ohmic loss (which are much more important for sustaining a large current density) in the case of the NPBI membrane are considerably lower than those of PBI. For example, the NPBI membrane gives a maximum power density 290 mW/cm$^2$ at 0.3 V, whereas the PBI membrane gives 210 mW/cm$^2$ at 0.3 V. This better fuel cell performance of NPBI membrane can be attributed to high H$_3$PO$_4$ acid content and elastomeric nature of NPBI membrane after doping which favors chain movement facilitating enhanced proton conductivity.
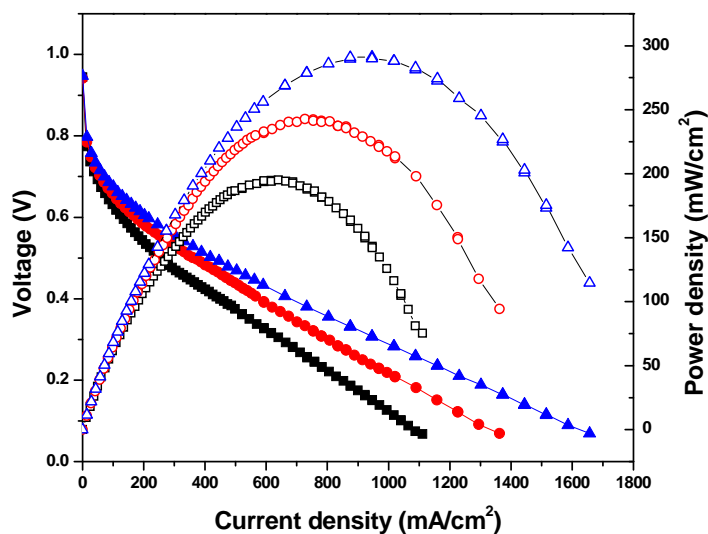
**Figure 2.26** Polarization curves obtained with NPBI membrane fuel cell at different temperatures with dry $H_2$ and $O_2$ (flow rate 0.4 slpm). The cell was conditioned for 30 min at open-circuit potential and at 0.2 V for 15 min before measurements. Key: (■□) 100, (●○) 125 and (▲△) 150 °C.
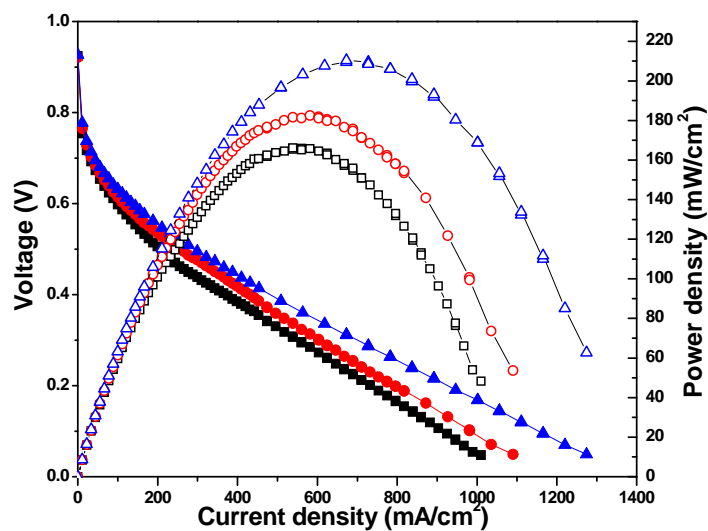


**Figure 2.27** Polarization curves obtained with PBI membrane fuel cell at different temperatures with dry $H_2$ and $O_2$ (flow rate 0.4 slpm). The cell was conditioned for 30 min at open-circuit potential and at 0.2 V for 15 min before measurements. Key: (■□) 100, (●○) 125 and (▲△) 150 °C.

**2.3.5    Synthesis and structural characterization of polybenzimidazole and Co-polybenzimidazole having free amino groups with different diacids**

Polybenzimidazole polymers containing pendant phenoxyamine groups were synthesized by solution polymerization method by condensing TAB with 5-(4-aminophenoxy) isophthalic acid hydrochloride in polyphosphoric acid. We used hydrochloride of the diacid, as free amine group has a tendency to undergo chemical changes with time and change in color is observed from white to pink and finally mud color which gave low molecular weight polymer even after heating for several hours with TAB in polyphosphoric acid. Where as, high molecular weight polymers in high yields could be obtained using 5-(4-aminophenoxy) isophthalic acid hydrochloride. Both, homopolymer of 5-(4-aminophenoxy) isophthalic acid hydrochloride with conventional TAB (scheme 2.6) and copolymers of TAB with a mixture of different mole ratios (90:10, 70:30, 50:50, 30:70 and 10:90) of 5-(4-aminophenoxy) isophthalic acid hydrochloride and isophthalic acid were synthesized in order to study the effect of pendant phenoxyamine content on proton conductivity, electrochemical and other properties of PBIs.

To study structure property relationship, few more new co-polybenzimidazoles containing phenoxyamine pendant groups with structural variations were also synthesized, by condensing 5-(4-aminophenoxy) isophthalic acid hydrochloride and other commercially available diacids such as terephthalic acid, pyridine 2,6 dicarboxylic acid, adipic acid, and sebacic acid in 50:50 mole ratio with TAB (Scheme 2.7).

Terephthalic acid gives para orientation and rigid structure; pyridine moiety gives extra basicity useful for phosphoric acid uptake for application as polymer electrolyte for fuel cell and enhances solubility; aliphatic moiety imparts hydrophobicity. Approximately 12 h heating is essential to form high molecular weight polymers. All the polymers remained soluble in polyphosphoric acid without precipitation. They form viscous solutions, which on pouring in hot water formed strong thread like structure; adipic acid based copolymer does not form threads. All these polymers, except adipic acid based, have film-forming properties and they form transparent, tough film on casting from DMAc solution.

Inherent viscosity was determined in DMAc (0.5 g.dL$^{-1}$ concentration at 30ºC) using Ubbelhode viscometer. The values are observed to be high, which are in the range from 0.62 - 1.52 dL.g$^{-1}$. The values for homo polybenzimidazole of AEDA (APBI) and co-polybenzimidazoles of AEDA and IPA are greater than one (Table-2.6). Copolybenzimidazole of 50 mole% terephthalic acid and AEDA (APBI-9) also has high inherent viscosity of 1.52 dL.g$^{-1}$. Co-polybenzimidazoles of AEDA with adipic acid (APBI-6), sebacic acid (APBI-7) and pyridine dicarboxylic acid (APBI-8) have inherent viscosity of 0.62, 0.71 and 0.82 dL.g$^{-1}$ respectively. All these polymers except APBI-6 form tough flexible films.

**Table 2.6** Inherent viscosities and film nature of amino group containing polybenzimidazoles.

| Polymer Code | Diacids used (Mole ratio %) | Inherent viscosity $\eta_{inh}$ (dL/g) | Film Color | Film Nature |
|---|---|---|---|---|
| APBI | AEDA **100%** | 1.2 | Pale yellow | Flexible |
| APBI-1 | AEDA / IPA **90:10** | 1.12 | Light brown | Flexible |
| APBI-2 | AEDA / IPA **70:30** | 1.29 | Light brown | Flexible |
| APBI-3 | AEDA / IPA **50:50** | 1.36 | Yellowish | Flexible |
| APBI-4 | AEDA / IPA **30:70** | 1.23 | Yellowish | Flexible |
| APBI-5 | AEDA / IPA **10:90** | 1.49 | Yellowish | Flexible |
| APBI-6 | AEDA / AA **50:50** | 0.62 | Dark brown | Brittle |
| APBI-7 | AEDA / SA **50:50** | 0.72 | Brown | Flexible |
| APBI-8 | AEDA / PDA **50:50** | 0.82 | Yellowish | Flexible |
| APBI-9 | AEDA / TPA **50:50** | 1.52 | Light brown | Flexible |

**AEDA:** 5-(4-aminophenoxy) isophthalic acid hydrochloride, **IPA:** Isophthalic acid, **AA:** Adipic acid, **SA:** Sebacic acid, **PDA:** Pyridine dicarboxylic acid, **TPA:** Terephthalic acid.

The polymers, thus obtained, were characterized by FTIR and $^1$H NMR spectroscopy. FTIR spectra of all polymers were scanned using thin films. The FT-IR spectra of APBI, APBI-1, APBI-2, APBI-3, APBI-4 & APBI-5 are shown in (Fig 2.28 & 2.29) and those of APBI-6, APBI-7, APBI-8, and APBI-9 in (Fig 2.30). The formation of polybenzimidazoles was confirmed by the characteristic absorption band in the range at 1618-1623 cm$^{-1}$ due to C=N stretching of imidazole ring and another characteristic band of breathing mode of imidazole ring appearing in the range of 1284 -1288 cm$^{-1}$.

The absorption band at 3190 cm$^{-1}$ is assigned to self-associated N-H interaction of PBI chains. Due to structural variations of these polymers these bands appear at different

wavelength in the range mentioned. The presence of free NH$_2$ group was confirmed by absorption band at 3350 cm$^{-1}$.
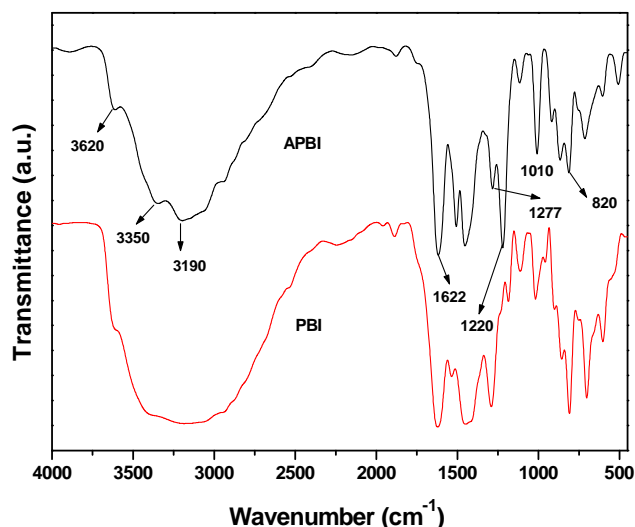


**Figure 2.28**   FTIR spectrum of amino group containing polybenzimidazole compared with PBI.
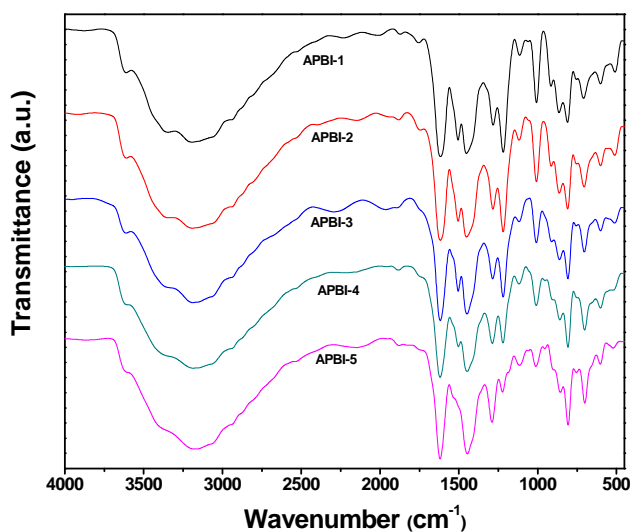


**Figure 2.29**   FTIR spectrum of amino group containing polybenzimidazoles of IPA.

In the (Figure 2.29) the intensity of band at 3335-3360 cm$^{-1}$ due to free amino group decreases as amino diacid percentage in co-PBI series of IPA decreases from 100 to 10%. Since polybenzimidazole show broad peak in this region due to N-H group, the absorption at 3335 – 3360 cm$^{-1}$, due to the free amino group, is masked out and could not be distinctly seen, instead a slight hump appears at this region. Band due to C-O-C linkage appears at 1216 cm$^{-1}$, the intensity of which decreases as AEDA content in co-polymer decreases. The Co-PBI of

aliphatic acids show absorption band at 2930-2937 cm$^{-1}$ due to aliphatic C-H stretching (Figure 2.30). Intensity of this peak is high for sebacic acid based polymer.

The presence of benzimidazole groups and free amino group in the polymer was further confirmed by $^1$H NMR spectrum of polybenzimidazole of AEDA and TAB (Figure 2.31). The protons at 13.16 and 5.18 δ ppm were assigned to hydrogen of N-H group of imidazole ring and hydrogen atoms of aromatic amine respectively and the aromatic protons with expected multiples and integration at 6.6–8.8 δ ppm substantiate the formation of polybenzimidazole with free amino groups.
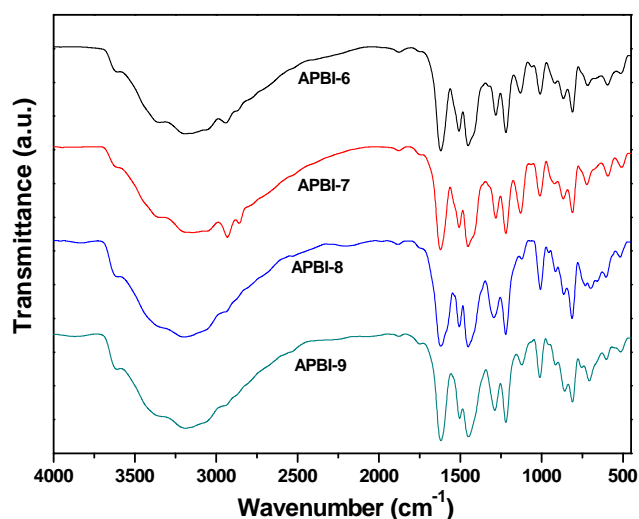


**Figure 2.30** FTIR spectra of amino group containing polybenzimidazoles with other diacids.
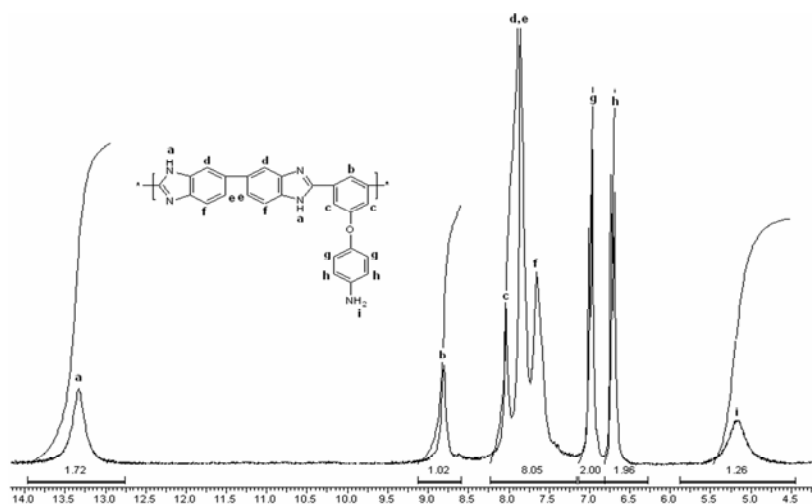


**Figure 2.31** $^1$H NMR spectrum of amino group containing polybenzimidazole.

### 2.3.6    Properties of APBIs

The properties of APBIs were evaluated by solubility measurements, X-ray diffraction, DSC, TGA and mechanical property study.

### 2.3.6.1 Solubility measurements

Solubility behavior of newly synthesized polymers was studied by dissolving 4 mg of polymers in 0.5 mL solvent. Commercial PBI is soluble only in aprotic solvents such as DMAc, after heating at high temperature for several hours in presence of lithium chloride. The polymers under study displayed good solubility compared to commercial PBI. They are soluble in all polar aprotic solvents such as DMF, DMAc, NMP, DMSO, (Table-2.7) at ambient temperature.

**Table 2.7** Solubility behavior of the amino groups containing polybenzimidazoles.

| Polymer | Solvents | | | | | | | | |
|---------|-----|-----|-------|------------|-----|------|------|-----|-----|
| Code | TFA | MSA | HCOOH | $H_2SO_4$ | DMF | DMSO | DMAc | NMP | THF |
| APBI | + + | + + | + + | + + | + + | + + | + + | + + | + - |
| APBI-1 | + + | + + | + + | + + | + + | + + | + + | + + | - - |
| APBI-2 | + + | + + | + + | + + | + + | + + | + + | + + | - - |
| APBI-3 | + + | + + | + + | + + | + + | + + | + + | + + | + - |
| APBI-4 | + + | + + | + + | + + | + + | + + | + + | + + | + - |
| APBI-5 | + + | + + | + + | + + | + + | + + | + + | + + | - - |
| APBI-6 | + + | + + | + + | + + | + + | + + | + + | + + | - - |
| APBI-7 | + + | + + | + + | + + | + + | + + | + + | + + | - - |
| APBI-8 | + + | + + | + + | + + | + + | + + | + + | + + | - - |
| APBI-9 | + + | + + | + + | + + | + + | + + | + + | + + | - - |
| PBI | + + | + | + + | + + | + | + | + | + | - - |

**+ +:** Soluble at room temperature, **+:** soluble on heating, **+ -:** swelling on heating and **- -:** insoluble on heating. **TFA:** Trifluro acetic acid, **MSA:** Methane sulfonic acid **$H_2SO_4$:** Conc. sulfuric acid, **DMF:** N,N-dimethylformamide**: DMAc**, N,N-dimethyl acetamide, **DMSO:** Dimethyl sulfoxide, **NMP:** N-methyl-2-pyrrolidone, **THF:** Tetrhydrofuran, **HCOOH:** Formic acid.

They are readily soluble in strong acids such as $H_2SO_4$, trifluroacetic acid, formic acid, methane sulfonic acid etc. However, these polymers are not soluble in common organic solvents such as chloroform, toluene, dioxane & acetic acid due to their polar nature. Polymers swell in tetrahydrofuran. The presence of phenyl ether and amino groups in side chain in these polymers enhances the solvent solubility.

### 2.3.6.2 Crystallinity

Crystalline nature of these polymer specimens in film form was studied by X-ray diffraction (Figure 2.32 & 2.33) No sharp peak for crystalline nature was observed. The amorphous nature of polybenzimidazoles could be attributed to their unsymmetrical structural units and the bulky phenoxyamine groups, which reduced the intra and inter polymer chain interactions, resulting in loose polymer chain packaging and aggregates.
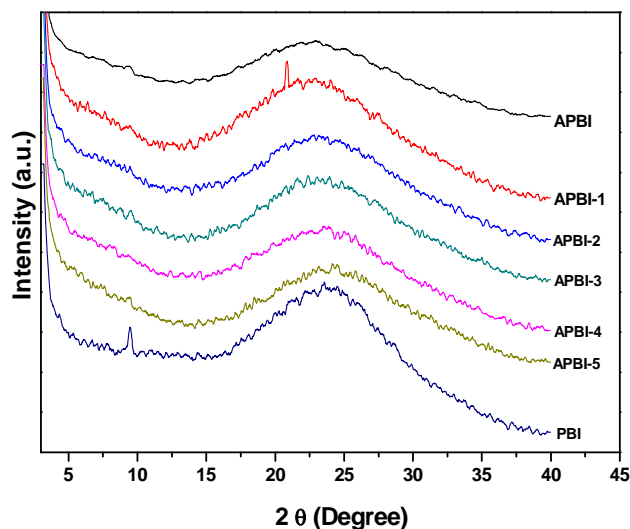


**Figure 2.32** Wide-angle X-ray diffraction patterns, of the amino group containing polybenzimidazoles with IPA compared with PBI.
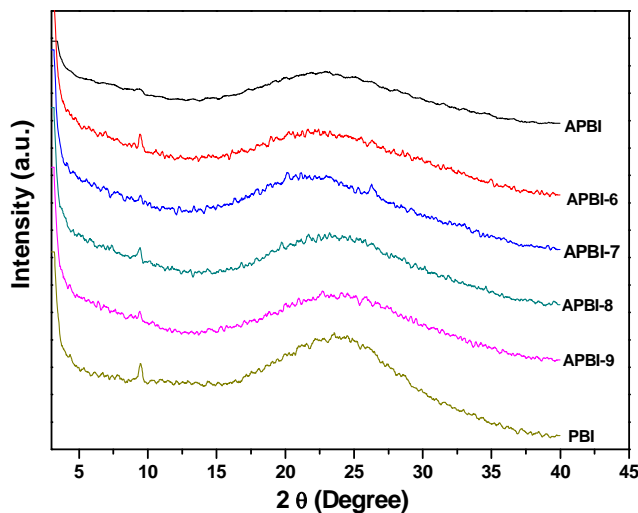


**Figure 2.33** Wide-angle X-ray diffraction patterns, of the amino group containing polybenzimidazoles with other diacids compared with PBI.

**2.3.6.3  Thermal properties of polymers**

➢  **Thermogravimetric analysis**

Thermal stability of these polymers was determined by thermogravimetric analysis (TGA) in nitrogen atmosphere at a heating rate of 10°C /min (Table 2.8). The thermograms are given in Figure 2.34 & 2.35. These polymers have a tendency to absorb moisture and they could not be de-moisturized even after heating at 150 °C for several hours as they hold moisture strongly.

All the polymers except homopolymer and commercial PBI show some weight loss after 200 °C, probably due to absorbed moisture. This loss is reflected in 5% weight loss and observed temperature (for 5% weight loss) is comparatively low. In fact, for copolymer APBI-7, the observed temperature for 5% weight loss is lower than the initial decomposition temperature (IDT).
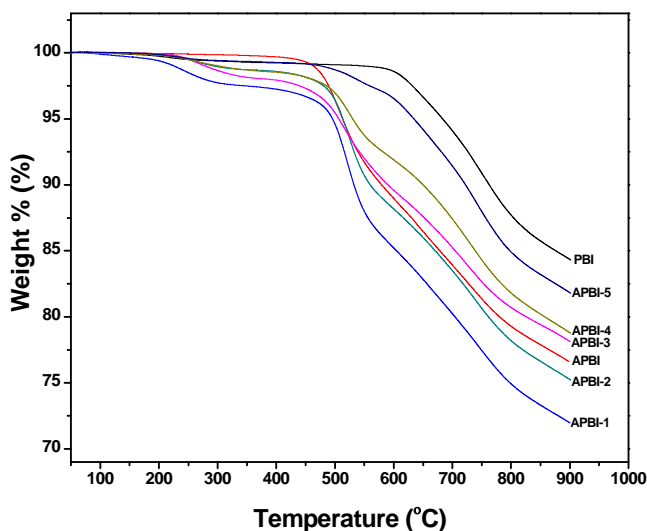


**Figure 2.34**  TGA thermograms of amino group containing polybenzimidazoles of IPA compared with PBI in $N_2$ at heating rate 10°C min$^{-1}$.

All the polymers show good thermal stability with no weight loss below 461°C. Homopolymer that has maximum pendant phenoxyamine groups has initial decomposition temperature (IDT) of 475°C and maximum decomposition temperature ($T_{max}$) of 508°C. Low IDT and $T_{max}$ compared to PBI are attributed to the presence of flexible phenoxyamine groups in side chain. Temperature for 5, 10 and 20% weight loss for homopolymer is 516, 579 and 777 °C respectively. Partial replacement of AEDA with aromatic diacids in co-polymers enhances thermal stability to some extent. In copolymer series of AEDA and IPA, initial

decomposition temperature of copolymers varies from 461-600°C. However, the exact reason for the lowest IDT, $T_{max}$ and $T_g$ values of APBI-3 containing 50 mol% of AEDA and IPA compared to other compositions is not known. Copolymer of AEDA with 90 mole % IPA, showed highest IDT of 600°C, close to that of PBI based on 100% IPA. Structure of diacids in copolymers has effect on thermal stability. Co-polymers containing 50 mole % of aliphatic adipic and sebacic acids show low IDT compared to copolymers containing 50 mole% of aromatic acids due to the presence of aliphatic carbons. $T_5$, $T_{10}$ and $T_{20}$ values of these two polymers are also low showing rapid weight loss.
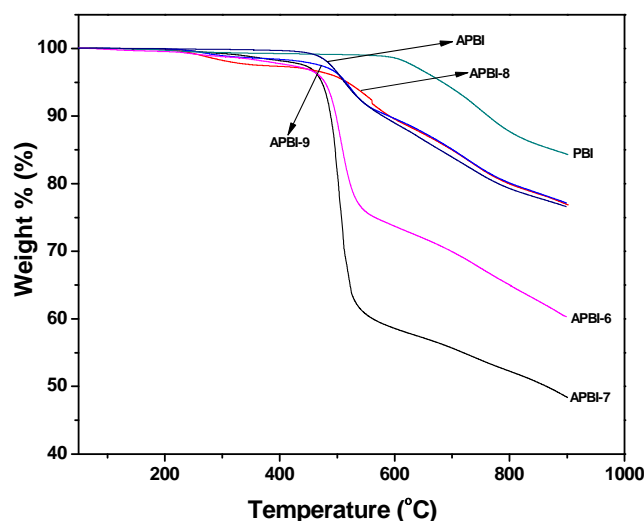


**Figure 2.35** TGA thermograms of amino group containing polybenzimidazoles of other diacids compared with PBI in $N_2$ at heating rate 10°C min$^{-1}$.

High thermal stability of pyridine ring is reflected on high *IDT, $T_{max}$* and *$T_{20}$* values of APBI-8 based on 50-mole% of pyridine 2, 6-dicarboxylic acid. Similarly, copolymer containing 50 mole % terephthalic acid, APBI-9, also shows high thermal stability due to para orientation

The values of residual weight vary from 48.6 - 82.2 wt% and the highest value 82.2 is observed for APBI-5, based on 90-mole% of IPA and 10-mole% of AEDA. Co-PBI based on aliphatic acids i.e. adipic and sebacic show low residue i.e. 48.6 and 60.5 wt % respectively (Table-2.7) due to the decomposition of aliphatic groups.

**Table 2.8** Thermal properties of amino groups containing polybenzimidazoles.

| Polymer Code | IDT (°C) | $T_5$ (°C) | $T_{10}$ (°C) | $T_{20}$ (°C) | $T_{max}$(°C) | Residue (wt %) | $T_g$ (°C) |
|---|---|---|---|---|---|---|---|
| APBI | 475 | 516 | 579 | 777 | 508 | 77.6 | 376 |
| APBI-1 | 498 | 509 | 553 | 766 | 520 | 72.8 | 402 |
| APBI-2 | 481 | 519 | 555 | 760 | 523 | 75.4 | 387 |
| APBI-3 | 461 | 510 | 592 | 823 | 516 | 78.5 | 382 |
| APBI-4 | 491 | 529 | 652 | 863 | 524 | 79.4 | 401 |
| APBI-5 | 600 | 631 | 722 | +900 | 533 | 82.2 | 435 |
| APBI-6 | 475 | 480 | 497 | 522 | 507 | 60.5 | 344 |
| APBI-7 | 486 | 475 | 491 | 502 | 509 | 48.6 | 313 |
| APBI-8 | 506 | 519 | 591 | 800 | 558 | 77.2 | 434 |
| APBI-9 | 493 | 518 | 582 | 810 | 553 | 77.1 | 401 |
| PBI | 603 | 679 | 760 | +900 | 751 | 84.5 | 431 |

**IDT**: Initial decomposition temperature, $T_5$, $T_{10}$, $T_{20}$ and $T_{max}$: Temperature at which 5%, 10%, 20% and maximum weight loss of polymer takes place respectively, $T_g$: Glass transition temperature

> ➢ **Glass transition temperature ($T_g$)**

PBI in general shows high glass transition temperature, due to the rigid structure. Incorporation of flexible groups in side chain is expected to lower $T_g$. Glass transition temperature of AEDA based PBIs was determined by differential scanning calorimeter (DSC) in nitrogen atmosphere at heating rate of 20 °C /min (Table-2.8) and the DSC thermograms of these polymers are shown in (Figure 2.36 & 2.37). All the copolymers showed single $T_g$ indicating random distribution. $T_g$ of these polymers varies from 313-435 °C depending on structure and mole ratio of diacids. PBI based on AEDA has $T_g$ of 376 °C, whereas $T_g$ of PBI based on IPA is 413 °C indicating that incorporation of flexible group in side chain lowers $T_g$. The Co-PBI's based on sebacic acid have lowest $T_g$ of 313 °C due to flexible alkane chain. Addition of IPA in AEDA increases $T_g$ of resultant copolymers. The $T_g$ of copolymers is also influenced by the structure of diacid. In copolymers based on 50 mole % of AEDA and 50 mole % of other acids, copolymer based on pyridine dicarboxylic acid has highest $T_g$ of 432 °C comparable to PBI based on IPA, whereas copolymer containing alkane groups have lowest $T_g$. Copolymer containing terephthalic acid has higher $T_g$ than that of IPA based copolymer due to possible orientation in terephthalic acid based copolymer forming close packing which facilitates hydrogen bonding. However, it may be noted that though polybenzimidazoles

based on AEDA have low $T_g$ values compared to commercial PBI, they are sufficiently high for applications as polymer electrolyte for (fuel cell) or membranes for separation technology. These polymers also have sufficiently high thermal stability suitable for high temperature applications.
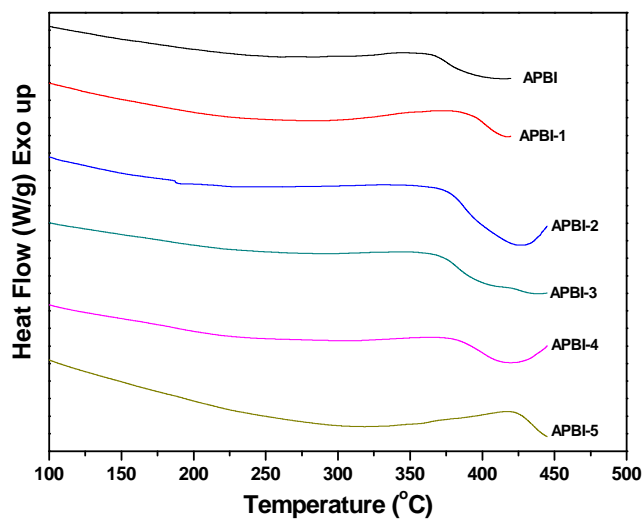


**Figure 2.36** DSC thermograms of amino group containing polybenzimidazole and co-polybenzimidazoles of IPA in $N_2$ at heating rate 20 °C min$^{-1}$.
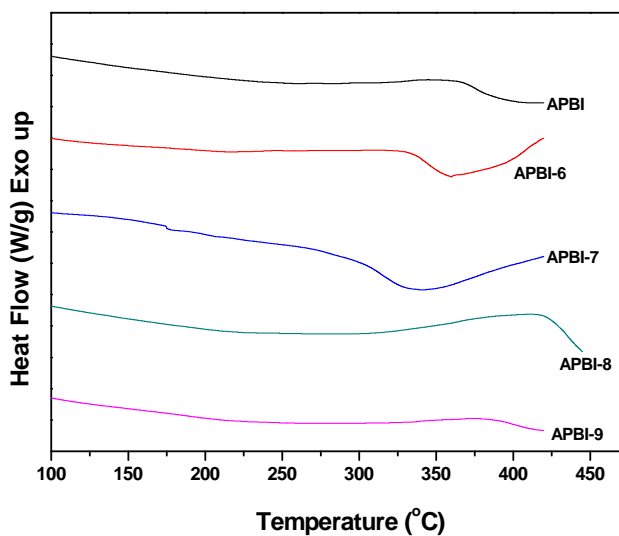


**Figure 2.37** DSC thermograms of amino group containing polybenzimidazole and co-polybenzimidazoles of other diacids in $N_2$ at heating rate 20 °C min$^{-1}$.

**2.3.6.4 Mechanical properties of polymers**

Polymer membranes should have good strength for applications such as polymer electrolyte for fuel cells or separation technology. Commercial PBI has superior mechanical properties due to rigid structure and any structural change is expected to affect mechanical properties. Commercial PBI has meta substituted phenyl rings in main chain where as, AEDA based PBI also has meta substituted phenyl ring in main chain and in addition, phenoxyamine pendant group attached to the phenyl ring. Data on tensile strength, modulus, toughness and elongation at break is tabulated in Table 2.9. The data reveals that the pendant phenoxyamine groups reduce the tensile strength of PBI from 151 MPa (PBI) to 72 MPa (APBI) (Table 2.9), probably, due to disruption of rigid polymer structure by flexible bulky pendant group increasing free volume of the polymer.

Tensile properties of co-PBIs of AEDA and IPA (Figure 2.38) reveals that the addition of 10 mole % IPA to AEDA reduces the tensile strength further from 72 MPa to 58 MPa, probably, due to disruption of regular polymer structure of APBI. Further addition of IPA increases tensile strength and copolymer containing 50 mole % of AEDA and IPA (APBI-3) has high tensile strength of 119 MPa probably due to equimolar monomer concentration which helps in formation of regular polymer structure. However, comparatively low $T_g$ observed for this copolymer does not support formation of rigid structure. Addition of more than 50 mole% IPA again reduces tensile strength. Similar trend is observed in case of modulus. Thus, modulus of polybenzimidazole of AEDA (APBI) is 2267 MPa, whereas modulus of co-polybenzimidazole containing 50 mole % of AEDA and 50 mole % of IPA (APBI-3) is 3540 MPa and that of 10 mole % of AEDA and 90 mole % of IPA (APBI-5) is 2222 MPa. Compared to APBI, the toughness of all copolybenzimidazoles of AEDA and IPA is higher.

Again, highest toughness of 58.1 MPa is shown by APBI-3. Similar trend was observed for elongation at break (Figure-2.38). High elongation at break of ~ 40% is shown by APBI-3 and APBI-4. These results indicate that the structural changes in copolymers due to change in mole ratio of diacid monomers has significant effect on mechanical properties of copolymers. The copolybenzimidazole APBI-3 containing equimolar monomer ratio of diacids has high

tensile strength, high modulus, high toughness and high elongation at break. Any deviation from this ratio reduces mechanical properties.

**Table 2.9** Mechanical properties of amino groups containing polybenzimidazoles

| Polymer Code | Diacid used (mole ratio %) | Tensile Stress (MPa) | Modulus (MPa) | Toughness (MPa) | Elongation at Break (%) |
|---|---|---|---|---|---|
| APBI | AEDA **100** | 72 | 2267 | 2.25 | 4.3 |
| APBI-1 | AEDA / IPA **90:10** | 58 | 2295 | 8.26 | 14.2 |
| APBI-2 | AEDA / IPA **70:30** | 84 | 2888 | 21.00 | 20.9 |
| APBI-3 | AEDA / IPA **50:50** | 119 | 3540 | 58.41 | 40.4 |
| APBI-4 | AEDA / IPA **30:70** | 72 | 2345 | 36.85 | 41.6 |
| APBI-5 | AEDA / IPA **10:90** | 64 | 2222 | 29.77 | 34.7 |
| APBI-6 | AEDA / AA **50:50** | NA | NA | NA | NA |
| APBI-7 | AEDA / SA **50:50** | 125 | 3191 | 8.10 | 4.9 |
| APBI-8 | AEDA / PDA **50:50** | 71 | 2546 | 5.26 | 6.8 |
| APBI-9 | AEDA / TPA **50:50** | 67 | 1760 | 28.53 | 35.13 |
| PBI | IPA **100** | 151 | 3771 | 5.77 | 6.28 |

**AEDA:** 5-(4-aminophenoxy) isophthalic acid hydrochloride, **IPA:** Isophthalic acid, **AA:** Adipic acid, **SA:** Sebacic acid, **PDA:** Pyridine dicarboxylic acid, **TPA:** Terephthalic acid.
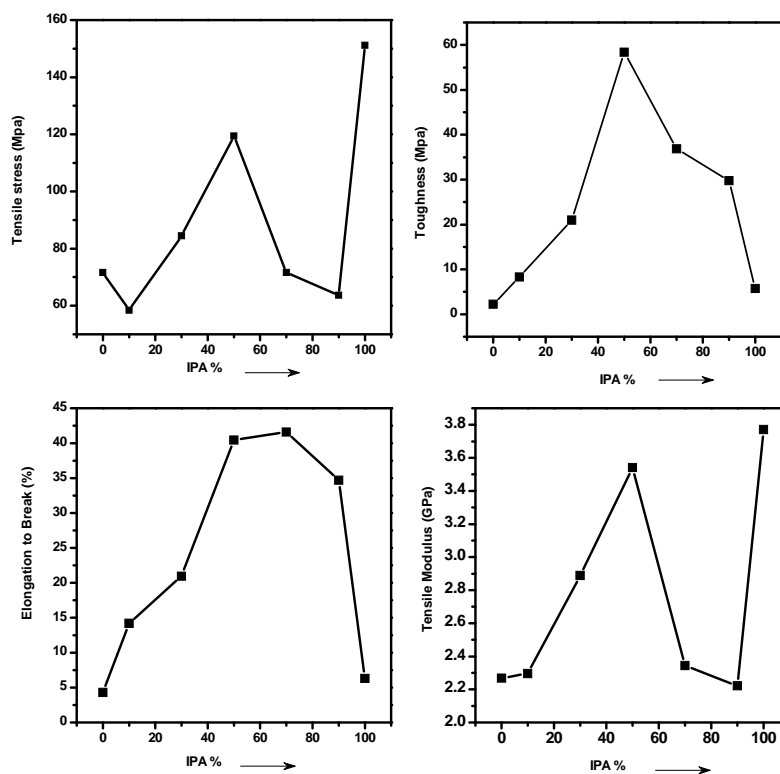


**Figure 2.38** Mechanical properties: comparative plot showing effect of IPA% on the co-polybenzimidazoles of AEDA.
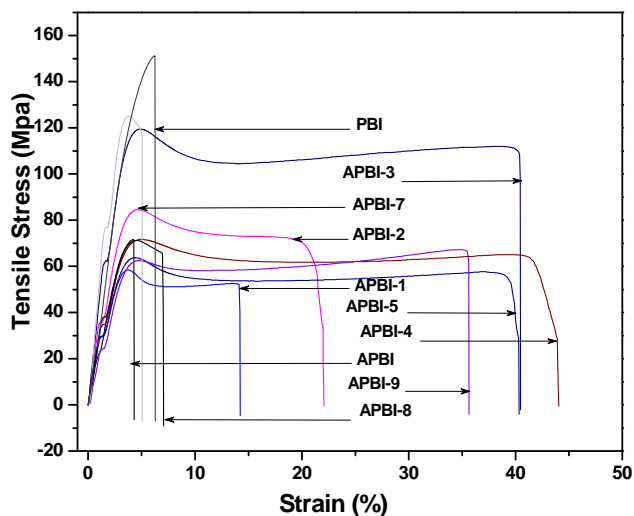
**Figure. 2.39** Tensile stress versus strain graph of APBI and copolymers.

Chemical structure of acids used for the synthesis of PBI also has effect on mechanical properties of co-polybenzimidazoles (Figure 2.39). Mechanical properties of co-polybenzimidazoles containing 50-mole % of AEDA and 50-mole % of different acids (APBI-3, APBI-7, APBI-8 and APBI-9) are shown in Table 2.9. Monomer composition of APBI-3 and APBI-9 is similar except the nature of linking. (Isophthalic acid is Meta linking where as, terephthalic acid is para linking). However, APBI-3 has high tensile properties, high modulus, high toughness and high elongation at break compared to APBI-9. Comparatively low mechanical properties were exhibited by APBI-8 containing pyridine moiety. Co-polybenzimidazole based on aliphatic sebacic acid (APBI-7) also shows high tensile strength of 117 MPa and high modulus 3191 MPa. Thus, mechanical properties of copolybenzimidazoles depend on chemical composition of polymer. Though polybenzimidazole containing pendent phenoxyamine groups has low tensile strength and modulus compared to commercial PBI, the observed strength is good enough for applications as high temperature membrane materials for separation technology, polymer electrolytes for fuel cell and others.

### 2.3.7     Fuel cell Characterization of pendant aminophenoxy group containing PEM

### 2.3.7.1 Oxidative stability study

Fenton reagent test was carried out with amino group containing APBIs and commercial PBI to examine the radical oxidative stability of these membranes (Figure 2.40 and Figure 2.41). The membranes (thickness: 90–100 µm) were immersed in 3% $H_2O_2$ containing 4 ppm of $Fe^{2+}$ (Mohr's salt, $(NH_4)_2Fe (SO_4)_2 \cdot 6H_2O$) at 70 °C for 12 h and the stability was related to the weight loss of the samples. Same samples were immersed further in fresh solutions of Fenton reagent and the samples were tested for 120 h after changing the Fenton reagent every 12 h.
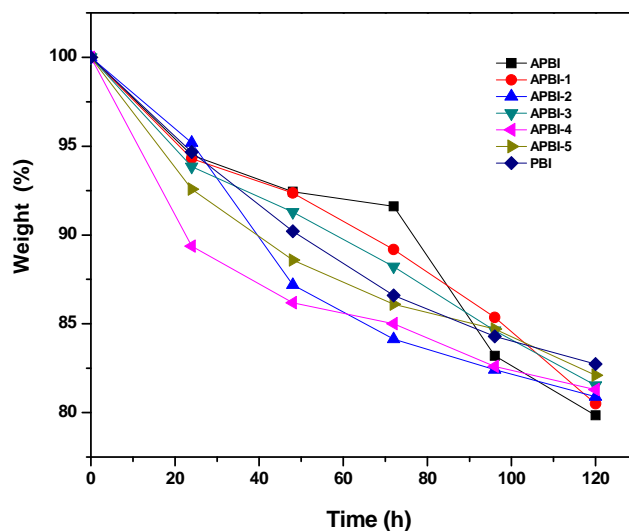


**Figure 2.40** Oxidative stability expressed as % weight loss in Fenton's test of amino group containing co-polybenzimidazoles of IPA compared with PBI.

As shown in Figure 2.40, amino group containing APBI, APBI-1-5 showed 8-17 % weight loss after 72 h in Fenton reagent test. The weight loss of APBI is 8% wt after 72 h, and it increases upto 20% after 120 h, while APBI-1- 5 and commercial PBI showed 12-16 % weight loss after the 72 h. The membrane samples of APBIs of IPA were still very tough upto 72 h indicating good oxidative stability of these membranes.

Figure 2.41 shows the oxidative stability of amino group containing polybenzimidazoles of other diacids. The weight loss of APBI-7 of sebacic acid and AEDA is 24 % after 72 h, which goes upto 38 % in120 h in Fenton reagent test. The high wt loss is due to aliphatic groups. Terephthalic acid containing APBI-9 also shows 21 % wt loss in 72 h and

upto 25 % wt loss in120 h. APBI-8 contains pyridine group shows similar oxidative stability as PBI.
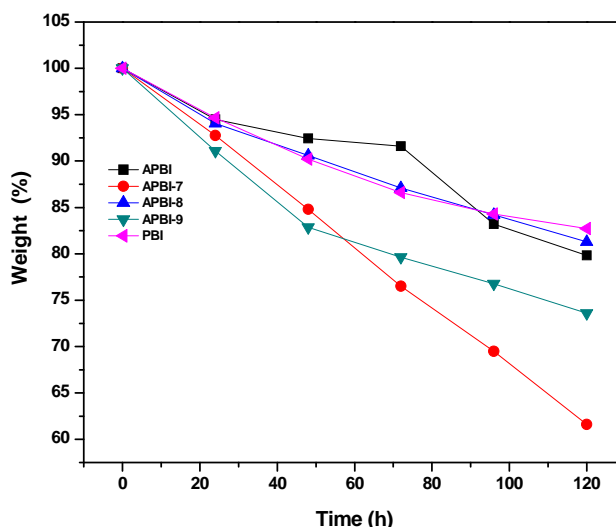


**Figure 2.41** Oxidative stability expressed as % weight loss in Fenton's test of amino group containing co-polybenzimidazoles of other diacids compared with PBI.

### 2.3.7.2 Phosphoric acid doping study

The acid uptake capacity of newly synthesized polymers was determined by doping membranes of APBIs and commercial PBI for comparison in 2-14 molar $H_3PO_4$ solutions for 24 h at room temperature. The time dependant doping study of APBIs and PBI was conducted in 12 & 14 molar $H_3PO_4$ at room temperature for 36 h to study the effect of time on doping level. The doping level is expressed as the wt % of $H_3PO_4$ of the polymer or copolymers.

Compared to PBI, APBIs show high acid uptake (wt %) in all concentration of acid as shown in Figure 2.42 and 2.43. Enhanced free volume of APBI due to bulky amino-phenoxy group in side chain and the presence of high content of basic free non-bonded N-H groups, and free amino groups which facilitate diffusion of phosphoric acid into matrix explain observed high acid uptake of APBI compared to rigid PBI. Upto 8 molar phosphoric acid, the percent of water (v/v) is more than that of phosphoric acid and it appears that the amino group being basic in nature support uptake of acid fast from the acid solution of low concentration also. However, acid uptake is faster above 8 molar acid solution (Figure-2.39), because above 8 molar solution content of phosphoric acid is more than water. Thus,

phosphoric acid uptake of APBI in 10 and 12 molar phosphoric acid increases and reaches to 400 wt % compared to 250 wt% for PBI in 12 molar phosphoric acid solution. APBI film dissolves in 14 molar phosphoric as it takes tremendous amount of acid due to the presence of amino groups and high free volume.
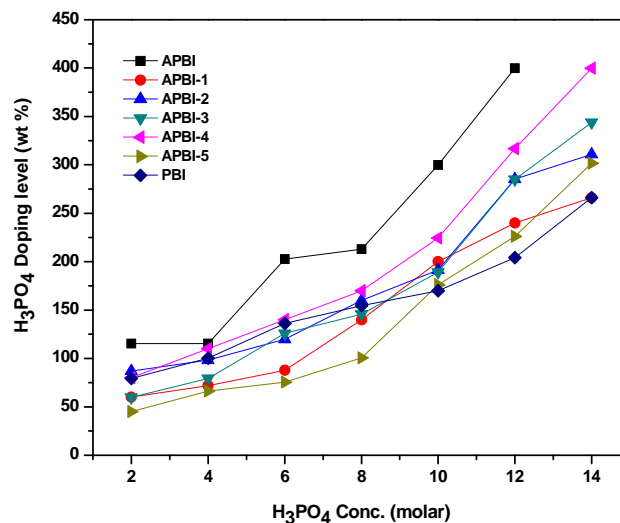


**Figure 2.42**  Doping level of phosphoric acid (wt%) in polymers as a function of the $H_3PO_4$ concentration for amino group containing co-polybenzimidazoles of IPA compared with PBI.
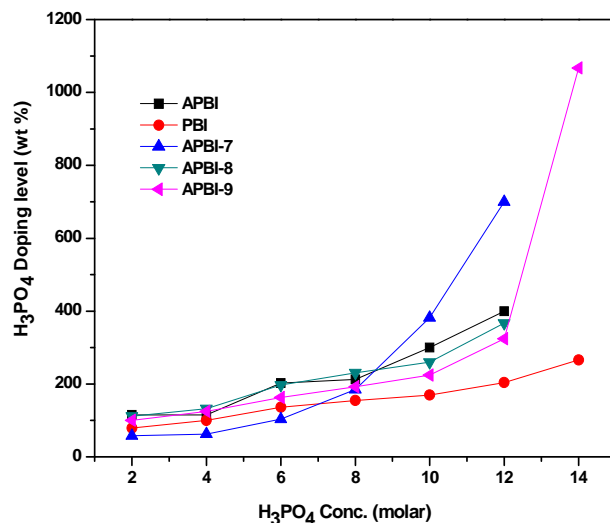


**Figure 2.43**  Doping level of phosphoric acid (wt%) in polymers as a function of the $H_3PO_4$ concentration for amino group containing co-polybenzimidazoles of other diacids compared with PBI.

Figure 2.43 shows a comparative doping level, in 2-14 molar $H_3PO_4$ solutions of amino group containing co-polybenzimidazoles of different diacids. APBI-7 containing sebacic acid

shows lowest doping level upto 6 molar $H_3PO_4$, while it increases above 8-12 molar $H_3PO_4$, solutions and its film dissolves in 14 molar $H_3PO_4$, solution. The water content (v/v), in $H_3PO_4$ upto 8 molar solution, is high compared to $H_3PO_4$ content. aliphatic groups being hydrophobic $H_3PO_4$ uptake of copolymer of AEDA and SA is low in 2-8 molar $H_3PO_4$. Once, $H_3PO_4$ content is increased in 10 molar and high molar $H_3PO_4$, the acid uptake increases due to flexibility of polymer chain and dissolves in 14 molar $H_3PO_4$ due to excessive acid uptake. The doping behavior of APBI-8 containing pyridine moiety is similar to APBI. It dissolves in 14 molar $H_3PO_4$ due to excessive uptake of phosphoric acid, because of presence of basic pyridine moiety and free $NH_2$ groups. Terephthalic acid containing APBI-9 shows similar doping behavior upto 12 molar $H_3PO_4$ solution as APBI shows, while in 14 molar $H_3PO_4$ solution its acid uptake goes upto 1100 wt%, it lose its mechanical strength at such higher doping level.
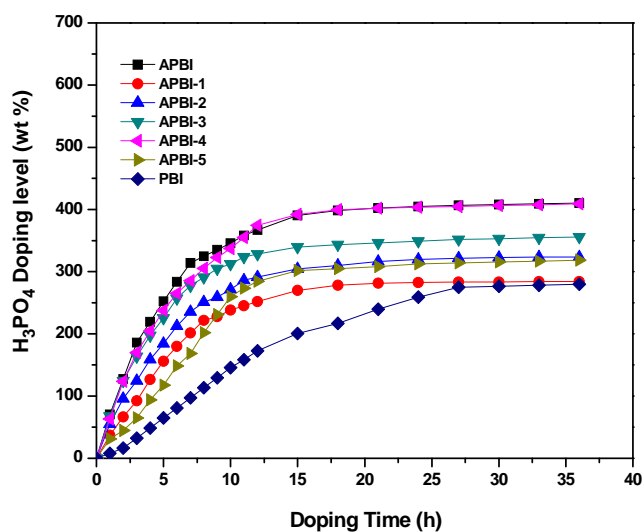


**Figure 2.44** Time dependant doping level of amino group containing Polybenzimidazoles of
IPA compared with PBI in $H_3PO_4$ at room temperature.

This is further substantiated by the time dependant acid uptake study in 12 & 14 molar $H_3PO_4$ solution (Figure2.44 & 2.45). In case of PBI, a steady increase in acid uptake with time upto 24-27 h and saturation thereafter is observed, whereas acid uptake in APBIs is comparatively fast and saturation point is reached within 12-15 h. This is, probably, due to the presence of free amino groups and nature of N-H group bonding in these polymers. The rigidity of PBI, due to the presence of high self associated H-N---H hydrogen bonding

between inter-chain imidazole groups, resists penetration of phosphoric acid into polymer matrix, whereas APBIs, having more un-bonded free N-H groups compared to PBI, as evidenced by the IR-study, gives access for easy penetration of phosphoric acid in polymer matrix. Thus, acid uptake in copolymers increases with increase in AEDA content in polymer.

The acid uptake in copolymers increases with increase in AEDA content in polymer. Thus, acid uptake of membranes of APBIs is high and fast compared to PBI. Interestingly, the membranes of APBIs have good strength and flexibility suitable for the preparation of PEM after controlled acid uptake. After confirming the stability of membranes of APBIs in phosphoric acid, the membranes for the proton conductivity study were doped with 12 and 14 molar of phosphoric acid.
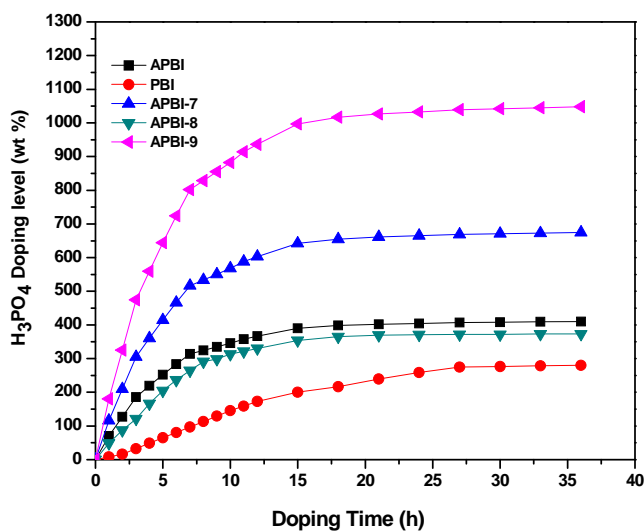


**Figure 2.45** Time dependant doping level of amino group containing co-polybenzimidazoles of other diacids compared with PBI in 85% $H_3PO_4$ at room temperature.

**2.3.7.3 Proton conductivity measurement**

Proton conductivity of PBI, APBI and copolymers, doped with 12 and 14 molar of phosphoric acid for 24 h was determined by AC impedance method at different temperature in the range of 25-175 °C as described in experimental part. As expected, proton conductivity of all polymer membranes increases with increase in temperature (Figure 2.46 & Figure 2.47). In case of PBI, proton conductivity increases from $3.96 \times 10^{-3}$ S/cm at 25 °C to $3.30 \times 10^{-2}$ S/cm

at 175 °C, where as the proton conductivity of APBI membrane is $3.72 \times 10^{-3}$ S/cm at 25 °C and $2.4 \times 10^{-2}$ S/cm at 175 °C (Figure 2.46).
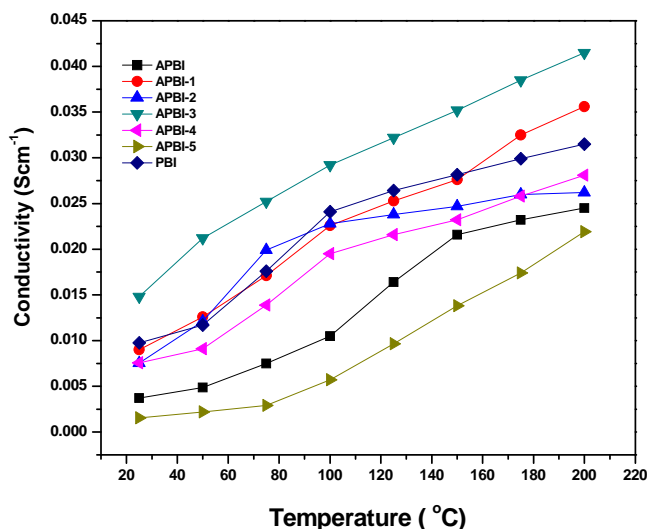


**Figure 2.46** Proton conductivities of amino group containing co-polybenzimidazoles with IPA compared with PBI at different temperature.
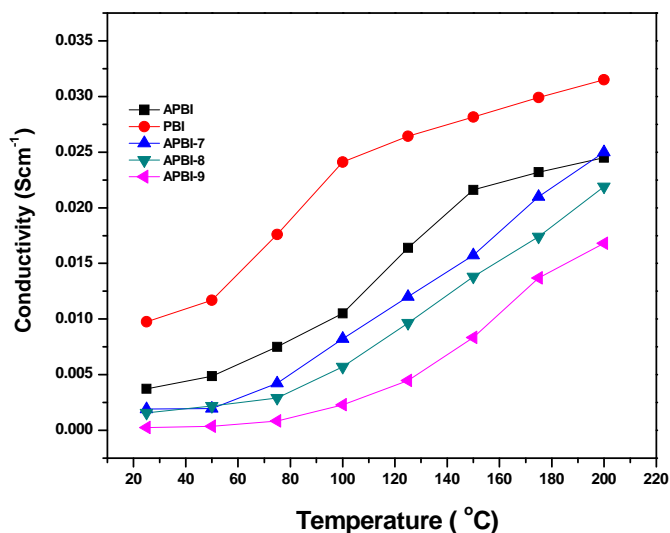


**Figure 2.47** Proton conductivities of amino group containing Polybenzimidazoles with other diacids compared with PBI at different temperature.

The conductivity data and doping level is summarized in Table 2.10. It appears that pendant phenoxy amine group does not enhance proton conductivity of PBI inspite of high doping level. Proton conductivity of all APBI polymers at 175 °C is at the order of $10^{-2}$ S/cm.

APBI-3 a copolymer of 50:50 AEDA and IPA shows the conductivity ($4.1 \times 10^{-2}$ S/cm) as compared to APBI ($2.4 \times 10^{-2}$ S/cm) and PBI ($3.30 \times 10^{-2}$ S/cm) at 175 °C. The proton

conductivity of all other copolymer is slightly lower compared to PBI. These results indicate that free amino group in pendant amino phenoxy group does not contribute to proton conductivity. For good proton conductivity, proton formed should be labile. A strongly bonded proton cannot be transported easily resulting in low proton conductivity. It appears that primary amine in these polymers form strong ionic bond with phosphoric acid and restricts mobility of protons, which explains low proton conductivity of these polymers compared to PBI.

**Table 2.10** Proton conductivity and Doping level in wt% and mol/repeat unit of PBI and APBIs at 175 °C.

| Polymer Code | Doping level of $H_3PO_4$ (wt%) | Doping level of $H_3PO_4$ (mole) | $\sigma_{max}$ (S cm$^{-1}$) |
|---|---|---|---|
| APBI | 337 | 14.3 | $2.4 \times 10^{-2}$ |
| APBI-1 | 414 | 17.10 | $3.5 \times 10^{-2}$ |
| APBI-2 | 363 | 14.19 | $2.6 \times 10^{-2}$ |
| APBI-3 | 418 | 15.45 | $4.1 \times 10^{-2}$ |
| APBI-4 | 436 | 15.13 | $2.8 \times 10^{-2}$ |
| APBI-5 | 420 | 13.66 | $2.2 \times 10^{-2}$ |
| APBI-7 | 287 | 11.13 | $2.5 \times 10^{-2}$ |
| APBI-8 | 300 | 11.11 | $2.2 \times 10^{-2}$ |
| APBI-9 | 348 | 12.86 | $1.7 \times 10^{-2}$ |
| PBI | 280 | 8.92 | $3.3 \times 10^{-2}$ |

#### 2.3.7.4 Membrane electrode assembly fabrication

The electrodes with a gas diffusion layer and a catalyst layer were fabricated by following the same procedure as mentioned in section 2.3.4.4. A polymer electrolyte membrane, APBI (90 μm) was doped in 12 molar $H_3PO_4$ for 24 h, was wiped out by tissue paper and dried at 100 °C under vacuum. The membrane electrode assemblies (MEAs) were made by hot-pressing the pretreated electrodes (9 cm$^2$) and the membrane at 120 °C and 130 atm pressure for 3 min.

#### 2.3.7.5 Polarization study

Figure 2.48 shows the fuel cell performance of APBI membrane in terms of polarization plots of MEA fabricated using 20% Pt/C for both anode and cathode in a single cell experiment , at 100, 125 and 150 °C with a dry $H_2/O_2$ gas flow rate of 0.4 slpm (standard

liters per minute). APBI membrane show lower performance than that of the PBI membrane. The open-circuit voltage (OCV) obtained with the APBI membrane is 0.9 V at 150 ℃, whereas for PBI it is 0.92 V. The APBI membrane gives a maximum power density 163 mW/cm$^2$ at 0.3 V, whereas the PBI membrane gives 210 mW/cm$^2$ at 0.3 V.  The lower fuel cell performance of APBI membrane can be attributed to low $H_3PO_4$ acid content and low proton conductivity of APBI membrane.
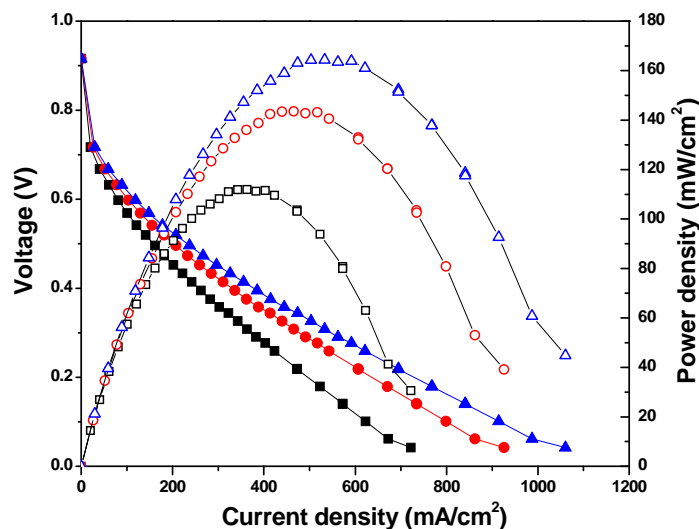


**Figure 2.48** Polarization curves obtained with APBI membrane fuel cell at different temperatures with dry $H_2$ and $O_2$ (flow rate 0.4 slpm). The cell was conditioned for 30 min at open-circuit potential and at 0.2 V for 15 min before measurements**.** Key: (■□) 100, (●○) 125 and (▲△) 150 ℃.

## 2.4  Conclusions

- Two new diacids namely, 5-(4-nitrophenoxy) isophthalic acid and 5-(4-aminophenoxy) isophthalic acid were successfully synthesized by simple condensation and oxidation, reduction reactions in high purity and high yields, by using a commercially available phenol like 3-5 dimethylphenol.

- A model compound, 4-(3,5-di(1H-benzo[dimidazol-2-yl]phenoxy)aniline having free amino group was synthesized to confirm the presence of free amino group in polymer.

- New series of polybenzimidazoles having pendant nitrophenoxy and  phenoxyamine groups were synthesized from a mixture of commercial diacids and  5-(4-nitrophenoxy) isophthalic acid or 5-(4-aminophenoxy) isophthalic acid with 3,3',4,4,'-

tetra amino biphenyl (TAB) using high temperature solution polycondensation in PPA.

- Most of these polymers were soluble in a wide range of solvents like NMP, DMAc, DMF, TFA, $H_2SO_4$, methane sulfonic acid compared to the commercial polybenzimidazole indicating that the incorporation of bulky pendant groups lead to a improvement in solubility.

- Incorporation of pendant functional phenoxy groups affects the thermal stability of these polymers significantly and hence they exhibited reasonably low thermal stability as compared to the commercial PBI. The pendant phenoxy groups lowered the glass transition temperatures ($T_g$) considerably.

- Incorporation of pendant functional phenoxy groups affects the packaging of polymer chains which increase the free volume in polymer chains of these polymers and hence they exhibited reasonably high phosphoric acid uptake as compared to the commercial PBI. High phosphoric acid uptake lowers the mechanical integrity of doped films to some extent.

- Nitrophenoxy groups improve the oxidative stability of polymers, while the phenoxyamine lowers the oxidative stability of polymers as compared to the commercial PBI.

- Nitrophenoxy groups improve the proton conductivity of polymers as it becomes elastomeric after doping with phosphoric acid at high temperature, while the phenoxyamine lowers the proton conductivity of polymers as compared to the commercial PBI.

## References

1.    Buckley, A.; Steutz, D.E.; Serad, G.A. *Encyclopedia* Vol.11, 2nd Edn.**1988**, p.572.

2.    Shaw, S. J. *Polymer International* **1996**, 41,193-207.

3.    Hergenrother, P. M.; Smith, J. G.; Connell, J. W. *Polymer* **1993**, 34, 856-865.

4.    Varma, I. K.; Veena S. M. *Journal of Polymer Science, Part A: Polymer Chemistry* **1976**, 14, 973.

5.    Varma, I. K.; Veena, S. M.; *Journal of Macromol Science Chem.* **1977**, 11, 845.

6.    Lakshmi Narayan, T. V.; Marvel, C. S. *Journal of Polymer Science, Part A: Polymer Chemistry* **1967**, 5, 1113-1118.

7.    Syuichi Inoue.; Yoshio Imai.; Keikichi Uno.; Yoshio Iwakura. *Die Makromolekulare Chemie* **1966,** 95, 236-247.

8.    Srinivasan, P. R.; Srinivasan, M.; Mahadevan, V. *Journal of Polymer Science, Part A: Polymer Chemistry* **1982**, 20, 1145-1150.

9.    Srinivasan, P. R.; Mahadevan, V.; Srinivasan, M. *Polymer* **1981**, 22, 1290-1291.

10.   Sung Moon.; Arthur L. Schwartz.; Jeffrey K. Hecht. *Journal of Polymer Science, Part A: Polymer Chemistry* **1970**, 8, 3665-3666.

11.   Brock, T.; Sherrington, D. C.; Tang, H.G. *Polymer* **1991**, 32, 353 -357.

12.   Ashok Reddy, T.; Srinivasan, M. *Journal of Polymer Science, Part A: Polymer Chemistry* **1988**, 26, 1051-1061.

13.   Srinivasan, P. R.; Mahadevan, V.; Srinivasan, M. *Journal of Polymer Science, Part A: Polymer Chemistry* **1982**, 20, 3095-3105.

14.   Behzad Pourabas.; Ahmad Banihashemi. *Polymer International* **2002**, 51, 1086-1099.

15.   Yoshio Iwakura.; Keikichi Uno.; Yoshio Imai.; Motoo Fukui. *Die Makromolekulare Chemie* **1964**, 77, 41-50.

16.   Moriyuki Sato.; Masaaki Yokoyama. Journal *of Polymer Science, Part A: Polymer Chemistry* **1981**, 19, 591-594.

17.   Junhan Cho.; Min Su Park.; Jin Hyun Choi.; Byung Chul Ji.; Sung Soo Han.; Won Seok Lyoo. *Journal of Polymer Science, Part B: Polymer Physics*,  **2001**, 39, 1778-1783.

18.   Keikichi Uno.; Kazuma Niume.; Yasuhisa Iwata.; Fujio Toda.; Yoshio Iwakura. *Journal of Polymer Science Polymer Chemistry Edition* **1977**, 15, 1309-1318.

19.   Juan Antonia Asensio.; Salvador Borros.; Pedro, Gomez-Romero *Journal of Polymer Science, Part A: Polymer Chemistry*, **2002**, 40, 3703–3710

20.   Thaddeus E. Helminiak, *US Patent* 4377546, March 22, **1983**.

21.   Sansone.; Michael, J. Kwiatek.; Mark, S. (Hoechst Celanese Corp.). *European patent* 385687, September 5, **1990**.

22.   Eui W Choe.;  Randolph, N. J. (Celanese Corp.).*US Patent* 4579915, April 1, **1986**.

23.    Floyd D. Trischler. *US Patent* 3578644, May 11, **1971**.

24.    Sansone, Michael J. (Hoechst Celanese Corp.)*US Patent* 4814400, March 21, **1989**.

25.    Julien Jouanneau.; Regis Mercier .; Laurent Gonon.; Gerard Gebel. *Macromolecules* **2007**, 40, 983 -990.

26.    Xavier Glipa.; Mustapha EI Haddad.; Deborah J. Jones.; Jacques Roziere. *Solid State Ionics* **1997**, 97, 323-331.

27.    Songa, J. M.; Chab, S.Y.; Lee, W. M. *Journal of Power Sources* **2001**, 94, 78

28.    Vogel, H.A,; Marvel, C.S., *Journal of Polymer Science, Part A: Polymer Chemistry* **1961**, 50, 511-539.

29.    Chung TS. *J. Macromol. Sci.-Rev. Macromol. Chem. Phys.* **1997**, C37, 277-301.

30.    Yu-Han Teng,; George A. Kaminski,; Zhong-Biao Zhang,; Ajit Sharma,; Dillip K. Mohanty. *Polymer* **2006**, 47, 4004.

31.    Junhan Cho,; Min Su Park,; Jin Hyun Choi,;  Byung Chul Ji,; Sung Soo Han,; Won  Seoklyoo. *Journal of Polymer Science, Part B: Polymer Physics*  **2001**, 39, 1778.

32.    Gourdoupi, N.; Andreopoulou, A. K.; Deimede, V.; Kallitsis, K. *Chemistry of Materials* **2003**, *15*, 5044-5050.

# Chapter 3

Hydroxyl Group based Polybenzimidazole Copolymers for Proton Exchange Membrane Fuel Cell- Synthesis and Characterization

### 3.1 Introduction

Polybenzimidazoles have been considered as promising alternative materials for the fabrication of proton-exchange membranes, and a good number of publications have appeared on this topic [1-8]. These polymers present very good thermal stability [9] and proton conductivity, especially when "doped" or loaded with acids [10].

Among many possible polybenzimidazole derivatives, the polymer most extensively examined has been poly[2,2'-(m-phenylene)-5,5'-bibenzimidazole] (PBI) which is the only one commercially available. This material has been used for the fabrication of proton-exchange membranes for fuel cells using, both $H_2$ [11-12] and methanol [13] as fuels.

Several laboratories have concentrated on the synthesis and development of new polybenzimidazoles; as a result, a variety of polybenzimidazoles having different units and functional groups have been reported as proton-conducting membranes [14-17]. Following these developments, we have been interested in pursuing the synthesis of other novel materials belonging to this very promising family of proton conducting membranes. In particular, the introduction of hydroxyl groups seems of interest and has been performed by using hydroxyl group containing aromatic diacid. This approach is useful for the synthesis of similar polymers for different applications (such as $K^+$, $Na^+$, and $Li^+$ conducting polymers) [18-20].

Though, the proton conductivity of PBI, doped with phosphoric acid is high at high temperature, compared to Nafion, it has low proton conductivity at low temperature (30-90 °C). For many applications, high proton conductivity at low temperature is desired. PBI, doped with alkali hydroxides, such as, NaOH/KOH found to show high proton conductivity [20] comparable to Nafion, at low temperature. Similarly, PBI containing sulfonic acid groups, obtained by the reaction of (4- bromomethyl) benzene sulfonate, also found to exhibit high proton conductivity [21] on doping with alkali hydroxides. These results are promising for further investigations on alkali doped structurally modified PBI. Considering the capability of phenolic hydroxyl groups to generate ionic species with alkali hydroxide, it is worth studying as polymer electrolyte for fuel cell. Hydroxyl group in phenol is capable of interacting with phosphoric acid, imidazole group in PBI and alkali hydroxide. Hence, a comparative study of

PBI and PBI containing hydroxyl groups, doped with phosphoric acid and alkali hydroxide (KOH) is interesting.

Hydroxyl groups containing PBI, based on 2,5 dihydroxy terephthalic acid, doped with phosphoric acid is known to show high proton conductivity [22-23]. However, Para linked two hydroxyl groups, due to interaction with imidazole groups [24] form a kind of cross-links, rendering this polymer insoluble in any solvent. So, this polymer is processed into membranes by direct casting the solution in PPA after polymerization without precipitation.

To avoid such difficulties in membrane preparation and controlled doping, we opted for 5-hydroxy isophthalic acid (HIPA) containing single hydroxyl group in the molecule for the synthesis of PBI containing hydroxyl groups. A meta linkage in both conventional PBI and present hydroxyl group containing PBI is additional advantage for comparison.

Phenolic hydroxyl groups, being capable of interacting with both, phosphoric acid and alkali hydroxides, hydroxyl groups containing PBIs are expected to have good proton conductivity on doping with phosphoric acid and alkali hydroxides. A reactive hydroxyl groups also offers wide scope for linking other functional units for specific applications and improving miscibility with other polymers.

Thus, present work was undertaken to study the effect of hydroxyl groups, on properties of polybenzimidazole. Accordingly, the present work describes synthesis of hydroxyl group containing polybenzimidazoles having meta linkages, by the condensation of this diacid and varying mixture of this diacid and isophthalic acid or other commercial diacids with 3,3',4,4,'-tetra amino biphenyl (TAB) in polyphosphoric acid at high temperature to obtain novel homo and co-polybenzimidazoles containing free hydroxyl side groups and characterization of these polymers as potential candidate as polymer electrolyte for fuel cell applications.

### 3.2   Experimental

### 3.2.1   Materials

3,3',4,4,'-tetra amino biphenyl (TAB), 5-hydroxy isophthalic acid, isophthalic acid , terephthalic acid, pyridine 2, 6-dicarboxylic acid, adipic acid and sebacic acid were purchased from Aldrich Chemicals, USA. 5-hydroxy isophthalic, isophthalic acid, adipic acid and sebacic acid were purified by recrystallization from methanol. Terephthalic acid was purified by sublimation. Pyridine 2, 6-dicarboxylic acid was recrystallized from 1:1 water/HCl 3,3',4,4,'-tetra amino biphenyl (TAB) was recrystallized from water. N-methyl-2-pyrollidinone (NMP), N, N-dimethylacetamide (DMAc) and N, N-dimethyl formamide (DMF) were distilled over calcium hydride. Methanol, ortho phosphoric acid (85%), phosphorus pentoxide and potassium permanganate were purchased from s.d.fine-chem. Ltd and used without further purification. Polyphosphoric acid (PPA) was prepared by heating 1:1.8 weight ratio of ortho phosphoric acid (85%) and phosphorus pentoxide for 6 h at 100 °C.

### 3.2.2   Analytical methods

All the analytical methods used to characterize the polymer and polymer membranes are same as described in chapter 2.

### 3.2.3   Synthesis of new homo and co-polybenzimidazoles containing hydroxyl groups.

Polybenzimidazoles containing hydroxyl groups were synthesized by condensing 3,3',4,4,'-tetra amino biphenyl (TAB) with 5-hydroxy isophthalic acid (HIPA) (Scheme 3.1). Co-polybenzimidazoles having hydroxyl groups were synthesized by condensing TAB with a mixture of HIPA and other diacids namely 1) isophthalic acid(IPA)  2) adipic acid(AA) 3) sebacic acid(SA) 4) 2,5-pyridine dicarboxylic acid(PDA)   and 5) terephthalic acid(TPA)   (scheme 3.2) by using high temperature one step solution polycondensation technique in polyphosphoric acid. A typical procedure for high temperature solution polycondensation is described below.

### 3.2.3.1 Synthesis of polybenzimidazole having free hydroxyl groups

To a 100 mL three necked round bottom flask equipped with a mechanical stirrer, nitrogen gas inlet and a guard tube was added 2.0 g (9.334 mmol) of TAB and 80 g of polyphosphoric acid and the mixture was heated to 140 °C with stirring under a stream of nitrogen. After the complete dissolution of TAB, 1.70 g (9.334 mmol) of 5-hydroxy isophthalic acid was added slowly with stirring and the temperature of the reaction mixture was raised to 170 °C. The diacid dissolved in 1 h giving homogeneous solution. The solution was then heated to 200 °C and maintained at this temperature for 12 h. The resulting viscous solution was then cooled and poured into 500 mL water to precipitate the polymer as fiber. The polymer was then filtered, washed repeatedly with water and stirred in 10% aqueous $Na_2CO_3$ solution overnight to eliminate residual phosphoric acid. The polymer was then washed repeatedly with water to neutrality and heated in boiling water for 6 h, three times. The polymer was dried at 100 °C for 24 h and 150 °C for another 24 h in a vacuum oven. A brown fibrous polymer was obtained. Yield of the polymer was 97%. The inherent viscosity (I.V) of this polymer at 0.5 g.dL$^{-1}$ concentration, measured in DMSO at 30 °C was 1.09 dL g$^{-1}$.
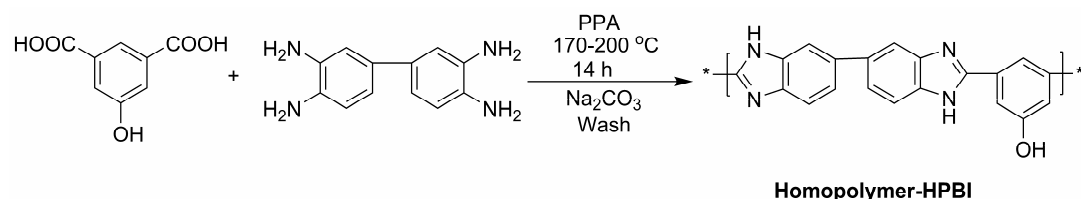


**Scheme 3.1** Synthesis of hydroxyl groups containing homo polybenzimidazole.

FT-IR (film, cm$^{-1}$): 1605 (C=N); 3395 (N–H stretching) 1609 (N–H deformation); 1010, 1220 (C-O stretching); 1536, 1447 (aromatic) (Figure-3.1).

$^1$H NMR [400 MHz, DMSO-d$_6$, ppm] showed signals of different protons at δ values of 13.22 (s, 2H, H$_a$); 10.22 (s, 1H, H$_b$); 8.60 (s, 1H, H$_c$); 8.10-7.60 (m, 8H, H$_{d-f}$) (Figure-3.4).

| Elemental analysis: | C% | H% | N% |
|---|---|---|---|
| **$C_{20}H_{12}N_4O$** | | | |
| Calculated: | 74.06 | 3.73 | 17.27 |
| Observed: | 73.11 | 3.9 | 16.72 |

**3.2.3.2 Synthesis of co-polybenzimidazole having a free hydroxyl groups with different diacids**

➢ **Synthesis of copolybenzimidazole HPBI-1 (HIPA 90%: IPA 10%)**

To a 100 mL three necked round bottom flask equipped with a mechanical stirrer, nitrogen gas inlet and a guard tube was added 2.0 g (9.334 mmol) of TAB and 20 g of polyphosphoric acid and the mixture was heated at 140 °C with stirring under a stream of nitrogen. After the complete dissolution of TAB, 1.53 g (8.400 mmol) of 5-hydroxy isophthalic acid and 0.155 g (0.933 mmol) isophthalic acid was added slowly with stirring. Then the temperature was raised to 170 °C, when diacid dissolved in 2 h giving homogeneous solution. The solution was heated to 200 °C and maintained at this temperature for 12 h. The resulting viscous solution was then cooled and poured into 500 mL water to precipitate the polymer as fiber. The polymer was then filtered, washed repeatedly with water and stirred with 10% aqueous $Na_2CO_3$ solution overnight to eliminate residual phosphoric acid.
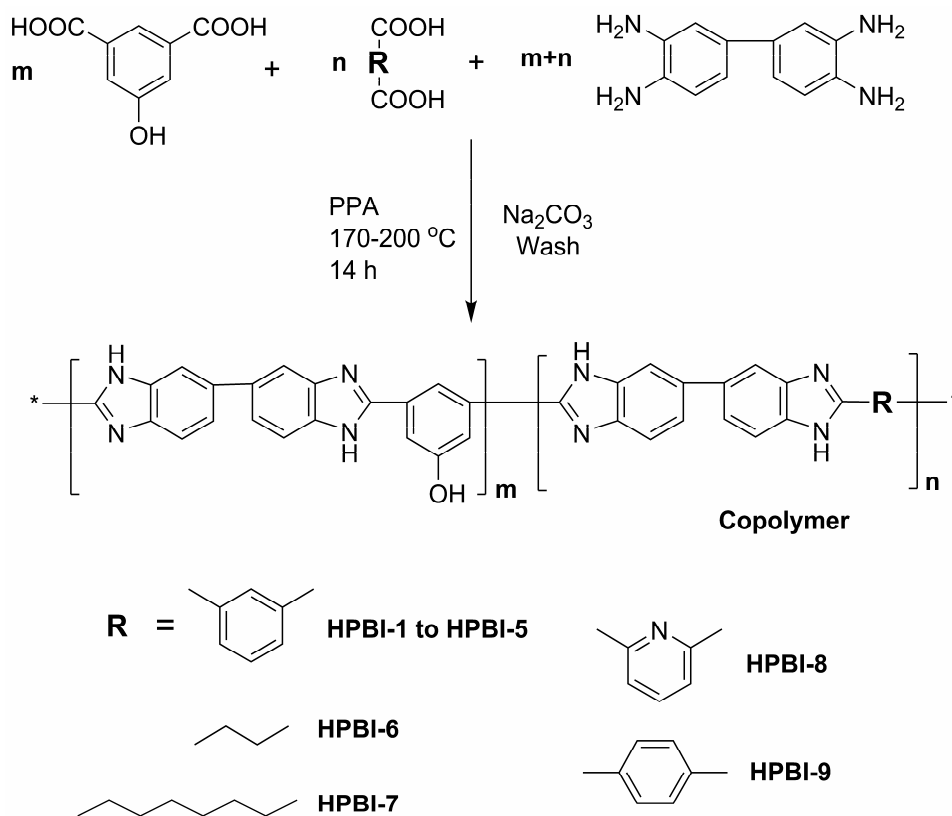


**Scheme 3.2** Synthesis of hydroxyl groups containing co-polybenzimidazoles.

The polymer was then washed repeatedly with water to neutrality and heated in boiling water for 6 h, three times. The polymer was dried at 100 °C for 24 h and 150 °C for

another 24 h. A brown fibrous polymer was obtained. Yield of the polymer was 98%. The inherent viscosity of this polymer, at 0.5 g.dL$^{-1}$ concentration, measured in DMSO at 30 ℃, was 1.03 dL g$^{-1}$. The ratio of 5-hydroxy isophthalic acid and isophthalic acid in this co-polybenzimidazole is 90:10 mol%.

Following the similar procedure co-polybenzimidazoles of HIPA and other diacids in different ratio were prepared with TAB. (tabulated in Table 3.1)

## 3.3   Results and discussion

### 3.3.1   Synthesis and structural characterization of polybenzimidazole and co-polybenzimidazoles having free hydroxyl groups

All the polybenzimidazole polymers containing hydroxyl groups were synthesized by solution polymerization in PPA by condensing TAB with HIPA or with a mixture of HIPA and isophthalic acid or other diacids as described in the experimental part (Scheme 3.1). PBIs containing different hydroxy content were prepared by condensing TAB with a mixture of HIPA and IPA in different mole ratio (90:10, 70:30, 50:50, 30:70, and 10:90) to study the effect of hydroxyl groups on properties of PBI. Few more new co-polybenzimidazoles containing hydroxyl groups with structural variations were synthesized, by condensing TAB with a mixture of 5-hydroxy isophthalic acid and other commercially available aromatic diacids such as terephthalic acid, pyridine 2,6 dicarboxylic acid, adipic acid, and sebacic acid in 50:50 mole ratio (Scheme-3.2) to study structure property relationship. Approximately 12 h heating is essential to form high molecular weight polymers and having inherent viscosity ~ 1dL/g. All the polymers remain soluble in polyphosphoric acid without precipitation although, they form viscous solutions, which on pouring in hot water form strong thread like structure.

Inherent viscosities were determined in DMSO (0.5 g.dL$^{-1}$ concentration at 30 ℃) using Ubbelhode viscometer. The values are observed to be high, in the range of 0.75-1.66 dL.g$^{-1}$. The I.V for homo polybenzimidazole of HIPA (HPBI) is 1.09 and for co-polybenzimidazoles of HIPA and IPA it is in the range of 1.03-1.66 dL.g$^{-1}$ (Table 3.1). All these polymers form tough and flexible films.

**Table 3.1**  Inherent viscosity and film nature of hydroxyl group containing polybenzimidazoles**.**

| Polymer Code | Diacids used (Mole ratio %) | Yield (%) | Inherent viscosity $\eta_{inh}$ (dL/g) | Film Color | Film Nature |
|---|---|---|---|---|---|
| HPBI | HIPA 100% | 97 | 1.09 | Brown | Flexible |
| HPBI-1 | HIPA / IPA 90:10 | 98 | 1.03 | Light brown | Flexible |
| HPBI-2 | HIPA / IPA 70:30 | 96 | 1.37 | Light brown | Flexible |
| HPBI-3 | HIPA / IPA 50:50 | 98 | 1.66 | Yellowish | Flexible |
| HPBI-4 | HIPA / IPA 30:70 | 97 | 1.40 | Yellowish | Flexible |
| HPBI-5 | HIPA / IPA 10:90 | 98 | 1.48 | Yellowish | Flexible |
| HPBI-6 | HIPA / AA 50:50 | 90 | 0.75 | Dark brown | Semi-flexible |
| HPBI-7 | HIPA / SA 50:50 | 92 | 0.90 | Light brown | Flexible |
| HPBI-8 | HIPA / PDA 50:50 | 95 | 1.10 | Yellowish | Flexible |
| HPBI-9 | HIPA / TPA 50:50 | 98 | 1.25 | Reddish | Flexible |

**HIPA:** 5-Hydroxy isophthalic acid, **IPA:** Isophthalic acid, **AA:** Adipic acid, **SA:** Sebacic acid, **PDA:** Pyridine dicarboxylic acid, **TPA:** Terephthalic acid.

The polymers, thus obtained, were characterized by FT-IR and ^{1}H NMR spectroscopy. FT-IR of all polymers was scanned using thin films. The FT-IR spectra of HPBI, PBI are shown in (Fig 3.1) The formation of polybenzimidazoles was confirmed by the characteristic absorption at 1602-1618 cm$^{-1}$ band due to C=N stretching of imidazole ring. Another characteristic band of breathing mode of imidazole ring appears in the range of 1283 -1287 cm$^{-1}$, which confirms the PBI formation.

The absorption band at 3188 -3195 cm$^{-1}$ is assigned to self-associated N-H interaction of PBI chains. Due to structural variations of these polymers these bands appear at different wavelength in the range mentioned. Absorption band at 1220 & 1010 cm$^{-1}$ are due to OH groups. Absorption band due to −OH group and −NH groups in imidazole appear as broad band at ~3300-3395 cm$^{-1}$. The Fig 3.2 shows FT-IR spectrum of co-PBI series of IPA and HIPA the intensity of band at 1220 cm$^{-1}$ due to hydroxyl group which decreases as hydroxy diacid percentage in co-PBI series of IPA decreases from 100 to 10%. The characteristic band of breathing mode of imidazole ring shifts from 1280 cm$^{-1}$ to 1290 cm$^{-1}$ as IPA% increases. The Figure-3.3 shows FT-IR spectrum of co-PBI series of HIPA and other commercial diacids such as adipic acid (HPBI-6), sebacic acid (HPBI-7), pyridine dicarboxylic acid (HPBI-8) and

terephthalic acid (HPBI-9). The spectrum of HPBI-6 and HPBI-7 shows characteristic peak of aliphatic C-H at 2930 cm$^{-1}$.
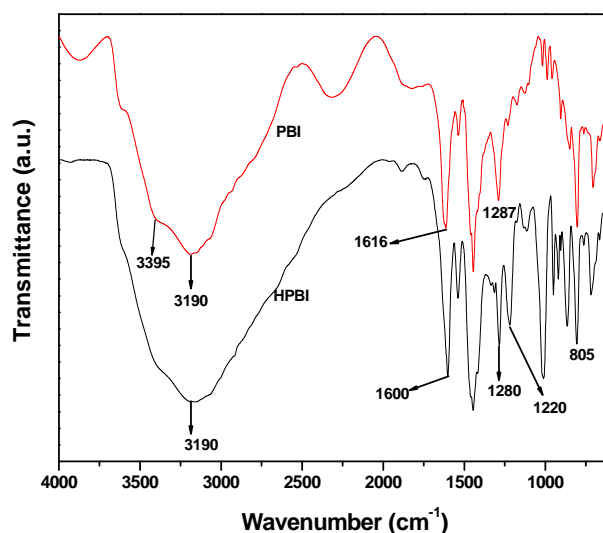


**Figure 3.1** FTIR spectrum of hydroxyl group containing polybenzimidazole compared with PBI
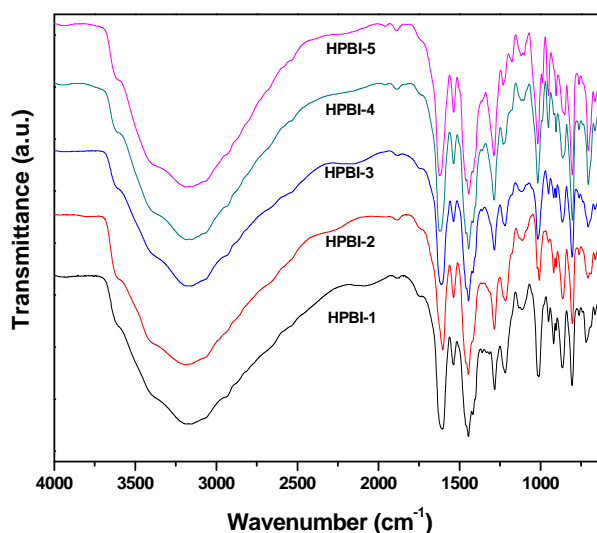


**Figure 3.2** FTIR spectrum of hydroxyl group containing polybenzimidazoles of IPA.

       Among the HPBI's synthesized from HIPA, only the $^1$H NMR spectrum of homopolymer (HPBI) was taken by dissolving polymer in DMSO-D$_6$. The $^1$H NMR spectrum of HPBI (Figure 3.4) showed proton at 13.22 δ assigned to hydrogen of N-H group of imidazole ring and proton at 10.19 δ to O-H group respectively which confirm the presence of benzimidazole groups and free hydroxyl groups in the polymer. The aromatic region showed

protons with expected multiples and integration at 7.6–8.6 δ due to the aromatic protons of both tetraamine and HIPA. The resolution of aromatic protons was not good in this case even though the spectrum was recorded on a 400 MHz NMR instrument. Thus, FTIR and $^1$HNMR confirm the structure of HPBI's.
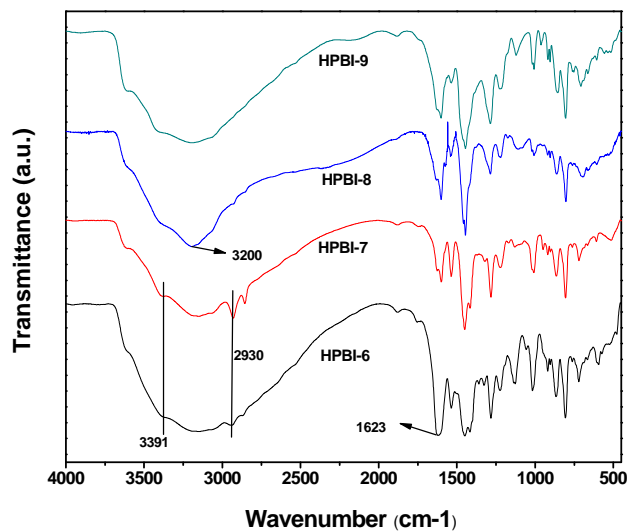


**Figure 3.3** FTIR spectrum of hydroxyl group containing polybenzimidazoles of other diacids.
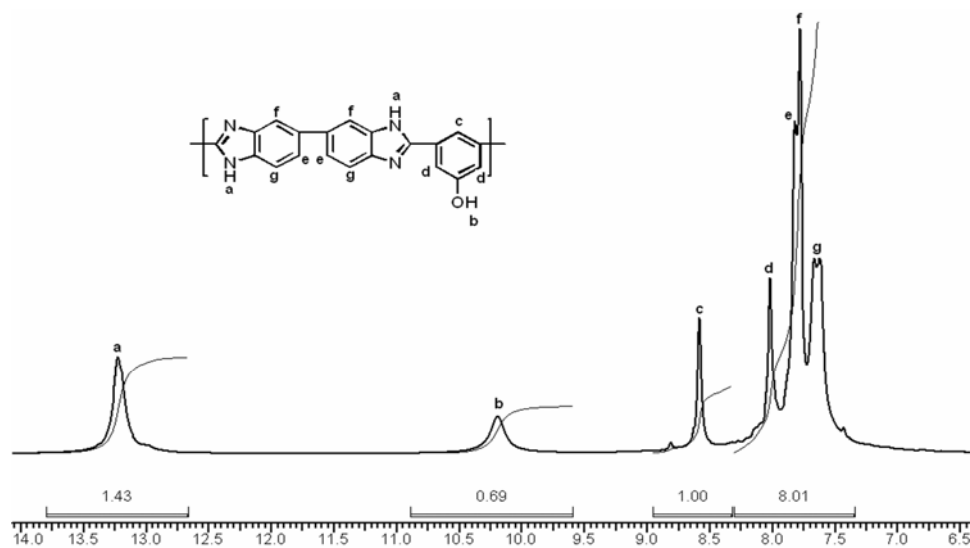


**Figure 3.4** $^1$H NMR spectrum of hydroxyl group containing polybenzimidazole (HPBI).

### 3.3.2 Properties of HPBI's

The properties of HPBI's were evaluated by solubility measurements, X-ray diffraction, DSC, TGA and mechanical property study.

### 3.3.2.1 Crystallinity

Crystalline nature of these polymer specimens (in film form) was studied by X-ray diffraction (Figure 3.5 and 3.6). No sharp peak for crystalline nature was observed. The amorphous nature of polybenzimidazoles could be attributed to their unsymmetrical structural units and the hydroxyl groups, which reduced the intra and interpolymer chain interactions, resulting in loose polymer chain packaging and aggregates.
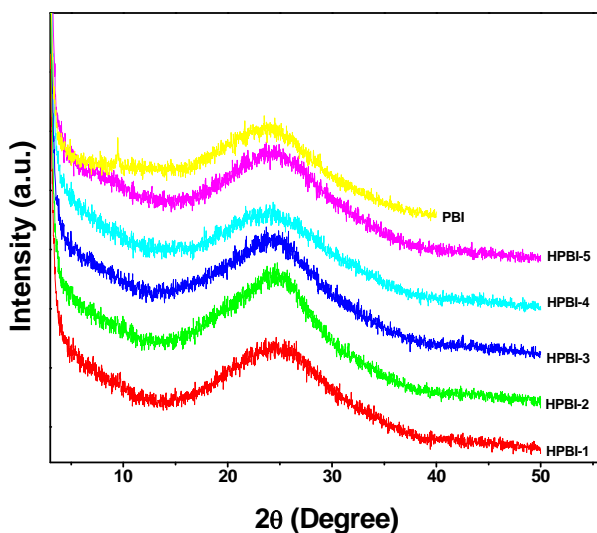


**Figure 3.5** Wide-angle X-ray diffractograms of hydroxyl group containing polybenzimidazoles of HIPA and IPA compared with PBI.
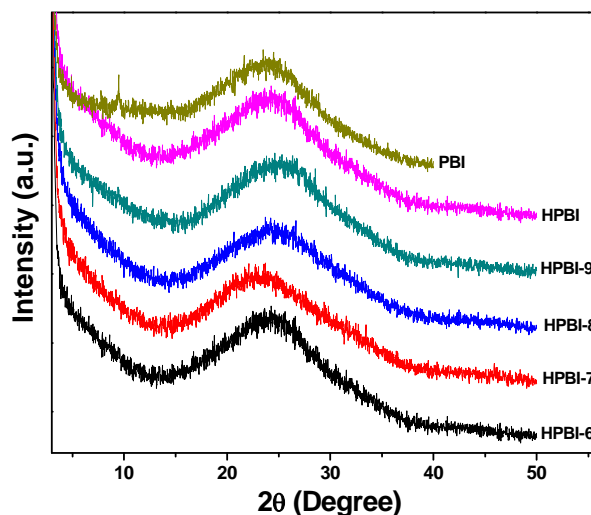


**Figure 3.6** Wide-angle X-ray diffractograms of hydroxyl group containing polybenzimidazoles of HIPA and different diacids compared with PBI.

**3.3.2.2 Solubility measurements**

The solubility of the HPBI's was studied quantitatively in various solvents and the results are shown in Table-3.2. PBI are rigid polymers with high softening point and polymer solubility plays a major role. Solubility behavior of newly synthesized polymers was studied by dissolving 4 mg of polymers in 0.5 mL solvent. Commercial PBI is soluble only in aprotic solvents such as DMAc, NMP and DMSO after heating at high temperature for several hours in presence of lithium chloride. The polymers under study displayed good solubility in strong acids such as $H_2SO_4$, trifluroacetic acid (TFA), formic acid, methane sulfonic acid etc. However, homopolymer (HPBI) is soluble in DMSO, but not soluble in DMAc, NMP. The co-polybenzimidazoles of IPA and HIPA are soluble in all polar aprotic solvents such as DMF, DMAc, NMP, DMSO, (Table 3.2) at ambient temp.

**Table 3.2** Solubility behavior of hydroxyl polybenzimidazole and co- polybenzimidazoles

| Polymer | Solvents | | | | | | | | |
|---------|-----|-----|-------|----------|-----|------|------|-----|-----|
| Code | TFA | MSA | HCOOH | $H_2SO_4$ | DMF | DMSO | DMAc | NMP | THF |
| HPBI | + | + + | + | + + | + | + + | - - | - - | - - |
| HPBI-1 | + + | + + | + | + + | + | + + | + + | + + | - - |
| HPBI-2 | + + | + + | + + | + + | + + | + + | + + | + + | - - |
| HPBI-3 | + + | + + | + + | + + | + + | + + | + + | + + | - - |
| HPBI-4 | + + | + + | + + | + + | + + | + + | + + | + + | - - |
| HPBI-5 | + + | + + | + + | + + | + + | + + | + + | + + | - - |
| HPBI-6 | + + | + + | + + | + + | - - | + + | - - | - - | - - |
| HPBI-7 | + + | + + | + + | + + | - - | + + | - - | - - | - - |
| HPBI-8 | + + | + + | + + | + + | + + | + + | + + | + + | - - |
| HPBI-9 | + + | + + | + + | + + | + - | + + | + - | + + | - - |
| PBI | + + | + | + + | + + | + | + | + | + | - - |

**+ +:** Soluble at room temperature, **+:** soluble on heating, **+ -:** swelling on heating and **- -:** insoluble on heating. **TFA:** Trifluro acetic acid, **MSA:** Methane sulfonic acid, **$H_2SO_4$:** Conc. sulfuric acid, **HCOOH:** Formic acid, **DMF:** N,N-dimethylformamide: **DMAc:** N,N-dimethyl acetamide, **DMSO:** Dimethyl sulfoxide, **NMP:** N-methyl-2-pyrrolidone, **THF:** Tetrhydrofuran.

The co-polybenzimidazoles of aliphatic acids and HIPA are not soluble in aprotic solvents such as DMAc, NMP and DMF but they are readily soluble in DMSO. HPBI-8 containing pyridine moiety has high solubility in aprotic solvents. All polymers are not soluble in common organic solvents such as chloroform, toluene, tetrahydrofuran, dioxane & acetic acid due to their polar nature.

### 3.3.2.3 Thermal properties of polymers

> **Thermogravimetric analysis**

The thermal stability of the hydroxyl group containing PBI, co-PBIs and the conventional PBI was analyzed by thermogravimetric analysis and the results are given in Table 3.3 and thermograms in Figure 3.7 and 3.8. HPBI's exhibited a two-step degradation pattern. The first step of degradation was observed between 300-400 °C due to the residual phosphoric acid as it forms ester linkage with hydroxyl group. [25] The second step at 540-627 °C indicates the decomposition of the polymer backbones.
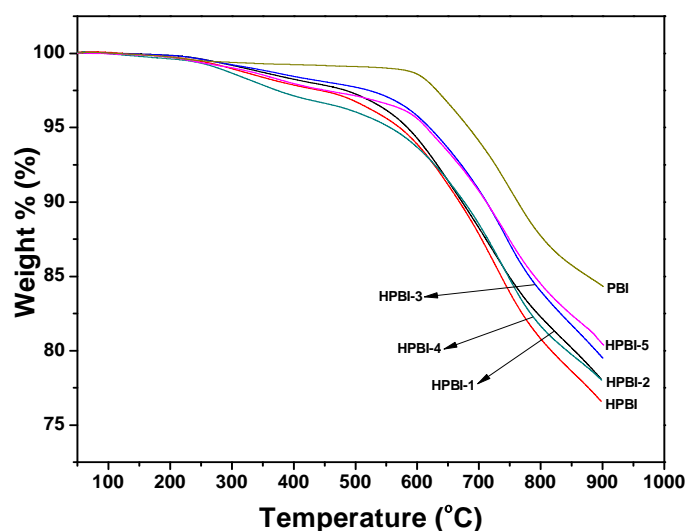


**Figure 3.7** TGA curves of hydroxyl group containing polybenzimidazoles of HIPA and IPA compared with PBI in $N_2$ at heating rate 10 °C $min^{-1}$.
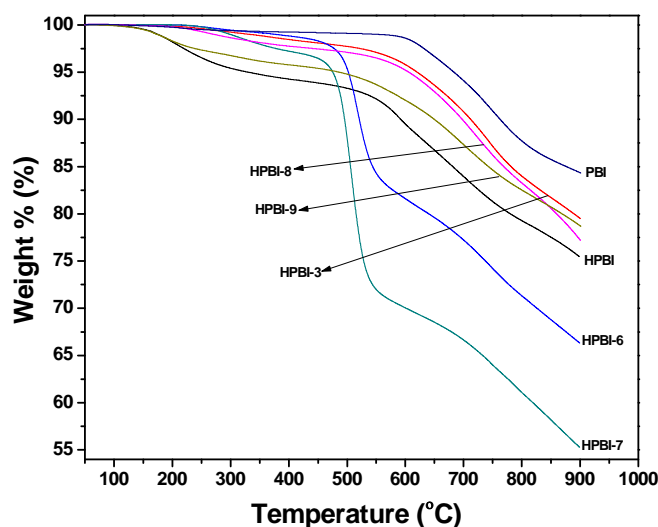


**Figure 3.8** TGA curves of hydroxyl group containing polybenzimidazoles of HIPA and different diacids compared with PBI in $N_2$ at heating rate 10 °C $min^{-1}$.

HPBI's showed slightly less thermal stability than the conventional PBI. For the conventional PBI, the onset for first step of degradation started around 600 °C. But the HPBI's showed an onset around 545 °C indicating their slightly less thermal stability than that of conventional PBI due to the presence of hydroxyl groups. However, thermal stability of synthesized hydroxyl group containing polybenzimidazoles is high enough for application as polymer electrolyte membranes for operation at high temperature.

**Table 3.3** Thermal properties of homo and co- polybenzimidazoles of HIPA

| Polymer Code | IDT (ºC) | $T_5$ (ºC) | $T_{10}$ (ºC) | $T_{max}$ (ºC) | Residue (wt %) | $T_g$ (ºC) |
|:---:|:---:|:---:|:---:|:---:|:---:|:---:|
| HPBI | 545 | 340 | 582 | 590 | 75 | 297 |
| HPBI-1 | 565 | 590 | 677 | 715 | 78.3 | 300 |
| HPBI-2 | 574 | 581 | 671 | 721 | 76.6 | 293 |
| HPBI-3 | 604 | 625 | 715 | 734 | 79.2 | 295 |
| HPBI-4 | 627 | 568 | 680 | 743 | 77.8 | 307 |
| HPBI-5 | 580 | 612 | 711 | 733 | 80.2 | 317 |
| HPBI-6 | 478 | 503 | 521 | 516 | 66.48 | 286 |
| HPBI-7 | 470 | 475 | 496 | 507 | 55.19 | 290 |
| HPBI-8 | 571 | 603 | 696 | 722 | 77.29 | 299 |
| HPBI-9 | 513 | 513 | 666 | 701 | 78.71 | 308 |
| PBI | 603 | 679 | 760 | 751 | 84.5 | 419 |

**IDT**: Initial decomposition temperature, $T_5$, $T_{10}$, and $T_{max}$: Temperature at which 5%, 10% and maximum weight loss of polymer takes place respectively, $T_g$: Glass transition temperature.

> ➢ **Glass transition temperature ($T_g$)**

PBI in general show high glass transition temperature due to rigid structure. Incorporation of functional groups in main chain is expected to lower $T_g$. Glass transition temperature of HIPA based PBIs was determined by differential scanning calorimeter (DSC) in nitrogen atmosphere at heating rate of 20 °C /min and the DSC thermograms of these polymers are shown in (Figure 3.9 & 3.10). All the HPBI polymers showed $T_g$ in the range of 280-320 °C, which are low as compared to the $T_g$ of conventional PBI. However, it may be noted that though polybenzimidazoles based on HIPA have low *$T_g$* values compared to commercial PBI, they are sufficient for applications in polymer electrolyte for fuel cell or membranes for separation technology at high temperature. These polymers also have sufficiently high thermal stability suitable for high temperature applications.
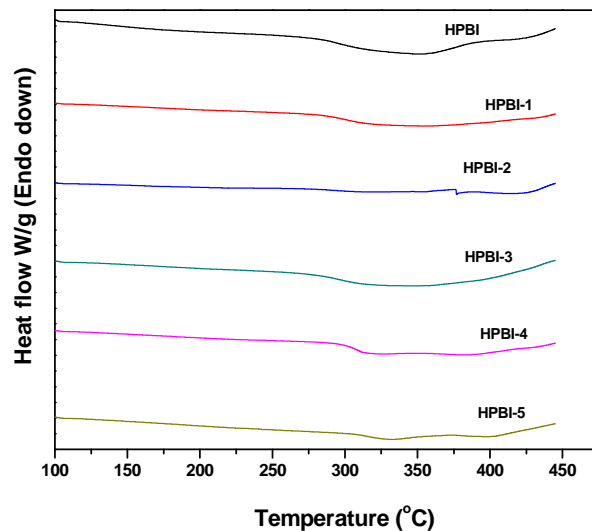
**Figure 3.9** DSC curves of hydroxyl group containing polybenzimidazoles of HIPA and IPA compared with PBI in $N_2$ at heating rate 20 °C min⁻¹.
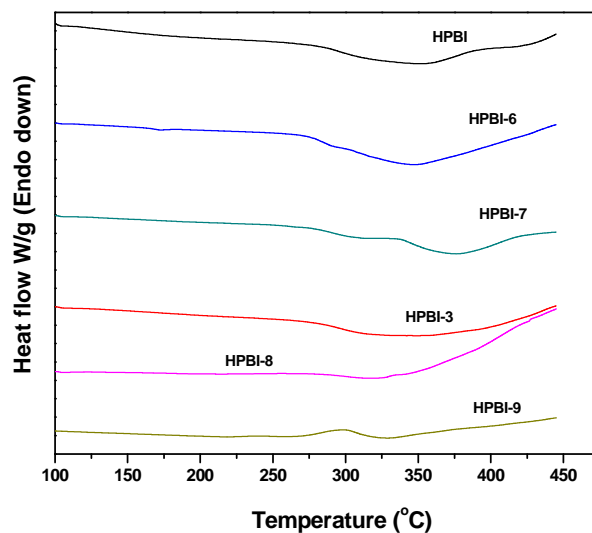


**Figure 3.10** DSC curves of hydroxyl group containing polybenzimidazoles of HIPA and different diacids compared with PBI in $N_2$ at heating rate 20 °C min⁻¹.

### 3.3.2.4 Mechanical properties of polymers

Polymer membranes should have good strength for applications such as polymer electrolyte for fuel cell or separation technology. Commercial PBI has superior mechanical properties due to rigid structure and any structural change is expected to affect mechanical properties. Commercial PBI has meta substituted phenyl rings in main chain where as, HIPA based PBI also has meta substituted phenyl ring in main chain and in addition, free hydroxyl

group attached to the phenyl ring. In the present study, it is observed that the free hydroxyl groups reduce the tensile strength of PBI from 151 MPa (PBI) to 130 MPa (HPBI) (Table 3.4), probably, due to disruption of rigid polymer structure by free hydroxyl group increasing free volume of the polymer.

**Table 3.4** Mechanical properties of hydroxyl group containing polybenzimidazoles.

| Polymer Code | Diacid used (mole ratio) | Tensile Stress (MPa) | Modulus (MPa) | Toughness (MPa) | Elongation at Break (%) |
|---|---|---|---|---|---|
| HPBI | HIPA **100** | 130 | 4410 | 24.73 | 8.97 |
| HPBI-1 | HIPA / IPA **90:10** | 94 | 4629 | 49.14 | 18.07 |
| HPBI-2 | HIPA / IPA **70:30** | 125 | 4270 | 38.50 | 16.36 |
| HPBI-3 | HIPA / IPA **50:50** | 121 | 4178 | 69.12 | 32.61 |
| HPBI-4 | HIPA / IPA **30:70** | 104 | 4239 | 38.50 | 20.13 |
| HPBI-5 | HIPA / IPA **10:90** | 117 | 4532 | 37.90 | 16.17 |
| HPBI-6 | HIPA / ADA **50:50** | 62 | 2640 | 10.58 | 9.59 |
| HPBI-7 | HIPA / SA **50:50** | 90 | 3003 | 12.29 | 8.26 |
| HPBI-8 | HIPA / PDA **50:50** | 84 | 4105 | 25.75 | 15.51 |
| HPBI-9 | HIPA / TPA **50:50** | 93 | 2445 | 41.51 | 25.44 |
| PBI | IPA **100** | 151 | 3771 | 5.77 | 6.28 |
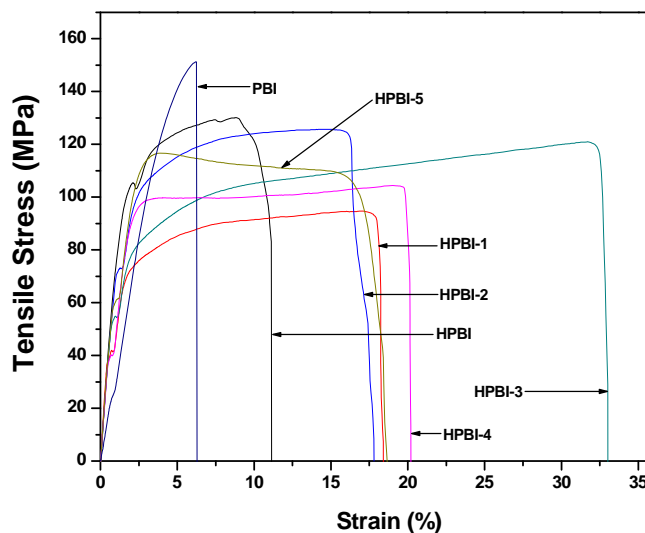


**Figure 3.11** Tensile stress verses Strain graph of hydroxyl group containing polybenzimidazoles of HIPA and IPA compared with PBI.

Tensile properties of co-PBIs of HIPA and IPA (Figure-3.11) reveals that addition of different mole % IPA to HIPA reduces the tensile strength further, probably due to disruption of

regular polymer structure of PBI. Modulus of HPBI's is higher than PBI, except for HPBI-6, 7 & 9. Thus, modulus of polybenzimidazole of HIPA (HPBI) is 4410 MPa and modulus of co-polybenzimidazole containing different mole % of IPA decreases from 4100 MPa to 4600 MPa compared to 3770 MPa of PBI. Both tensile strength and modulus of PBI of aliphatic acids is low. Compared to PBI and HPBI the toughness of all copolybenzimidazoles of HIPA and IPA are higher. Highest toughness of 69.12 MPa is shown by HPBI-3. No particular trend was observed in tensile properties of HPBI's.
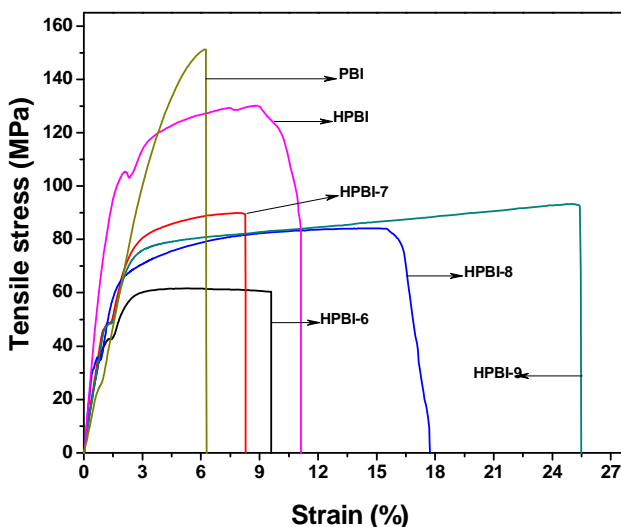


**Figure 3.12**  Tensile stress verses Strain graph of hydroxyl group containing polybenzimidazoles of HIPA and  different diacids compared with PBI.

Tensile properties of co-PBIs of HIPA and other diacids also show slightly low tensile strength as compared to PBI. HPBI-6 containing adipic acid shows lowest tensile stress of 62 MPa, this may be due to the low inherent viscosity of HPBI-6. While, other polymers HPBI-7, HPBI-8 and HPBI-9 show tensile strength in range of 80-95 MPa (Figure-3.12). These results indicate that the structural change in diacid monomers has significant effect on mechanical properties of copolymers. Chemical structure of acids used for the synthesis of PBI also has effect on mechanical properties of co-polybenzimidazoles (Figure-3.12). Thus mechanical properties of copolybenzimidazoles depend on chemical composition of polymer. Though mechanical properties of HPBI's are low compared to PBI, observed properties are high enough for many applications.

### 3.3.3    Fuel cell Characterization of hydroxyl group containing PEM
### 3.3.3.1 oxidative stability study

Fenton reagent test was carried out with HPBI's and commercial PBI to examine the radical oxidative stability of these polymer membranes. The membranes (thickness: 40-60 μm) were soaked in 3% $H_2O_2$ containing 4 ppm $Fe^{2+}$ (Mohr's salt, $(NH_4)_2Fe(SO_4)_2 \cdot 6H_2O$) at 70 °C for 12 h and the stability was determined by the weight loss of the membranes. Same sample was used upto 96 h by replacing Fenton reagent solution after every 12 h with fresh solution.
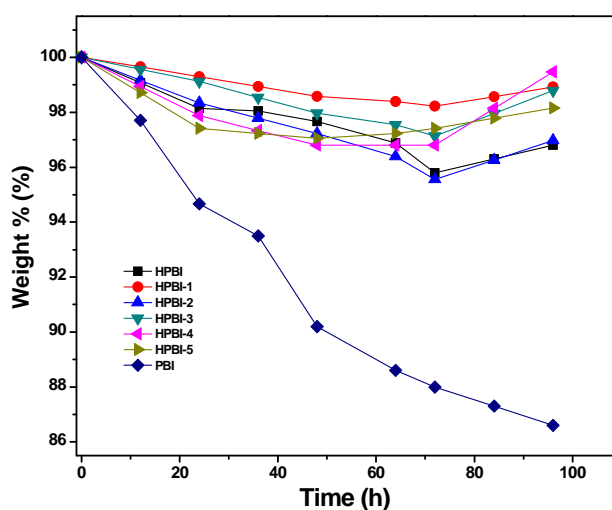


**Figure 3.13** Oxidative stability expressed as weight loss in Fenton's test of hydroxyl group containing -polybenzimidazole of HIPA and  IPA compared with PBI.

It may be observed from Figure-3.13, that HPBI's of IPA, showed low weight loss after the Fenton reagent test for 96 h. Films were still very tough indicating excellent oxidative stability of these membranes. Hydroxyl group containing HPBI's showed 3-4 % weight loss after the 96 h of Fenton reagent test while commercial PBI showed 13 % weight loss after the 96 h of Fenton reagent test and they were still very tough indicating excellent oxidative stability of these membranes as compared to commercial PBI.

Figure-3.14 shows the oxidative stability of hydroxyl group containing polybenzimidazoles with other diacids. HPBI-6 containing adipic acid shows 12 % wt loss after 96 h in Fenton reagent test high wt loss is due to the presence of short aliphatic chains, which degrade fast and form small fragments. Weight loss in case of aromatic HPBI-8 and HPBI-9 is 5%. High oxidative stability of hydroxyl group containing PBI may attribute to

radical scavenging property of phenol. It may be noted that after certain period in Fenton reagent some weight gain is observed instead of loss cause for which is not known.
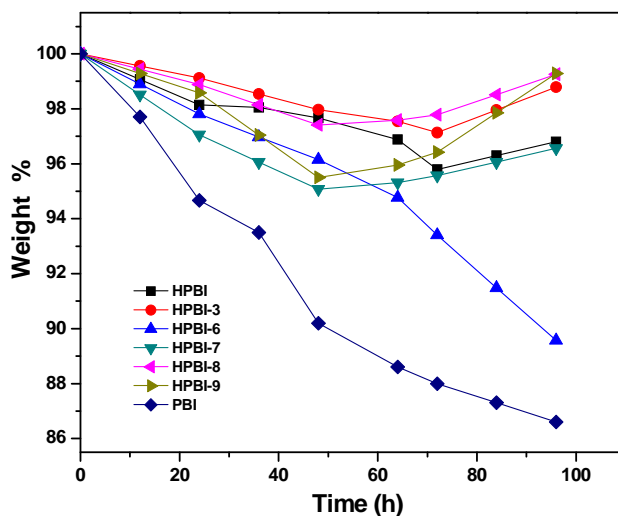


**Figure 3.14** Oxidative stability expressed as weight loss in Fenton's test of hydroxyl group containing polybenzimidazoles of HIPA and different diacids compared with PBI.

### 3.3.3.2 Alkali (KOH) doping study

Doping of PBI with strong alkali, such as, LiOH, NaOH and KOH is well documented and PBI doped with 6 molar KOH showed highest ionic conductivity. [20] So, HPBI's in the present study were doped with 6M KOH solution at ambient temperature by immersing weighed membranes in aqueous 6M KOH solution for 10 days. Membranes were weighed again after withdrawing from KOH solution and wiping adhered solution. The water uptake along with KOH was determined by formula (eqn no.1)

$$\text{Water uptake}\,[\%] = \frac{W_{wet} - W_{dry}}{W_{dry}} \times 100 \qquad\qquad [1]$$

Where, $W_{wet}$ is the weight of the sample after removing from KOH solution and $W_{dry}$ is the weight of the dried sample after removing from KOH solution. These membranes were dried under vacuum at 120 °C for 24 h till constant weight was obtained. The KOH uptake sample was determined by the equation (eqn no. 2),

$$\text{KOH uptake}\,[\%] = \frac{W'_{dry} - W_{dry}}{W_{dry}} \times 100 \qquad\qquad [2]$$

Where $W_{dry}$ is the weight of the dried sample before immersing in KOH solution and $W'_{dry}$ is the weight of KOH dope sample after vacuum drying.

Table-3.5 shows water uptake along with KOH and only KOH uptake of HPBI's in comparison with PBI. The highest uptake of KOH (398 wt%) and water (769 wt%) is shown by HPBI having highest hydroxyl groups. Compared to PBI, all HPBI's show high water and KOH uptake values, which increase with increase in hydroxyl groups in the polymer. Thus, acidic and hydrophilic phenolic hydroxyl groups enhance both KOH and water uptake.

**Table 3.5** KOH doping level with and without water in wt% of doped PBI and HPBI's at RT.

| Polymer Code | Doping level of KOH with water (wt%) | Doping level of dry KOH (wt%) | Water uptake (wt%) |
|:---:|:---:|:---:|:---:|
| HPBI | 1167 | 398 | 769 |
| HPBI-1 | 750 | 300 | 350 |
| HPBI-2 | 360 | 183 | 177 |
| HPBI-3 | 274 | 150 | 124 |
| HPBI-4 | 259 | 144 | 115 |
| HPBI-5 | 222 | 132 | 90 |
| PBI | 220 | 140 | 86 |

### 3.3.3.3 Conductivity measurement of alkali (KOH) doped HPBI's

For the conductivity measurements, HPBI-2, HPBI-3, HPBI-4, HPBI-5 and PBI films were doped in 6 molar of KOH solution for 10 days, while, HPBI and HPBI-1 films were doped in 3 molar of KOH solution for 24 h to control KOH uptake low (~130 wt%) for comparison with PBI. The dope films were used as such without drying as alkaline conductivity is water dependant. Temperature dependant conductivity of alkali doped polymer films was determined by the same method used for proton conductivity measurements of phosphoric acid doped films as described in experimental part in chapter 2 in the temperature range of 30 to 110 °C under 85 % humidity. Figure-3.15 represents the conductivity vs. temperature graph. The HPBI's films exhibit high proton conductivities compared to that of PBI. Specifically, HPBI-2 shows high conductivity ($5.6 \times 10^{-2}$ S.cm$^{-1}$) followed by HPBI-3 ($5.1 \times 10^{-2}$ S.cm$^{-1}$) and HPBI-1 ($4.1 \times 10^{-2}$ S.cm$^{-1}$) at 90 °C. Interestingly, these values are more than that obtained for PBI ($1.0 \times 10^{-2}$ S.cm$^{-1}$) at 90 °C.
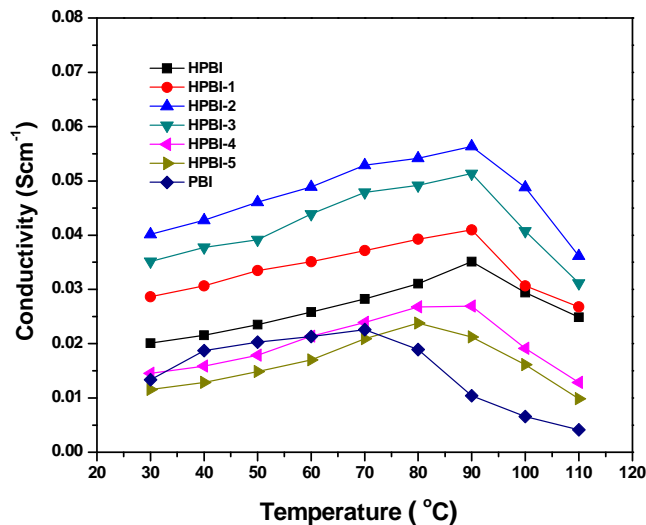
**Figure 3.15** Conductivities of alkali doped(KOH) hydroxyl group containing polybenzimidazoles of HIPA and IPA compared with PBI at different temperature.

  High proton conductivities of alkali doped HPBI's can be attributed to presence of free hydroxyl groups in polymer which after doping with the KOH form phenolate ions and generate $^-$OH ions responsible for alkaline conductivity. High conductivity of HPBI even at low doping level (120 wt%) compared to PBI with higher doping level (140 wt%) indicate that hydroxyl groups enhance conductivity. Another interesting feature of KOH-doped HPBI's is that their conductivity increases upto 90 °C, while conductivity of KOH doped PBI, start decreasing after 70 °C. It appears that OH groups hold water upto 90 °C, while PBI starts loosing water above 70 °C. Thus, incorporation of hydroxyl groups in PBI enhances alkaline conductivity significantly. From the results in Table 5.6, it appears that conductivity of HPBI could be enhanced still further by increasing doping level.

**Table 3.6** Proton conductivity and doping level in wt% and mol/repeat unit of KOH doped hydroxyl group containing polybenzimidazoles compared with PBI at 90 °C

| Polymer Code | Doping level of dry KOH (wt %) | Doping level of dry KOH (mole) | $\sigma_{max}$ (S cm$^{-1}$) |
|:---:|:---:|:---:|:---:|
| HPBI | 120 | 6.94 | $3.5 \times 10^{-2}$ |
| HPBI-1 | 130 | 7.48 | $4.1 \times 10^{-2}$ |
| HPBI-2 | 183 | 10.48 | $5.6 \times 10^{-2}$ |
| HPBI-3 | 150 | 8.45 | $5.1 \times 10^{-2}$ |
| HPBI-4 | 144 | 8.04 | $2.7 \times 10^{-2}$ |
| HPBI-5 | 132 | 7.29 | $2.1 \times 10^{-2}$ |
| PBI | 140 | 7.70 | $1.0 \times 10^{-2}$ |

### 3.3.3.4 Phosphoric acid doping study

The acid uptake capacity of newly synthesized polymers was determined by doping membranes of HPBI's and commercial PBI in various molar concentrations of $H_3PO_4$ solutions for 48 h at room temperature. It is well known that PBI is generally doped in the 85% $H_3PO_4$ at room temperature, so we also studied the time dependant doping of HPBI's and PBI in the 85% $H_3PO_4$ at room temperature for 110 h to study the effect of time on doping level. The doping level is expressed as the wt% of $H_3PO_4$ of the polymer or copolymers. Compared to PBI, HPBI's of IPA show low acid uptake in all concentration of acid as shown in Figure-3.16. The acid uptake is slow upto 10M $H_3PO_4$ solution, although a steady increase in acid uptake with increase in concentration is observed. The acid uptake of HPBI's is in the range of 143-295 wt% of $H_3PO_4$ of the polymer in 10M $H_3PO_4$ compared to 320 wt% for PBI. The acid uptake increases in higher molar phosphoric acid. Thus, in 14M $H_3PO_4$ solution the acid uptake of HPBI's in the range of 240-345 wt% of $H_3PO_4$ of the polymer compared to 380 wt% for PBI. The homopolymer, HPBI shows lowest acid uptake of 242 wt% of $H_3PO_4$ of the polymer. Thus phenolic OH groups reduce $H_3PO_4$ uptake of PBI.

In case of co-polybenzimidazoles of HIPA and other diacids acid uptake of HPBI-6 and HPBI-7 containing aliphatic groups, is higher, 550 and 320 wt% of $H_3PO_4$ respectively, compared to HPBI-8 and HPBI-9 (Figure-3.17).
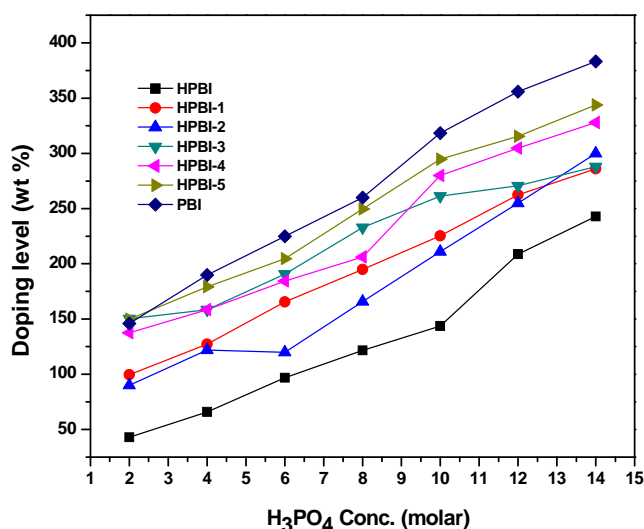


**Figure 3.16** Doping level of phosphoric acid (wt% of $H_3PO_4$) in polymers as a function of the $H_3PO_4$ concentration for hydroxyl group containing polybenzimidazoles of HIPA and IPA compared with PBI.
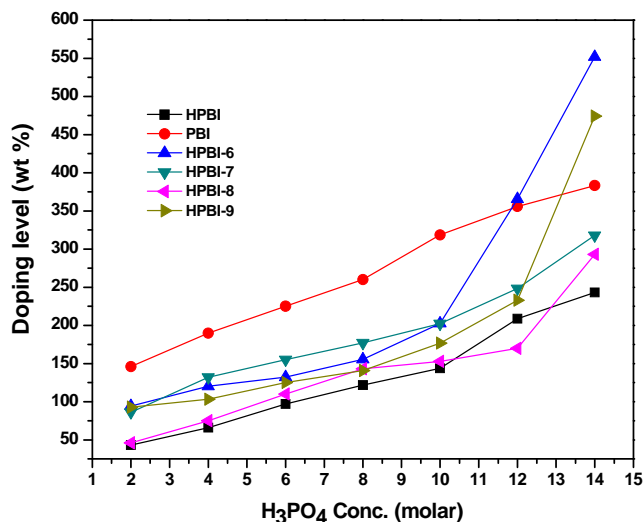
**Figure 3.17** Doping level of phosphoric acid (wt% of $H_3PO_4$) in polymers as a function of the $H_3PO_4$ concentration for hydroxyl group containing polybenzimidazoles of HIPA and other diacids compared with PBI.
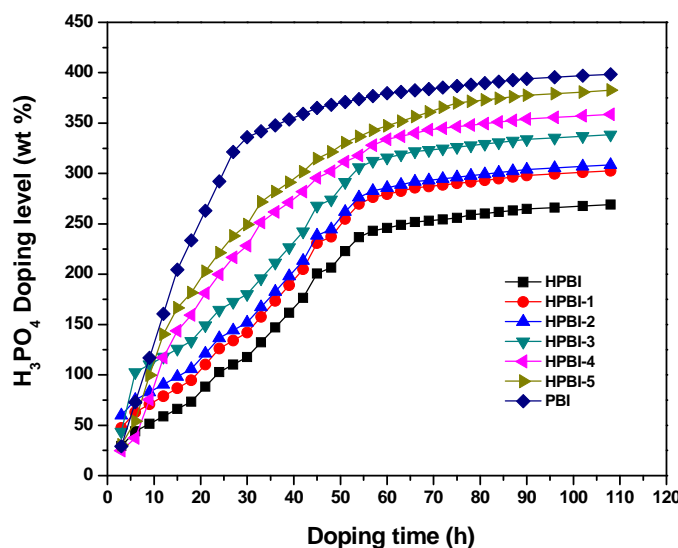


**Figure 3.18** Time dependant doping level of hydroxyl group containing polybenzimidazole of HIPA and IPA compared with PBI in 85% $H_3PO_4$ at room temperature.

This is further substantiated by the time dependant acid uptake study in 85% $H_3PO_4$ solution in Figure-3.18 & 3.19 In case of PBI, a steady increase in acid uptake with time upto 24-27 h and saturation thereafter is observed. Whereas, acid uptake in HPBI's is comparatively slow and saturation point is reached after 45-50 h. The acid uptake in copolymers increases with increase in IPA content in polymer. Thus, acid uptake of membranes of HPBI's is low and slow compared to PBI. Low acid uptake of hydroxyl group

containing PBI is, presumably, due to the formation of phosphonic ester with hydroxyl groups which inhibits easy access for the diffusion of phosphoric acid in polymer matrix. After confirming the good doping level and stability of membranes of HPBI's in 85% phosphoric acid, the membranes for the proton conductivity study were doped with 85% phosphoric acid.
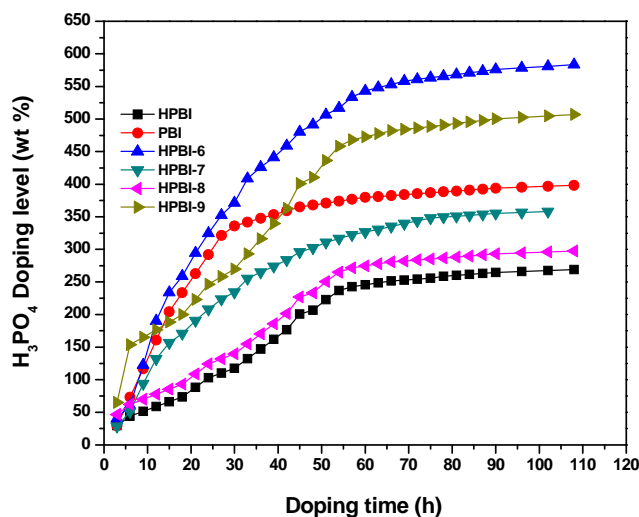


**Figure 3.19** Time dependant doping level of hydroxyl group containing polybenzimidazoles of HIPA and other diacids compared with PBI in 85% $H_3PO_4$ at room temperature.

### 3.3.3.5 Proton conductivity measurement

For the proton conductivity measurements, HPBI's and PBI films were doped with 85% $H_3PO_4$ for 50 h and dried under vacuum for 24 h at 110 °C. Temperature dependant conductivity of doped polymer films was determined in the temperature range of 25 to 175 °C as described in experimental part of chapter 2. Figure-3.20 represents the conductivity vs. temperature graph. The HPBI's membranes exhibit high proton conductivities compared to that of PBI. Specifically, HPBI shows high conductivity ($5.6 \times 10^{-2}$ S.cm$^{-1}$) followed by HPBI-1 ($4.6 \times 10^{-2}$ S.cm$^{-1}$) and HPBI-2 ($4.20 \times 10^{-2}$ S.cm$^{-1}$) at 175 °C. Interestingly, these values are more than that obtained for PBI ($3.24 \times 10^{-2}$ S.cm$^{-1}$) at 175 °C.

High proton conductivities of HPBI's at near about same phosphoric acid doping level as of PBI are probably, due to the formation of phosphonic ester with hydroxyl groups. Bonded phosphoric acid to the hydroxyl groups increase the protonating sites in the polymer matrix and help in fast proton transport in HPBI, which explains observed high proton conductivity in HPBI. Interestingly, the copolymers of IPA show decrease in conductivity as

IPA % in polymer increases. While the copolymer HPBI-6 and HPBI-7 of aliphatic acids (Figure 3.21) show less proton conductivity though they have more acid uptake as compared to other HPBI's. Thus, incorporation of hydroxyl groups in PBI enhances proton conductivity significantly.
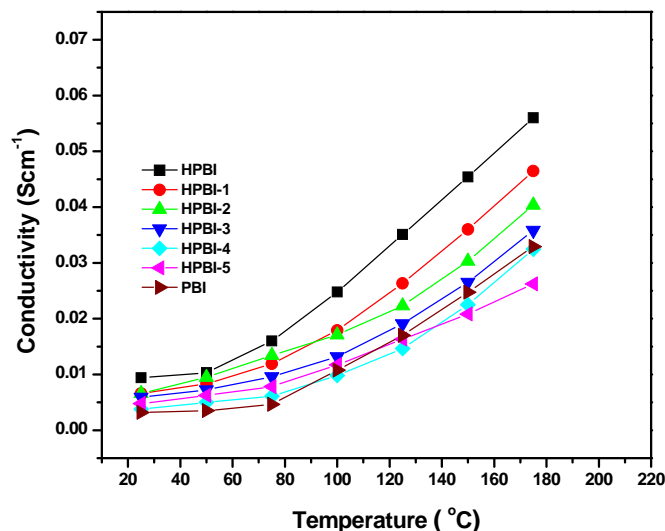


**Figure 3.20** Proton conductivities of hydroxyl group containing polybenzimidazoles of HIPA and  IPA compared with PBI  at different temperature.

Thus, PBI containing phenolic hydroxyl groups possess good thermal stability, good mechanical properties, high oxidative stability and high proton conductivity on doping with KOH and phosphoric acid suitable for low and high temperature application respectively, as polymer electrolyte for PEMFC.
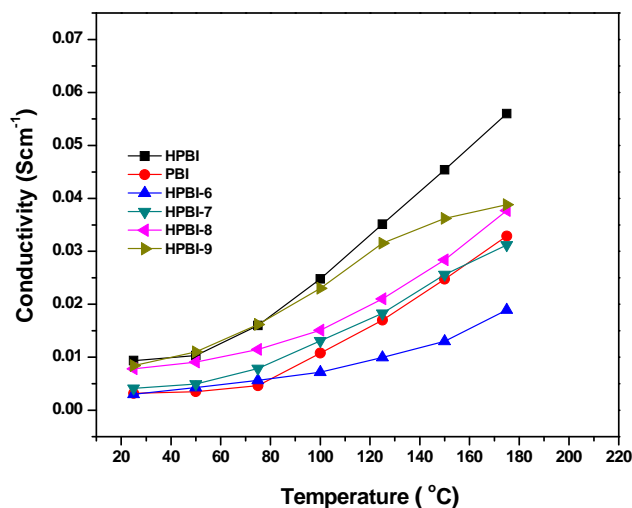


**Figure 3.21** Proton conductivities of hydroxyl group containing polybenzimidazoles of HIPA and  other diacids compared with PBI  at different temperature.

**Table 3.7** Proton conductivity and Doping level in wt% and mol/repeat unit of hydroxyl group containing polybenzimidazoles of HIPA compared with PBI at 175 °C.

| Polymer Code | Doping level of $H_3PO_4$ (wt %) | Doping level of $H_3PO_4$ (mole) | $\sigma_{max}$ (S cm$^{-1}$) |
|---|---|---|---|
| HPBI | 240 | 8.94 | $5.6 \times 10^{-2}$ |
| HPBI-1 | 250 | 8.23 | $4.6 \times 10^{-2}$ |
| HPBI-2 | 255 | 8.29 | $4.0 \times 10^{-2}$ |
| HPBI-3 | 260 | 8.39 | $3.6 \times 10^{-2}$ |
| HPBI-4 | 265 | 8.47 | $3.2 \times 10^{-2}$ |
| HPBI-5 | 265 | 8.38 | $2.6 \times 10^{-2}$ |
| HPBI-6 | 340 | 10.93 | $1.9 \times 10^{-2}$ |
| HPBI-7 | 361 | 12.65 | $3.1 \times 10^{-2}$ |
| HPBI-8 | 250 | 8.06 | $3.7 \times 10^{-2}$ |
| HPBI-9 | 300 | 9.41 | $3.8 \times 10^{-2}$ |
| PBI | 280 | 8.92 | $3.3 \times 10^{-2}$ |

### 3.3.3.6 Membrane electrode assembly fabrication

The electrodes with a gas diffusion layer and a catalyst layer were fabricated by following the same procedure as mention in section 2.3.4.4. A polymer electrolyte membrane, HPBI (90 μm) was doped in 85% $H_3PO_4$ for 48 h was wiped out by tissue paper and dried at 100 °C under vacuum. The membrane and electrode assemblies (MEAs) were made by hot-pressing the pretreated electrodes (9 cm$^2$) and the membrane under the conditions of 120 °C, 130 atm for 3 min.

### 3.3.3.7 Polarization study

Figure 3.22 shows the fuel cell performance of HPBI membrane in terms of polarization plots of MEA fabricated using 20% Pt/C for both anode and cathode in a single cell experiment , at 100, 125 and 150 °C with a dry $H_2/O_2$ gas flow rate of 0.4 slpm (standard liters per minute). HPBI membrane show better performance than that of the PBI membrane. The open-circuit voltage (OCV) obtained with the HPBI membrane is 0.92 V at 150 °C, whereas for PBI also it is 0.92 V. However, the activation loss and ohmic loss (which are much more important for sustaining a large current density) in the case of the HPBI membrane are considerably lower than those of PBI. For example, the HPBI membrane gives a maximum power density 238 mW/cm$^2$ at 0.3 V, whereas the PBI membrane gives 210 mW/cm$^2$ at 0.3 V. This better fuel cell performance of HPBI membrane can be attributed to bonded phosphoric

acid to the hydroxyl groups increases the protonating sites in the polymer matrix and help in fast proton transport in HPBI which explains observed fuel cell performance of HPBI.
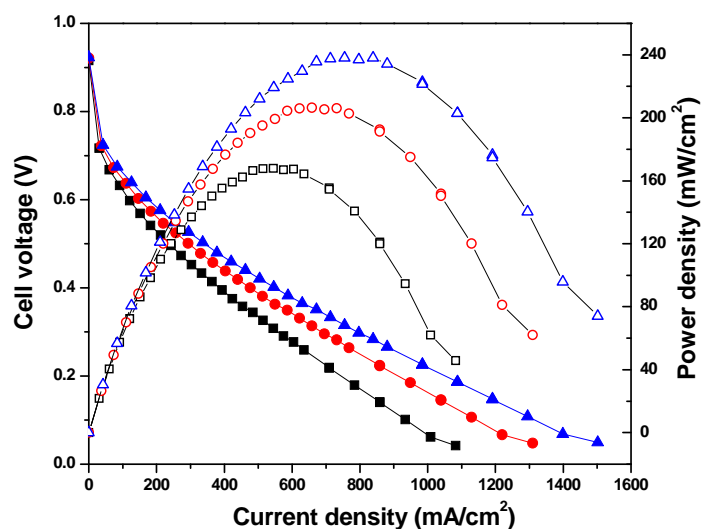


**Figure 3.22**   Polarization curves obtained with HPBI membrane fuel cell at different temperatures with dry $H_2$ and $O_2$ (flow rate 0.4 slpm). The cell was conditioned for 30 min at open-circuit potential and at 0.2 V for 15 min before measurements. Key: (■□) 100, (●○) 125 and (▲△) 150 °C.

## 3.4   Conclusions

- New series of polybenzimidazoles having free hydroxyl groups were synthesized from m-phenylene diacid namely 5-(hydroxy) isophthalic acid with 3,3',4,4,'-tetra amino biphenyl (TAB) and other commercial diacids using high temperature solution polycondensation in PPA.

- Most of these polymers were soluble in a wide range of solvents like NMP, DMSO, TFA, $H_2SO_4$, methane sulfonic acid.

- Incorporation of free hydroxyl groups, though reduces the thermal stability of these polymers to some extent compared to PBI, they exhibited reasonably good thermal stability suitable for high temperature applications.

- Hydroxyl groups improve the oxidative stability of polymers, as compared to the commercial PBI as hydroxyl groups act as radical quencher.

- Hydroxyl groups improve the proton conductivity of polymers as it forms phosphonic ester after doping with phosphoric acid, and increase the protonating sites in the polymer matrix and help in fast proton transport in HPBI as compared to the commercial PBI.

- KOH doped HPBI and $H_3PO_4$ doped HPBI have high proton conductivity compared to PBI and they are suitable as polymer electrolyte for PEMFC.

## References

1. Fontanella, J. J.; Wintersgill, M. C.; Wainright, J. S.; Savinell, R. F.; Litt, M. *Electrochim Acta* 1998, **43**, 1289-1294.

2. Bouchet, R.; Siebert, E. Solid State Ionics 1999, **118**, 287-299.

3. Xing, B.; Savadogo, O. *J New Mater Electrochem Systems* 1999, **2**, 95-101.

4. Kawahara, M.; Morita, J.; Rikukawa, M.; Sanui, K.; Ogata, N. *Electrochim Acta* 2000, **45**, 1395-1398.

5. Kawahara, M.; Rikukawa, M.; Sanui, K. *Polym Adv Technol* 2000, **11**, 544-547.

6. Glipa, X.; Bonnet, B.; Mula, B.; Jones, D. J.; Roziere, J. *J Mater Chem* 1999, **9**, 3045-3049.

7. Litt, M.; Ameri, R.; Wang, Y.; Savinell, R.; Wainwright, *J. Mater Res Soc Symp Proc* 1999, 548, 313-323.

8. Savinell, R. F.; Litt, M. U.S. Patent 5,525,436, 1996.

9. Samms, S. R.; Wasmus, S.; Savinell, R. F. *J Electrochem Soc* 1996, **143**, 1225-1232.

10. Wainright, J. S.; Wang, J. T.; Weng, D.; Savinell, R. F.; Litt, M. *J Electrochem Soc* 1995, **142**, L121-L123.

11. Wang, J. T.; Savinell, R. F.; Wainright, J. S.; Litt, M.; Yu, H. *Electrochim Acta* 1996, **41**, 193-197.

12. Wang, J. T.; Wainright, J. S.; Savinell, R. F.; Litt, M. *J Appl Electrochem* 1996, **26**, 751-756.

13. Gieselman, M. B.; Reynolds, J. R. *Macromolecules* 1992, **25**, 4832-4834.

14. Shih-Wei Chuang.; Steve Lien-Chung Hsu. *J Polym Sci Part A: Polymer Chemistry*, 2006, **44**, 4508-4513.

15. Xiao, L.; Zhang, H.; Jana, T.; Scanlon, E.; Chen, R.; Choe, E.-W.; Ramanathan, L. S.; Yu, S.; Benicewicz, B. C. *Fuel Cells* 2005, **5**, 287-295.

16. Shengbo Qing.; Wei Huang.; Deyue Yan. *J Polym Sci Part A: Polymer Chemistry*, 2005, **43**, 4363-4372.

17. Juan Antonia Asensio.; Salvador Borros.; Pedro, Gomez-Romero. *J Polym Sci Part A: Polymer Chemistry*, 2002, **40**, 3703–3710

18. Jacques Roziere.; Deborah J. Jones.; Mathieu Marrony.; Xavier Glipa.; Bernard Mula. *Solid State Ionics*, 2001, **145**, 61-68

19. Varcoe, J. R.; Slade, R. C. T. *Fuel Cells*, 2005, No. 2

20. Xing, B.; Savadogo, O.*Electrochemistry Communications* 2000, **2** (10), 697.

21. Rozière Jacques.; Jones J Deborah.; Marrony Mathieu.; Xavier Glipa.; Mula Bernard. *Solid State Ionics* 2001, **145** (1-4), 61.

22.  Seonghan Yu. *Novel polybenzimidazole derivatives for high temperature PEM fuel cells*, PhD, Rensselaer Polytechnic Institute, Troy, 2006.

23.  Yu, S.; Xiao, L.; Benicewicz, B. C. *Fuel Cells* 2008, **8** (3-4), 165.

24.  Sikkema.; Doetze J. *Polymer* 1998, **39** (24), 5981.

25.  Kosolapoff, G. M. Organophosphorus Compounds: John wiley & Sons, Inc., 1950

# Chapter

# 4

Benzimidazole Group based Polybenzimidazole Copolymers for Proton Exchange Membrane Fuel Cell - Synthesis and Characterization

### 4.1   Introduction

Aromatic polybenzimidazoles (PBIs), as mentioned in earlier chapter, due to their high mechanical properties [1] excellent thermal stability, good chemical resistance, good flame resistance, have made deep inroads in various applications [2]. Presently, it has received considerable attention for the development of high temperature polymer electrolyte membrane for proton exchange membrane fuel cell (PEMFC) and direct methanol fuel cells (DMFC).

In order to enhance solvent solubility and proton conductivity at low temperature and other properties to suit desired application, various functional groups have been introduced [3-15] in PBI; most of these groups are introduced in main chain. Functional groups in side chain are expected to modify the properties of PBI significantly. However, much information on PBI containing bulky pendant group is not available. PBI, due to amphoteric nature of imidazole groups, conducts protons on doping with strong acids. Enhancing benzimidazole groups in PBI by introducing these groups in side chain also, may enhance proton conductivity of PBI. Pendant imidazole groups tethered in polysulfone [16] polysiloxane [17] and styrene-maleimide copolymer [18] imparts proton conductivity to these polymers and these polymers on doping with phosphoric acid exhibit good proton conductivity. Polymers with pendant benzimidazole group have been used for other applications also. Polystyrene having pendant benzimidazole group has been used to prepare polymer supported reagents and catalysts [19].

In most of the above mentioned cases, benzimidazole group is tethered to preformed polymer by suitable chemical reactions wherein benzimidazole group is randomly distributed in a polymer chain and it is difficult to control the number of benzimidazole groups in the polymer. Polymers containing desired number of functional groups can be synthesized by polycondensation of monomers having preformed functional groups.

With this perspective, we synthesized a diacid monomer containing pendant benzimidazole group and present work describes the synthesis and characterization of a novel aromatic diacid containing pendant benzimidazole group and polybenzimidazoles containing pendant benzimidazole groups. Proton conductivity and other properties related to polymer

electrolyte for fuel cell have also been studied to assess possible applications of these polymers as polymer electrolyte for fuel cells. These polymers may also find applications as high temperature polymer electrolytes for fuel cell or high temperature membranes in separation technology.

## 4.2 Experimental

### 4.2.1 Materials

Ortho-phenylene diamine (Fluka, Switzerland) was purified by sublimation. 3,5 dimethyl benzoic acid (Aldrich Chemicals, USA), was used as received), Ethyl acetate (Merck, India), potassium permanganate, pyridine, methanol, hydrochloric acid, formic acid, ortho phosphoric acid (85%), phosphorus pentoxide and sodium bicarbonate (S. D. Fine Chem. India) were used as received. 3,3',4,4,'-tetra amino biphenyl (TAB), (Aldrich Chemicals, USA) was recrystallized from water. Isophthalic acid (Fluka, Switzerland) was purified by recrystallization from methanol. Terephthalic acid and pyridine 2, 6-dicarboxylic acid (Aldrich Chemicals, USA) were purified by sublimation, and recrystallization from 1:1 water/HCl respectively. N-methyl-2-pyrollidinone (NMP) and N, N-dimethylacetamide (DMAc) (S. D. Fine Chem., India) were dried over phosphorus pentoxide and vacuum distilled. Polyphosphoric acid (PPA) was prepared by heating 1:1.8 weight ratio of ortho phosphoric acid (85%) and phosphorus pentoxide for 6h at 100 $^\circ$C.

### 4.2.2 Analytical methods

All the analytical methods used to characterize the polymer and polymer membranes are described in chapter 2 earlier.

### 4.2.3 Synthesis of new substituted aromatic diacid

### 4.2.3.1 Synthesis of 5-(1H-benzo[d]imidazol-2-yl) isophthalic acid (BIPA)

This diacid was synthesized in two steps by the reaction of o-phenylene diamine with 3,5 dimethylbenzoic acid in the presence of polyphosphoric acid as solvent and dehydrating agent, followed by the oxidation of the product to the corresponding diacid using potassium permanganate and pyridine. Various steps involved in this synthesis are outlined in Scheme 4.1.

**(i) Synthesis of 2-(3,5-dimethylphenyl)-1H-benzo[d]imidazole (I)**

To a 250 mL three necked round bottom flask, equipped with an overhead mechanical stirrer, nitrogen inlet and calcium chloride guard tube, was added 10.90 g (100.79 mmol) of O-phenylene diamine and 150 g of polyphosphoric acid and the mixture was heated to 140 °C with stirring under a stream of nitrogen. After the complete dissolution of O-phenylene diamine, 15 g (99.88 mmol) of 3,5 dimethylbenzoic acid was added slowly with stirring and the temperature of the reaction mixture was raised to 170 °C. The acid dissolved in half hour giving homogeneous solution. The solution was then heated to 200 °C and maintained at this temperature for 8 h. The resulting viscous solution was then cooled and poured into 2000 mL of water to precipitate the product as powder. The product was then filtered, washed repeatedly with deionised water to remove excess of phosphoric acid and O-phenylene diamine. The product was stirred in 10% aqueous $Na_2CO_3$ solution overnight to eliminate residual phosphoric acid. The crude product was filtered, washed with large excess of water, dried and recrystallized from acetone.

Yield: 21 g (95 %)

Melting point: 101-103 °C

FTIR: IR (neat, cm$^{-1}$): 1605 (C=N stretching); 1274 (imidazole breathing mode); 846 (-C-N stretching); 1524, 1444 (aromatic). (Figure 4.1)

$^1$H NMR [200 MHz, DMSO-d$_6$, ppm] showed signals of different protons at δ values of 7.76 (s, 2H, H$_a$); 7.6 (dd, 2H, H$_b$); 7.2 (dd, 2H, H$_c$); 7.1 (s, 2H, H$_d$); 2.33 (s, 6H, H$_e$). (Figure 4.2)

$^{13}$C NMR [400 MHz, DMSO-d$_6$, δ, ppm ] showed values of 152, 138.52, 131.75, 130.37, 124.71, 122.53 and 21.34. (Figure 4.3)

| Elemental analysis: | C% | H% | N% |
|---|---|---|---|
| $C_{15}H_{14}N_2$ | | | |
| Calculated: | 81.05% | 6.35% | 12.60% |
| Observed: | 80.65% | 6.55% | 12.44% |
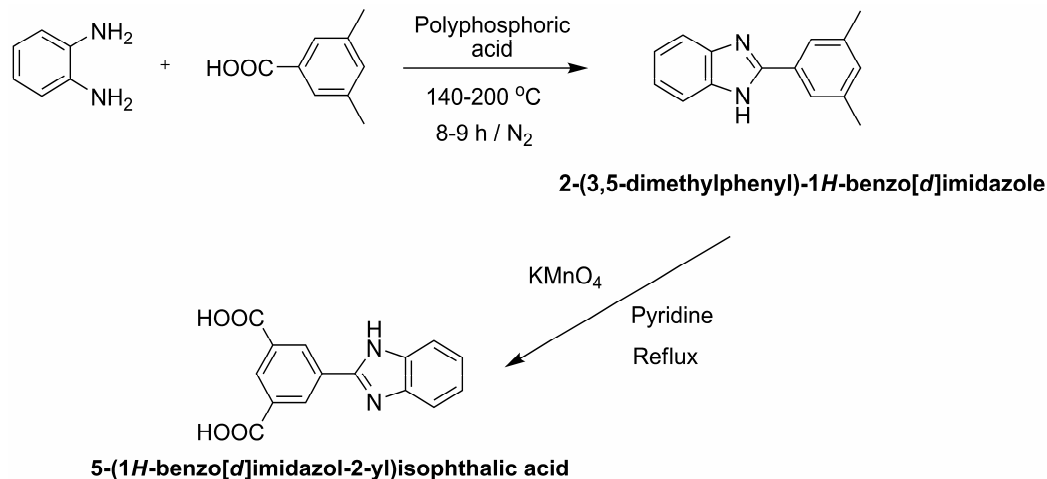
**Scheme 4.1**. Synthesis of 5-(1H-benzo[d]imidazol-2-yl)isophthalic acid **(BIPA)**

**(ii)Synthesis of 5-(1H-benzo[d]imidazol-2-yl) isophthalic acid**

      To a 500 mL three necked round bottom flask equipped with a thermo-well, a reflux condenser and a mechanical stirrer were added 20.0 g (89.97 mmol) 2-(3,5-dimethylphenyl)-1H-benzo[d]imidazole, 65 mL water and 140 mL pyridine and the solution was heated to reflux. To this solution 85 g (552.5 mmol) solid $KMnO_4$ was added at a slow rate with stirring to maintain a slow reflux. Water was added occasionally to replace the loss by evaporation and to wash down the permanganate. The solution was then refluxed 12 h and 85 mL methanol was added to destroy excess permanganate. The $MnO_2$ was suction filtered while hot and washed with boiling water. Filtrate and washings were combined and the pyridine was removed by vacuum distillation. After cooling, the solution was acidified with concentrated HCl and the precipitate obtained was filtered and washed with water several times. The diacid obtained was again dissolved in aqueous sodium carbonate solution, treated with charcoal, filtered and acidified. The precipitated solid was dried at 80 °C under vacuum and recrystallized from formic acid.

Yield: 21.2 g (85%)  Melting point: 258 – 260 °C.

FTIR (neat, $cm^{-1}$): 1702 (C=O); 1616 (C=N stretching); 1257 (imidazole breathing mode); 840 (-C-N stretching); 1578, 1420 (aromatic). (Figure 4.4)

$^1$H NMR [200 MHz, DMSO-$d_6$, ppm] showed signals of different protons at δ values of 13.5 (s, 1H, $H_a$); 9.03 (s, 2H, $H_b$); 8.57 (s, 2H, $H_c$); 7.67 (d, 2H, $H_d$); 7.28 (d, 2H, $H_e$). (Figure 4.5)

^{13}C NMR [400 MHz, DMSO-$d_6$, δ, ppm ] showed values of 166.16, 149.50, 139.18, 132.17, 130.94, 122.58, 126.62 and 115.35 (Figure 4.6), consistent with structure.

| Elemental analysis: | C% | H% | N% |
|---|---|---|---|
| $C_{15}H_{10}N_2O_4$ | | | |
| Calculated: | 63.83% | 3.57% | 9.92% |
| Observed: | 63.1% | 3.17% | 9.55% |

### 4.2.4    Synthesis of new substituted homo and co-polybenzimidazoles

Polybenzimidazoles having free benzimidazole groups were synthesized from 5-(1H-benzo[d]imidazol-2-yl) isophthalic acid (BIPA) by condensing with 3,3',4,4,'-tetra amino biphenyl (TAB) and other diacids. Homo polybenzimidazole was synthesized by condensing BIPA and TAB (Scheme 4.2) while co-polybenzimidazoles were synthesized by condensing a mixture of BIPA and IPA in different ratio with TAB. Other co-polybenzimidazoles having 50:50 mole ratios of BIPA and different diacids, namely, pyridine 2, 6-dicarboxylic acid (PDA) and terephthalic acid (TPA) were also synthesized by using one step solution polycondensation in polyphosphoric acid (Scheme 4.3) detailed procedure used for polycondensation is described below.

### 4.2.4.1 Synthesis of polybenzimidazole having pendant benzimidazole groups (BPBI)

To a 100 mL three necked round bottom flask, equipped with a mechanical stirrer, nitrogen gas inlet and a guard tube, was added 2.0 g (9.334 mmol) 3,3',4,4,'-tetra amino biphenyl (TAB) and 80 g of polyphosphoric acid and the mixture was heated to 140 °C with stirring under a stream of nitrogen. After the complete dissolution of TAB, 2.63 g (9.334 mmol) of 5-(1H-benzo[d]imidazol-2-yl) isophthalic acid was added slowly with stirring and the temperature of the reaction mixture was raised to 170 °C. The diacid dissolved in 1 h giving homogeneous solution. The solution was then heated to 200 °C and maintained at this temperature for 12 h. The resulting viscous solution was then cooled and poured into 500 mL water to precipitate the polymer as fiber. The polymer was then filtered, washed repeatedly with water and stirred in 10% aqueous $Na_2CO_3$ solution overnight to eliminate residual phosphoric acid. The polymer was then washed with water to neutrality and heated in boiling

water for 6 h, three times. The purified polymer was dried at 100 °C for 24 h and at 150 °C for another 24 h in a vacuum oven. A brown fibrous polymer was obtained. Yield of the polymer was 98%. The inherent viscosity of this polymer at 0.5 g.dL$^{-1}$ concentration, measured in DMSO at 30 °C was 0.90 dL g$^{-1}$.

FTIR (film, cm$^{-1}$): 1605 (C=N); 3395 (N–H stretching); 3191 (N–H deformation); 1010, and 1220 (C-O stretching); 1536 and 1447 (aromatic). (Figure 4.7)

$^1$H NMR [400 MHz, DMSO-d$_6$, ppm] showed signals of different protons at δ values of 13.5 (s, 2H, H$_a$); 9.25 (s, 3H, H$_b$); 8.20 (s, 1H, H$_c$); 8.10-7.60 (m, 8H, H$_{d-h}$). (Figure 4.9)

| Elemental analysis: | C% | H% | N% |
|---|---|---|---|
| $C_{20}H_{12}N_4O$ | | | |
| Calculated: | 76.40% | 3.80% | 19.80% |
| Observed: | 75.41% | 3.90% | 18.72% |
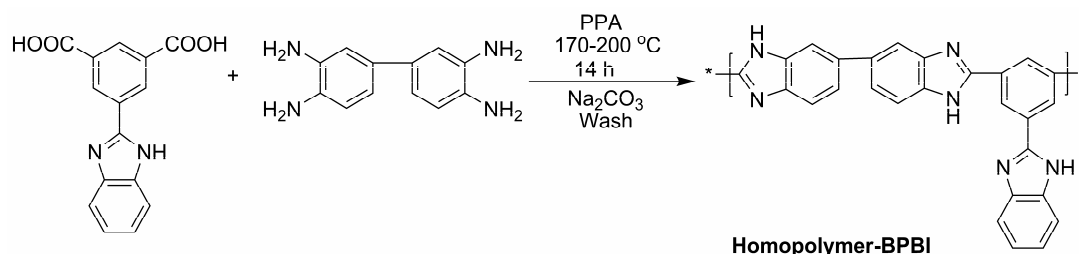


**Scheme 4.2** Synthesis of benzimidazole groups containing homo polybenzimidazole.

### 4.2.4.2 Synthesis of co-polybenzimidazole having pendant benzimidazole groups with different diacids

> **Synthesis of copolybenzimidazole BPBI-1 (BIPA 90%: IPA 10%)**

To a 100 mL three necked round bottom flask, equipped with a mechanical stirrer, nitrogen gas inlet and a guard tube, was added 2.0 g (9.334 mmol) 3,3',4,4,'-tetra amino biphenyl (TAB) and 20 g of polyphosphoric acid and the mixture was heated to 140 °C with stirring under a stream of nitrogen. After the complete dissolution of TAB, 2.36 g (8.4 mmol) of 5-(1H-benzo[d]imidazol-2-yl) isophthalic acid and 0.155 g (0.93 mmol) isophthalic acid were added slowly with stirring. Then the temperature was raised to 170 °C, when diacids dissolved in 2h giving homogeneous solution. The solution was heated to 200 °C and

maintained at this temperature for 12 h. The resulting viscous solution was then cooled and poured into 500 mL water to precipitate the polymer as fiber.
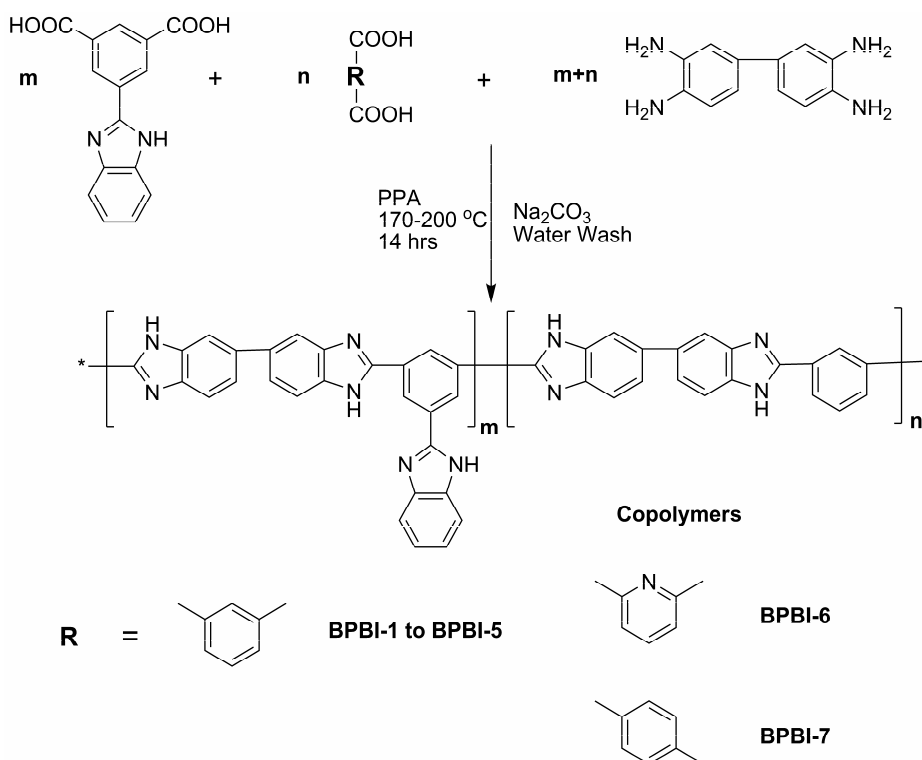


**Scheme 4.3** Synthesis of benzimidazole groups containing copolybenzimidazoles of BIPA and other diacids.

The polymer was then filtered, washed repeatedly with water and stirred with 10% aqueous $Na_2CO_3$ solution overnight to eliminate residual phosphoric acid. The polymer was then washed with water to neutrality and heated in boiling water for 6 h, three times. The purified polymer was dried at 100 °C for 24 h and 150 °C for another 24 h in a vacuum oven. A brown fibrous polymer was obtained.

Yield of the polymer was 99%. The inherent viscosity of this polymer, at 0.5 g.dL$^{-1}$ concentration, measured in DMAc at 30 °C, was 1.03 dL g$^{-1}$. The ratio of 5-(1H-benzo[d]imidazol-2-yl) isophthalic acid and isophthalic acid in this co-polybenzimidazole is 90:10 mol%.

Other co-polybenzimidazoles of BIPA and other diacids in different ratio prepared by following this procedure are tabulated in Table 4.1.

## 4.3   Results and Discussion

### 4.3.1   Synthesis and characterization of monomers

### 4.3.1.1 Synthesis and characterization of 5-(1H-benzo[d]imidazol-2-yl) isophthalic acid

This diacid was synthesized from 3,5 dimethyl benzoic acid and o-phenylene diamine in two steps (Scheme 4.1) by reacting o-phenylene diamine with 3,5 dimethylbenzoic acid in the presence of a polyphosphoric acid to obtain 2-(3,5-dimethylphenyl)-1H-benzo[d]imidazole, which was then oxidized to the corresponding diacid using potassium permanganate and pyridine. Pure diacid was obtained by recrystallization from formic acid. Various steps involved in this synthesis are outlined in Scheme 4.1.

Elemental analysis, FTIR, $^1$H-NMR, and $^{13}$C-NMR spectra confirmed the formation of 2-(3,5-dimethylphenyl)-1H-benzo[d]imidazole. The elemental analysis values were found to be in good agreement with the calculated values. FTIR spectrum of 2-(3,5-dimethylphenyl)-1H-benzo[d]imidazole (Figure 4.1) showed bands at 1524 and 1444 cm$^{-1}$ due to asymmetric and symmetric aromatic C-H stretching vibrations. The band at 1274 is due to imidazole breathing mode of imidazole ring. The bands at 1605 and 846 cm$^{-1}$are due to the C=N stretching and –C-N stretching vibration respectively.
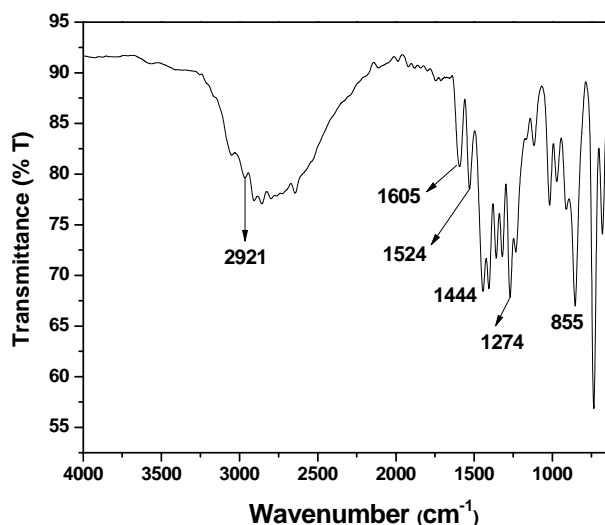


**Figure 4.1** FTIR spectrum of 2-(3,5-dimethylphenyl)-1H-benzo[d]imidazole

$^1$H NMR spectrum of 2-(3,5-dimethylphenyl)-1H-benzo[d]imidazole (Figure 4.2) showed signal at 2.33 δ ppm corresponding to the protons of –CH3, attached to the aromatic ring, in addition to signals corresponding to aromatic protons in the region 7.0-7.8 δ ppm with expected multiplicity and integration equivalent to seven protons. The $^{13}$C NMR

spectrum of 2-(3,5-dimethylphenyl)-1H-benzo[d]imidazole shows aromatic carbons at 122–152 δ ppm with expected values and two carbons of methyl groups appear at 21.34 δ ppm (Figure 4.3).
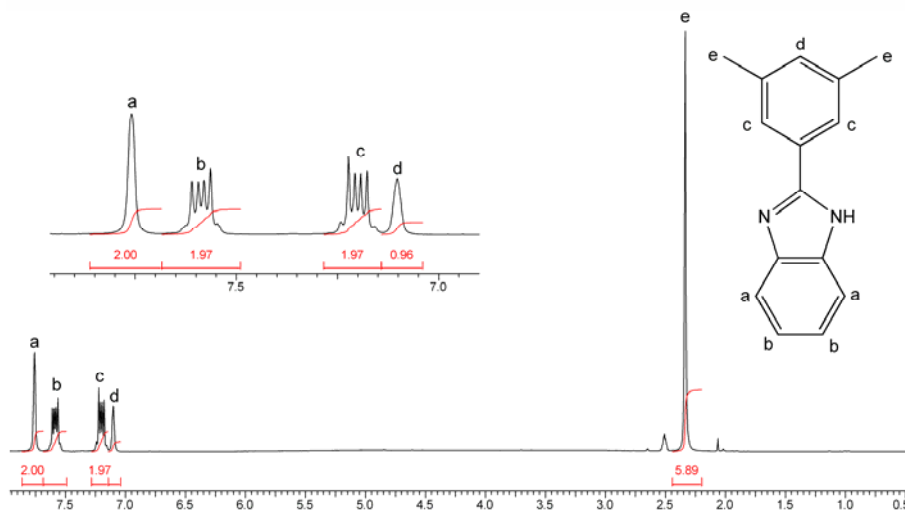


**Figure 4.2** $^1$H NMR spectrum of 2-(3,5-dimethylphenyl)-1H-benzo[d]imidazole.
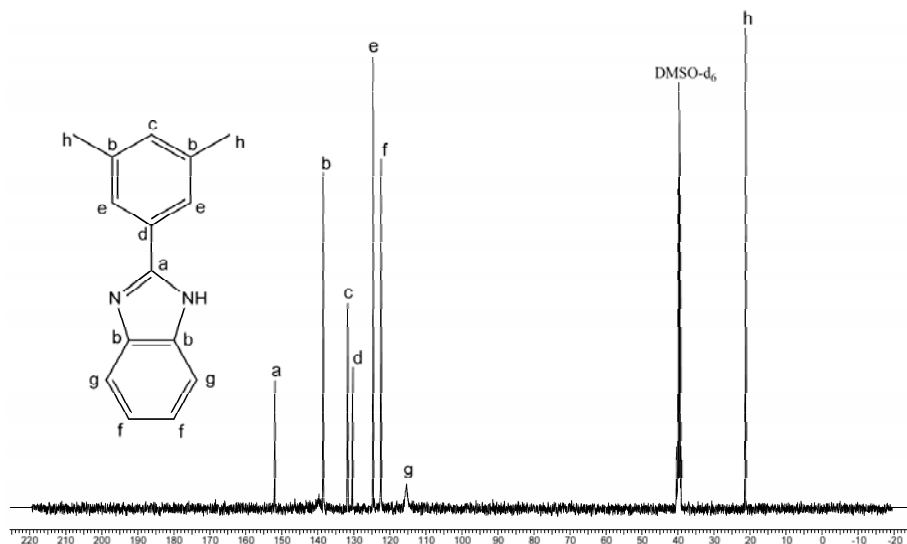


**Figure 4.3** $^{13}$C NMR spectrum of 2-(3,5-dimethylphenyl)-1H-benzo[d]imidazole.

In the second step, 5-(1H-benzo[d]imidazol-2-yl) isophthalic acid was prepared by the oxidation of 2-(3,5-dimethylphenyl)-1H-benzo[d]imidazole using aqueous KMnO₄-pyridine. The dicarboxylic acid was recrystallized from formic acid. In the oxidation step excess KMnO₄ was added to ensure complete oxidation of the methyl groups (upto the point till the color of KMnO₄ did not fade on refluxing). This helped in improving the yield and purity of diacid, which in turn helped in increasing the molecular weight of polymer. The chemical

structure of the diacid was confirmed by means of elemental analysis, FTIR, ^{1}H NMR, and ^{13}C NMR spectra. Elemental analysis is in good agreement with calculated values.
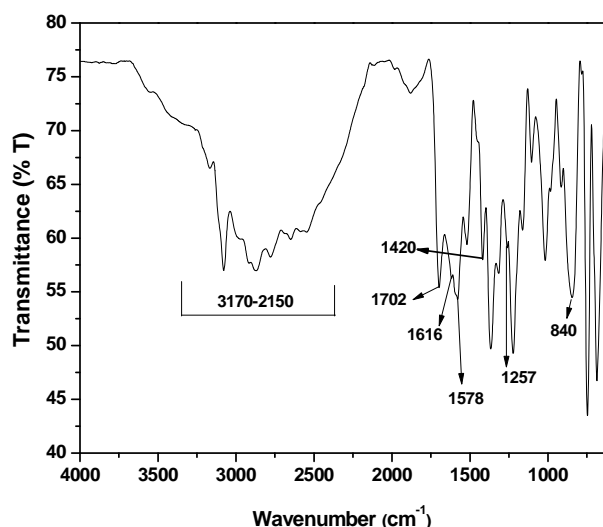


**Figure 4.4** FTIR spectrum of 5-(1H-benzo[d]imidazol-2-yl) isophthalic acid

FTIR spectrum of 5-(1H-benzo[d]imidazol-2-yl) isophthalic acid (Figure 4.4) showed new absorptions in the region 2150-3170 due to hydrogen bonded –OH of carboxyl group and at 1702 cm^{-1} due to C=O of carboxyl group along with the bands at 1578 and 1420 cm^{-1} due to asymmetric and symmetric C-H stretching vibrations. The band at 1257 is due to imidazole breathing mode vibration of imidazole ring. The bands at 1616 and 840 cm^{-1} are due to the C=N and –C-N stretching vibration respectively.
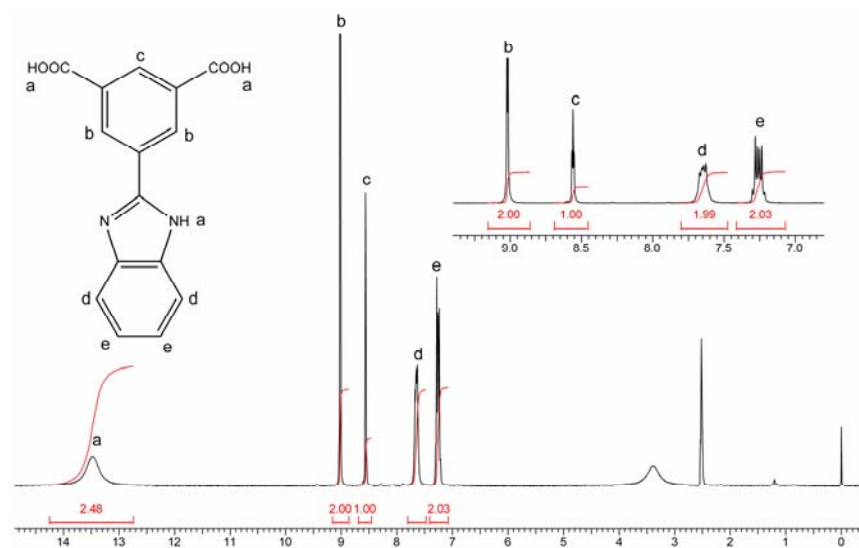


**Figure 4.5** ^{1}H NMR spectrum of 5-(1H-benzo[d]imidazol-2-yl) isophthalic acid.
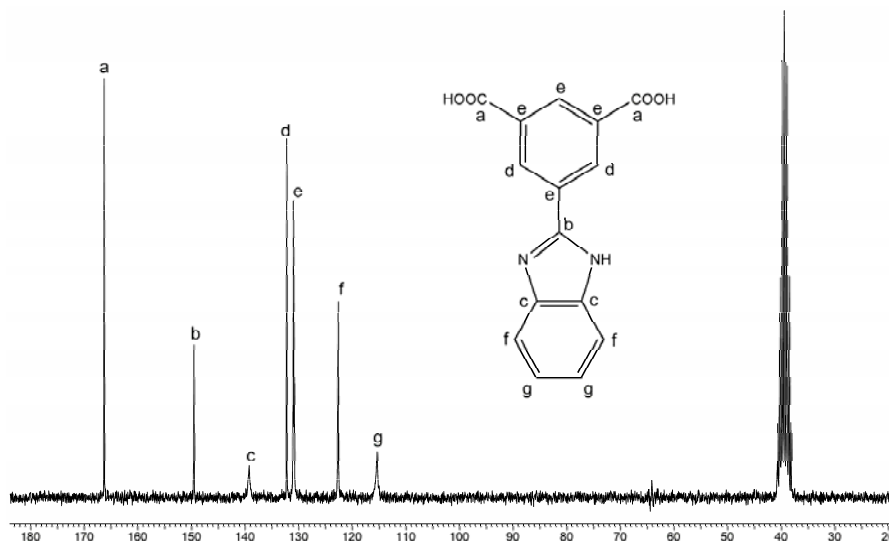
**Figure 4.6** ^{13}C NMR spectrum of 5-(1H-benzo[d]imidazol-2-yl) isophthalic acid.

^{1}H NMR spectrum of 5-(1H-benzo[d]imidazol-2-yl) isophthalic acid (Figure 4.5) shows aromatic protons at 7.25–9.03 δ ppm with expected multiples and integration and absence of methyl protons. ^{13}C NMR spectrum of 5-(1H-benzo[d]imidazol-2-yl) isophthalic acid (Figure 4.6) shows aromatic carbons at 115–167 δ ppm with expected values and methyl carbons at 21.34 δ ppm disappear and appear as carbons of carboxyl group at 166.16 δ ppm. Thus, elemental analysis, FTIR, ^{1}H NMR and ^{13}C NMR confirm the expected structure of the diacid.

### 4.3.2 Synthesis and structural characterization of polybenzimidazole and Co-polybenzimidazole having pendant Benzimidazole groups with different diacids.

All polymers were synthesized by one pot solution polycondensation in PPA at high temperature as described in experimental part. Both, homopolymer of 5-(1H-benzo[d]imidazol-2-yl) isophthalic acid (BIPA) with conventional 3,3',4,4,'-tetra amino biphenyl (TAB) and copolymers of TAB with a mixture of different mole ratio (90:10, 70:30, 50:50, 30:70 and 10:90) of BIPA and isophthalic acid were synthesized in order to study the effect of free benzimidazole groups on properties of PBIs. Two more new co-polybenzimidazoles containing benzimidazole groups with structural variations were synthesized, by condensing a mixture of BIPA and terephthalic acid or pyridine 2,6 dicarboxylic acid in 50:50 mole ratio with TAB (Scheme 4.2 & 4.3) to study structure property

relationship. Approximately 12 h heating at 200 °C is essential to form high molecular weight polymers. All the polymers remain soluble in polyphosphoric acid without precipitation, although, they form viscous solutions, which on pouring in hot water form strong thread like structure.

**Table 4.1** Inherent viscosity and film nature of benzimidazole PBI and Co-PBIs

| Polymer Code | Diacids used (mole ratio) | Yield (%) | Inherent viscosity $\eta_{inh}$ (dL/g) | Film Color | Film Nature |
|---|---|---|---|---|---|
| **BPBI** | BIPA **100%** | 98 | 0.90 | Yellowish | Flexible |
| **BPBI-1** | BIPA / IPA **90:10** | 99 | 1.03 | Yellowish | Flexible |
| **BPBI-2** | BIPA / IPA **70:30** | 96 | 1.20 | Yellowish | Flexible |
| **BPBI-3** | BIPA / IPA **50:50** | 96 | 1.40 | Light brown | Flexible |
| **BPBI-4** | BIPA / IPA **30:70** | 98 | 1.60 | Light brown | Flexible |
| **BPBI-5** | BIPA / IPA **10:90** | 97 | 1.65 | brown | Flexible |
| **BPBI-6** | BIPA / PDA **50:50** | 95 | 0.95 | Yellowish | Flexible |
| **BPBI-7** | BIPA / TPA **50:50** | 98 | 1.7 | Reddish | Flexible |

**BIPA:** 5-(1H-benzo[d]imidazol-2-yl) isophthalic acid, **IPA:** Isophthalic acid, **PDA:** Pyridine dicarboxylic acid, **TPA:** Terephthalic acid.

Inherent viscosities of these polymers were determined in DMAc (0.5 $gdL^{-1}$ concentration at 30 °C) using Ubbelhode viscometer. The values are observed to be high, in the range of 0.90-1.66 $dL.g^{-1}$ (Table 4.1). Co-polybenzimidazole with terephthalic acid shows highest viscosity and forms a tough and flexible film which is reddish in color. All these polymers form tough flexible films.
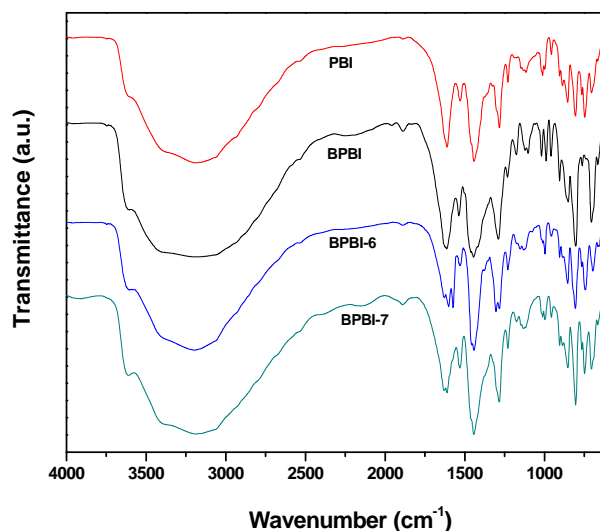


**Figure 4.7** FTIR spectra of co-polybenzimidazoles of BIPA and PDA,TPA diacids.
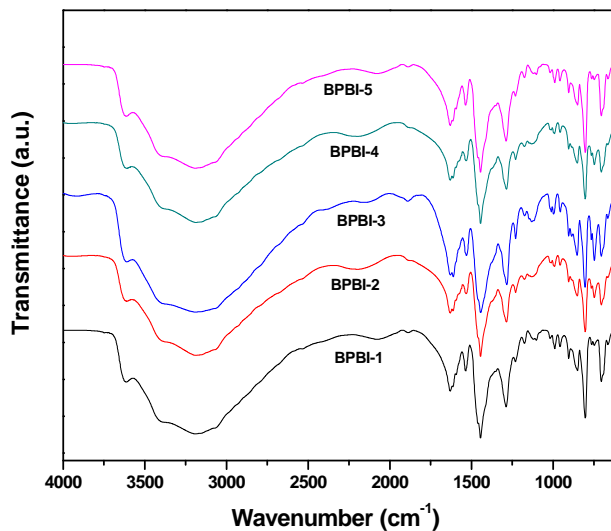
**Figure 4.8** FTIR spectra of co-polybenzimidazoles of BIPA and IPA.

The polymers, thus obtained, were characterized by FTIR and ^{1}H NMR spectroscopy. FTIR of all the polymers was scanned using thin films. The FTIR spectra of BPBI's and PBI are shown in (Figure 4.7 & 4.8) The formation of polybenzimidazoles was confirmed by the characteristic absorption at 1630 cm$^{-1}$ band due to C=N stretching of imidazole rings. Another characteristic band of breathing mode of imidazole ring appears in the range of 1283 -1287 cm$^{-1}$, which confirms the formation of imidazole groups.

The absorption band at 3188 -3195 cm$^{-1}$ is assigned to self-associated N-H interaction of PBI chains. Due to structural variations of these polymers these bands appear at different wavelength in the range mentioned.
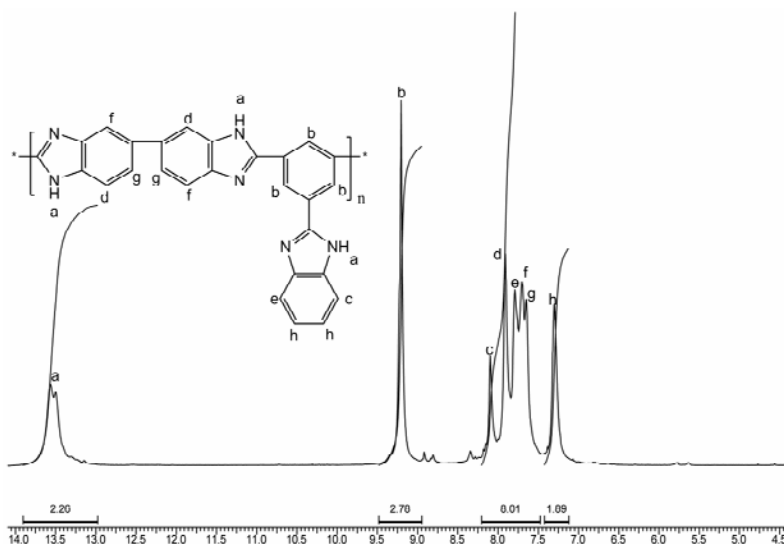


**Figure 4.9** ^{1}H NMR spectrum of benzimidazole group containing polybenzimidazole (BPBI).

Among the BPBI's synthesized from BIPA, only the $^1$H NMR spectrum of homopolymer (BPBI) was scanned by dissolving polymer in DMSO-D$_6$. The $^1$H NMR spectrum of BPBI (Figure 4.9) showed more than two protons at 13.5 $\delta$ ppm assigned to hydrogen of N-H group of imidazole ring, which confirms the presence of benzimidazole groups in polymer chain and free benzimidazole groups in the polymer. The aromatic region showed protons with expected multiples and integration at 7.1–9.4 $\delta$ due to the aromatic protons of both TAB and BIPA. The resolution of aromatic protons was not good in this case even though the spectrum was recorded on a 400 MHz NMR instrument.

### 4.3.3   Properties of BPBI's

The properties of BPBI's were evaluated by solubility measurements, X-ray diffraction, DSC, TGA and mechanical property study.

### 4.3.3.1 Solubility measurements

The solubility of the BPBI's was studied qualitatively in various solvents and the results are shown in Table 4.2. PBI's are rigid polymers having high softening point and polymer solubility plays a major role.  Solubility behavior of newly synthesized polymers was studied by dissolving 4 mg of polymers in 0.5 mL solvent. Commercial PBI is soluble in aprotic solvents such as DMAc, NMP and DMSO after heating at high temperature for several hours in presence of lithium chloride.

The polymers under study displayed good solubility in aprotic solvents such as DMF, NMP, DMAc and DMSO at ambient temp. However, BPBI is soluble in DMAc, NMP and DMSO. The co-polybenzimidazoles of IPA and BIPA are soluble in all polar aprotic solvents such as DMF, DMAc, NMP, DMSO, (Table 4.2) at ambient temp. All polymers are soluble in strong acids such as H$_2$SO$_4$, TFA, formic acid and methane sulfonic acid. However they are not soluble in common organic solvents such as chloroform, toluene, tetrahydrofuran, dioxane and acetic acid due to their polar nature.

**Table 4.2** Solubility behavior of homo and co- Polybenzimidazoles containing pendant benzimidazole groups

| Polymer Code | Solvents | | | | | | | | |
|---|---|---|---|---|---|---|---|---|---|
| | TFA | MSA | HCOOH | $H_2SO_4$ | DMF | DMSO | DMAc | NMP | THF |
| BPBI | + + | + + | + + | + + | + | + + | + + | + + | - - |
| BPBI-1 | + + | + + | + | + + | + | + + | + + | + + | - - |
| BPBI-2 | + + | + + | + + | + + | + + | + + | + + | + + | - - |
| BPBI-3 | + + | + + | + + | + + | + + | + + | + + | + + | - - |
| BPBI-4 | + + | + + | + + | + + | + + | + + | + + | + + | - - |
| BPBI-5 | + + | + + | + + | + + | + + | + + | + + | + + | - - |
| BPBI-6 | + + | + + | + + | + + | + + | + + | + + | + + | - - |
| BPBI-7 | + + | + + | + + | + + | + | + + | + + | + + | - - |
| PBI | + + | + + | + + | + + | + | + | + | + | - - |

**+ +:** Soluble at room temperature, **+:** soluble on heating, **+ -:** swelling on heating and **- -:** insoluble on heating.   **TFA:** Trifluro acetic acid, **HCOOH:** Formic acid, **MSA**: Methane sulfonic acid, **$H_2SO_4$:** Conc. sulfuric acid, **DMF:** N,N-dimethylformamide**, DMAc**: N,N-dimethyl acetamide, **DMSO:** Dimethylsulfoxide, **NMP:** N-methyl-2-pyrrolidone, **THF:** Tetrhydrofuran.

### 4.3.3.2 Crystallinity

Crystalline nature of these polymer specimens (in film form) was studied by wide angle X-ray diffraction (Figure 4.10). No sharp peak for crystalline nature was observed. All PBIs from BIPA showed amorphous pattern indicating loss of crystallinity with increasing bulky benzimidazole moiety in the side chain of polymer **(**Figure 4.10).
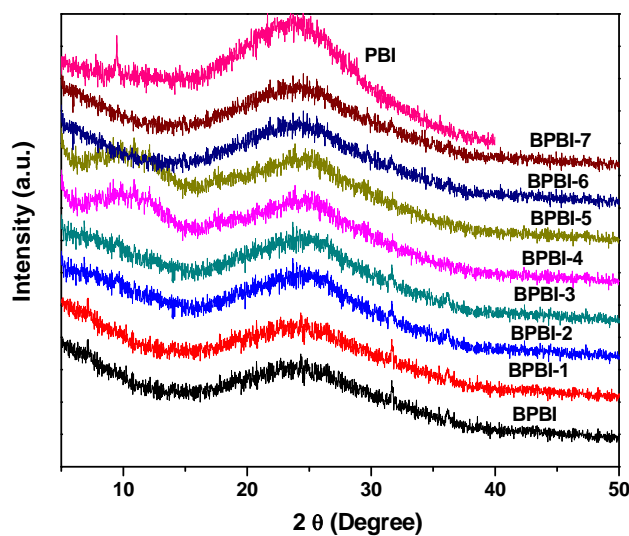


**Figure 4.10** Wide-angle X-ray diffractograms polybenzimidazoles containing pendant benzimidazole groups compared with PBI.

This is attributed to the flexibility of benzimidazole group, which increases the disorder in chains, thereby causing less chain packing. Amorphous nature of these polymers is also reflected in enhanced polymer solubility. The amorphous nature of polybenzimidazoles of BIPA could be attributed to the bulky benzimidazole groups in side chain, which reduced the intra and interpolymer chain interactions, resulting in loose polymer chain packaging and aggregates.

### 4.3.3.3 Thermal stability of polymers
> **Thermogravimetric analysis**

The thermal stability of the benzimidazole group containing PBI, co-PBIs and the conventional PBI was analyzed by thermogravimetric analysis and the results are given in Table 4.3 and Thermograms in Figure 4.11.
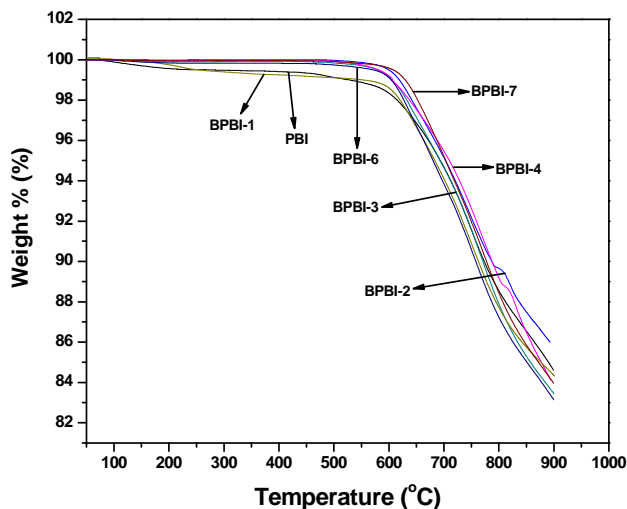


**Figure 4.11** TGA curves of polybenzimidazoles containing pendant benzimidazole groups compared with PBI in $N_2$ at heating rate 10 °C min$^{-1}$.

BPBI showed more thermal stability than the conventional PBI. For the conventional PBI, the onset of degradation started around 600 °C, while for the BPBI the onset is around 616 °C indicating its high thermal stability. Co-polymers BPBI-7 of BIPA and TPA showed highest IDT of 629 °C. Both IDT and $T_{10}$ values of BPBI indicate high thermal stability of these polymers. These results show that the synthesized benzimidazole group containing polybenzimidazoles can be used as polymer electrolyte membranes for operation at high temperature and also as polymeric material for other high temperature applications.

**Table 4.3** Thermal properties of homo and co- polybenzimidazoles of BIPA

| Polymer Code | IDT (ºC) | $T_{10}$ (ºC) | $T_{20}$ (ºC) | $T_{max}$ (ºC) | Residue (wt %) | $T_g$ (ºC) |
|:---:|:---:|:---:|:---:|:---:|:---:|:---:|
| BPBI | 616 | 772 | 900+ | 740 | 84.65 | 412 |
| BPBI-1 | 626 | 765 | 900+ | 735 | 84.50 | 410 |
| BPBI-2 | 590 | 760 | 900+ | 750 | 83.70 | 416 |
| BPBI-3 | 592 | 771 | 900+ | 770 | 84.19 | 421 |
| BPBI-4 | 590 | 788 | 900+ | 764 | 85.95 | 417 |
| BPBI-5 | 612 | 786 | 900+ | 740 | 83.10 | 410 |
| BPBI-6 | 599 | 758 | 900+ | 751 | 86.95 | 422 |
| BPBI-7 | 629 | 780 | 900+ | 750 | 86.20 | 402 |
| PBI | 603 | 760 | 900+ | 751 | 84.50 | 419 |

**IDT**: Initial decomposition temperature, $T_{10}$, $T_{20}$, and $T_{max}$: Temperature at which 10%, 20% and maximum weight loss of polymer takes place respectively, $T_g$: Glass transition temperature.

➢ **Glass transition temperature** *(T_g)*

PBI in general show high glass transition temperature due to rigid structure. Incorporation of functional groups in main chain is expected to lower $T_g$. Glass transition temperature of BIPA based PBIs was determined by differential scanning calorimeter (DSC) in nitrogen atmosphere at heating rate of 20 °C /min and the DSC thermograms of these polymers are shown in (Figure 4.12).
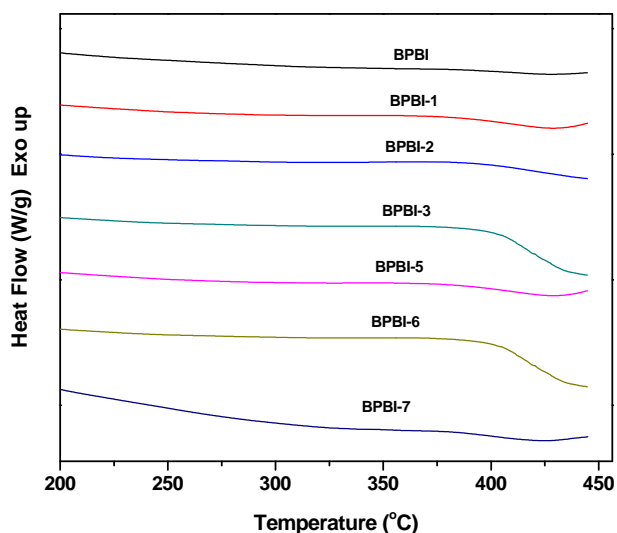


**Figure 4.12** DSC curves of polybenzimidazoles containing pendant benzimidazole groups compared with PBI in N₂ at heating rate 20 °C min⁻¹.

All the BPBI polymers showed $T_g$ in the range of 400-421 °C, which are near about same as compared to the $T_g$ of conventional PBI (Table 4.3). High $T_g$ of these polymers is,

probably, due to restriction to chain movement by the rigid and bulky pendant benzimidazole groups in the polymers.

### 4.3.3.4 Mechanical properties of polymers

Commercial PBI has superior mechanical properties due to rigid structure and any structural change is expected to affect mechanical properties. Commercial PBI has meta substituted phenyl rings in main chain where as, BIPA based PBI also has meta substituted phenyl ring in main chain and in addition, pendant benzimidazole group attached to the phenyl ring. In the present study, it was observed that the pendant benzimidazole groups reduces the tensile strength of PBI from 151 MPa (PBI) to 56 MPa (BPBI) (Table 4.4), probably due to disruption of rigid polymer structure by pendant benzimidazole group in side chain decreasing the interaction between imidazole groups and increasing free volume of the polymer.
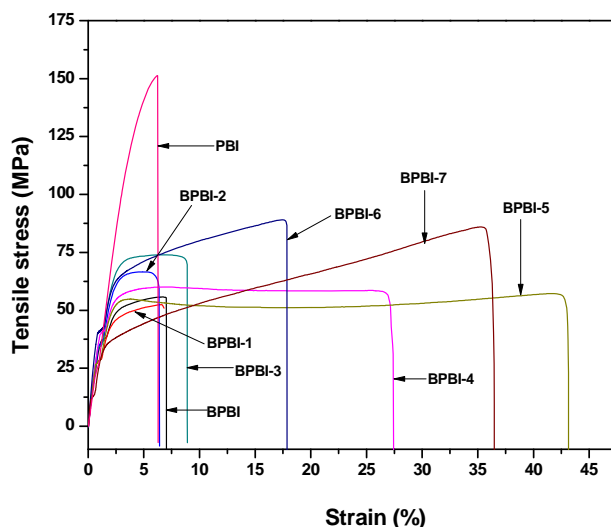


**Figure 4.13** Tensile stress versus strain graph of polybenzimidazoles containing pendant benzimidazole groups compared with PBI.

Tensile properties of co-PBIs of BIPA and IPA (Figure 4.13) reveals that addition of different mole % IPA to BIPA does not improve the tensile strength above 74 MPa, probably due to disruption of regular polymer structure of PBI. Similar trend is observed in case of modulus. Thus, modulus of polybenzimidazole of BIPA (BPBI) is 2198 MPa whereas, modulus of co-polybenzimidazole containing different mole % of BIPA is also in the range of 1517 MPa to 2615 MPa compared to 3771 MPa of PBI. The toughness of PBI (5.77 MPa) is low,

compared to BPBI polymers (5.84 - 55.21 MPa). In copolymer series of BIPA and IPA toughness increases with increase in IPA content. Compared to BPBI toughness (6.41MPa) the toughness of all copolybenzimidazoles of BIPA is higher. Highest toughness of 55.21 MPa is shown by BPBI-5. However, no definite trend was observed in case of tensile stress and modulus.

Similar trend was observed for elongation at break (Figure 4.13). High elongation at break of ~43.06% is shown by BPBI-5. These results indicate that the composition of diacid monomers in co-polymers has significant effect on mechanical properties of copolymers. Thus, mechanical properties of copolybenzimidazoles depend on chemical composition of polymer. Though polybenzimidazole containing pendent benzimidazole groups has low tensile strength and modulus compared to commercial PBI, the observed strength is good enough for applications as high temperature membrane materials for separation technology, polymer electrolytes for fuel cell and others.

**Table 4.4** Mechanical properties of polybenzimidazoles containing pendant benzimidazole groups

| Polymer Code | Diacid used (mole ratio) | Tensile Stress (MPa) | Modulus (MPa) | Toughness (MPa) | Elongation at Break (%) |
|---|---|---|---|---|---|
| **BPBI** | BIPA 100 | 56 | 2198 | 6.47 | 6.27 |
| **BPBI-1** | BIPA / IPA 90:10 | 52 | 2258 | 5.84 | 6.66 |
| **BPBI-2** | BIPA / IPA 70:30 | 67 | 2303 | 6.88 | 7.07 |
| **BPBI-3** | BIPA / IPA 50:50 | 74 | 2389 | 11.22 | 8.94 |
| **BPBI-4** | BIPA / IPA 30:70 | 60 | 1966 | 38.48 | 27.47 |
| **BPBI-5** | BIPA / IPA 10:90 | 58 | 2215 | 55.21 | 43.06 |
| **BPBI-6** | BIPA / PDA 50:50 | 87 | 2615 | 35.32 | 17.97 |
| **BPBI-7** | BIPA / TPA 50:50 | 86 | 1517 | 45.07 | 36.30 |
| **PBI** | IPA 100 | 151 | 3771 | 5.77 | 6.28 |

**4.3.4    Fuel cell Characterization of pendant benzimidazole group containing PEM**

**4.3.4.1 Oxidative stability study**

Fenton reagent test was carried out with BPBI's and commercial PBI to examine the radical oxidative stability of these polymer membranes. The membranes (thickness: 40-60 μm) were soaked in 3% $H_2O_2$ containing 4 ppm $Fe^{2+}$ (Mohr's salt, $(NH_4)_2Fe(SO_4)_2 \cdot 6H_2O$) at 70 °C for 12 h and the stability is expressed in terms of weight loss in membrane on immersing in Fenton's reagent for desired time. The radical stability of the samples was tested for different time period upto 96 h. The Fenton's reagent was replaced with fresh reagent after every 12 h.

Figure 4.14 shows oxidative stability of homo and copolymers of BPBI and IPA. Weight loss of BPBI after 96 h is 12% compared to 17% for PBI. Weight loss of other copolymers is in the range of 5-16% depending on the composition of the polymer. No definite trend in oxidative stability was observed. From the results it appears that pendant benzimidazole groups are more stable to oxidative degradation and they enhance oxidative stability of BPBI's due to flexibility of these polymers. All the membranes remain strong and flexible after the test.
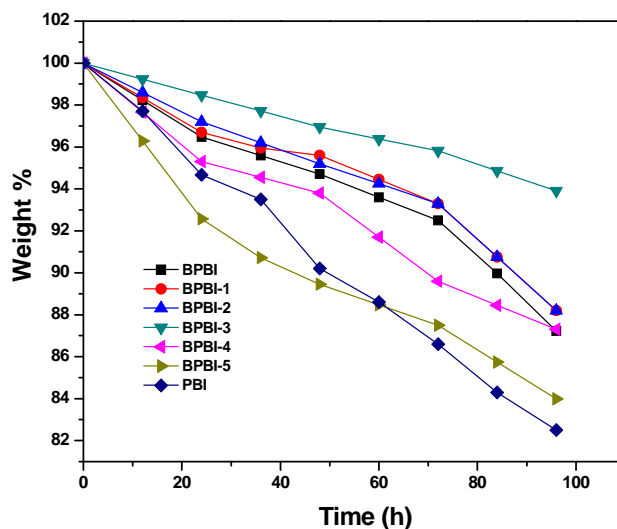


**Figure 4.14**  Oxidative stability expressed as weight loss in Fenton's test of pendant benzimidazole groups  containing polybenzimidazoles of IPA compared with PBI.
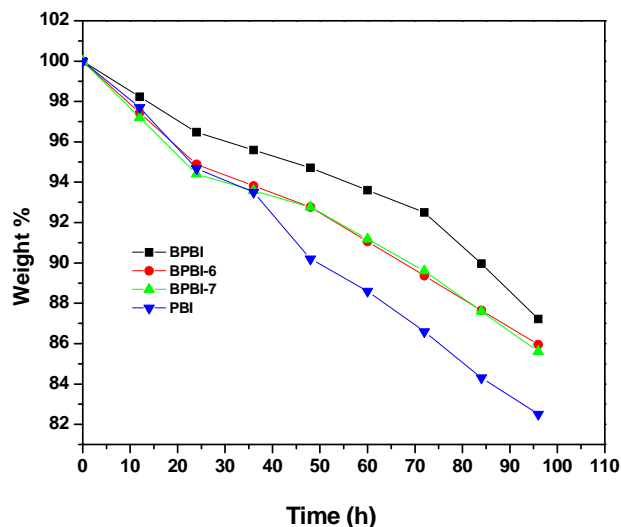
**Figure 4.15** Oxidative stability expressed as weight loss in Fenton's test of co-polybenzimidazoles of BIPA, PDA and TPA compared with PBI.

Figure 4.15 shows oxidative stability of copolymers of BIPA with TPA and PDA. Weight loss of these polymers is higher than BPBI but lower than PBI. Thus, structures of polymers have effect on oxidative stability of PBI. It may be noted that weight loss in BPBI's is gradual, whereas in PBI weight loss is fast after 36 h.

### 4.3.4.2 Phosphoric acid doping study

The acid uptake capacity of newly synthesized polymers was determined by doping membranes of BPBI's and commercial PBI in various molar concentrations of $H_3PO_4$ solutions for 24 h at room temperature. The doping level is defined as the wt% of $H_3PO_4$ in the polymer or copolymers. Its is known that doping levels of PBI depends on time period of doping, so we also studied the time dependant doping of BPBI's and PBI in the $H_3PO_4$ at room temperature for 36 h to study the effect of time on doping level. The doping level is expressed as the wt% of $H_3PO_4$ in the polymer or copolymers.

Compared to PBI, BPBI's show high acid uptake in all concentration of acid as observed in Figure 4.16. The acid uptake is slow upto 10M $H_3PO_4$ solution, although a steady increase in acid uptake with increase in concentration is observed. The acid uptake of BPBI's is 245 wt% of $H_3PO_4$ as compared to 165 wt% for PBI in 10M $H_3PO_4$. The homopolymer, BPBI shows highest acid uptake of 245 wt% of $H_3PO_4$ in 10 molar $H_3PO_4$. However, BPBI, BPBI-1 and BPBI-6 dissolve in the 12 and 14 molar of $H_3PO_4$. Thus, the presence of free

benzimidazole groups in the polymer enhances acid uptake, presumably, due to the formation of phosphoric acid complex with benzimidazole groups and enhanced free volume, which gives easy access for the diffusion of phosphoric acid in polymer matrix. In 14 molar $H_3PO_4$, acid uptake of BPBI's is in the range of 325-470 wt% compared to 265 wt% for PBI. Highest acid uptake of 470 wt% is shown by BPBI-3. Exact cause for high and fast acid uptake and high oxidative stability of BPBI-3 is not known. Probably, a particular microstructure of the copolymer due to regular structure obtained by the presence of equimolar BIPA and IPA may be responsible for these properties.
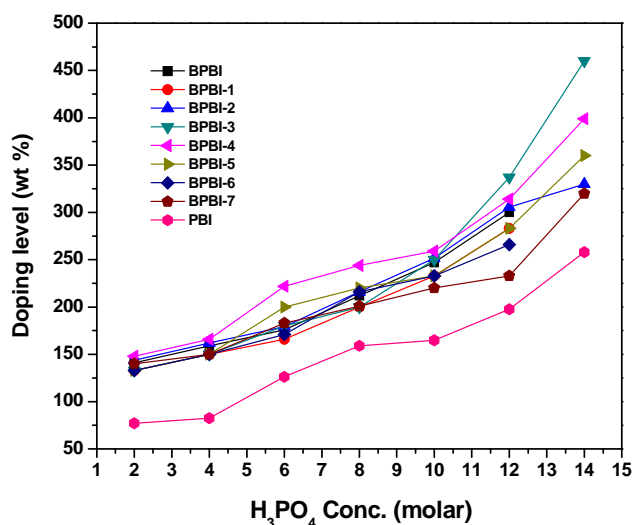


**Figure 4.16** Doping level of phosphoric acid (wt%) in polymers as a function of the $H_3PO_4$ concentration for polybenzimidazole containing pendant benzimidazole groups of IPA and other diacids compared with PBI.

This is further substantiated by the time dependant acid uptake study in 10 molar and 14 molar $H_3PO_4$ solutions shown in Figure 4.17. Since, BPBI, BPBI-1 and BPBI-6 films dissolve in the 12 and 14 molar $H_3PO_4$, they were studied in 10 molar $H_3PO_4$, while other BPBI polymers were doped in 85% $H_3PO_4$ solution. In case of PBI, a steady increase in acid uptake with time upto 24-27 h and saturation thereafter is observed. Whereas, acid uptake in BPBI's is comparatively fast and saturation point is reached after 15-16 h.

Thus, acid uptake of membranes of BPBI's is high and fast compared to PBI. Interestingly, the membranes of BPBI's have good strength and flexibility suitable for the preparation of PEM even after high acid uptake. After confirming the doping level and

stability of membranes of BPBI's in 10 and 14 molar phosphoric acid solutions, the membranes for the proton conductivity study were doped in 10 and 14 M phosphoric acid.
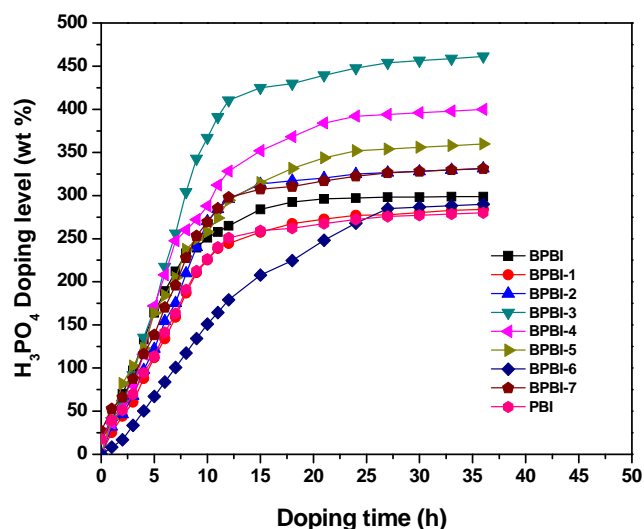


**Figure 4.17** Time dependant doping level of polybenzimidazoles containing pendant benzimidazole groups in $H_3PO_4$ at room temperature.

### 4.3.4.3 Proton conductivity measurement

Proton conductivity of BPBI, PBI and BPBI's , doped with phosphoric acid for 24 h was determined by AC impedance method at different temperature in the range of 25-175 °C as described in experimental part. BPBI, BPBI-1, BPBI-2 and BPBI-6 and BPBI-7 were doped in 10 molar $H_3PO_4$, while BPBI-3, BPBI-4, BPBI-5 and PBI membrane were doped in 14 molar $H_3PO_4$.
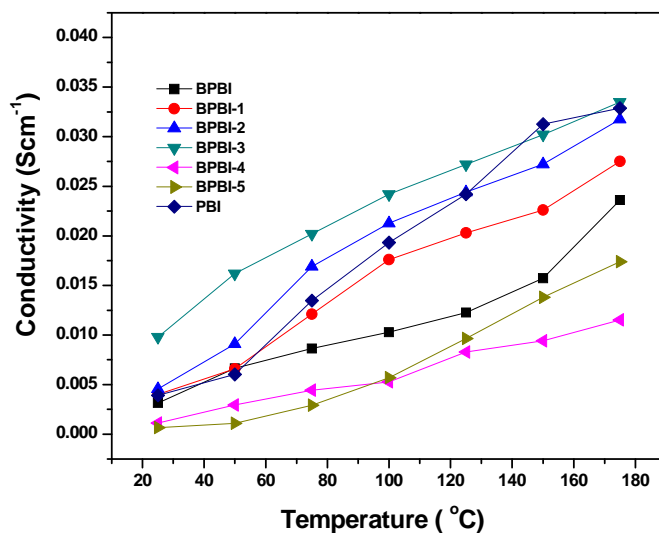


**Figure 4.18** Proton conductivities of polybenzimidazoles containing pendant benzimidazole groups ( IPA based polymers) compared with PBI at different temperature.
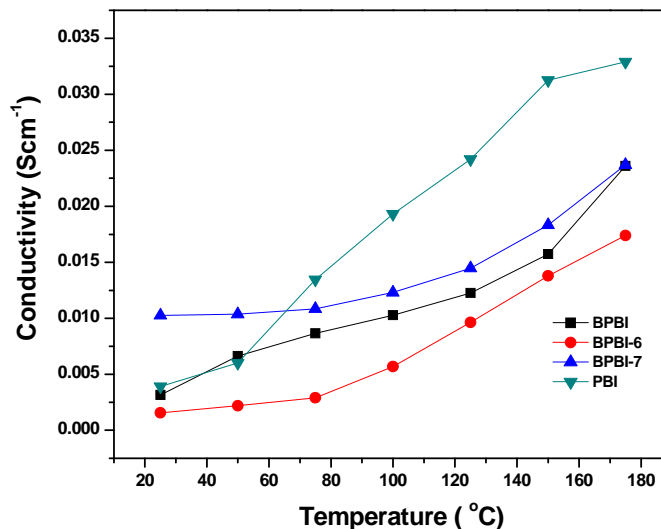
**Figure 4.19** Proton conductivities of PBI containing pendant benzimidazole groups (TPA and PDA based polymers) compared with PBI at different temperature.

As expected, proton conductivity of all polymer membranes increases with increase in temperature (Figure 4.18 & Figure 4.19). In case of PBI, proton conductivity increases from $3.96 \times 10^{-3}$ S/cm at 25 °C to $3.30 \times 10^{-2}$ S/cm at 175 °C, where as the proton conductivity of BPBI membrane is $3.15 \times 10^{-3}$ S/cm at 25 °C and $2.3 \times 10^{-2}$ S/cm at 175 °C.

The conductivity data and doping level is summarized in Table-4.5. All BPBI's shows high proton conductivity in the order of $10^{-2}$ S/cm at 175 °C. Slightly low proton conductivity of BPBI-1, BPBI-2, BPBI-6 and BPBI-7, compared to PBI is due to the low doping level of these polymers. BPBI-3 with high doping level shows highest proton conductivity of $3.9 \times 10^{-2}$ S/cm at 175 °C.

**Table 4.5** Proton conductivity and Doping level in wt% and mol/repeat unit of PBI and BPBI's at 175 °C

| Polymer Code | Doping level of $H_3PO_4$ (wt %) | Doping level of $H_3PO_4$ (mole) | $\sigma_{max}$ (S cm$^{-1}$) |
|:---:|:---:|:---:|:---:|
| BPBI | 234 | 10.12 | $2.3 \times 10^{-2}$ |
| BPBI-1 | 240 | 10.10 | $2.7 \times 10^{-2}$ |
| BPBI-2 | 250 | 9.93 | $3.1 \times 10^{-2}$ |
| BPBI-3 | 320 | 11.95 | $3.9 \times 10^{-2}$ |
| BPBI-4 | 290 | 10.14 | $2.5 \times 10^{-2}$ |
| BPBI-5 | 280 | 9.13 | $2.7 \times 10^{-2}$ |
| BPBI-6 | 220 | 8.22 | $2.5 \times 10^{-2}$ |
| BPBI-7 | 230 | 8.59 | $2.2 \times 10^{-2}$ |
| PBI | 280 | 8.92 | $3.3 \times 10^{-2}$ |

### 4.3.4.4 Membrane electrode assembly fabrication

The electrodes with a gas diffusion layer and a catalyst layer were fabricated by following the same procedure as mention in section 2.3.4.4. A polymer electrolyte membrane, BPBI (80 µm) was doped in 10 molar $H_3PO_4$ for 24 was wiped out by tissue paper and dried at 100 °C under vacuum. The membrane and electrode assemblies (MEAs) were made by hot-pressing the pretreated electrodes (9 $cm^2$) and the membrane under the conditions of 120 °C, 130 atm for 3 min.

### 4.3.4.5 Polarization study

Figure 4.20 shows the fuel cell performance of BPBI membrane in terms of polarization plots of MEA fabricated using 20% Pt/C for both anode and cathode in a single cell experiment , at 100, 125 and 150 °C with a dry $H_2/O_2$ gas flow rate of 0.4 slpm (standard liters per minute). BPBI membrane show lower performance than that of the PBI membrane. The open-circuit voltage (OCV) obtained with the APBI membrane is 0.88 V at 150 °C, whereas for PBI it is 0.92 V. The BPBI membrane gives a maximum power density 137 $mW/cm^2$ at 0.3 V, whereas the PBI membrane gives 210 $mW/cm^2$ at 0.3 V.  This lower fuel cell performance of APBI membrane can be attributed to low $H_3PO_4$ acid content and low proton conductivity of APBI membrane.
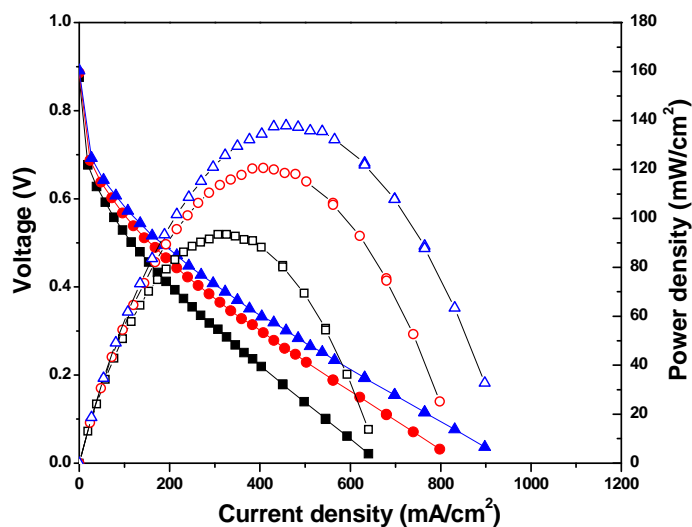


**Figure 4.20** Polarization curves obtained with BPBI membrane fuel cell at different temperatures with dry $H_2$ and $O_2$ (flow rate 0.4 slpm). The cell was conditioned for 30 min at open-circuit potential and at 0.2 V for 15 min before measurements**.** Key: (■□) 100, (●○) 125 and (▲△) 150 °C.

### 4.4   Conclusions

- A new diacid namely, 5-(1H-benzo[d]imidazol-2-yl) isophthalic acid was successfully synthesized by simple cyclization and oxidation reactions in high purity and high yield, by using a commercially available acid like 3-5 dimethylbenzoic acid.

- New series of polybenzimidazoles having pendant benzimidazole groups were synthesized from substituted m-phenylene diacid namely 5-(1H-benzo[d]imidazol-2-yl) isophthalic acid with 3,3',4,4,'-tetra amino biphenyl (TAB) and commercial diacids using high temperature solution polycondensation in PPA.

- Most of these polymers were soluble in a wide range of solvents like NMP, DMAc, DMF, TFA, $H_2SO_4$, methane sulfonic acid compared to the commercial polybenzimidazole indicating that the incorporation of bulky pendant groups lead to an improvement in solubility.

- Incorporation of pendant benzimidazole group enhances the thermal stability of these polymers significantly and hence they exhibited good thermal stability as compared to the commercial PBI.

- Pendant benzimidazole groups improve the oxidative stability of polymers as compared to the commercial PBI.

- Though, significant enhancement in proton conductivity of PBI is not achieved by incorporation of pendant benzimidazole groups, these proton conductivity of these polymers is sufficiently high for application as polymer electrolyte for PEMFC

**References**

1.  Buckley, A.; Steutz, D. E.; Serad, G. A. '*Encyclopedia* Vol. 11,2nd Edn., 1988, p. 572.

2.  High temp. adhesives: S. J. Shaw,  *Polymer International* 41 (1996) 193-207.

3.  Hergenrother, P. M.,  Smith Jr. J. G.  and Connell, J. W. *Polymer*,  **1993**, 34, ,  856-865.

4.  Varma, I. K.; Veena, S, M. *Journal of polymer Science Part A: Polymer Chemistry*  1976, 14, 973 and Varma, I. K. and Veena, *S. M. J. Macromol. Sci. Chem.* **1977**, 11,845.

5.  Lakshmi Narayan, T. V.; Marvel, C. S. *Journal of polymer Science Part A-1: Polymer Chemistry* **1967**, 5, 1113-1118.

6.  Syuichi Inoue.; Yoshio Imai.; Keikichi Uno.; Yoshio Iwakura. *Die Makromolekulare Chemie* **1966**, 95, 236-247.

7.  Srinivasan, P. R.; Srinivasan, M.; Mahadevan, V. *Journal of Polymer Science: Polymer Chemistry Edition*, **1982**, 20, 1145-1150.

8.  . Srinivasan, P. R.; Mahadevan, V.; Srinivasan, M. *Polymer*, **1981,** 22, 1290-1291.

9.  Sung Moon.; Arthur L. Schwartz.; Jeffrey K. Hecht. *Journal of Polymer Science Part A-1: Polymer Chemistry* **1970**, 8, 3665-3666.

10. Brock, T.; Sherrington, D. C.; Tang,  H. G. *Polymer*, **1991**, 32, 353-357.

11.  Ashok Reddy, T.; Srinivasan, M. *Journal of Polymer Science Part A: Polymer Chemistry* **1988**, 26, 1051-1061.

12. Srinivasan, P. R.; Mahadevan, V.; Srinivasan, M. *Journal of Polymer Science: Polymer Chemistry Edition* **1982**, 20, 3095-3105.

13. Behzad Pourabas.; Ahmad Banihashemi. *Polymer International* **2002**, 51, 1086-1099.

14.  Yoshio Iwakura.; Keikichi Uno.; Yoshio Imai.; Motoo Fukui. *Die Makromolekulare Chemie* **1964,** 77, 41-50.

15.  Moriyuki Sato.; Masaaki Yokoyama.  *Journal of Polymer Science: Polymer Chemistry Edition* **1981**, 19, 591-594.

16.  Yongzhu, Fu.; Arumugam Manthiram.; Michael D. Guiver. *Electrochemistry Communications* **2006**, 8, 1386-1390.

17. Persson, J.C.; Jannasch, P. *Macromolecules* **2005**; 38, 3283–9.

18.  Hongting Pu.; Lei Qiao.; *Macromol. Chem..phys*., **2005**, 206, 263-267.

19. Nai-Hong Li.; Jean M.J. Frechet. *Reactive Polymers* **1987**, 6, 311-321.

# Chapter 5

Blends of Polybenzimidazole with Sulfonated-PEEK and Commercial PVOH for Proton Exchange Membrane Fuel Cell- Preparation and Characterization

## 5.1   Introduction

Polymer electrolyte membrane is one of the key components of proton exchange membrane electrolyte fuel cells (PEMFC). This membrane should have several desirable features like good mechanical properties, high thermal stability, good chemical resistance, high proton conductivity and low cost. Presently, perfluorinated ionomer [1-3] (Nafion°) is commercially available polymer used as polymer electrolyte for fuel cell. However, its high cost, high fuel permeability, high water drag and low operating temperature (below 80 °C), among other drawbacks, have made it essential to search for alternate polymer electrolytes capable of operating above 130 °C in order to ameliorate the deactivation of platinum catalyst due to the adsorption of carbon monoxide [4]. Although many heterocyclic thermally stable polymers such as PBI [5-8], sulfonated polyimides [9] and polyoxadiazoles [10-11] amongst others are, considered as possible alternatives for Nafion, PBI doped with phosphoric acid is considered to be the most promising one due to several reasons. Commercial PBI, a condensation product of isophthalic acid and 3,3',4,4,'-tetra amino biphenyl (TAB), has high thermal stability, good mechanical property, high chemical resistance, low gas and methanol permeability, zero water drag and excellent proton transport properties at high temperature [12-15]. However, compared to Nafion, PBI has low proton conductivity and more significantly an adverse    tendency to loose efficiency with time due to the leaching out of unbound phosphoric acid by methanol or water formed during the electrochemical processes thus seriously undermining its durability in a fuel cell.

Consequently, various methods have been attempted to improve the proton conductivity of PBI including the synthesis of different types of structural analogues of PBI. One such method is the introduction of sulfonic acid groups by substituting N-H of imidazole group by a sulfonic acid group containing moiety [16-17]. Another method is the use of polymer blends to get improved properties. For example, Kerres et.al. [18-19] have recently described the use of acid-base blends of sulfonated polymers with polymers containing primary or secondary or tertiary nitrogen, while   Savinell et.al. [20] have described  the use of blends of basic polymers such as PBI with  sulfonated  polymers. Barbara Kosmala [21] describes  the  blends  of  PBI  with  sulfonated  polyphenyleneoxide (sPPO) as polymer

electrolytes for fuel cell. Bjerrum et al. [22-23] describes the blends of PBI with sulfonated polysulfone as polymer electrolytes for fuel cell. Kerres et al. [24] recommend the use of acid-base type binary blends of PBI with SPEEK or its metal salts and ternary blends of PBI, SPEEK and another basic polymer as polymer electrolytes. Blends of PBI and thermoplastic polymers such as sulfonated polysulfone have been used as polymer electrolytes [25]. Most of these blends, however suffer from the limitation of poor mechanical properties as they require large quantity of sulfonated polymer for high proton conductivity resulting in brittleness of membranes. Thus, most of the blends studied as polymer electrolytes for fuel cell are acid-base blends of PBI and sulfonated polymers or blends of polymers containing amine groups and sulfonated polymers [24]. The sulfonic acid groups in these polymers interact with imidazole groups or free amino groups in these polymers. However, blend of PBI containing free amino groups and sulfonated polymer as acid-base blend for polymer electrolyte for fuel cell has not been investigated. Infact, PBI containing pendant free aminophenoxy groups are not reported in literature. As apart of this thesis, we synthesized PBI containing pendant aminophenoxy groups as detailed in chapter 2. As extension of this work, an acid-base blend of PBI containing pendant aminophenoxy groups (APBI) and sulfonated PEEK (SPEEK) as polymer electrolyte for fuel cell has been investigated in the present work.

Polyvinyl alcohol (PVOH) is another polymer which interacts with $H_3PO_4$ to form gel capable of conducting protons. Blends of two polymers for example, PBI and PVOH, which conduct protons on doping with common dopant, $H_3PO_4$ is worth considering. However, proton transport behavior of blends of PBI with PVOH as polymer electrolyte has not been investigated in details. In this work we also report the performance of a new kind of blends. More specifically, we investigate the blends of PBI and PVOH as polymer electrolyte for hydrogen oxygen fuel cells focusing more on the systematic effect of PVOH on proton conductivity and other properties of PBI. Thus, this chapter describes preparation, characterization and evaluation of blends of APBI and SPEEK and blends of PBI and PVOH as polymer electrolyte for fuel cell.

## 5.2  Experimental

### 5.2.1  Materials

Polybenzimidazole (PBI) was synthesized by reported procedure [26]. Poly (ether ether ketone) (PEEK) was procured from Gharda Chemicals Limited, India under the trade name of Gatone™ 5300P. Concentrated sulphuric acid (98%) and LiCl were purchased from Loba chemicals, India. Polyvinyl alcohol (PVOH) (Mn 125000) was obtained from s.d. fine chemicals, India. Phosphoric acid and polyphosphoric acid were purchased from Merck, India and isophthalic acid and 3,3',4,4,'-tetra amino biphenyl (TAB) from Aldrich chemicals. Dimethylacetamide (DMAc) (Spectrochem) was dried over $CaH_2$ and distilled under reduced pressure. Isophthalic acid and TAB were recrystallized from methanol and water respectively.

### 5.2.2  Analytical methods

All the analytical methods used to characterize the blend membranes are same as described in chapter two except SEM and water uptake. For SEM the membranes were freeze fractured in liquid nitrogen, and the surface morphology was studied by scanning electron microscopy (SEM) using a Hitachi S2150 microscope. The water uptake and sample loss of blend membranes was determined by immersing weighed dry membrane samples (1 x 1 cm pieces) of blend membrane in distilled water for 24 h at ambient temperature. The membranes after removing from distilled water were dried with tissue paper to remove adhered water and weighed again. The water uptake was determined by formula (eqn no.1)

$$\text{Water uptake}\,[\%] = \frac{W_{wet} - W_{dry}}{W_{dry}} \times 100 \qquad\qquad [1]$$

where, $W_{dry}$ is the weight of the dried sample before immersing in water and $W_{wet}$ the weight of the sample after removing from water. The same sample was dried under vacuum oven at 120 °C for 24 h and weighed again. The sample loss was determined by the equation (eqn no. 2),

$$\text{Sample loss}\,[\%] = \frac{W_{dry} - W'_{dry}}{W_{dry}} \times 100$$

$$[2]$$

where $W_{dry}$ is the weight of the dried sample before measurement and $W'_{dry}$ is the weight after vacuum drying the sample, immersed in water.

### 5.2.3    Preparation of APBI-SPEEK Membranes

#### 5.2.3.1 Sulfonation of Polyether ether ketone

The sulphonation of PEEK in granule form was carried out in a round bottom flask by following procedure described in literature [27]. A solution of 12.5 g PEEK in 200 mL conc. $H_2SO_4$ was stirred mechanically for a period of 3 h at 45 °C. A polymer with 70% degree of sulphonation was obtained. The sulphonated PEEK (SPEEK) was then precipitated by drop-wise addition of the solution to 500 mL of ice cold distilled water. The product was washed till the excess acid was removed and dried in an oven at 70 °C for 12 h. This dried product was kept in a dessicator. Elemental analysis Found: C, 62.94%; H, 4.62 %; S, 6.11%.

#### 5.2.3.2 SPEEK blending with polybenzimidazole having amino group (APBI)

APBI in the powder form was dried under vacuum for 24 h at 150 °C in order to remove the absorbed moisture. 5 g of dried APBI was added slowly in small quantities to 100mL of dry DMAc with stirring for one hour. The temperature of the solution was increased upto 150 °C and heated for half hour. A homogeneous solution was formed, which was filtered through polypropylene cloth at hot condition in order to remove any particle present in solution. A solution of SPEEK (5 wt%) in DMAc was prepared by following similar procedure. Triethyl amine was added to neutralize SPEEK. These two solutions were used to prepare the blend membranes of SPEEK-APBI.

Solutions of APBI (5 wt %) and SPEEK-Net$_3$H$^+$(5 wt %) in DMAc were mixed in different proportions as listed in Table 5.1 and heated for 15 min at 100 °C with stirring. Membranes of the blend having 100 μm thicknesses were prepared by solution casting by pouring the solution onto a glass Petri dish and heating at 80 °C for 24 h in an oven. After solvent evaporation, the Petri dish with the polymer membranes were cooled to ambient temperature, and subsequently the Petri dish were immersed in a water bath. After 5–30 min, the membranes came off the Petri dish.

The membranes were post-treated first in hot 10% HCl solution for 24 h at 80 °C, and then at 60 °C in hot distilled water for 24 h to remove excess acid from the membranes. To remove any excess of solvent, the membranes were dried under vacuum at 120 °C for 2 days. Membranes of 10 μm thickness for recording IR spectra were cast by the same method.

**Table 5.1** Blend Composition of APBI/SPEEK polymer blends.

| Polymer blend Code | Polymers used | Composition APBI/SPEEK wt% |
|:---:|:---:|:---:|
| APBI | APBI | 100/0 |
| APS-1 | APBI/SPEEK | 75/25 |
| APS-2 | APBI/SPEEK | 50/50 |
| APS-3 | APBI/SPEEK | 25/75 |
| SPEEK | SPEEK | 0/100 |

**APBI**: Amino group containing polybenzimidazole; **SPEEK**: Sulfonated polyether ether ketone.

### 5.2.4 Preparation of PBI-PVOH blend membranes

Blends of PBI and PVOH were prepared by mixing of solutions of PBI and PVOH in DMAc. Solution of PBI (5%) was prepared by adding 5 g of PBI, dried at 150 °C for 24 h in a vacuum oven, to 110 mL of dry DMAc in 1 h with stirring. To this, 150 mg (3 wt%) LiCl was added and mixture was heated to 150 °C for 1 h. The homogeneous solution formed was filtered through propylene cloth at hot condition. The solid content of the solution was determined by evaporating the solvent from weighed quantity of the solution in a vacuum oven at 150 °C, till constant weight was obtained. The solution of PVOH in DMAc was prepared without using LiCl, by following similar procedure.

**Table 5.2** Blend Composition of PBI/PVOH polymer blends.

| Blend Code | Polymers used | Composition PBI/PVOH wt% |
|:---:|:---:|:---:|
| PBI | PBI | 100/0 |
| Blend-1 | PBI/PVOH | 90/10 |
| Blend -2 | PBI/PVOH | 80/20 |
| Blend -3 | PBI/PVOH | 70/30 |
| Blend -4 | PBI/PVOH | 60/40 |
| Blend -5 | PBI/PVOH | 50/50 |

**PBI**: Commercial polybenzimidazole; **PVOH**: Polyvinyl alcohol.

**5.2.4.1 Preparation of membranes of the blend**

Solutions of PBI and PVOH in DMAc were mixed in different proportions as listed in Table 5.2 and heated for 1 h at 150 °C with stirring. Membranes of the blends (50 cm²) having 100 μm thicknesses were prepared by solution casting by pouring the solution onto a Petri dish and heating at 80 °C for 24 h in an oven. To remove any excess of solvent, the membranes were dried under vacuum at 150 °C for 2 days. Membranes of 10 μm thickness for Fourier Transform Infrared Spectroscopy (FTIR) were cast by the same method.

## 5.3 Results and Discussion

### 5.3.1 Preparation and structural characterization of APBI-SPEEK blends

Blends of APBI and SPEEK were prepared as described in the experimental part. PEEK was sulfonated using sulfuric acid and degree of sulfonation was calculated using the elemental analysis results. From the elemental analysis results it was proved that degree of sulfonation of PEEK used in present work is ~70%.

The polymer blends, thus obtained, were characterized by FTIR spectroscopy. FTIR spectra of all polymer blends were scanned using thin membranes. The FT-IR spectra of APBI, APBI\SPEEK blends and SPEEK are shown in Figure 5.1.

It is known from the literature that the ionic interactions in the blend of polymeric acids and bases can be observed via FTIR spectroscopy. The FTIR analysis of the acid–base blend membranes showed characteristic bands indicating the ionic crosslink formation between the sulfonated and basic polymers occurring by proton transfer. The IR spectra of acid–base interaction bands found in SPEEK/PBI blends have been reported previously [28] and the characteristic bands have been observed between 1300 and 1800 cm$^{-1}$.

In the present work the characteristic bands have also been observed in the range of 1300–1800 cm$^{-1}$ for the SPEEK/APBI blend membranes. In the Figure 5.1, absorption band at 3190 cm$^{-1}$ is assigned to self-associated N-H interaction of PBI chains in APBI. The intensity of band at 3335-3360 cm$^{-1}$ due to free amino group decreases as APBI percentage in blend decreases from 100 to 25%. Also the breathing mode of APBI, which appears as a sharp band at 1286 cm$^{-1}$ disappears due acid–base interaction in N-H group of APBI and SO$_3$H groups of

SPEEK. This shows the ionic interaction between the sulfonic acid groups and the benzimidazole.
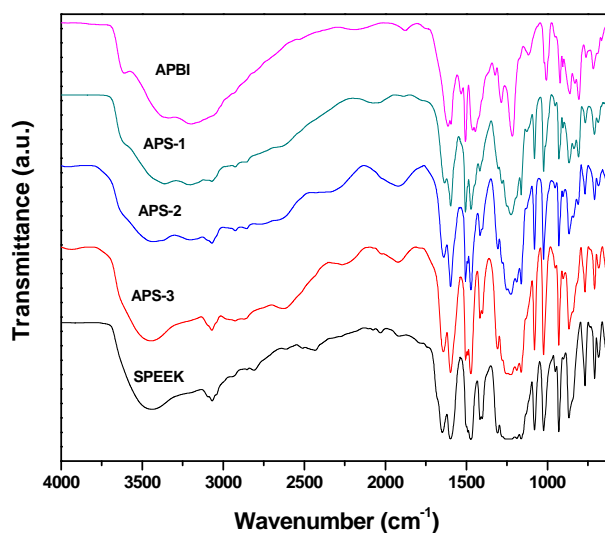


**Figure 5.1**   FTIR spectra of amino group containing PBI and the sulfonated PEEK blends compared with APBI.

### 5.3.2   Properties of APBI-SPEEK blends

The properties of APBI-SPEEK blends were evaluated by SEM, X-ray diffraction, TGA and mechanical property study.

#### 5.3.2.1 Crystallinity

Crystalline nature of these polymer blend specimens (in membrane form) was studied by X-ray diffraction (Figure 5.2). No sharp peak for crystalline nature was observed. The amorphous nature of polymer blends could be attributed to their unsymmetrical structural units and the amino groups, which reduced the intra and interpolymer chain interactions, resulting in loose polymer chain packaging and aggregates.
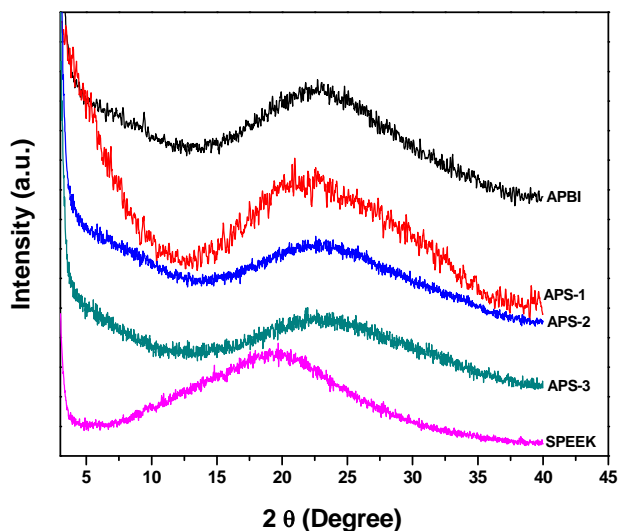


**Figure 5.2**   Wide-angle X-ray diffractograms of amino group containing PBI and the sulfonated PEEK blends compared with APBI.

#### 5.3.2.2 Scanning electron microscopy

For morphology characterization, the APBI, SPEEK and APBI/SPEEK blends of all compositions were freeze-fractured in liquid nitrogen. The fractured surface of APBI, SPEEK and APBI/SPEEK blends (Figure 5.3) was observed by SEM at X 10000 magnification. The SEM images of APBI and SPEEK show complete homogeneity as they are single polymer. APBI/SPEEK blends having SPEEK 25% and 50% also show complete homogeneity and lack of discrete domain in freeze-fractured surfaces, they show plate-like structures which indicate a greater uniformity of mixing. APBI/ SPEEK blend having composition 25:75 % show a discrete

domain in freeze-fractured surface which indicates lack of homogeneity or uniformity of mixing.
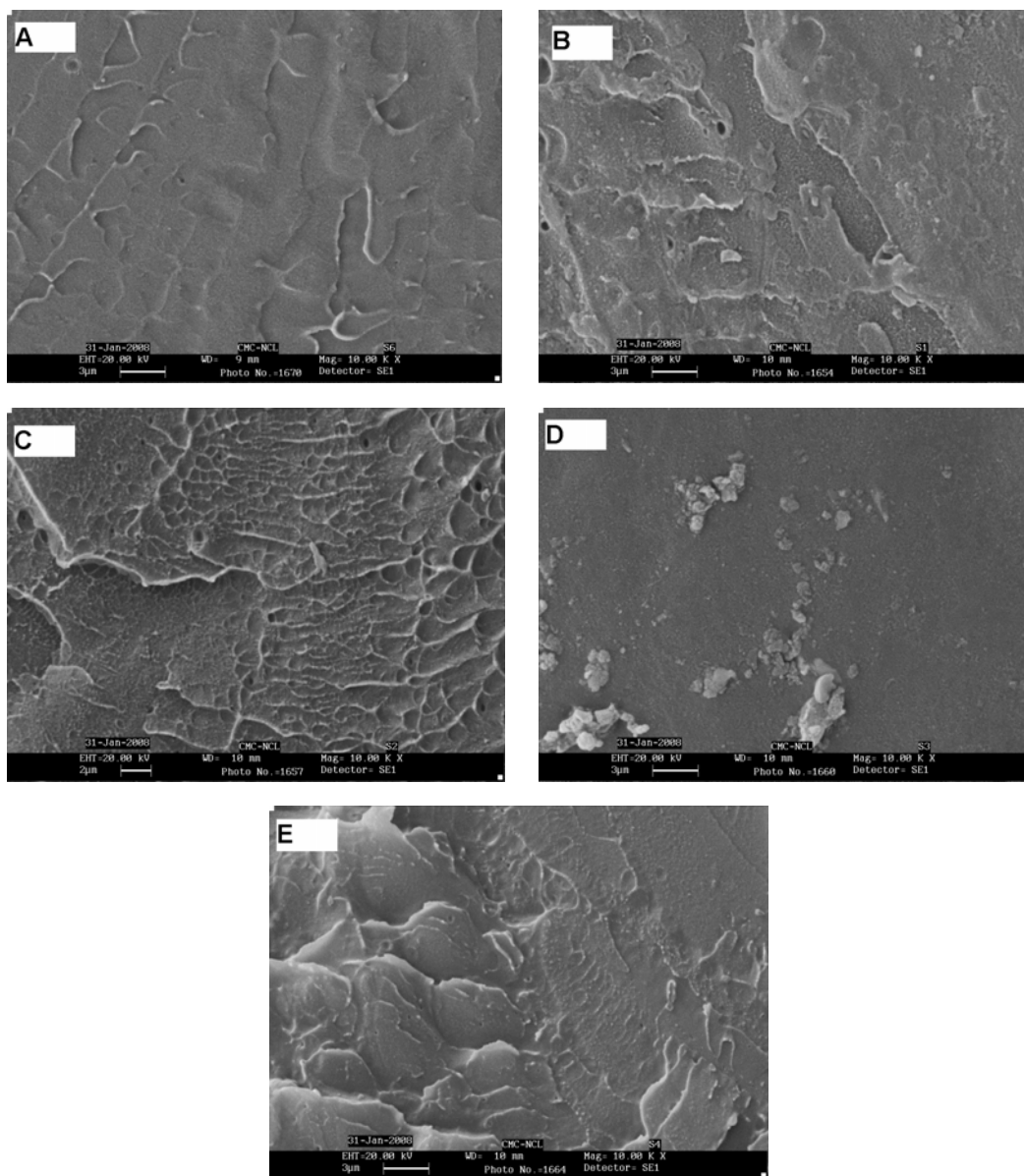


**Figure 5.3** Scanning electron microscopy (SEM) images of cross-section of APBI, SPEEK and blends by freeze fracturing A) APBI-100, B) APBI-75-SPEEK-25, C) APBI-50-SPEEK-50, D)APBI-25-SPEEK-75 E) SPEEK-100.

**5.3.2.3 Thermal properties of polymer blends**

➤ **Thermogravimetric analysis**

The thermal stability of the amino group containing PBI and the sulfonated PEEK blends was analyzed by thermogravimetric analysis and the results are given in Figure 5.4 & Table 5.2. All Blends exhibited a two-step degradation pattern (Figure 5.4). The first step of degradation was observed between 300-400 °C due to the decomposition of sulfonic acid groups. The second step decomposition occurs at 470-600 °C due to the decomposition of APBI and PEEK polymer main chain.

Low values of initial decomposition temperature (IDT) (376-392 °C), $T_{10}$ (379-444 °C) and $T_{20}$ (465 – 560 °C) compared to APBI indicate that the sulfonated PEEK lowers thermal stability of APBI-SPEEK blends.
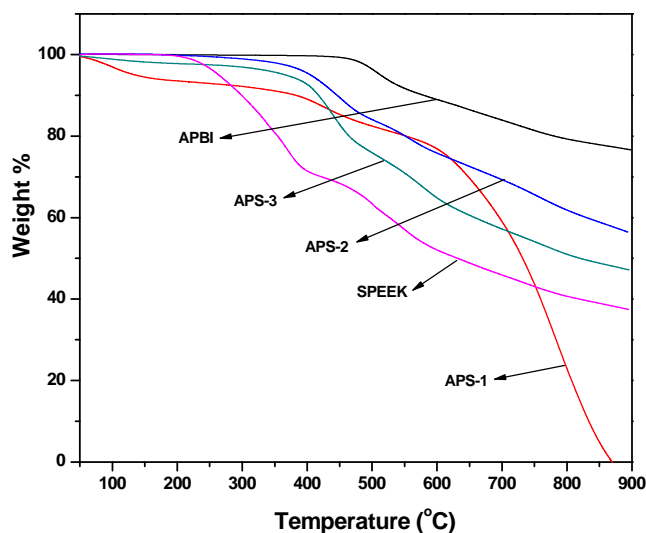


**Figure 5.4** TGA curves of amino group containing PBI and the sulfonated PEEK blends in N$_2$ at heating rate 10°C min$^{-1}$.

For the APBI, the onset for first step of degradation started around 475 °C. But the APBI-SPEEK blends show an onset around 380 °C indicating their less thermal stability. The thermal stability of blends decreases with increase in SPEEK content. However thermal stability of blends is better than the SPEEK. These results show that the thermal stability of APBI-SPEEK blend membranes is high enough for application as polymer electrolyte membranes for fuel cell for operation at high temperature.

**Table 5.3**   Thermal properties of amino group containing PBI and the sulfonated PEEK blends.

| Polymer blend code | IDT (ºC) | $T_{10}$ (ºC) | $T_{20}$ (ºC) | $T_{max}$ (ºC) | Residue (wt %) |
|:---:|:---:|:---:|:---:|:---:|:---:|
| APBI | 475 | 579 | 777 | 508 | 77.6 |
| APS-1 | 392 | 379 | 553 | 757 | 78.3 |
| APS-2 | 384 | 444 | 551 | 588 | 56.36 |
| APS-3 | 376 | 417 | 465 | 528 | 47.18 |
| SPEEK | 215 | 297 | 415 | 486 | 37.46 |

**IDT**: Initial decomposition temperature, $T_5$, $T_{10}$, and $T_{max}$: Temperature at which 5%, 10% and maximum weight loss of polymer blend takes place respectively**.**

### 5.3.2.4 Mechanical properties of  polymer blends

The values of tensile properties of APBI-SEEK blends are summarized in Table 5.4 and Figure 5.5 shows the tensile stress verses strain graph of amino group containing PBI and the sulfonated PEEK blends. APBI has tensile strength of 72 MPa. In the present study, it is observed that the sulfonated PEEK reduce the tensile strength of APBI from 72 MPa to 57 MPa (APBI-25-SPEEK-75) (Table 5.3), probably due to disruption of rigid polymer structure by sulfonated PEEK increasing free volume of the polymer blends. Tensile properties of APBI-SPEEK polymer blends have no specific trend. However, observed strength is sufficiently high for application as PEM for fuel cell.

**Table 5.4** Mechanical properties of amino group containing PBI and the sulfonated PEEK blends.

| Polymer blend code | Tensile stress (MPa) | Modulus (MPa) | Toughness (MPa) | Elongation at break (%) |
|:---:|:---:|:---:|:---:|:---:|
| APBI | 72 | 2267 | 2.25 | 4.3 |
| APS-1 | 59 | 2102 | 1.83 | 8.5 |
| APS-2 | 37 | 1647 | 1.08 | 2.0 |
| APS-3 | 57 | 4178 | 69.12 | 2.7 |
| SPEEK | 31 | 1313 | 1.95 | 4.22 |
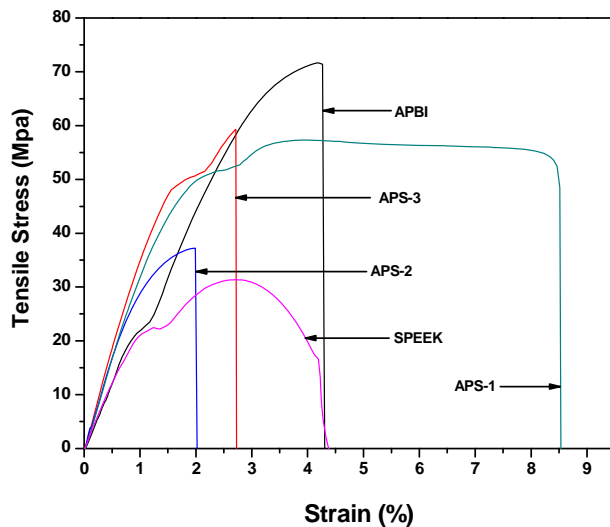
**Figure 5.5** Tensile stress versus strain graph of amino group containing PBI and the sulfonated PEEK blends.

### 5.3.3    Fuel cell characterization of APBI-SPEEK blend membranes

### 5.3.3.1 Oxidative stability study

Fenton reagent test was carried out with blends of amino group containing PBI and the sulfonated PEEK and APBI to examine the radical oxidative stability of these polymer blend membranes. The membranes (thickness: 40-60 μm) were soaked in 3% $H_2O_2$ containing 4 ppm $Fe^{2+}$ (Mohr's salt, $(NH_4)_2Fe(SO_4)_2 \cdot 6H_2O$) at 70 °C for 12 h and the stability was characterized by the remaining weight of the membranes, same sample was used upto 96 h by taking fresh solution after every 12 h.
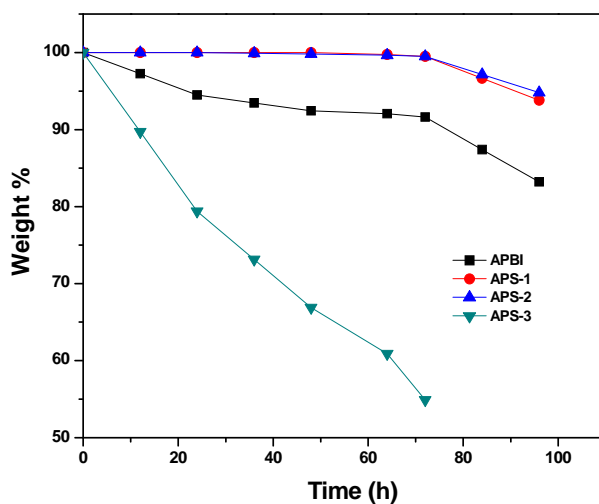


**Figure 5.6** Oxidative stability expressed as weight loss in Fenton's test of amino group containing PBI and the sulfonated PEEK blends.

As observed in Figure 5.6, no weight loss was observed till 72 h, for blends containing 25 and 50% SPEEK, while they show only 4% wt loss after 96 h in Fenton's reagent and the membranes  were still very tough indicating excellent oxidative stability of these blend membranes. The blend APBI-25-SPEEK-75 shows 45 % weight loss in 72 h and became brittle, indicating the dissolution of SPEEK from the blend membrane while, amino group containing APBI showed 15 % weight loss after the 96 h of Fenton reagent test and SPEEK dissolved in Fenton reagent test solution. High oxidative stability of blends is due to hydrogen bonding between $-NH-$, $NH_2$ of APBI and $SO_3H$ of SPEEK.

### 5.3.3.2 Phosphoric acid doping study

APBI-SPEEK blend membranes were doped with phosphoric acid by immersing in 85% $H_3PO_4$ for 72 h at 80 °C, while APBI membrane was doped in 12 molar $H_3PO_4$ for 24 h at ambient temperature. Uptake of phosphoric acid in APBI-SPEEK blend membranes at room temperature was very low. During doping, the membranes take water present in 85% $H_3PO_4$ along with phosphoric acid. Extent of doping and water uptake of APBI and blend membranes was determined as described in experimental part. Compared to APBI, blend membrane of APBI-75-SPEEK-25 takes more water and $H_3PO_4$ as it is doped in 85 wt% $H_3PO_4$. The doping level decreases significantly with increase in SPEEK content in blend membrane.

**Table 5.5** $H_3PO_4$ and water uptake of amino group containing PBI and the sulfonated PEEK blends compared with APBI and SPEEK doped at 80 °C for 72 h and Proton conductivity at 175 °C.

| Polymer Code | Doping level of $H_3PO_4$ along with water (wt %) | Water uptake along with $H_3PO_4$ (wt %) | Doping level of $H_3PO_4$ after drying (wt %)) | $\sigma_{max}$ (S cm$^{-1}$) |
|---|---|---|---|---|
| APBI* | 413 | 76 | 337 | $2.40 \times 10^{-2}$ |
| APS-1 | 580 | 130 | 450 | $2.99 \times 10^{-2}$ |
| APS-2 | 203 | 19 | 184 | $1.10 \times 10^{-2}$ |
| APS-3 | 71 | 9.5 | 59 | $8.56 \times 10^{-4}$ |
| SPEEK | - - | - - | - - | $1.99 \times 10^{-2}$ |

**\***APBI membrane doped in 12 molar $H_3PO_4$ at room temperature.

### 5.3.3.3 Proton conductivity measurement

For the proton conductivity measurements, APBI-SPEEK blend membranes were doped with phosphoric acid by immersing in 85% $H_3PO_4$ for 72 h at 80 °C, while APBI membrane was doped in 12 molar $H_3PO_4$ for 24 h at ambient temperature and dried under vacuum for 24 h at 110 °C. Temperature dependant conductivity of doped polymer membranes was determined in the temperature range of 25 to 175 °C as described in experimental part of chapter 2.
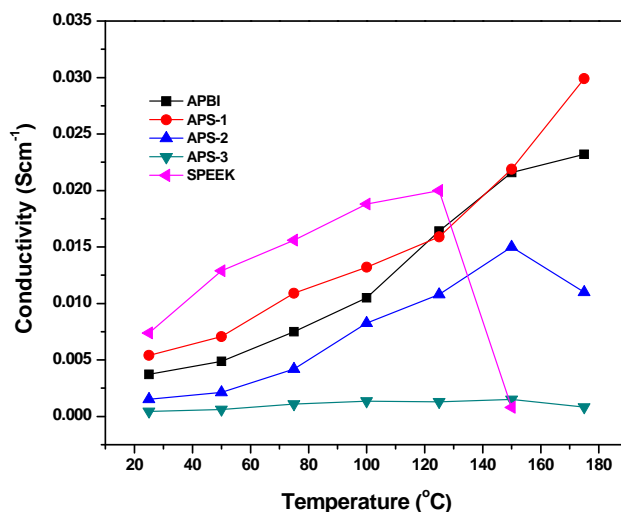


**Figure 5.7** Proton conductivities of amino group containing PBI and the sulfonated PEEK blends compared with APBI and SPEEK at different temperature.

Figure 5.7 represents the conductivity vs. temperature graph. The SPEEK-100 membrane was treated by immersing in distilled water at room temperature for 24 h, prior to conductivity measurement in the temperature range of 25 to 150 °C. The APBI-75-SPEEK-25 blend membrane exhibited high proton conductivity ($2.99 \times 10^{-2}$ S.cm$^{-1}$) compared to that of APBI ($2.40 \times 10^{-2}$ S.cm$^{-1}$) at 175 °C (Table 5.5). These conductivity values decrease with increase in SPEEK content in blends.

### 5.3.3.4 Membrane electrode assembly fabrication

The electrodes with a gas diffusion layer and a catalyst layer were fabricated by following the same procedure as mentioned in section 2.3.4.4. A polymer electrolyte membrane, APBI-75-SPEEK-25 (110 μm), doped in 85% $H_3PO_4$ for 72 h at 80 °C, was wiped out by tissue paper and dried at 100 °C under vacuum. The membrane and electrode

assemblies (MEAs) were made by hot-pressing the pretreated electrodes (9 cm$^2$) and the membrane under the conditions of 120 °C, 130 atm for 3 min.

### 5.3.3.5 Polarization study

Figure 5.8 shows the fuel cell performance of APS-1 blend membrane in terms of polarization plots of MEA fabricated using 20% Pt/C for both anode and cathode in a single cell experiment, at 100, 125 and 150 °C with a dry H$_2$/O$_2$ gas flow rate of 0.4 slpm (standard liters per minute). The blend membrane shows better performance than that of the APBI membrane. The open-circuit voltage (OCV) obtained with the APBI-75-SPEEK-25 blend membrane is 0.93 V at 150 °C, whereas for APBI it is 0.90 V. The APBI-75-SPEEK-25 blend membrane gives a maximum power density 179 mW/cm$^2$ at 0.3 V, whereas the APBI membrane gives 163 mW/cm$^2$ at 0.3 V.  This better fuel cell performance of APBI-75-SPEEK-25 blend membrane can be attributed to bonded phosphoric acid to the amino groups and amino sulfonate complex of APBI and SPEEK, which increases the protonating sites in the polymer matrix and help in fast proton transport in APS-1blend which explains observed good fuel cell performance of blend.
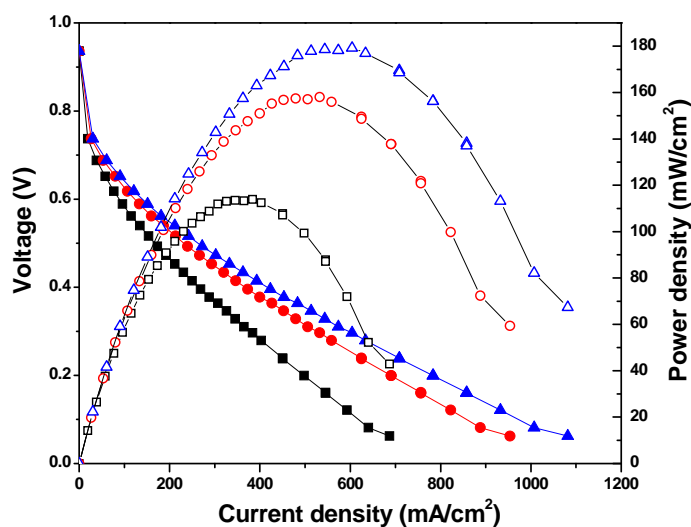


**Figure 5.8**  Polarization curves obtained with APS-1 blend membrane fuel cell at different temperatures with dry H$_2$ and O$_2$ (flow rate 0.4 slpm). The cell was conditioned for 30 min at open-circuit potential and at 0.2 V for 15 min before measurements. Key: (■□) 100, (●○) 125 and (▲△) 150 °C.

### 5.3.4    Preparation and structural characterization of PBI-PVOH blends

Membranes of polymer blends were prepared by solution casting technique, wherein solutions of both polymers after mixing were heated to 150 °C prior to casting. The membranes obtained after mixing at room temperature without heating (even after sonication) have lower softening point. Five blend membranes having PBI:PVOH weight percent ratio of 90:10 (Blend-1), 80:20 (Blend-2), 70:30 (Blend-3), 60:40 (Blend-4) and 50:50 (Blend-5) were prepared (Table 5.2). All the membranes were observed to be transparent and flexible.
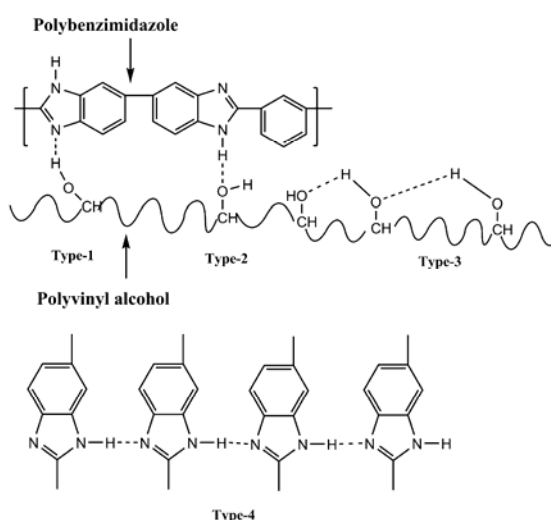


**Scheme 5.1** Various types of hydrogen bonding in blends

Miscibility of polymers has a profound effect on the properties of blends since it critically depends on the specific interactions between polymer chains. For example, aromatic PBIs possess both donor and acceptor hydrogen bonding sites capable of participating in specific interactions, while PVOH has hydroxyl groups capable of participating in hydrogen bonding. Indeed, both, N-H and C=N groups in PBI and OH groups of PVOH can interact by inter and intra-molecular hydrogen bonding. Possible interactions occurring on blending PBI and PVOH have been shown in Scheme 5.1, which include (i) inter-molecular hydrogen bonding between hydroxyl (OH) of PVOH and C=N (type-1) and N-H (type-2) groups of benzimidazole in PBI, (ii) intramolecular hydrogen bonding between hydroxyl groups of PVOH (type-3) and (iii) intramolecular hydrogen bonding between N-H groups of

benzimidazole in PBI (type-4). Intermolecular hydrogen bonding between two polymers enhances miscibility.

FTIR technique has been widely used to study the specific interactions, particularly, hydrogen bonding between the polymers. These interactions can be detected by the shifts in absorption of particular groups, involved in specific interactions in IR spectroscopy. Since probable interactions between PBI and PVOH are by hydrogen bonding between benzimidazole group in PBI and O-H groups in PVOH, the specific area of interest in IR spectra are 1000-1280 cm$^{-1}$ for C-O stretching frequency for hydroxyl groups in PVOH, [29] 1280 cm$^{-1}$ for benzimidazole breathing mode and 3000-3600 cm$^{-1}$ for O-H groups in PVOH and N-H and imidazole group in PBI. IR spectra of present blends have been described below region wise. Adams et.al [29] has reported various interactions between PBI and copolymer of PVOH and polyvinyl acetate.

> **FTIR spectroscopy.**

*Region of 1320-1180 cm$^{-1}$*

In this region, absorption bands by C-O stretching in PVOH are observed in the range of 1000-1200 cm$^{-1}$, although this is affected by hydrogen bonding. For example, PVOH has a strong and broad absorption at 1252 cm$^{-1}$, which is likely due to the self-association of the hydroxyls through hydrogen bonding and other hydroxyl unit of the vinyl alcohol moieties. There is no significant absorption by PBI in this region. The blends exhibit this absorption more strongly. In blend-1 & 2 a major absorption peak is observed at 1260 cm$^{-1}$ with a distinct shoulder at 1287 cm$^{-1}$, which corresponds to the breathing mode of imidazole ring. As we move from blend 3 to blend 5 the absorption band broadens, although  the balance of the absorption also changes, so that in blends 3 and 4 the peak at 1266 cm$^{-1}$ is quite pronounced and the 1287 cm$^{-1}$ absorption is with less shoulder while in blend 5 it shows a single peak at 1265 cm$^{-1}$ (Figure 5.9.a). This is attributed to hydrogen bonding of **type-1** and **type-2** with PBI.

Hydrogen bonding between PBI & PVOH is expected to increase with the PVOH content in the blend and accordingly the absorption peak values in IR spectra of blend-3 to blend-5 suggest that the hydrogen bonding (type 1and 2) with PBI is sufficiently strong to

compete with self-association in both blend components. Region 1560-1680 cm$^{-1}$ in PBI exhibits a peak at 1625 cm$^{-1}$ C=N stretching bands typical of PBIs (see Figure 5.9.b) and as expected its intensity in the blend decreases as PVOH percentage increases.
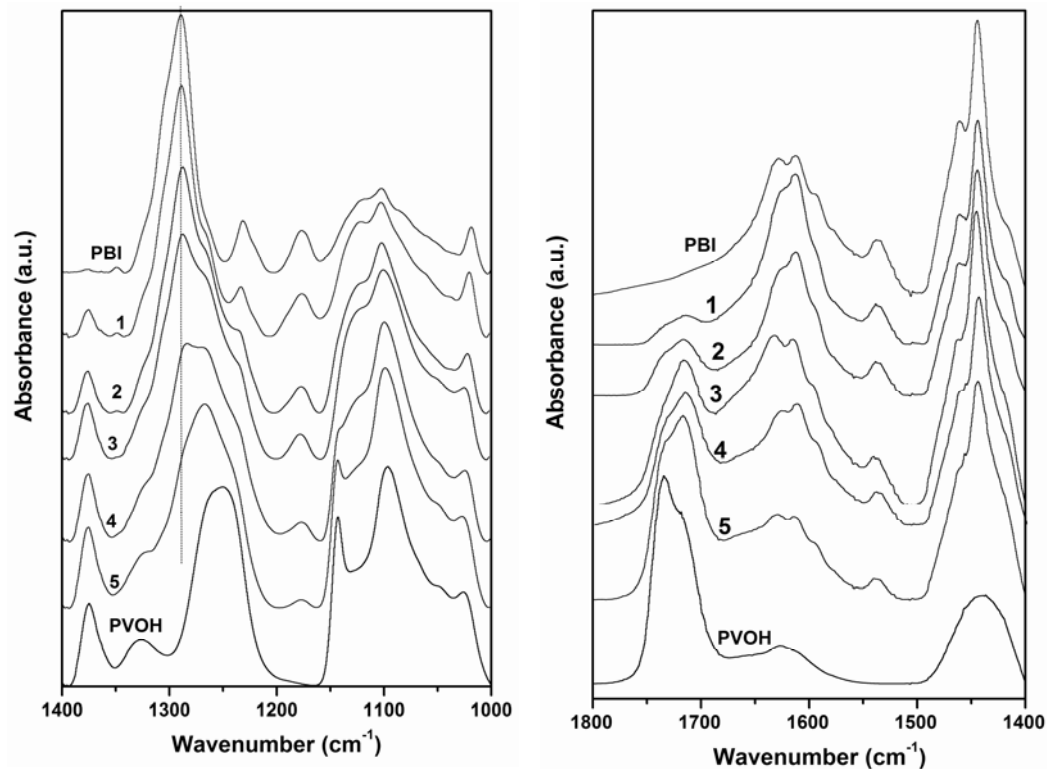


**Figure 5.9.a** FTIR spectra of PBI, PVOH and blends 1-5 in the region 1000-1400 cm$^{-1}$

**Figure 5.9.b** FTIR spectra of PBI, PVOH and blends 1-5 in the region 1400-1800 cm$^{-1}$

PVOH sample used in this study was expected to be fully hydrolyzed. IR spectra show some absorption at 1725 cm$^{-1}$ due to the presence of acetate groups. As the commercial PVOH sample is prepared by hydrolysis of poly vinyl acetate, it is likely to contain some unhydrolyzed acetate groups. Blends show peak at 1725 cm$^{-1}$ due to C=O stretch and represents non-associated species. Its intensity in blends increases as PVOH percentage increases.

*Region 2650-3700 cm$^{-1}$*

Musto et.al. [30] have reported 2500-3500 cm$^{-1}$ region in IR spectrum of PBI as the most sensitive region for hydrogen bonding. In PBI, absorption peak at 3195 cm$^{-1}$ and 3390 cm$^{-1}$ are assigned to self-association N-H interactions and non-interacting free N-H groups respectively. IR spectra in Fig 5.1.c shows the pronounced changes as we move through blend

1-3 due to progressive change in the PBI:PVOH ratio through blend series. The self association peak (3195 cm$^{-1}$) and free N-H (3390 cm$^{-1}$) are present in blends 1-3 but their intensity decreases as PVOH content in blend increases due to hydrogen bonding with PVOH. In these blends PVOH content is less compared to PBI content. But in blend 4-5 these absorption peaks vanishes as PVOH content increases. In blend 5, it shows single strong absorption at 3360 cm$^{-1}$, which confirms the hydrogen bonding of hydroxyl groups to N-H groups of PBI (Figure 5.9.c). Thus, IR study indicates the interactions between PBI and PVOH via hydrogen bonding for the formation of miscible blends.
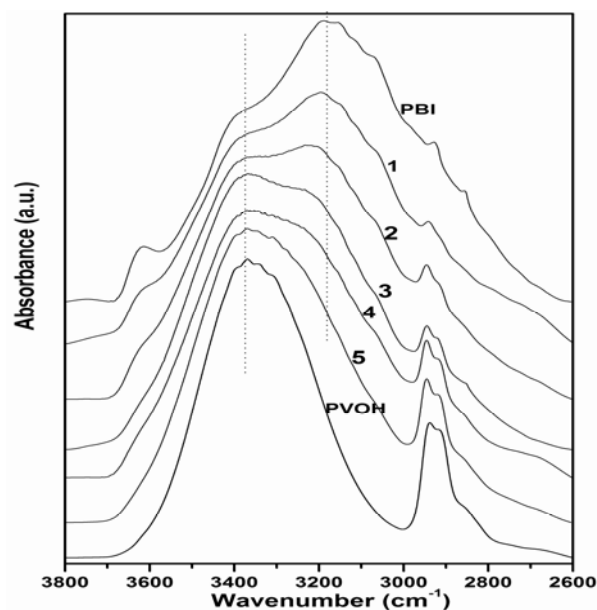


**Figure 5.9.c** FTIR spectra of PBI, PVOH and blends 1-5 in the region 2600-3600 cm$^{-1}$.

### 5.3.5 Properties of PBI-PVOH blends

The properties of PBI-PVOH blends were evaluated by SEM, X-ray diffraction, DSC, TGA and mechanical property study.

### 5.3.5.1 Crystallinity of blends

WAXD spectra of these blends are shown in Figure 5.10, where PBI clearly shows a broad scattering resulting from the amorphous structure. PVOH membrane, however, shows a characteristic scattering for an orthorhombic lattice centered at 20º, indicating a semi crystalline structure [31]. With the addition PBI to PVOH, the degree of crystallinity progressively reduces and blends-1 and 2 with 90 and 80% of PBI content respectively finally show amorphous nature. Since crystallinity in PVOH is mainly due to the intramolecular hydrogen bonding, addition of PBI can easily disturb the order in PVOH due to the interaction between imidazole groups in PBI and hydroxyl groups in PVOH, thus resulting in the observed decrease in crystallinity.
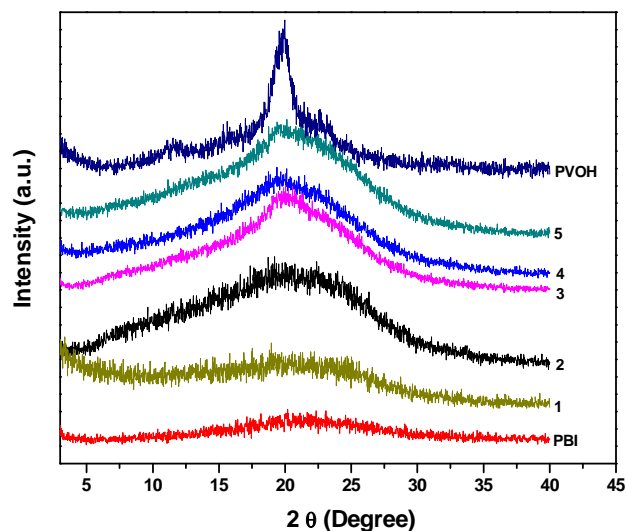


**Figure 5.10** Wide Angle X-ray (WAXD) scattering graphs of Blends 1-5 and PBI

### 5.3.5.2 Scanning electron microscopy (SEM)

For morphology characterization, the PBI/PVOH blends of all compositions were freeze-fractured in liquid nitrogen. The fractured surface of blends (Figure 5.11) was observed by SEM at X 10000 magnification. All SEM images show complete homogeneity and lack of discrete domain in freeze-fractured surfaces of PBI/PVOH blends. All the blends show

homogeneity as plate-like structures are seen, which indicates perhaps a greater uniformity of mixing. The morphological evidence thus supports the I.R analysis and DSC results of the formation of miscible blends.
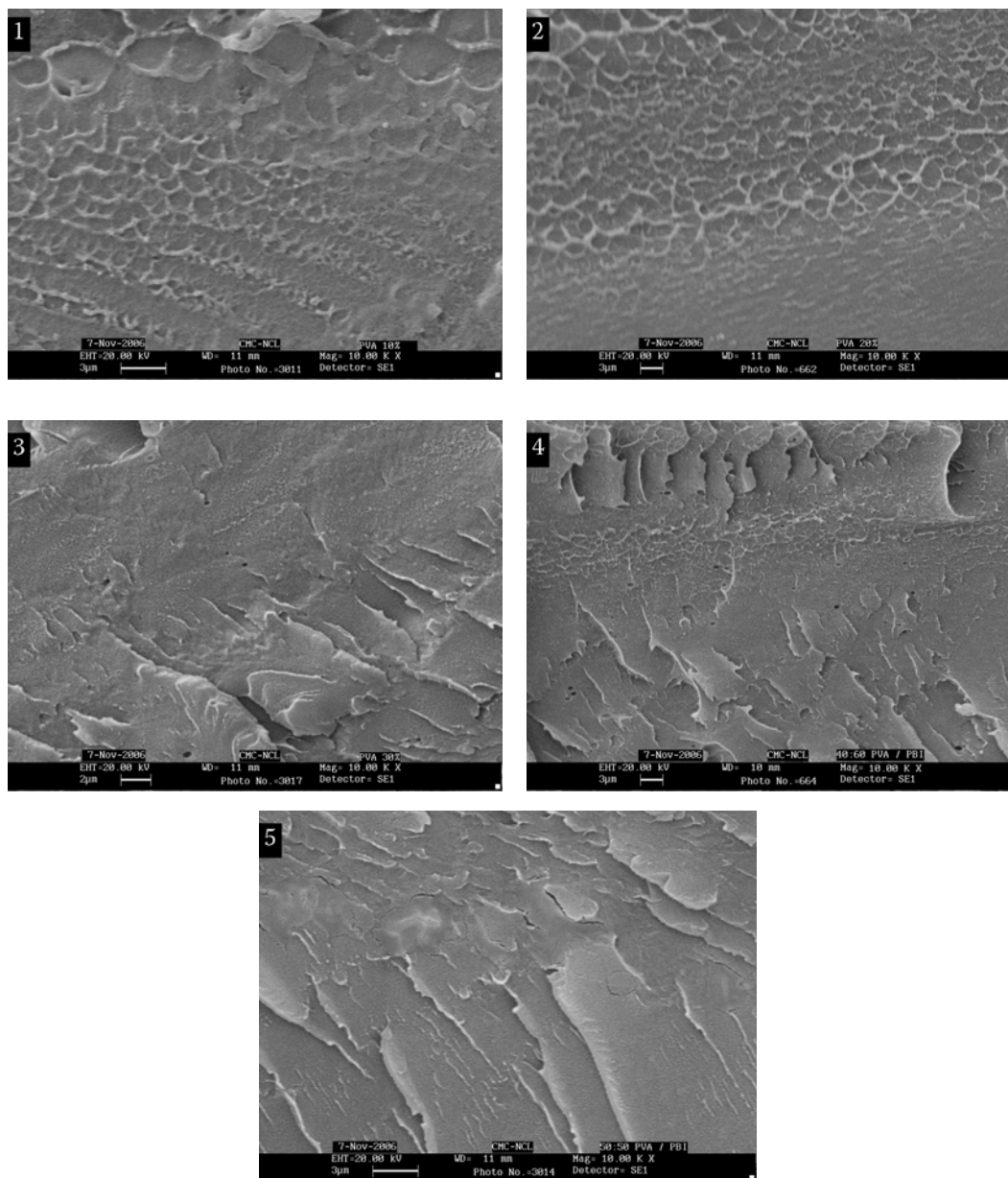


**Figure 5.11** Scanning electron microscopy (SEM) images of cross-section of blends 1-5 by freeze fracturing **1**) PVOH-10-PBI-90, **2**) PVOH-20-PBI-80, **3**) PVOH-30-PBI-70, **4**) PVOH-40-PBI-60  **5**) PVOH-50-PBI-50.

**5.3.5.3 Thermal properties of blends**

> **Differential scanning calorimetry**

The glass transition temperature ($T_g$) of the blends was determined by differential scanning calorimetry (DSC) from 50 to 450 °C in nitrogen atmosphere at a heating rate of 20 °C /min. The DSC curves, recorded at the second heating are depicted in Figure 5.12. The glass transition temperature of PVOH is observed at 71 °C (Figure 5.12) and the softening point at 180 °C. The absence of endotherm at 71 °C region in all blends substantiates the formation of miscible blends. Exact $T_g$ of the blends could not be located correctly. However it appears that the $T_g$ of these blends are in the range of 275-300 °C.
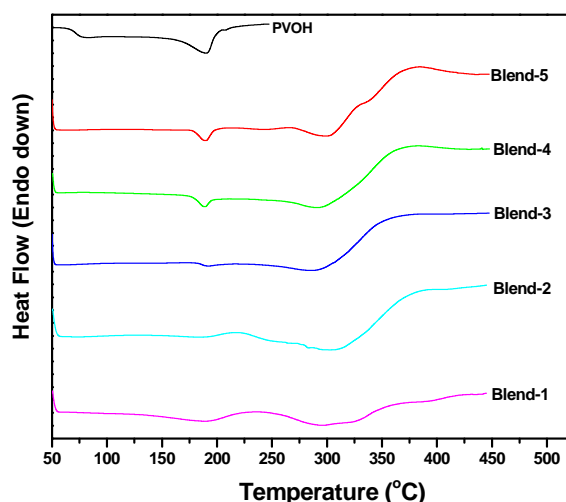


**Figure 5.12** DSC thermograms of Blends 1-5 and PVOH in nitrogen atmosphere at a heating rate of 20 °C min$^{-1}$.

> **Thermal gravimetric analysis**

Thermal behavior of blend membranes show interesting changes (Figure 5.13). The membranes were dried in a vacuum oven at 150 °C for two days prior to thermo gravimetric measurements to remove solvent. PBI is known for high thermal stability having initial decomposition temperature $T_{IDT} \sim 600$ °C. Interestingly the addition of PVOH to PBI significantly reduces the thermal stability of these blends. Thus, initial decomposition temperature of blend of PBI containing 10% of PVOH is ~ 287 °C. Low $T_{IDT}$ of blend-1 is mainly due to decomposition of PVOH in the blend. $T_{IDT}$ of PVOH is 295 °C, which is higher than that of blend-1.
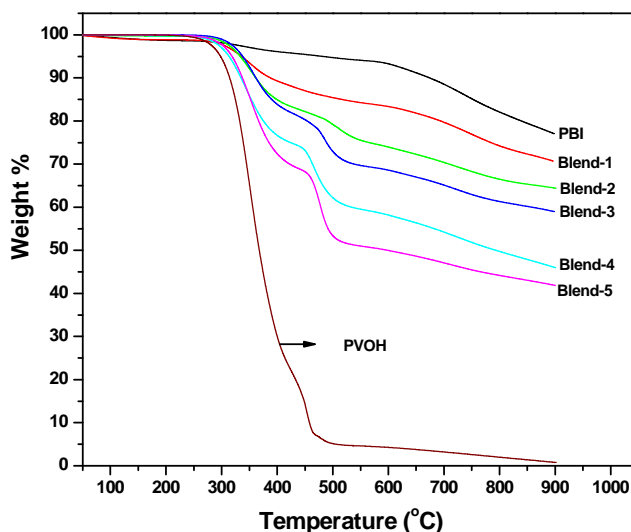
**Figure 5.13** TGA curves of PBI, PVOH and 1-5 Blends in $N_2$ at heating rate 10 °C min$^{-1}$.

This shows that the addition of low percentage of PVOH presumably disrupts self associated hydrogen bonding in PBI and also intra molecular hydrogen bonding of PVOH and thus PVOH without hydrogen bonding decomposes at lower temperature. Further addition of PVOH increases $T_{IDT}$ slightly. Thus, blend-2 containing 20% of PVOH and blend-5 containing 50% PVOH have $T_{IDT}$ of 310 and 314 °C respectively. This increase in $T_{IDT}$ of blends compared to $T_{IDT}$ of PVOH is due to hydrogen bonding of PVOH with PBI in blends. Temperature for 10% ($T_{10}$) and 20% ($T_{20}$) weight loss also decreases with increase in PVOH content in blends. DTG curves show two regions of maximum rate of weight loss, one around 340 – 355 °C mainly due to loss of PVOH and another around 718-736 °C due to decomposition of PBI. Residue decreases with increase in PVOH content due to loss of PVOH**.**

#### 5.3.5.4  Mechanical properties of blends

Figure 5.14 shows the effect of PVOH on mechanical properties of PBI in blends of PBI containing   10-50 wt% PVOH (Blends 1–5). The addition of PVOH to PBI results in an overall reduction in tensile strength. The initial reduction in tensile strength of PBI from 151 MPa to 99 MPa by the addition of 10% of PVOH may be probably due to the disruption of self-associated hydrogen bonding in PBI by PVOH. Further addition of PVOH up to 30% increases tensile strength to 132 MPa. This slight enhancement in tensile strength may be attributed to hydrogen bonding of PVOH with PBI. However, tensile strength again reduces to 115 and 90 MPa by further addition of 40 and 50% PVOH respectively, probably due to

plasticizing effect of PVOH. A similar trend is also observed for tensile modulus. Thus, tensile modulus decreased by ~18% from 3771 to 3088 MPa by the addition of 10% PVOH. As we move to higher wt% of PVOH in PBI, the tensile modulus also increases from 3088 to 3647 and 3785 MPa for blends containing 20 and 30 wt% PVOH respectively.
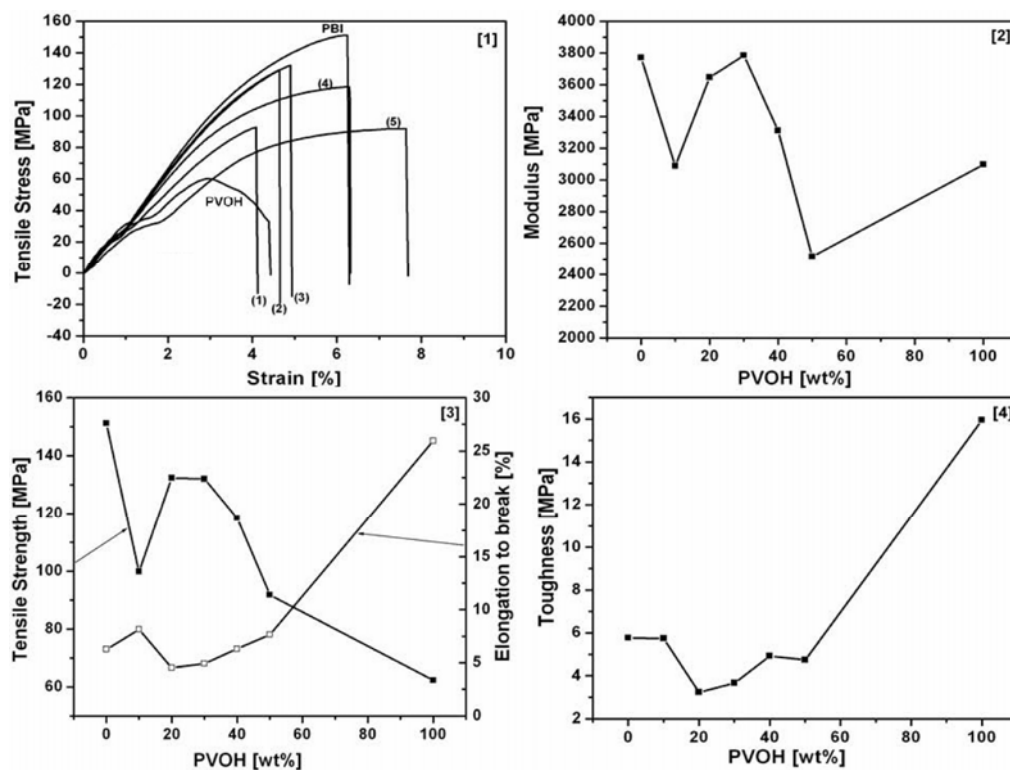


**Figure 5.14** [1] Variations in tensile stress (MPa) as a function of strain (%) for PBI, PVOH and 1-5 PBI/PVOH blend membranes. [2] Shows the plot of the variation in tensile modulus (MPa) as a function of wt% of PVOH in blends. [3] Is a plot of tensile strength and elongation to break (%) as a function of wt% of PVOH in blends [4] shows the variation in the toughness (MPa) as a function of wt % of PVOH in blends.

The tensile modulus again decreases to 3311 and 2516 MPa for blends containing 40 and 50% PVOH. These observations indicate that PVOH disrupts self-associated hydrogen bonding of PBI followed by hydrogen bonding with PBI depending on quantity of PVOH and finally acts as plasticizer. Interestingly, the toughness of PBI is not much affected by the addition of 10% PVOH although it decreases as PVOH content is increased to 30% followed by a slight further increase for 40 and 50% addition respectively. Elongation at break is high for blend containing 10% PVOH (80%) compared to 72% for PBI. It decreases to 64% for blend containing 20%

PVOH. However, it increases as PVOH content is increased further. Mechanical properties of blends are superior to that of PVOH. Though, the mechanical properties of blend membranes are low compared to PBI, they are high enough as membranes for fuel cell.

### 5.3.6    Fuel cell Characterization of PVOH-PBI blends PEM
### 5.3.6.1 Oxidative stability study

PBI is known [32] to undergo oxidative degradation by the radicals formed during the decomposition of hydrogen peroxide formed at cathode during the fuel cell operation. This results in the overall reduction in life of PEM and stack arising primarily due to membrane degradation issues.  In order to have some idea on the durability of these blend membranes, oxidative stability was determined by Fenton test as described in the experimental part.
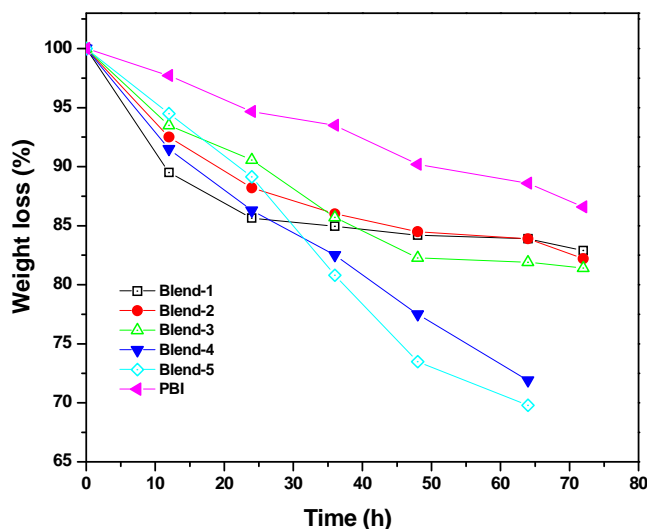


**Figure 5.15** Oxidative stability graph of PBI:PVOH blends and PBI by Fenton test.

The membranes (thickness: 40–60 μm) were soaked in 3% $H_2O_2$ containing 4 ppm of $Fe^{2+}$ (Mohr's salt, $(NH_4)_2Fe(SO_4)_2 \cdot 6H_2O$) at 70 °C for 12 h and the stability was determined by the weight loss of the membranes. The same sample was used upto 72 h by taking a fresh solution after every 12 h. As observed in Figure 5.15, commercial PBI showed a weight loss of 10% after the 72 h immersion in Fenton reagent. The blend membranes, Blend-4 and Blend-5, however, displayed much poorer radical oxidative stability than Blends 1-3, and commercial PBI. Membranes of Blends 4 & 5 broke into pieces after 60 h and they could not be weighed. Thus blends, in general, have low oxidative stability compared to that of PBI.

**5.3.6.2 Water uptake and sample loss study of PBI/PVOH blends in water**

PBI is known [33] to absorb water at ambient temperature on exposure to air and the addition of PVOH is expected to modify water uptake properties of PBI. Water uptake of PBI and blend membranes was determined as described in experimental part (Table 5.6). PBI membranes absorb 16.5% water of its weight. Water uptake increases with increase in PVOH content in blend membranes and water uptake of blend-5 containing 50% PVOH is ~ 24%. PVOH being soluble in water, some loss in weight was expected for blend membranes due to leaching out of PVOH in water. Weight loss in blends is in the range of 3.5-6.5%. Such weight loss was also observed in blends of PBI and polyvinylpyrrolidone [34].

**Table 5.6** Water uptake and sample loss of PBI and 1-5 blends during the swelling experiment.

| Membranes | Blend composition (PBI/PVOH wt. ratio) | Equilibrium water uptake (Wt %) | Sample wt loss (Wt %) |
|-----------|----------------------------------------|--------------------------------|-----------------------|
| PBI       | 100/0                                  | 16.5                           | -                     |
| Blend-1   | 90/10                                  | 15.8                           | 4                     |
| Blend-2   | 80/20                                  | 16.3                           | 5.2                   |
| Blend-3   | 70/30                                  | 17.4                           | 6.5                   |
| Blend-4   | 60/40                                  | 19.5                           | 5.6                   |
| Blend-5   | 50/50                                  | 23.9                           | 3.5                   |

**5.3.6.3 Phosphoric acid doping study**

Blend membranes were doped with phosphoric acid by immersing in 85% $H_3PO_4$ for 24 h at ambient temperature. During doping, the membranes take water present in 85% $H_3PO_4$ along with phosphoric acid. Extent of doping and water uptake of PBI and blend membranes was determined as described in experimental part. Compared to PBI, all blend membranes takes more water and $H_3PO_4$ and uptake increases with PVOH content in blend membranes. Thus, acid uptake along with water of PBI membrane is 3.22 times of its weight, whereas that of blend membrane containing 50% PVOH is 4.84 times. Similarly, phosphoric acid uptake, as determined by drying the doped membranes in vacuum oven at 110 °C, of PBI membrane is 2.5 times of its weight and that of blend membrane containing 50% PVOH is 3.80 times. Phosphoric acid uptake also increases with increase in PVOH content in blends

(Figure 5.16). Water uptake during acid doping remains nearly same for all the blend membranes though it is higher than that of PBI membrane.
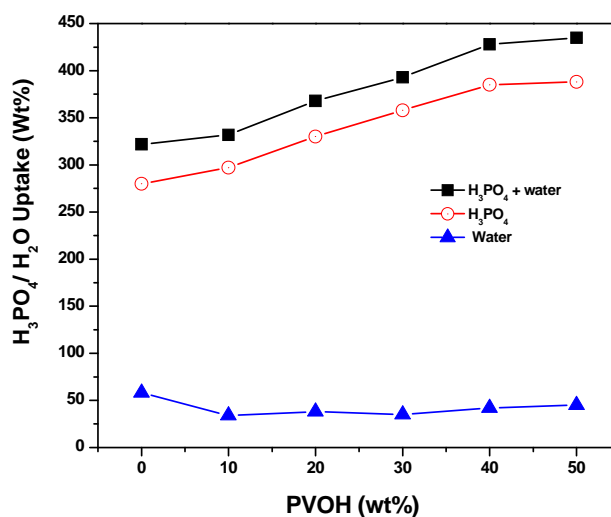


**Figure 5.16** $H_3PO_4$ and Water uptake of PBI and Blends 1-5 (■ $H_3PO_4$ uptake with water, ○ $H_3PO_4$ uptake after vacuum drying of doped membrane, ▲ water uptake during doping).

### 5.3.6.4 Proton conductivity measurement

For the proton conductivity measurements, membranes of blends and PBI were doped with 85% $H_3PO_4$ for 24 h and dried under vacuum for 24 h at 110 °C. It is well known [35] that PVOH form a gel membrane by absorbing phosphoric acid. It forms a complex with $H_3PO_4$, although it can not be used in a fuel cell due to the lack of mechanical strength and over swelling. By blending with PBI it gets mechanical strength and thus can avoid over-swelling to some extend even after doping with $H_3PO_4$. Temperature dependant conductivity of doped blend membranes was determined in the temperature range of 100 to 190 °C. Figure 5.17 represents the conductivity vs. temperature graph. The blend membranes exhibit high proton conductivities compared to that of PBI. Specifically, blend-5 shows high conductivity ($6.95 \times 10^{-2}$ S.cm$^{-1}$) followed by blend-4 ($5.96 \times 10^{-2}$ S.cm$^{-1}$) and blend-3 ($5.61 \times 10^{-2}$ S.cm$^{-1}$) at 190 °C. Interestingly, these values are more than that obtained for PBI ($3.92 \times 10^{-2}$ S.cm$^{-1}$) at 190 °C (Table 5.7).

One way to explain the higher proton conductivity of blends is due to the higher phosphoric acid content. Hydroxyl groups of PVOH have large affinity for $H_3PO_4$ molecule

and they form many types of complex species and so more phosphoric acid is available to facilitate proton transport in the polymer electrolyte matrix.
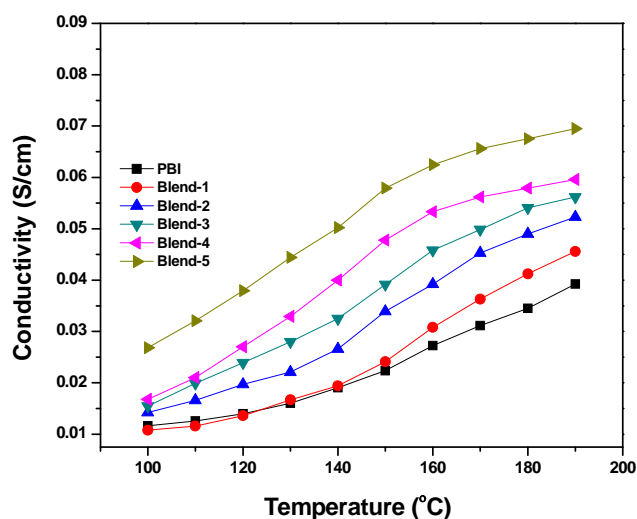


**Figure 5.17** Temperature dependence of proton conductivity of $H_3PO_4$ doped PBI and 1-5 PBI/PVOH blend membranes.

**Table 5.7** Proton conductivity and Doping level in wt% of PBI and PBI/PVOH blends at 190 °C.

| Polymer Code | Doping level of $H_3PO_4$ (wt %) | $\sigma_{max}$ (S cm$^{-1}$) |
|:---:|:---:|:---:|
| Blend-1 | 296 | $4.56 \times 10^{-2}$ |
| Blend-2 | 330 | $5.34 \times 10^{-2}$ |
| Blend-3 | 350 | $5.61 \times 10^{-2}$ |
| Blend-4 | 380 | $5.96 \times 10^{-2}$ |
| Blend-5 | 385 | $6.95 \times 10^{-2}$ |
| PBI | 280 | $3.92 \times 10^{-2}$ |

**5.3.6.5 Membrane electrode assembly fabrication**

The electrodes with a gas diffusion layer and a catalyst layer were fabricated by following the same procedure as mentioned in section 2.3.4.4. A polymer electrolyte membrane, Blend-2 (110 µm), doped in 85 wt% $H_3PO_4$ for 24, was wiped out by tissue paper and dried at 100 °C under vacuum. The membrane and electrode assemblies (MEAs) were made by hot-pressing the pretreated electrodes (9 cm$^2$) and the membrane under the conditions of 120 °C, 130 atm for 3 min.

**5.3.6.6 Polarization study**

Figure 5.18 shows the fuel cell performance of blend-2(PBI-80%-PVOH-20%) membrane in terms of polarization plots of MEA fabricated using 20% Pt/C for both anode and cathode in a single cell experiment, at 100, 125 and 150 °C with a dry $H_2/O_2$ gas flow rate of 0.4 slpm (standard liters per minute). We selected the blend-2 membrane for carrying out performance analysis mainly because of its superior oxidative stability than that of other blends. Blend-2 membrane show better performance than that of the PBI membrane. The open-circuit voltage (OCV) obtained with the blend-2 membrane is 0.95 V at 150 °C, whereas for PBI it is 0.92 V. However, the activation loss and ohmic loss (which are much more important for sustaining a large current density) in the case of the blend-2 membrane are considerably lower than those of PBI. For example, the blend-2 membrane gives a maximum power density 254 mW/cm² at 0.4 V, whereas the PBI membrane gives 210 mW/cm² at 0.3 V. This better fuel cell performance of blend-2 membrane can be attributed to high $H_3PO_4$ acid content due to PVOH which favors chain movement facilitating enhanced proton conductivity.
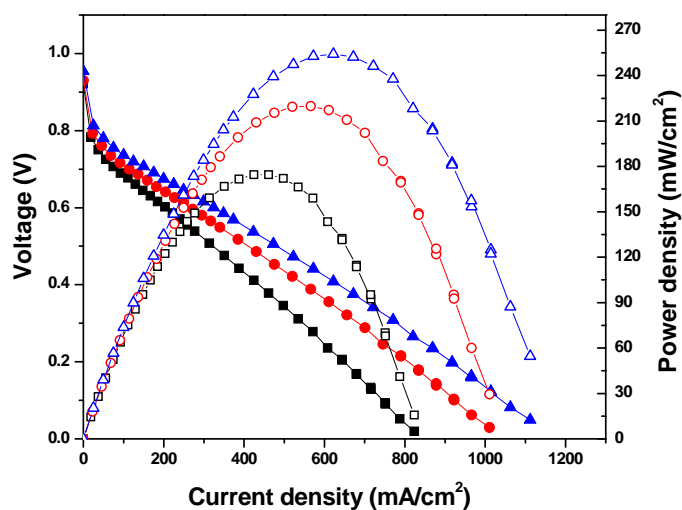


**Figure 5.18** Polarization curves obtained with Blend-2 membrane fuel cell at different temperatures with dry $H_2$ and $O_2$ (flow rate 0.4 slpm). The cell was conditioned for 30 min at open-circuit potential and at 0.2 V for 15 min before measurements. Key: (■□) 100, (●○) 125 and (▲Δ) 150 °C.

### 5.4 Conclusions

- Blend membranes of amino group containing polybenzimidazole (APBI) and sulfonated polyether ether ketone (SPEEK) in varying ratio were prepared by solution casting technique and characterized by IR spectroscopy, SEM analysis, XRD analysis, thermal analysis, and mechanical properties.

- APBI/SPEEK form miscible blends. However, miscibility decreases as SPEEK content increases. In SEM it shows good miscibility upto 50% SPEEK content.

- Thermal stability of the APBI-SPEEK blends is less than that of APBI due to the presence of sulfonic acid groups in the SPEEK. However thermal stability of blends is better than the SPEEK.

- Mechanical properties of the APBI-SPEEK blends are low than that of APBI due to the presence of the SPEEK. However, mechanical properties of blends are better than the SPEEK.

- APBI-SPEEK blends show better oxidative stability than APBI and SPEEK due to hydrogen bonding between $-NH-$, $NH_2$ of APBI and $SO_3H$ of SPEEK.

- Phosphoric acid doping level in APBI-SPEEK blends decreases significantly with increase in SPEEK content in blend membrane.

- In APBI-SPEEK blends, proton conductivity decreases with increase in SPEEK content in blends. Blend membrane APS-1 shows better conductivity than APBI.

- APS-1 shows better fuel cell performance than that of APBI which can be attributed to bonded phosphoric acid to the amino groups and amino sulfonate complex of APBI and SPEEK, which increases the protonating sites in the polymer matrix and help in fast proton transport in APS-1.

- Blend membranes of polybenzimidazole and polyvinyl alcohol in varying ratio were prepared by solution casting technique and characterized by IR spectroscopy, thermal analysis, SEM analysis, mechanical properties and XRD analysis.

- PBI-PVOH polymers form miscible blends having good thermal stability and mechanical properties.

- Thermal stability of the PBI-PVOH blends is less than that of PBI due to the presence of the aliphatic PVOH. However thermal stability of blends is better than the PVOH.

- Mechanical properties of the PBI-PVOH blends are low than that of PBI due to the presence of the PVOH. However mechanical properties of blends are much better than the PVOH.

- PBI-PVOH blends show lower oxidative stabilities than PBI due to the presence of the water soluble aliphatic PVOH.

- Phosphoric acid doping level in PBI-PVOH blends increases significantly with increase in PVOH content in blend membrane.

- In PBI-PVOH blends, proton conductivity increases with increase in PVOH content. Blend membranes show better conductivity than PBI.

- Blend-2 shows better fuel cell performance than that of PBI in polarization study, which can be attributed to high $H_3PO_4$ doping level compared to PBI, which favors chain movement facilitating enhanced proton conductivity.

### References
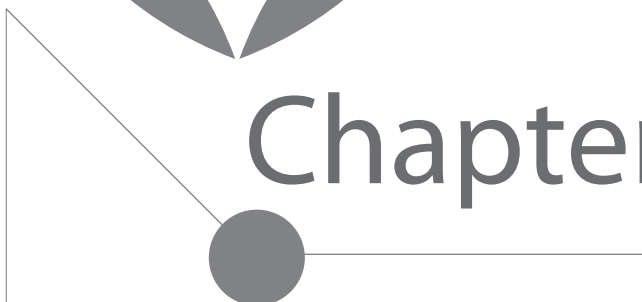
1. Xiaoming, R.; Mahlon, S. W.; Shimshon, G. *Journal of the Electrochemical Society* **1996**, 143, L12.

2. Antonucci, P.L.; Arico, A.S.; Creti, P.; Ramunni, E.; Antonucci, V. *Solid State Ionics* **1999**, 125, 431.

3. Masahiro, W.; Hiroyuki, U.; Yasuhiro, S.; Masaomi, E.; Paul, S. *Journal of the Electrochemical Society* **1996**, 143, 3847.

4. Qingfeng, L.; Ronghuan, H.; Ji-An, G.; Jens Oluf, J.; Niels, J. B. *Journal of the Electrochemical Society* **2003**, 150, A1599.

5. Wang, J. T.; Savinell, R.F.; Wainright, J. S.; Litt, M.; Yu, H. *Electrochimica Acta* **1996**, 41,193.

6. Juan Antonio, A.; Salvador, B.; Pedro, G.-R. *Journal of the Electrochemical Society* **2004**, *151*, A304.

7. Savadogo, O.; Xing, B. *Journal of New Mater. Electrochem. Syst.* **2000**, 3, 345.

8. Li, Q.; Hjuler, H. A.; Bjerrum, N. J. *Journal of Applied Electrochem* **2001**, 31, 773.

9. Gebel,G.; Aldebert, P.; Pineri, M. *Polymer*, **1993**, 34, 333.

10. Roeder, J.; Gomes, D.; .; Ponce, M.L.; Abetz, V.; Nunes, S. P. *Macromolecular Chemistry and Physics* **2007**, 208, 467.

11. Gomes, D.; Roeder, J.; Ponce, M.L.; Nunes, S. P. *Journal of Power Sources* **2008**,175, 49.

12. Wainright, J. S.; Wang, J. T.; Weng, D., Savinell, R. F.; Litt, M. H. *Journal of Electrochemical Society* **1995,** 142, L121.

13. Ma, Y. L.; Wainright, J. S.; Litt, M. H.; Savinell, R. F. *Journal of the Electrochemical Society* **2004**, 151, A8.

14. Samms, S. R.; Wasmus, S.; Savinell, R. F. *Journal of the Electrochemical Society* **2005**, 143, 1225.

15. Wainright, J. S.; Litt, M. H.; Savinell, R. F. *Fuel Cell Handbook* **2003**.

16. Glipa, X.; Mustapha, E. H.; Jones D. J.; Roziere, J. *Solid State Ionics* **1997**, 97, 323.

17. Gieselman, M.B. ; Reynolds, J. R. *Macromolecules* **1992**, 25, 4832.

18. Zhang, W.; Tang, C. M.; Kerres, J. *Separation and Purification Technology* **2001**, 22-23, 209.

19. Kerres, J.; Ullrich, A. *Separation and Purification Technology* **2001**, 22-23, 1.

20. Savinell, Robert F.; Litt, Morton H., Proton conducting polymers used as membranes; *US Patent* 5,525,436, **1996**.

21. Barbara, K.; Schauer, J. *Journal of Applied Polymer Science,* **2002,** 85, 1118.

22. Deimede, V.; Voyiatzis, G. A.; Kallitsis, J. K.; Qingfeng, L.; Bjerrum, N. J. *Macromolecules* **2000**, 33, 7609.

23. Hasiotis, C.; Qingfeng, L.; Deimede, V.; Kallitsis, J. K.; Kontoyannis, C. G.; Bjerrum, N. J. *Journal of the Electrochemical Society* **2001**, 148.

24. Kerres, J.; Ullrich, A.; Haring, T. Engineering ionomeric blends and engineering ionomeric blend membranes; *US Patent* 6,723,757, **2004**.

25. Bjerrum, N. J.; Li, Q.; Hjuler, H. A. Polymer electrolyte membrane fuel cells; *US Patent* 6,946,211, **2005**.

26. Vogel, H.A.; Marvel, C.S. *Journal of Polymer Science: Part-A* **1961**, 50, 511.

27. Lakshmi, V. V.; Choudhary, V.; Varma. I. K. *Macromolecular Symposia,* **2004**, 210, 21-29.

28. Kerres, J. A.; Ullrich, A.; Haring, Th.; Baldauf, M.; Gebhard U.; Preidel, W. *J. New Mater. Electrochem. Syst.* **2000**, 3, 229-239.

29. Adams, G. W.; Cowie, J. M. *Polymer* **1999**, 40, 1993.

30. Musto, P.; Wu, L.; Karasz, F. E.; MacKnight, W. J. *Polymer* **1991**, 32, 3.

31. Krumova, M.;  Lopez, D.; Benavente, R.; Mijangos, C.; Perena,J. M. *Polymer* **2000**, 41, 9265.

32. Li, Q.; Pan, C.; Jensen, O. J.; Noy´e, P.; Bjerrum, N. J. *Chem. Mater* **2007**, 19, 350.

33. Li, Q.; He, R.; Jensen J. O.; Bjerrum, N.J. *Fuel Cells* **2004,** 3, 147.

34. Hongting, P.; Qizhi, L.; Qiao, L.; Zhenglong, Y. *Polymer engineering and science* **2005**, 1395.

35. Vargas, R.A.; Garcia, A.; Vargas, M.A. *Electrochemica Acta* **1998**, 43, 1271.

# Chapter 6

Carboxylic and Sulfonic Acid Group based Polyimide Copolymers for Proton Exchange Membrane Fuel Cell- Synthesis and Characterization

### 6.1 Introduction

Aromatic polyimides are high performance heterocyclic polymers having high thermal stability, excellent mechanical and electrical properties, high chemical resistance and good film forming property and therefore are widely used in electronics, adhesives, coatings, composite materials and many others [1-2]. Recently, sulfonated polyimides (SPI) have been proposed [3-6] as polymer electrolytes for proton exchange membrane fuel cell (PEMFC). SPI, exhibit high proton conductivity [7-9] comparable to state of art polymer electrolyte membrane for fuel cell (PEMFC) namely, Nafion. A number of SPI with structural [10-14] variations have been evaluated as polymer electrolytes for fuel cell with a view to replace expensive Nafion. Most of the sulfonated polyimides [3-4,12] evaluated as polymer electrolytes for fuel cell have sulfonic acid groups in main chain, where as Nafion has sulfonic acid groups in side chain linked through ether linkage, which gives better flexibility to sulfonic acid groups. One of the major drawbacks of SPI with sulfonic acid group in main chain is their poor solvent solubility in the completely imidized state. Probably, sulfonic acid group attached to aromatic bulky group in side chain of polyimide should enhance the solubility of polymers due to increase in free volume and disruption of rigidity of polyimide. Moreover, polyimide with pendant phenyl sulfonic acid group linked to main chain via flexible ether group should have better flexibility compared to PI with sulfonic acid group attached to main chain. Such flexible sulfonic acid group in side chain of SPI may help to form hydrophilic and hydrophobic domains leading to channels for better proton conduction as in the case of Nafion [15]. Yin et.al [8] has underlined the importance of sulfopropoxy group in the side chain, where the formation of micro-phase separated structure, improved hydrolytic stability and increased proton conductivity above 70% RH is marked.

Another major hindrance for successful application of SPI in PEMFC is poor hydrolytic stability. Common SPI having five membered imide rings are prone to hydrolysis even in slightly acidic environment in presence of water causing degradation of MEA leading to short life time of membrane [3, 17]. Increase in basicity of the diamine can also improve the hydrolytic stability so the substitution of the electron donating group or flexible linkages like ether (C-O-C) attached ortho to the amine group may play a vital role in the hydrolytic

stability of the SPI [8]. SPI derived form six membered imide ring by using 1,4,5,8-naphthalene tetracarboxylic dianhydride (NTDA) have good hydrolytic stability. However, these polyimides have extremely rigid structure and exhibit poor solvent solubility, which limits the application of these polymers [18-19]. Polyimide derived from NTDA and a phenyl diamine containing phenyl sulfonic acid group linked to phenyl group of diamine via a flexible linkage is anticipated to be good material as polymer electrolyte for fuel cell further more the sulfonic group present in the side chain offers the site for the chemical reaction to modify the properties of polymer for tailor made application. In some literatures, interaction of sulfonic group with various imidazole have proved to be polymer electrolytes as anhydrous proton conductor, where the SPI supplies the proton to the heterocyclic bases and proton transports via acid-base complex formation, thus eliminating the need of water besides improving mechanical strength [20-22] .

One of the major problems of sulfonated PI is the stability of membrane in water. Membranes of SPI tend to crack in water. So, often copolymer with non-sulfonated diamine is preferred. However, such copolymers, due to low sulfonic acid groups, show low proton conductivity. Aromatic carboxylic acid groups may support proton conductivity and copolymer of sulfonated diamine and diamine containing carboxyl group may be useful as polymer electrolyte. Thus, the membranes based on copolyimides of sulfonated and carboxylated diamines are expected to have good stability in water and good proton conductivity compared to membrane based on copolyimides of sulfonated and non-sulfonated diamines. With this view in mind, in the present study, we synthesized two new diamines containing pendant phenoxy carboxyl and phenyl sulfonic acid groups, namely, 4-(2,4-diaminophenoxy) benzoic acid and 3-(3,5-diaminobenzoyl)benzene sulfonic acid to study the effect of phenyl sulfonic acid group and pendant phenyl carboxyl groups on proton conductivity and hydrolytic stability of SPIs.

## 6.2  Experimental

### 6.2.1    Materials

1-choro-2,4-dinitrobenzene, 3,5-dinitrobenzoyl chloride (Fluka, Switzerland), Aluminum chloride, 4-hydroxy benzaldehyde, triethylamine, chloroform, benzene, ethyl acetate, sulfuric acid and fuming sulfuric acid (60%, $SO_3$) (Merck, India) were used as received. 1,4,5,8-Naphthalene tetracarboxylic dianhydride (NTDA) (Aldrich Chemicals, USA) was purified by sublimation. Benzene (Merck, India) was first dried over $CaCl_2$, then refluxed with sodium and distilled, while m-cresol (Merck, India) was distilled twice. Hydrochloric acid, sodium chloride and sodium bicarbonate (S. D. Fine Chem., India) were used as received. Dimethylformamide (DMF) was dried over $CaH_2$ and vacuum distilled. N-methyl-2-pyrollidinone (NMP) and N,N-dimethylacetamide (DMAc) (S. D. Fine Chem., India) were dried over phosphorus pentoxide and vacuum distilled.

### 6.2.2    Analytical methods

All the analytical methods used to characterize the polymer and polymer membranes are same as described in chapter 2 except hydrolytic stability, water uptake and ion exchange capacity (IEC). The water uptake of polymer membranes was determined by immersing weighed dry samples (1 x 1 cm pieces) of polymer membrane in distilled water for 24 h at ambient temperature. The membranes after removing from distilled water were dried with tissue paper to remove adhered water and weighed again. The water uptake was determined by formula (eqn no.1)

$$\text{Water uptake}\,[\%] = \frac{W_{wet} - W_{dry}}{W_{dry}} \times 100 \qquad [1]$$

where, $W_{dry}$ is the weight of the dried sample before immersing in water and $W_{wet}$ the weight of the sample after removing adhered water. The same sample was dried under vacuum oven at 120 °C for 24 h and weighed again.

Ion exchange capacity (IEC) of sulfonated membranes was calculated from the molar ratio of sulfonated diamine to nonsulfonated diamine in feed, and also evaluated by means of titration. In titration method, a sample of membrane ($2 \times 2$ cm) in proton form was soaked in 15 wt% NaCl solution for 24 h at 30 °C to exchange $H^+$ ion with $Na^+$ ion. Then, $H^+$ ion

released into the solution was titrated with a 0.05 N NaOH solution using phenolphthalein as the indicator.

### 6.2.3    Synthesis of new substituted aromatic diamines
### 6.2.3.1 Synthesis of 4-(2,4-diaminophenoxy) benzoic acid (DAPBA)

This diamine was synthesized in three steps, by nucleophilic substitution reaction of 4-Hydroxy benzaldehyde with 1-choro-2,4-dinitrobenzene in the presence of an acid acceptor, triethylamine, followed by oxidation of resultant 4-(2,4-dinitrophenoxy) benzaldehyde to the corresponding acid using sodium dichromate in $H_2SO_4$. After that, 4-(2,4-dinitrophenoxy)benzoic acid was reduced to 4-(2,4-diaminophenoxy) benzoic acid using catalytic hydrogenation. Various steps involved in this synthesis are outlined in Scheme 6.1.

**(i)Preparation of 4-(2,4-dinitrophenoxy)benzaldehyde (I)**

4-Hydroxy benzaldehyde 12.2 g (100 mmol) and 1-chloro-2,4-dinitrobenzene 20.25 g (0.1 mol) were dissolved in acetone (150 mL) in a 250 mL round bottomed flask fitted with a reflux condenser. Triethylamine 16.66 mL (120 mmol) was added to this solution and mixture was heated to reflux for 48 h with stirring. Solvent acetone and excess triethylamine were distilled off and the residue was dissolved in chloroform (250 mL). The chloroform solution was washed with 5% HCl, 2% NaOH and repeatedly with water till free from alkali in a separating funnel and then dried with anhydrous $Na_2SO_4$. The solution, after filtration, was treated with activated charcoal, filtered and cooled. The compound separated was dried in a vacuum oven at 50 °C.

Yield was 26 g (90%). Melting Point: 120 °C.

FT-IR (KBr, cm$^{-1}$): 1710 (C=O); 1532, 1346 ($NO_2$ stretching); 1280, 1070 (C–O–C stretching); 1616, 1572 (aromatic). (Figure 6.1-A)

$^1$H NMR [200 MHz, CDCl$_3$, δ ppm]: 10.9 (S, 1H, H$_f$); 9.2 (d, 1H, H$_a$); 8.7 (d, 1H, H$_b$); 8.3 (d, 2H, H$_e$); 7.8 (dd, 2H, H$_d$); 7.7 (dd, 1H, H$_c$). (Figure 6.2-A)

$^{13}$C NMR [400 MHz, CDCl$_3$, δ ppm] showed values of 190.51, 158.95, 154.31, 142.6, 140.39, 133.93, 132.36, 129.20, 122.24, 120.70, 120.06. (Figure 6.3-A)

| **Elemental analysis:** | C% | H% | N% |
|---|---|---|---|
| **$C_{13}H_8N_2O_6$** | | | |
| Calculated: | 54.16% | 2.77% | 9.72% |
| Observed: | 54.09% | 2.80% | 9.75% |

**(ii) Preparation of 4-(2,4-dinitrophenoxy)benzoic acid (II)**

4-(2,4-dinitrophenoxy)benzaldehyde 20.16 g (70 mmol) was dissolved in acetone (100 mL) in a 500 mL round bottomed flask. Sodium dichromate 36.55 g (319 mmol) dissolved in water (82 mL) was added to above solution. $H_2SO_4$ (60 mL) was added drop-wise to this solution in 1 h and stirred for 12 h at room temperature. The reaction mixture was poured in 1 L of water. The precipitate was filtered and dissolved in 5% aqueous NaOH solution. The solution was filtered and neutralized with 10% $H_2SO_4$ solution. The precipitate obtained was filtered and washed with water and product was recrystallized from methanol.
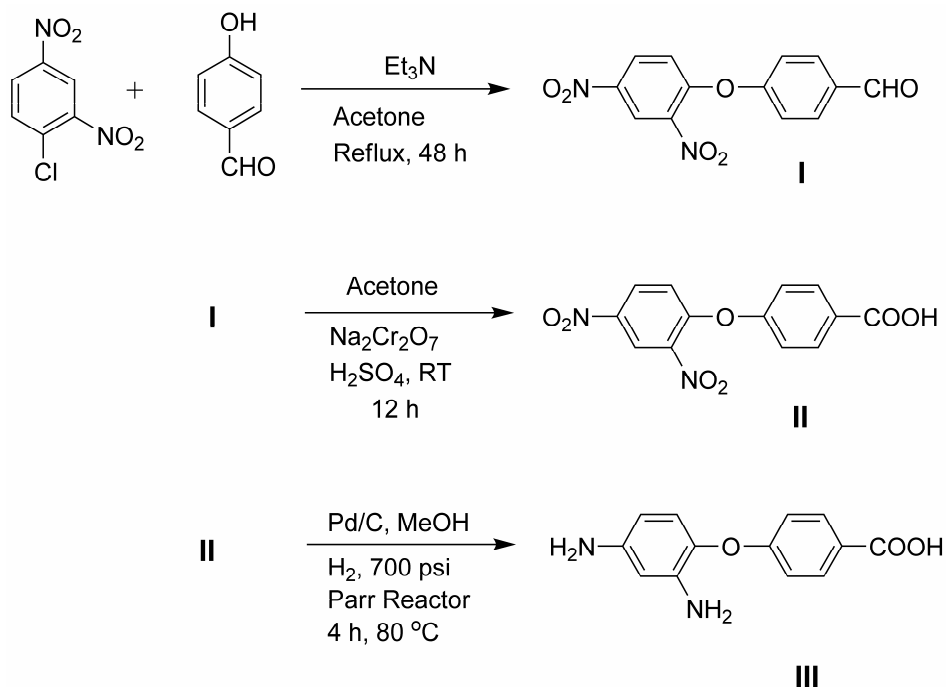


**Scheme 6.1** Synthesis of 4-(2,4-diaminophenoxy) benzoic acid (DAPBA)

Yield was 15.96 g (70%). Melting Point: 260–263 °C.

FT-IR (KBr, cm$^{-1}$): 1680 (C=O); 1532, 1346 (NO2 stretching); 1280, 1070 (C–O–C stretching); 1616, 1572(aromatic). (Figure 6.1-B)

$^1$H NMR [200 MHz, DMSO-$d_6$, δ ppm]: 9.25 (d, 1H, $H_a$); 8.78 (d, 1H, $H_b$); 8.38 (d, 2H, $H_e$); 7.68(dd, 2H, $H_d$); 7.6(d, 1H, $H_c$). (Figure 6.2-B)

$^{13}$C NMR [400 MHz, DMSO-$d_6$, δ ppm] showed values of 166.48, 157.95, 153.65, 142.06, 139.76, 131.97, 129.67, 127.96, 121.88 and 119.32.(Figure 6.3-B)

| **Elemental analysis:** | C% | H% | N% |
|---|---|---|---|
| **$C_{13}H_8N_2O_7$** | | | |
| Calculated: | 51.31% | 2.63% | 9.21% |
| Observed: | 51.19% | 2.69% | 9.29% |

### (iii) Preparation of 4-(2,4-diaminophenoxy) benzoic acid (DAPBA) (III)

A pressure vessel (Parr reactor), was charged with 4-(2,4-dinitrophenoxy)benzoic acid 10.0 g (40 mmol) dissolved in methanol (150 mL) and 5% Pd/C (0.5 g). The reactor was flushed with hydrogen 2–3 times. The mixture was heated at 80 °C with stirring for 4 h under 700 psi of hydrogen pressure. The reactor was cooled to room temperature. The solution was filtered to remove catalyst, treated with activated charcoal and filtered. The filtrate was concentrated by distilling off methanol and cooled. The solid separated was filtered, washed with ice-cold methanol and dried under vacuum at 50 °C.

Yield was 8.5 g (85%). Melting Point: 186 °C.

FT-IR (KBr, cm$^{-1}$): 1670 (C=O); 3376 (N–H stretching); 1604 (N–H deformation); 1280, 1070 (C–O–C stretching) and 1616, 1572 (aromatic). (Figure 6.1-C)

$^1$H NMR [200 MHz, DMSO-$d_6$, δ ppm]: 7.8 (d, 2H, $H_e$); 7.6 (d, 2H, $H_d$); 7.55 (d, 1H, $H_c$) 6.75 (d, 1H, $H_b$); 6.5 (m, 1H, $H_a$); 5.4 (s, 4H, $NH_2$). (Figure 6.2-C)

$^{13}$C NMR [400 MHz, DMSO-$d_6$, δ ppm] showed values of 172.39, 167.84, 151.74, 145.94, 136.69, 136.60, 128.91, 127.25, 120.35, 108.80 and 106.75. (Figure 6.3-C)

| **Elemental analysis:** | C% | H% | N% |
|---|---|---|---|
| **$C_{13}H_{12}N_2O_3$** | | | |
| Calculated: | 63.93% | 4.91% | 11.47% |
| Observed: | 63.85% | 4.95% | 11.54% |

### 6.2.3.2 Synthesis of 3-(3,5-diaminobenzoyl)benzene sulfonic acid dihydrochloride (DABBSA)

This diamine was synthesized in three steps, by Freidel-Crafts acylation reaction of 3,5-dinitrobenzoyl chloride with benzene in the presence of an aluminum chloride as the catalyst [23], followed by sulfonation of resultant (3,5-dinitrophenyl)(phenyl)methanone to the corresponding sulfonic acid using fuming sulfuric acid (60%, $SO_3$) in $H_2SO_4$ followed by the reduction of 3-(3,5-dinitrobenzoyl)benzenesulfonic acid to 3-(3,5-diaminobenzoyl) benzenesulfonic acid using stannous chloride dihydrate and hydrochloric acid. Various steps involved in this synthesis are outlined in Scheme 6.2.

### (i)Preparation of (3,5-dinitrophenyl)(phenyl)methanone (I)

A 500 mL completely dried three-necked round bottom flask equipped with a thermo-well, a reflux condenser and a mechanical stirrer was charged with 30 g (130 mmol) 3,5-dinitrobenzoyl chloride and 250 mL of dry benzene and the solution was stirred at room temperature. To this solution 18 g (135 mmol) solid $AlCl_3$ was added part by part at a slow rate for over 1 h maintaining the room temperature. After the addition, the mixture was refluxed for 4 h. The red solution was poured into a large quantity of ice water containing a 10 mL of conc. HCl. The resulting precipitate was filtered, and washed with water till neutral. The obtained solid was dried in vacuum at 60 °C for 6 h.  The product was recrystallized from chloroform.  Yield was 31.9 g (90%). Melting Point: 132-133 °C.

FT-IR (KBr, cm$^{-1}$): 1666 (C=O); 1535, 1348 (NO$_2$ stretching) and 1616, 1572 (aromatic). (Figure 6.4-A)

$^1$H NMR [200 MHz, CDCl$_3$, δ ppm]: 9.3 (S, 1H, H$_a$); 8.9 (d, 2H, H$_b$); 7.8-7.9 (d, 1H, H$_b$); 7.6 (d, 2H, H$_d$). (Figure 6.5-A)

$^{13}$C NMR [200 MHz, CDCl$_3$, δ ppm] showed values of 191.67, 148.52, 140.69, 135.06, 134.23, 130.01, 129.15 and 121.54. (Figure 6.6-A)

| **Elemental analysis:** | C% | H% | N% |
|---|---|---|---|
| **C₁₃H₈N₂O₆** | | | |
| Calculated: | 57.36% | 2.96% | 10.29% |
| Observed: | 57.10% | 2.90% | 10.15% |

**(ii)Preparation of 3-(3,5-dinitrobenzoyl)benzenesulfonic acid (II)**

A 250 mL three-necked round bottom flask equipped with a thermo-well, a reflux condenser, addition funnel and a mechanical stirrer was charged with 50 mL of concentrated sulfuric acid. At room temperature, 25 g (91.9 mmol) of 3,5-dinitrophenyl)(phenyl) methanone was added slowly to it with stirring. After the solid was dissolved, 50 mL of fuming sulfuric acid (60%, $SO_3$) was added drop-wise in 1 h and the solution was slowly heated to 120 °C and kept at this temperature for 12 h. The solution was cooled to room temperature and it was poured into 500 mL of ice water. The product was salted out by adding 100 g of NaCl into the solution. The solid was filtered, redissolved in 450 mL of water and neutralized to the pH of 6–7 with 10% HCl solution to precipitate the product. The precipitate was filtered and washed by acetone and then dried at 80 °C under vacuum for 12 h. Yield was 30.70 g (95%). Melting Point: 132-133 °C.

FT-IR (KBr; cm$^{-1}$): 1666 (C=O, aromatic ketone); 1209, 1030 cm$^{-1}$ (O=S=O); 1616, 1572 (aromatic). (Figure 6.4-B)

$^1$H NMR (200 MHz; DMSO-d$_6$, δ ppm): 9.2 (s, 1H, H$_a$); 8.8 (s, 2H, H$_b$); 8.2 (s, 1H, H$_c$); 8.0 (d, 1H, h$_d$); 7.8 (d, 1H, H$_e$); 7.62 (dd, 1H, H$_f$). (Figure 6.5-B)

$^{13}$C NMR [200 MHz, DMSO-d$_6$, δ ppm] showed values of 191.71, 148.45, 147.99, 139.58, 134.83, 130.81, 129.19, 128.62, 126.57 and 121.48(Figure 6.6-B)

| **Elemental analysis:** | C% | H% | N% | S% |
|---|---|---|---|---|
| **C$_{13}$H$_{10}$N$_2$O$_9$S** | | | | |
| Calculated: | 42.17% | 2.72% | 7.57% | 8.66% |
| Observed: | 42.01% | 2.65% | 7.47% | 8.45% |

**(ii) Preparation of 3-(3,5-diaminobenzoyl)benzenesulfonic acid dihydrochloride (DABBSA)(III)**

A 500 mL three-necked round bottom flask equipped with a reflux condenser, dropping funnel, mechanical stirrer and nitrogen gas inlet was charged with 20 g (56.77 mmol) of 3-(3,5-dinitrobenzoyl)benzenesulfonic acid, 132 g (567.7 mmol) of stannous chloride dihydrate, 200 mL of ethanol and 40 mL of water. Then, under nitrogen protection 100 mL conc. hydrochloric acid was added drop-wise for 1 h and the reaction mixture was stirred at 50 °C for 4 h. The resulting precipitate was filtered, and then dissolved in sodium

hydroxide solution. The solution was filtered, and the filtrate was acidified with hydrochloric

acid. The resulting precipitate was filtered, washed with water and ethanol successively, and

dried in vacuum at 80 °C for 12 h to give product. The product diamine was recrystallized

from conc. HCl in hydrochloride form as 3-(3,5-diaminobenzoyl) benzenesulfonic acid

dihydrochloride. Yield was 14.51 g (70%). Melting Point: 230-232 °C.

FT-IR (KBr; cm$^{-1}$): 1666 (C=O, aromatic ketone); 1209, 1030 cm$^{-1}$ (O=S=O); 1616, 1572

(aromatic). (Figure 6.4-C)

$^1$H NMR (200 MHz; DMSO-d$_6$, δ ppm): 8.5 NH$_2$HCl (s, 6H, H$_a$); 7.9 (dd, 2H, H$_b$); 7.8 (s, 1H,

H$_c$); 7.6 (s, 1H, h$_d$); 6.9-7.1 (m, 3H, H$_e$). (Figure 6.5-C)

$^{13}$C NMR (200 MHz, DMSO-d$_6$, δ ppm) showed values of 194.62, 148.19, 147.33, 138.95,

136.28, 135.02, 129.93, 128.42 and 115.00. (Figure 6.6-C)

| **Elemental analysis:** | C% | H% | N% | S% |
|---|---|---|---|---|
| **C$_{13}$H$_{16}$Cl$_2$N$_2$O$_5$S** | | | | |
| Calculated: | 40.74% | 4.21% | 7.31% | 8.37% |
| Observed: | 40.01% | 4.15% | 7.27% | 8.25% |
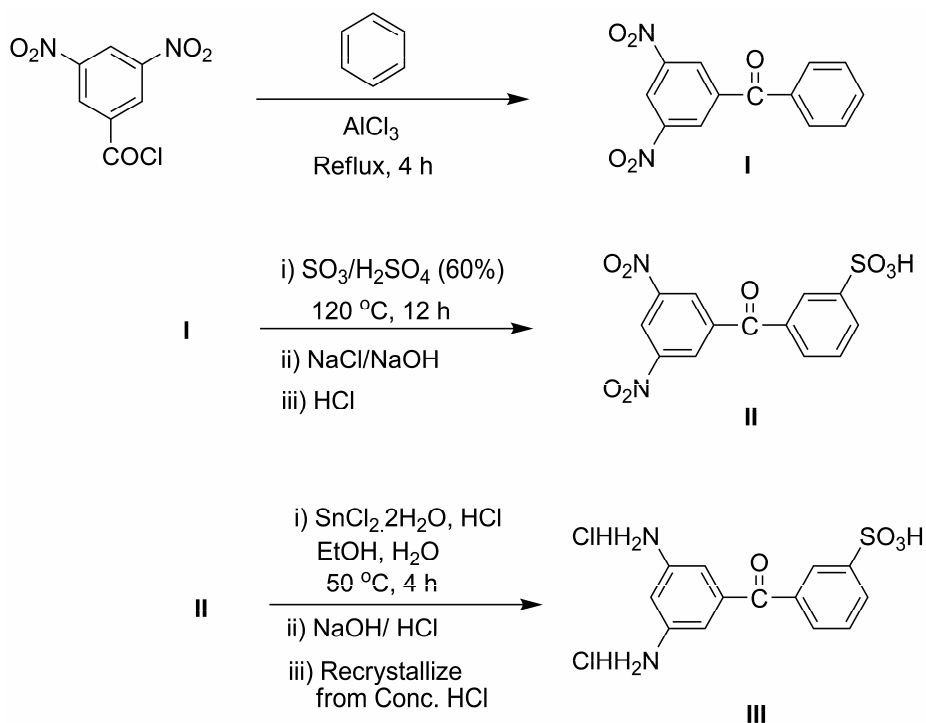


**Scheme 6.2** Synthesis of 3-(3,5-diaminobenzoyl)benzenesulfonic acid dihydrochloride
(DABBSA).

### 6.2.4  Synthesis of new substituted homo and co-polyimides

Polyimides containing sulfonic and carboxylic acid groups were synthesized by condensing 1,4,5,8-naphthalene tetracarboxylic dianhydride (NTDA) with DABBSA and DAPBA  (Scheme 6.3 and 6.4). Co-polyimides having sulfonic and carboxylic acid groups were synthesized by condensing NTDA with a mixture of DABBSA and DAPBA (scheme 6.5) by using high temperature solution polycondensation technique in m-cresol. A typical procedure for high temperature solution polycondensation is described below.

### 6.2.4.1  Synthesis of polyimide having pendant sulfonic acid groups

A 50 mL three-necked round bottom flask equipped with mechanical stirrer, nitrogen gas inlet and guard tube was charged with 4 g (10.95 mmol) of DABBSA, 40 mL of m-cresol and 4 mL of TEA. After DABBSA was completely dissolved, 2.937 g (10.95 mmol) of NTDA was added to the flask. The reaction solution was stirred at 80 °C for 4 h and at 180 °C for 12 h. After cooling to room temperature, the viscous solution was poured into acetone. The precipitated polymer in fiber form was collected by filtration, washed with acetone and dried in vacuum at 100 °C for 24 h.
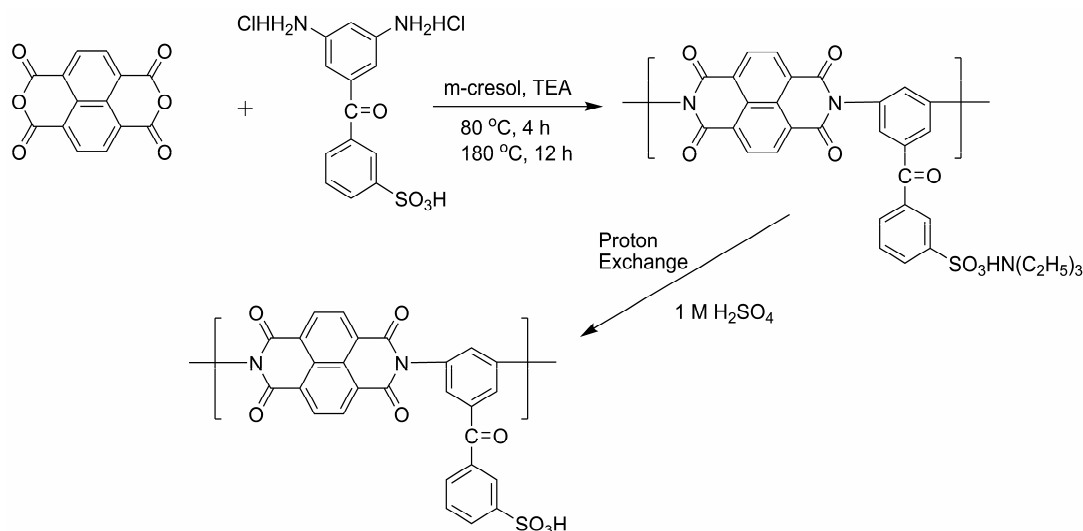


**Scheme  6.3** Synthesis  of  polyimide  from  3-(3,5-diaminobenzoyl)benzenesulfonic  acid dihydrochloride (DABBSA).

Yield  of  the  polymer  was  96%.  The  inherent  viscosity  of  this  polymer  at  0.5g.dL$^{-1}$ concentration, measured in DMAc at 30 °C was 1.18 dL.g$^{-1}$.

FT-IR (film, cm$^{-1}$): 1720, 1678 and 1345 (C=O, naphthalimide, aromatic ketone); 1209, 1032 (O=S=O); 1580, 1456 (aromatic). (Figure 6.7)

| **Elemental analysis:** | C% | H% | N% | S% |
|---|---|---|---|---|
| **C$_{27}$H$_{12}$N$_2$O$_8$S** | | | | |
| Calculated: | 63.15% | 4.66% | 6.69% | 5.11% |
| Observed: | 62.30% | 4.17% | 6.76% | 4.95% |

### 6.2.4.2 Synthesis of polyimides having pendant carboxyl acid groups

A 50 mL three-necked round bottom flask equipped with mechanical stirrer, nitrogen gas inlet and guard tube was charged with 3 g (12.28 mmol) of DAPBA and 30 mL of m-cresol. After DAPBA was completely dissolved, 3.294 g (12.28 mmol) of NTDA was added to the flask. The reaction solution was stirred at 80 °C for 4 h and at 180 °C for 12 h. After cooling to room temperature, the viscous solution was poured into acetone. The precipitated polymer in fiber form, was collected by filtration, washed with acetone and dried in vacuum at 100 °C for 24 h.
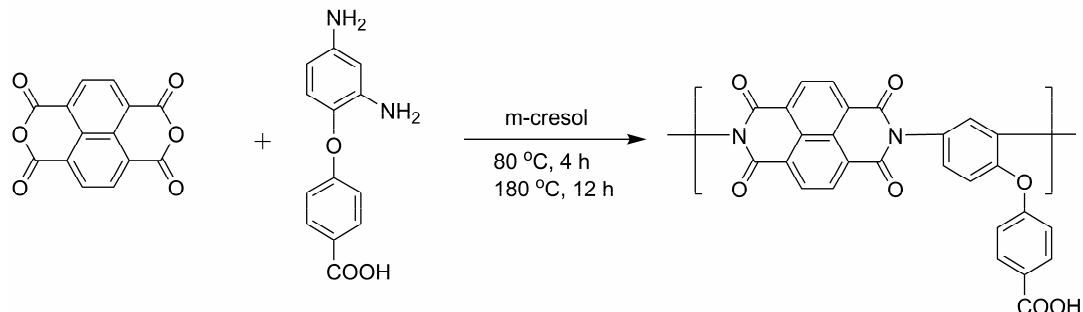


**Scheme 6.4** Synthesis of polyimide from 4-(2,4-diaminophenoxy) benzoic acid (DAPBA)

Yield of the polymer was 97%. The inherent viscosity of this polymer at 0.5g.dL$^{-1}$ concentration, measured in DMAc at 30 °C was 0.75 dL.g$^{-1}$.

FT-IR (film, cm$^{-1}$): 1720, 1678 and 1345 (C=O, naphthalimide, aromatic ketone); 1220, 1120 (-C-O-C- stretching); 1584, 1498 (aromatic). (Figure 6.7)

| **Elemental analysis:** | C% | H% | N% |
|---|---|---|---|
| **C$_{27}$H$_{12}$N$_2$O$_7$** | | | |
| Calculated: | 67.93% | 2.74% | 5.87% |
| Observed: | 67.30% | 2.77% | 5.56% |

**6.2.4.3 Synthesis of co-polyimides having pendant sulfonic and carboxyl acid groups**

A 50 mL three-necked round bottom flask equipped with mechanical stirrer, nitrogen gas inlet and guard tube was charged with 4.037 g (11.052 mmol) of DABBSA, 0.3 g (1.228 mmol) of DAPBA, 30 mL of m-cresol and 4.5 mL of TEA. After DABBSA and DAPBA were completely dissolved, 3.294 g (12.28 mmol) of NTDA was added to the flask. The reaction solution was stirred at 80 °C for 4 h and at 180 °C for 12 h. After cooling to room temperature, the viscous solution was poured into acetone. The precipitated polymer in fiber form was collected by filtration, washed with acetone and dried in vacuum at 100 °C for 24 h.
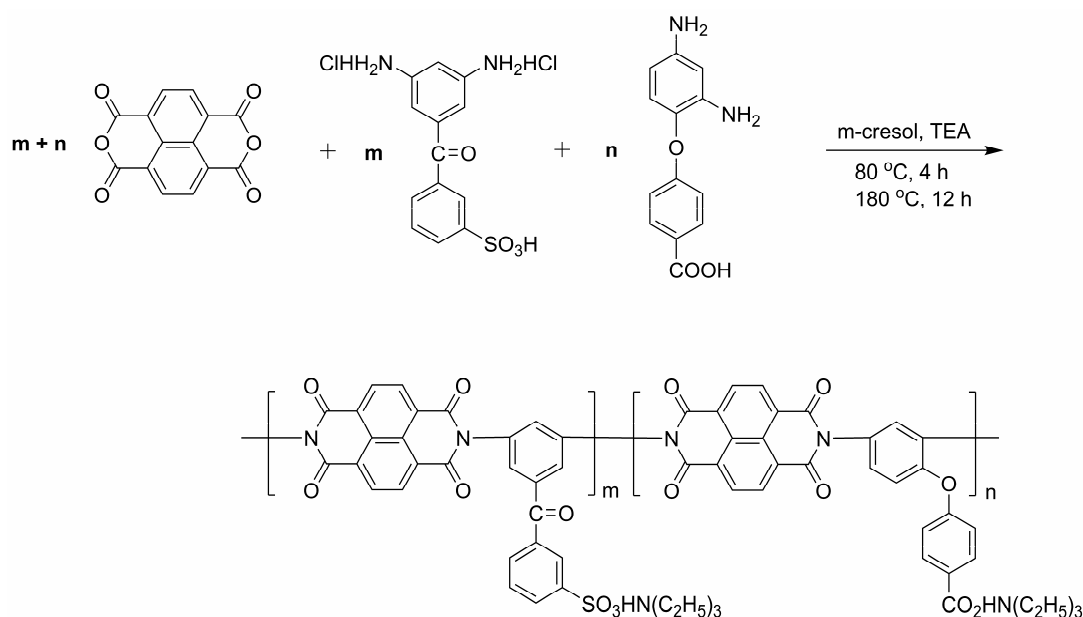


**Scheme 6.5** Synthesis of co-polyimides from DABBSA and DAPBA

Yield of the polymer was 95%. The inherent viscosity of this polymer at $0.5 g.dL^{-1}$ concentration, measured in DMAc at 30 °C was $0.91 \, dL.g^{-1}$.

Following the similar procedure co-polyimides of DABBSA and DAPBA with NTDA in different ratio were prepared. (Table 6.1)

**6.2.4.4 Membrane preparation**

Polymer membranes of 90-100 μm thickness, used for mechanical properties study, proton conductivity measurement and fuel cell studies were obtained by solution casting method. Three percent solution of polymer was prepared in DMAc and the solution was filtered through a 10 μm filter to remove any particles. The clear polymer solution was poured

into a clean Petri dish (diameter 7.5 cm). The DMAc was evaporated slowly in a leveled oven at 80 °C for 15 h. The membranes were removed and heated in boiling distilled water for 6 h to remove the traces of DMAc solvent and subsequently dried at 150°C for two days under reduced pressure.

## 6.3    Results and Discussion

### 6.3.1    Synthesis and characterization of monomers
### 6.3.1.1 Synthesis and characterization of 4-(2,4-diaminophenoxy) benzoic acid

4-(2,4-diaminophenoxy) benzoic acid can be prepared by different routes. Conventional route could be condensation of p-cresol with 1-chloro-2,4-dinitrobenzene followed by oxidation of methyl group of resultant 2,4-dinitro-4'-methyl diphenyl ether to carboxyl group and subsequent reduction of nitro groups to amino groups. We attempted this route. However, the yield of pure acid after oxidation of 2,4-dinitro-4'-methyl diphenyl ether with alkaline potassium permanganate was low. So, in this work, the new diamine monomer, 4-(2,4-diaminophenoxy) benzoic acid, which contains pendant benzoic acid group, was prepared by unconventional route in three steps starting from 4- hydroxy benzaldehyde according to the reaction sequence described in Scheme 6.1.

4-(2,4-dinitrophenoxy)benzaldehyde (I) was readily synthesized in high yield (90%) from 1-chloro-2,4-dinitrobenzene and 4-hydroxy benzaldehyde as described in experimental part which was oxidized with sodium dichromate and $H_2SO_4$ at room temperature to give 4-(2,4-dinitrophenoxy)benzoic acid (II) in 70% yield. Dinitro compound was reduced to corresponding diamine monomer by hydrogenation in parr reactor and the resulting diamine was recrystallized from methanol. The chemical structure of intermediates and final compounds was confirmed by elemental analysis, FT-IR, $^1$H NMR and $^{13}$C NMR spectroscopy. The elemental analysis values were found to be in good agreement with the calculated values. The FT-IR spectrum 4-(2,4-dinitrophenoxy)benzaldehyde (Figure 6.1 A) shows absorption bands at 1532 and 1346 cm$^{-1}$ due to asymmetric and symmetric –NO$_2$ stretching vibration, while 1280 and 1070 cm$^{-1}$  bands are assigned to C–O–C asymmetric and symmetric stretching. Band at 870 cm$^{-1}$ corresponds to aromatic C–N stretching vibration of C–NO$_2$ group. Characteristic absorption band of aldehyde due to (C=O) stretching is observed at

1710 cm$^{-1}$. After oxidation (Figure 6.1 B), aldehyde peak at 1710 cm$^{-1}$ disappears and peak at 1680 cm$^{-1}$ of COOH group appears. The FT-IR spectrum of 4-(2,4-diaminophenoxy)benzoic acid (Figure 6.1 C) showed bands at 3381 cm$^{-1}$ due to N–H stretching and the bands at 1532 and 1346 cm$^{-1}$ of NO$_2$ group disappear. Bands at 1670 and 1216 cm$^{-1}$ are due to carbonyl of COOH and ether linkage, respectively.
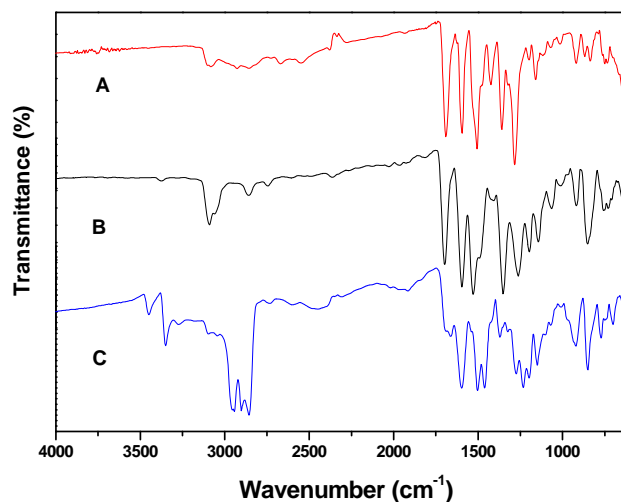


**Figure 6.1** FTIR spectra of A) 4-(2,4-dinitrophenoxy)benzaldehyde
B) 4-(2,4-dinitrophenoxy)benzoic acid  C) 4-(2,4-diaminophenoxy)benzoic acid.

The $^1$H NMR spectrum of 4-(2,4-dinitrophenoxy)benzaldehyde shows aromatic protons at 7.50–9.25 δ ppm with expected multiples and integration. The single proton of aldehyde group appears at 10.9 δ ppm (Figure 6.2 A). The $^1$H NMR spectrum of 4-(2,4-dinitrophenoxy)benzoic acid (Figure 6.2 B) shows aromatic protons at 7.50–9.25 δ ppm with expected multiples and integration. Signals of aldehyde proton disappeared. Protons of 4-(2,4-diaminophenoxy)benzoic acid at 5.0–5.4 δ ppm correspond to –NH$_2$ protons. Aromatic protons in the region 6.5–8.0 δ ppm showed the expected multiplicity and integration values as shown (Figure 6.2 C).
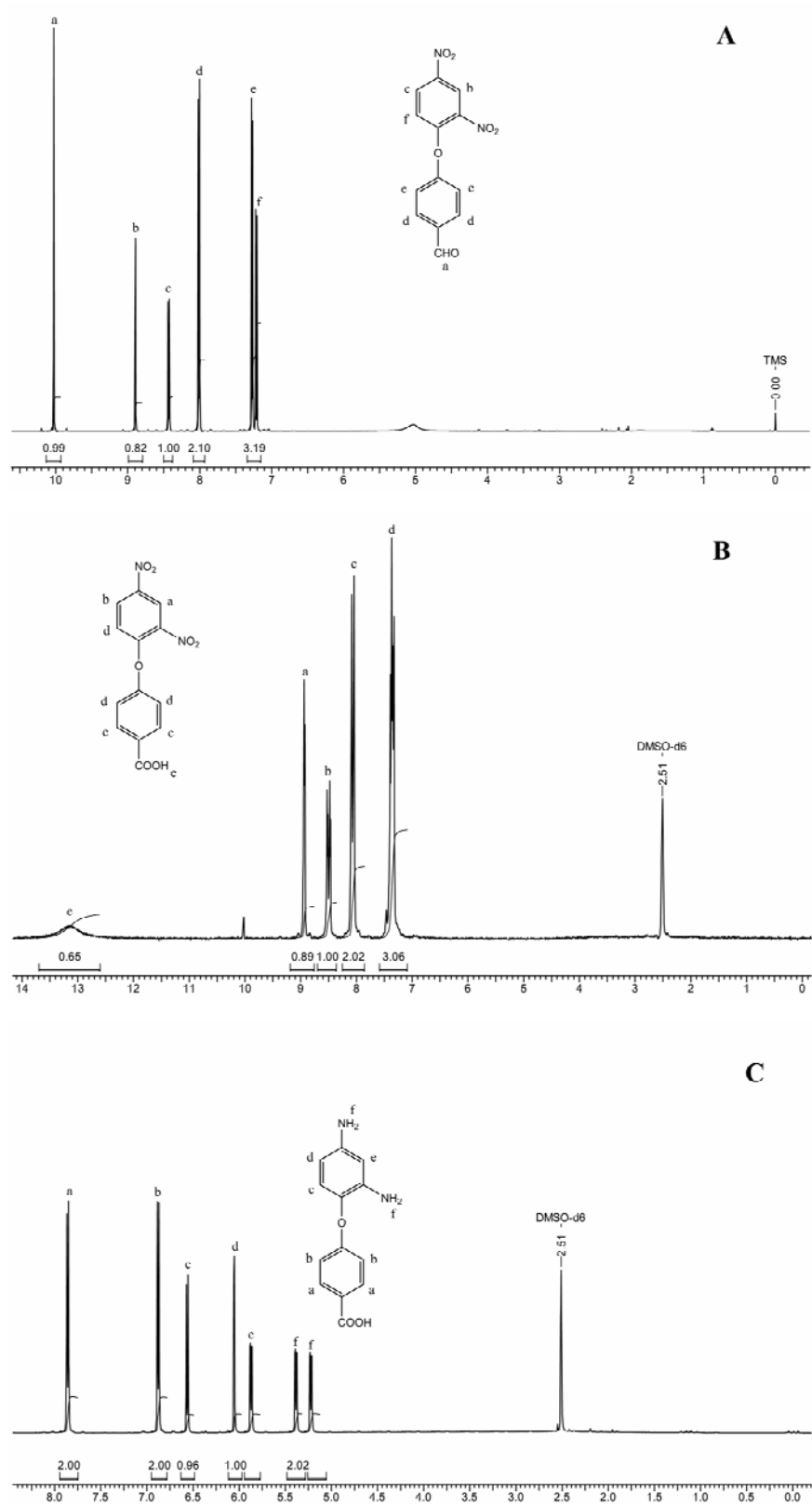
**Figure 6.2** ¹H NMR spectra of A) 4-(2,4-dinitrophenoxy)benzaldehyde
B) 4-(2,4-dinitrophenoxy)benzoic acid  C) 4-(2,4-diaminophenoxy)benzoic acid.
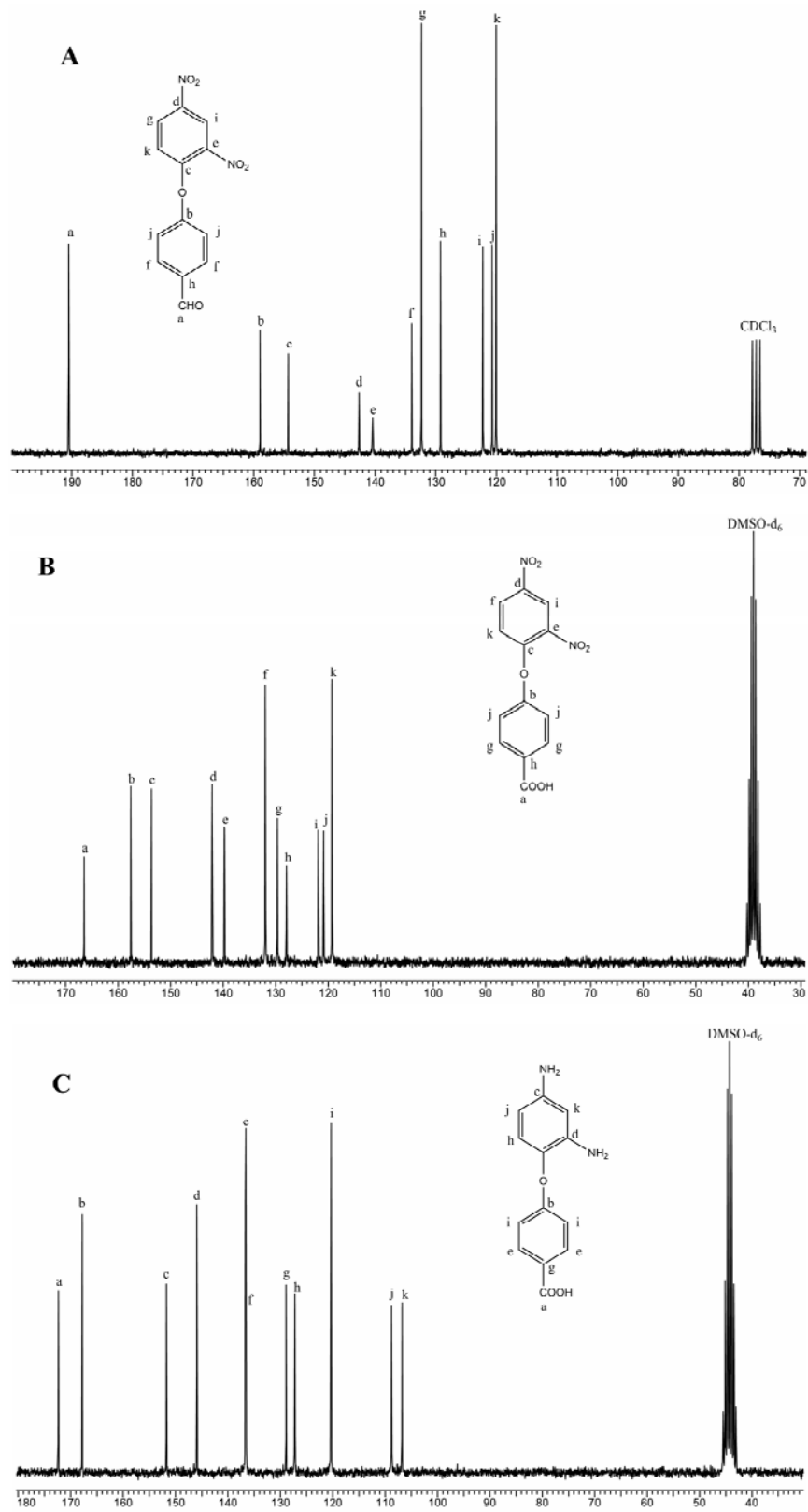
**Figure 6.3** $^{13}$C NMR spectra of A) 4-(2,4-dinitrophenoxy)benzaldehyde

B) 4-(2,4-dinitrophenoxy)benzoic acid  C) 4-(2,4-diaminophenoxy)benzoic acid.

The $^{13}$C NMR spectrum of 4-(2,4-dinitrophenoxy)benzaldehyde showed δ ppm values corresponding to 13 carbon atoms and were in good agreement with the proposed structure. Aromatic carbons in the range of 120–160 δ ppm and single carbon of aldehyde group appear at 192 δ ppm (Figure 6.3 A). $^{13}$C NMR spectrum of 4-(2,4-diaminophenoxy)benzoic acid (Figure 6.3 B) shows aromatic carbons at 118–157 δ ppm as expected and aldehyde carbon at 192 δ ppm disappear and carbon of carboxyl group appeared  as a single peak at 167 δ ppm. $^{13}$C NMR spectrum of 4-(2,4-diaminophenoxy)benzoic acid has δ-values close to that of dinitro acid compound. Aromatic carbons observed in the region 105–168 δ ppm and carbon of carboxyl group appeared  as a single peak at 174 δ ppm showed the expected values as shown in (Figure 6.3 C). Thus, elemental and spectral analysis confirm the structure of 4-(2,4-diaminophenoxy) benzoic acid and intermediate compounds.

### 6.3.1.2 Synthesis and characterization of 3-(3,5-diaminobenzoyl) benzenesulfonic acid

The novel diamine bearing sulfonated aromatic pendant group was synthesized from 3,5-dinitrobenzoyl chloride and benzene as the starting material by means of Freidel-Crafts acylation followed by sulfonation and reduction, as shown in Scheme 6.2. Freidel-Crafts acylation was performed using aluminum chloride as the catalyst and refluxing the reaction mixture for 4 h. Dinitro-compound having one sulfo group per pendant phenyl group was prepared by sulfonation with fuming sulfuric acid (60%, SO$_3$) at 40 °C for 1 h and at 120 °C for 12 h, respectively. The reduction reaction was conducted at 50 °C with stannous chloride dihydrate and hydrochloric acid. The product diamine was recrystallized from conc. HCl in hydrochloride form as 3-(3,5-diaminobenzoyl) benzenesulfonic acid dihydrochloride. The chemical structure of intermediates and final compounds was confirmed by elemental analysis, FT-IR, $^1$H NMR and $^{13}$C NMR spectroscopy. The elemental analysis values were found to be in good agreement with the calculated values.

The FT-IR spectrum (3,5-dinitrophenyl)(phenyl)methanone (Figure 6.4 A) shows absorption bands at 1535 and 1348 cm$^{-1}$ due to asymmetric and symmetric –NO$_2$ stretching vibration while band at 1627 cm$^{-1}$ corresponds to aromatic C–N stretching vibration of C–NO$_2$ group. Absorption band of ketone due to (C=O) stretching is observed at 1666 cm$^{-1}$.

After sulfonation (Figure 6.4 B), peaks at 1209 cm$^{-1}$ and 1030 cm$^{-1}$ appear due to O=S=O bond of SO$_3$H groups. The FT-IR spectrum of 3-(3,5-diaminobenzoyl) benzenesulfonic acid dihydrochloride (Figure 6.4 C) showed bands at 3495 and 3312 cm$^{-1}$ due to N–H stretching and the bands at 1535 and 1348 cm$^{-1}$ of NO$_2$ group disappear. Bands at 1666 and 1222, 1030 cm$^{-1}$ are due to carbonyl of ketone linkage and O=S=O bond of SO$_3$H groups, respectively.
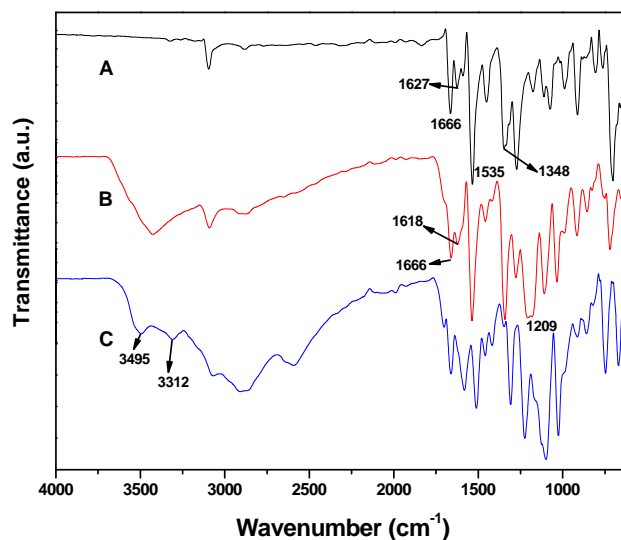


**Figure 6.4** FTIR spectra of A) 3,5-dinitrophenyl)(phenyl)methanone
B) 3-(3,5-dinitrobenzoyl)benzenesulfonic acid C) DABBSA.

The $^1$H NMR spectrum of (3,5-dinitrophenyl)(phenyl)methanone shows aromatic protons at 7.50–9.40 δ ppm with expected multiples and integration. The single proton sandwiched between two NO$_2$ groups appears at 9.4 δ ppm (Figure 6.5 A). The $^1$H NMR spectrum of 3-(3,5-dinitrobenzoyl)benzenesulfonic acid (Figure 6.5 B) shows aromatic protons at 7.50–9.25 δ ppm with expected multiples and integration. In $^1$H NMR the aromatic protons of 3-(3,5-diaminobenzoyl) benzenesulfonic acid hydrochloride shifted to downfield since it is in hydrochloride form. Aromatic protons in the region 7.0–8.55 δ ppm showed the expected multiplicity and integration values as shown (Figure 6.5 C). Protons of 3-(3,5-diaminobenzoyl) benzenesulfonic acid at 8.55 δ ppm correspond to –NH$_2$ protons.
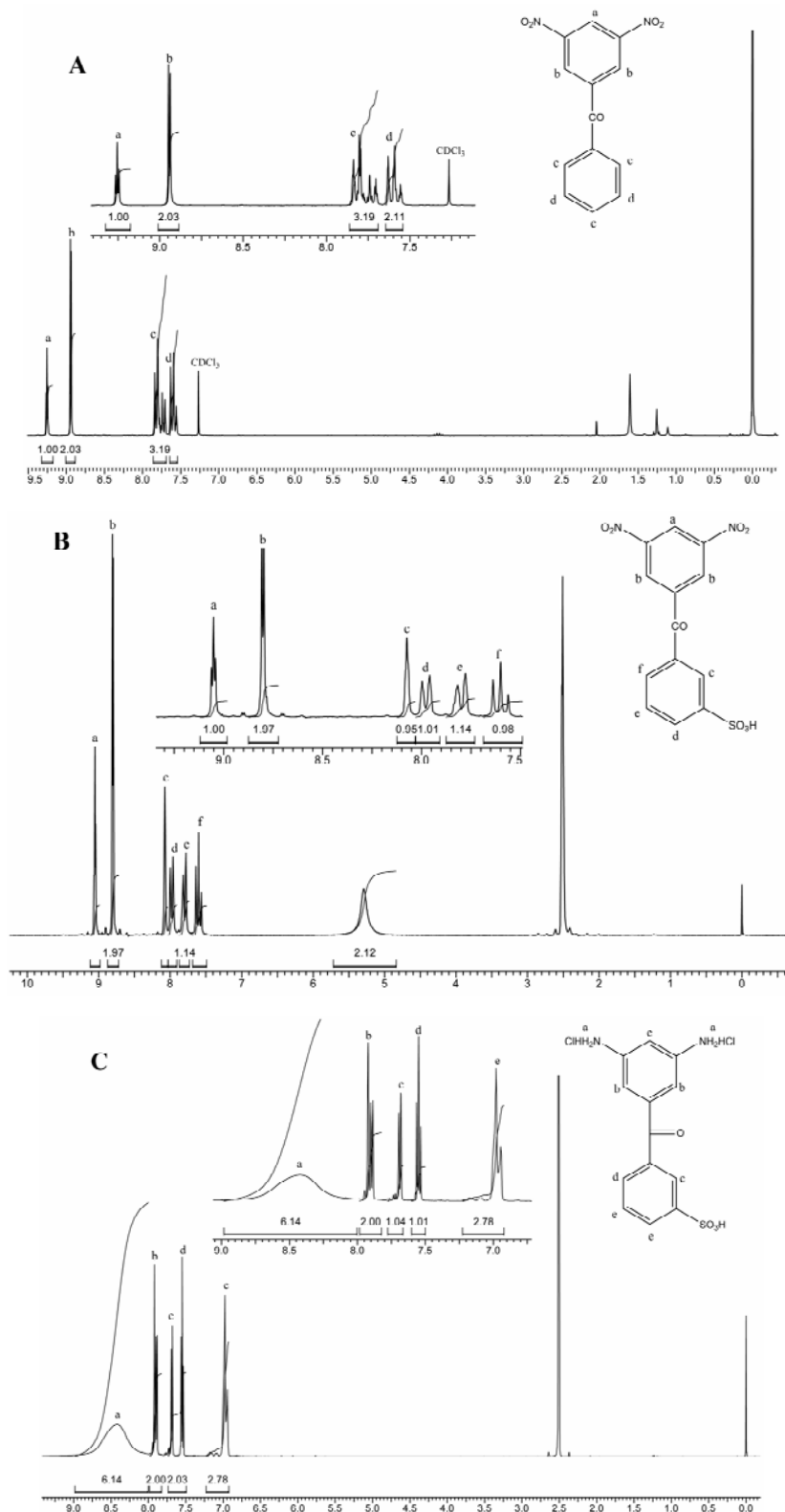
**Figure 6.5** ^{1}H NMR spectra of A) 3,5-dinitrophenyl)(phenyl)methanone B) 3-(3,5-dinitrobenzoyl)benzenesulfonic acid C) DABBSA.
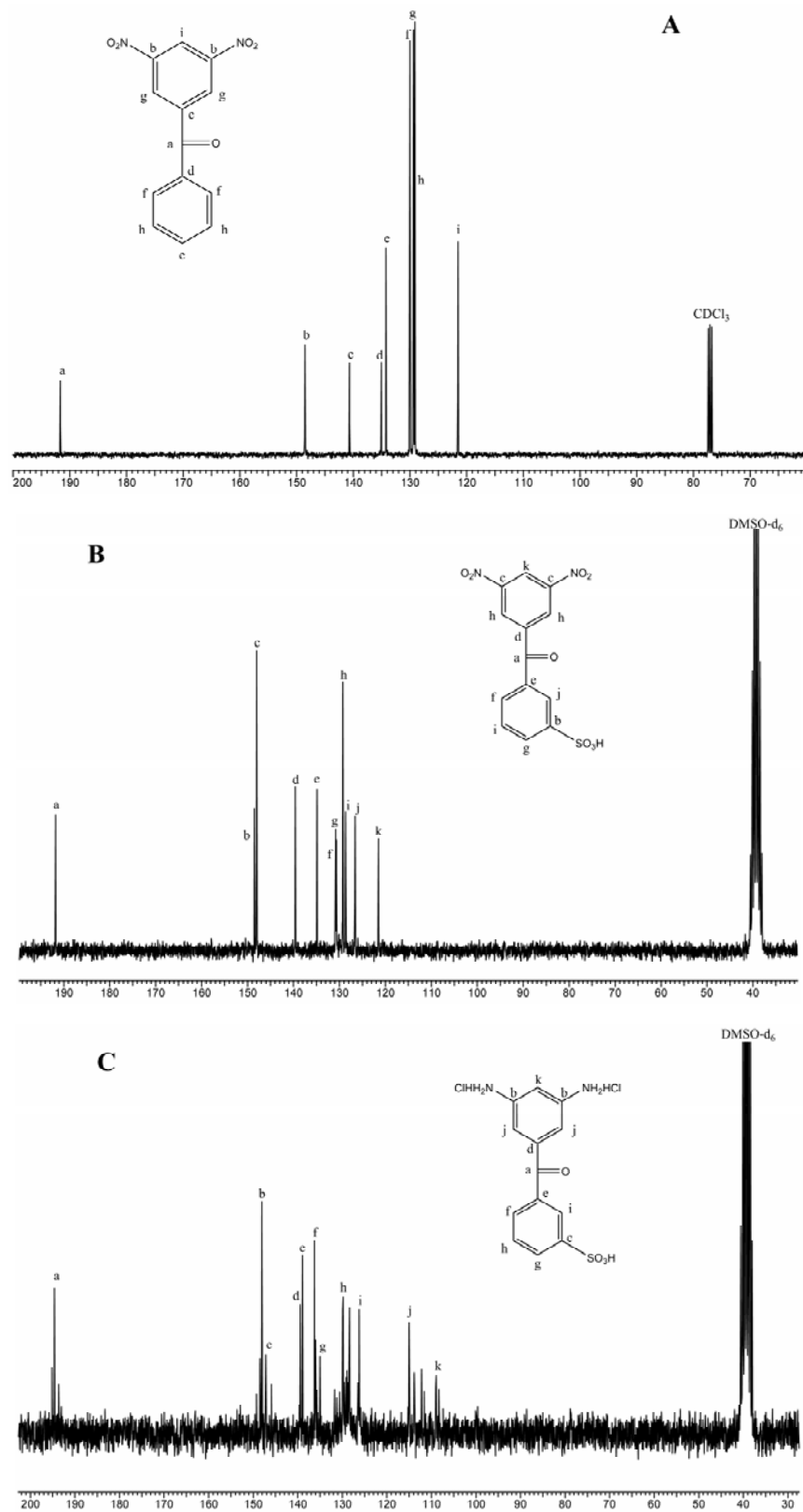
**Figure 6.6** $^{13}$C NMR spectra of A) 3,5-dinitrophenyl)(phenyl)methanone

         B) 3-(3,5-dinitrobenzoyl) benzenesulfonic acid  C) DABBSA.

The ¹³C NMR spectrum of 3,5-dinitrophenyl)(phenyl)methanone showed δ ppm values corresponding to 13 carbon atoms and were in good agreement with the proposed structure of aromatic carbons in the range of 120–191 δ ppm and single carbon of keto group appear at 191.67 δ ppm (Figure 6.6 A). ¹³C NMR spectrum of 3-(3,5-dinitrobenzoyl) benzenesulfonic acid  (Figure 6.6 B) shows aromatic carbons at 121–191 δ ppm as expected. ¹³C NMR spectrum of 3-(3,5-diaminobenzoyl) benzenesulfonic acid dihydrochloride has δ-values close to that of dinitro acid compound. Aromatic carbons observed in the region 115–195 δ ppm and carbon of keto group appeared  as a single peak at 194.62 δ ppm showed the expected values as shown in (Figure 6.6 C).

Thus, elemental and spectral analysis confirm the structure of 3-(3,5-diaminobenzoyl) benzenesulfonic acid dihydrochloride and intermediate compounds .

### 6.3.2    Synthesis and structural characterization of polyimides and co-polyimides having free carboxyl and sulphonic acid groups

Polyimide polymers containing pendant benzoylsulfonic and phenoxycarboxyl acid groups were synthesized by one-pot, high temperature polycondensation method by condensing 3-(3,5-diaminobenzoyl) benzenesulfonic acid dihydrochloride (DABBSA) and 4-(2,4-diaminophenoxy) benzoic acid (DAPBA) with NTDA in m-cresol. We used hydrochloride of the sulfonated diamine (DABBSA), as free amine groups has a tendency to undergo chemical changes with time and change in color is observed from white to pink and finally mud color, which gave low molecular weight polymer even after heating for several hours with NTDA in m-cresol. Where as, high molecular weight polymers in high yields could be obtained using 3-(3,5-diaminobenzoyl) benzenesulfonic acid dihydrochloride. Both, homopolymer of DABBSA and DAPBA with NTDA (scheme 6.3 and 6.4) and copolymers of NTDA with a mixture of different mole ratios (90:10, 80:20 and 70:30,) of DABBSA and DAPBA (scheme 6.5) were synthesized in order to study the effect of pendant benzoylsulfonic and phenoxycarboxyl acid content on proton conductivity, electrochemical and other properties of polyimides.

The synthesis of high molecular weight six-membered ring polyimides has been reported to be successful at 180-190 ℃ in *m*-cresol, in the presence of acid catalysts [24].

Generally high molecular weight polyimides are obtained when benzoic acid and isoquinoline are added sequentially as catalysts in the polymerization. However, in the present case, high molecular weight polymer was obtained without using these catalysts. These catalysts had no effect in enhancing molecular weight of the polymers. This may due to the use of sulfonated diamine in hydrochloride form, which gives triethylamine hydrochloride during dissolution of amine. Triethylamine hydrochloride may serve as acid catalyst during the polymerization reaction. Approximately 12 h heating is essential to form high molecular weight polymers. All the polymers remained soluble in m-cresol without precipitation. They form viscous solutions, which on pouring in acetone formed strong thread like structure. All these polymers have film-forming properties and they form transparent, flexible film on casting from DMAc solution.

Inherent viscosity was determined in triethylammonium sulfonate salt form in DMAc (0.5 g.dL$^{-1}$ concentration at 30 °C) using Ubbelhode viscometer. The values are observed to be high, which are in the range from 0.70 - 1.20 dL.g$^{-1}$. The values for homo polyimide of DABBSA (SBPI) is greater than one, while homo polyimide of DAPBA (CPI) and co-polyimides of DABBSA and DAPBA are less than one (Table 6.1). All these polymers except SCPI-1 form flexible membranes.

**Table 6.1** Inherent viscosities and film nature of polyimides and co-polyimides having free carboxyl and sulphonic acid groups

| Polymer Code | Diamines used (mole ratio %) DABBSA / DAPBA | Inherent viscosity $\eta_{inh}$ (dL/g) | Film Color | Film Nature |
|---|---|---|---|---|
| SBPI | 100/0 | 1.2 | Brownish yellow | Flexible |
| SCPI-1 | 90/10 | 0.91 | Light brown | Brittle |
| SCPI -2 | 80/20 | 0.84 | Reddish | Flexible |
| SCPI-3 | 70/30 | 0.70 | Reddish | Flexible |
| CPI | 0/100 | 0.75 | Dark brown | Flexible |

.

**DABBSA:** 3-(3,5-diaminobenzoyl) benzenesulfonic acid dihydrochloride, **DAPBA:** 4-(2,4-diaminophenoxy) benzoic acid

The polymers, thus obtained, were characterized by FT-IR and $^1$H NMR spectroscopy. FTIR spectra of all polymers were scanned using thin membranes. The FT-IR spectra of SBPI, SCPI-1, SCPI-2, SCPI-3 and CPI are shown in (Figure 6.7). The formation of polyimides was

confirmed by the characteristic naphthalimide absorption bands at 1720, 1678, and 1345 cm^{-1}, as well as those associated with the sulfonic acid groups. The symmetric and asymmetric stretches of the sulfonic acid groups appeared at 1030 and 1200 cm^{-1}, respectively. The homopolymer of DAPBA (CPI) also shows the absorption bands at 1720, 1678 and 1345 cm^{-1} (C=O, naphthalimide, aromatic ketone), 1220, 1120 cm^{-1} (-C-O-C- stretching) 1584, 1498 cm^{-1} (aromatic). Figure 6.7 shows the FT-IR spectra for the SCPI series of polymers. In co-polyimides the intensity of the peak at 1498 cm^{-1} due to aromatic C-H of phenyl ring increases as the content of carboxyl diamine increases.
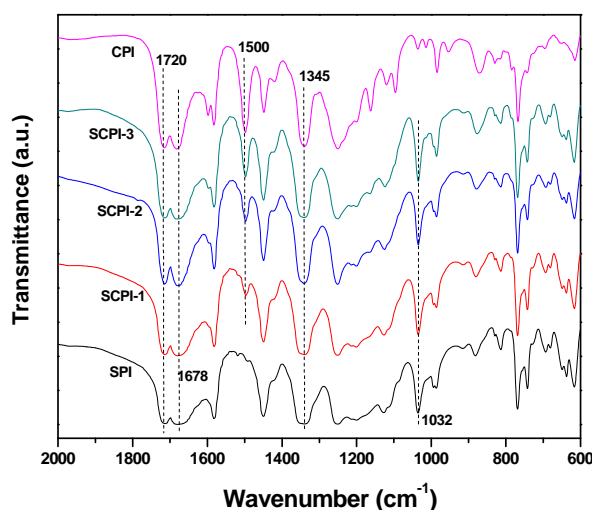


**Figure 6.7** FTIR spectra of polyimides and co-polyimides having free carboxyl and sulphonic acid groups.

### 6.3.3    Properties of polyimides and co- polyimides

The properties of polyimides and co-polyimides having free carboxyl and sulphonic acid groups (Triethylamine salt form) were evaluated by solubility measurements, X-ray diffraction, and TGA.

### 6.3.3.1 Solubility measurements

Solubility behavior of newly synthesized polyimides was studied by dissolving 4.0 mg of polymers in 0.5 mL solvent. The polymers in the present study displayed good solubility pattern. They are soluble in polar aprotic solvents such as m-Cresol, DMAc, NMP and DMSO (Table 6.2) at ambient temperature. However, these polymers are not soluble in common organic solvents such as chloroform, toluene, tetrahydrofuran and dioxane due to their polar nature. The presence of flexible phenyl ether and benzoyl functionalized groups in side chain in these polymers enhances the solvent solubility.

**Table 6.2** Solubility behaviors of polyimides and co-polyimides having free carboxyl and sulphonic acid groups (Triethylamine salt form)

| Polymer | Solvents | | | | | |
|---------|----------|-----|------|------|-----|-----|
| Code | m-Cresol | DMF | DMSO | DMAc | NMP | THF |
| SBPI | + + | + | + + | + + | + + | - - |
| SCPI-1 | + + | + | + + | + + | + + | - - |
| SCPI -2 | + + | + | + + | + + | + + | - - |
| SCPI-3 | + + | + | + | + + | + + | - - |
| CPI | + + | + + | + + | + + | + + | - - |

+ +, Soluble at room temperature: +, soluble on heating, and - -, insoluble on heating.
 **DMF:** N, N-dimethylformamide**: DMAc**: N, N-dimethyl acetamide, **DMSO:** Dimethyl sulfoxide, **NMP:** N-methyl-2-pyrrolidone, **THF:** Tetrhydrofuran.

### 6.3.3.2 Crystallinity

Crystalline nature of these polymer specimens in film form was studied by X-ray diffraction (Figure 6.8) No sharp peak for crystalline nature was observed. The amorphous nature of polyimides could be attributed to their unsymmetrical structural units and the bulky sulfo benzoyl and phenoxycarboxyl groups, which reduced the intra and inter polymer chain interactions, resulting in loose polymer chain packaging and aggregates.
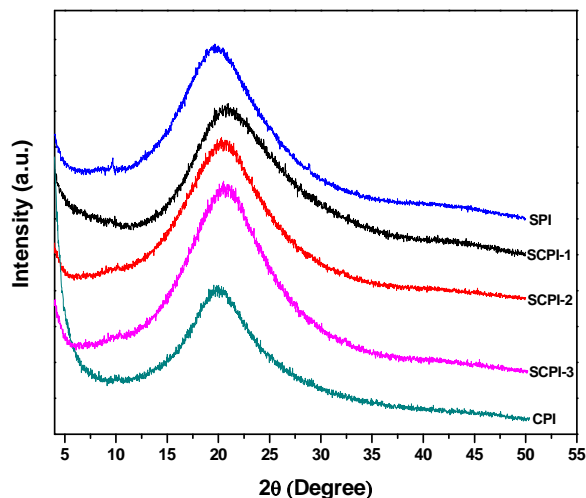
**Figure 6.8** Wide-angle X-ray diffraction patterns, of the polyimides and co-polyimides having free carboxyl and sulphonic acid groups.

### 6.3.3.3 Thermal properties of polymers

The thermal behavior of the polyimides and co-polyimides having free carboxyl and sulphonic acid groups was analyzed by thermo gravimetric analysis at a heating rate of 10 °C /min in nitrogen atmosphere and the thermograms are given in Figure 6.9. The initial weight loss observed upto 200 °C in some cases is probably due to loss of absorbed moisture. There are three stages of weight loss in the TGA curves.
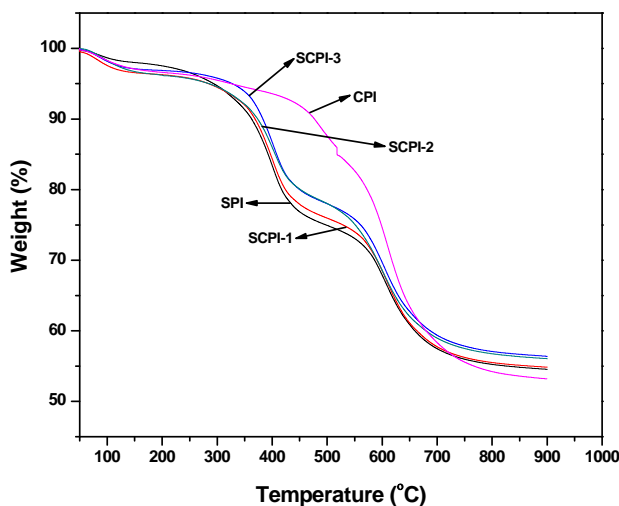


**Figure 6.9** TGA thermograms of the polyimides and co-polyimides having free carboxyl and sulphonic acid groups in $N_2$ at heating rate 10 °C min$^{-1}$.

The first weight loss before 200 °C is attributed to the absorbed water elimination. The second weight loss, corresponding to the decomposition of sulfonic acid group, occurs

from 280 °C to 400 °C. The third weight loss, due to the degradation of polymer backbone, starts above 400 °C. These polymers have sufficiently high thermal stability for application as PEM for fuel cell, which is usually operated at the temperature lower than 200 °C.

### 6.3.4 Fuel cell characterization of carboxyl and sulphonic acid groups containing PEM
### 6.3.4.1 Hydrolytic stability and water uptake

The stability test toward water of the polyimide membranes was performed by the immersion of the membranes in distilled water at 70 °C and characterized by the loss of mechanical properties of the hydrated membranes. The criterion for the judgment of the loss of mechanical properties is that the membrane sheet breaks when it is lightly bent.

**Table 6.3** Hydrolytic stability and water uptake values of sulfonated polyimide and co-polyimides having free carboxyl and sulphonic acid groups.

| Polymer Code | Membrane Thickness ( μm) | Hydrolytic satability (h) | Water uptake (%w/w) |
|---|---|---|---|
| SBPI | 100 | 168 | 48 |
| SCPI-1 | 96 | 48 | 43 |
| SCPI -2 | 95 | 72 | 33 |
| SCPI-3 | 98 | 120 | 25 |

Table 6.3 lists the values of the thickness, water uptake, and water stability of the polyimide membranes. Usually, the water stability of polymer membranes is strongly dependant on the water uptake. Membranes with lower water uptake should have better water stability. However, in this case, although SBPI had higher water uptake, it has high hydrolytic stability. In fact, SBPI displayed better water stability than other co-polyimides SCPI-1, SCPI-2 and SCPI-3 containing some nonsulfonated diamine moiety (DAPBA) and having lower IECs. High hydrolytic stability of DABBSA based polyimides is probably, due to flexibility of polymer and position of sulfonic acid groups in the polymers. Polyimide having sulfonic acid groups in side chain has better hydrolytic stability compared to PI having sulfonic acid groups in main chain. This indicates that the substitution position of the sulfonic acid groups has a significant influence on the membrane stability. The longer the distance

between the sulfonic acid group and the amine group, better the water stability of the resulting sulfonated polyimides.

The water uptake of sulfonated polyimide and co-polyimides having free carboxyl and sulphonic acid groups was measured as described in the experimental part. Sulfonated polyimide (SBPI) shows highest water uptake of 48 %, while SCPI-1, SCPI-2 and SCPI-3 have less water uptake. Water uptake of copolyimides decreases as the carboxyl group content increases. This is probably due to hydrophobic nature of phenyl carboxyl groups.

### 6.3.4.2 Ion exchange capacity

The measured IEC values in $[(mmol-SO_3^- + mmol-COO^-)\ g^{-1}]$ and theoretical IEC values in $[(mmol-SO_3^-\ g^{-1}]$ were shown in Table 6.4. IEC values of these polymers are in the range of 1.5-1.84 mmol g$^{-1}$ for the dry membranes. Slightly higher IEC values compared to calculated values are due to carboxyl groups. The gradual decrease in the DABBSA content lowers IEC values in the SCPI membranes, which led to decrease in both the proton conductivity and the water uptake content of the SCPI membranes.

**Table 6.4** Ion exchange capacity and proton conductivity values of sulfonated polyimide and co-polyimides having free carboxyl and sulphonic acid groups.

| Polymer Code | IEC (meq/g) Calculated | IEC (meq/g) Measured | $\sigma_{max}$ (S cm$^{-1}$) at 90 °C |
|---|---|---|---|
| SBPI | 1.90 | 1.84 | $9.49 \times 10^{-2}$ |
| SCPI-1 | 1.73 | 1.80 | $8.81 \times 10^{-2}$ |
| SCPI -2 | 1.55 | 1.70 | $6.55 \times 10^{-2}$ |
| SCPI-3 | 1.37 | 1.50 | $5.00 \times 10^{-2}$ |
| Nafion | 0.91 | 0.90 | $1.14 \times 10^{-1}$ |

### 6.3.4.3 Proton conductivity measurement

For the proton conductivity measurements, SBPI, SCPI's membranes were treated by immersing in 1 M H$_2$SO$_4$ for 24 h at room temperature, followed by washing in distilled water at room temperature for another 24 h, while Nafion 115 (127 μm, DuPont Co.) membrane was treated with boiling 5% H$_2$O$_2$ and 1 M H$_2$SO$_4$ for 1 h to remove organic and metallic impurities respectively, and then washed in distilled water for 24 h. Temperature dependant

conductivity of treated polymer membranes was determined in the temperature range of 30 to 90 °C as described in experimental part of chapter 2 maintaining the 90 % relative humidity. Figure 6.10 represents the conductivity vs. temperature graph. The SBPI membrane exhibits high proton conductivity ($9.49 \times 10^{-2}$ S.cm$^{-1}$) compared to that of SCPI-1 ($8.81 \times 10^{-2}$ S.cm$^{-1}$) followed by, SCPI-2 membrane ($6.55 \times 10^{-2}$ S.cm$^{-1}$) and SCPI-3 ($5.00 \times 10^{-2}$ S.cm$^{-1}$) at 90 °C. These values decrease as carboxyl groups in membrane increases. But all proton conductivities are less than that of Nafion ($1.14 \times 10^{-1}$ S.cm$^{-1}$). Slightly low proton conductivities of SCPIs compared to SBPI is due to low IEC values of these polymers. It appears that carboxyl groups do not contribute much toward proton conductivity.
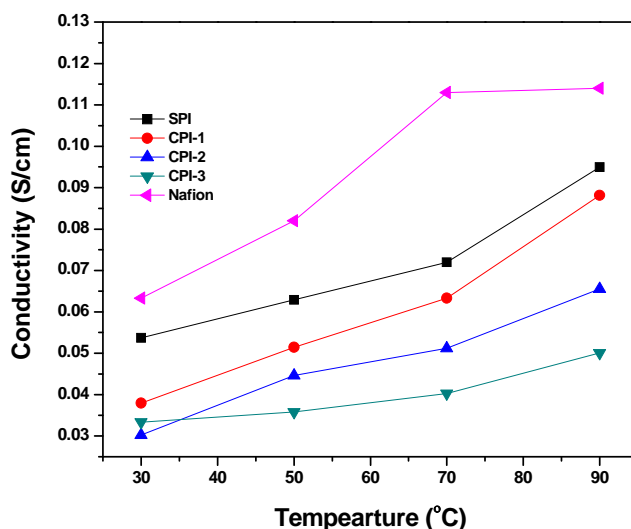


**Figure 6.10** Proton conductivities of the sulfonated polyimide and co-polyimides having free carboxyl and sulphonic acid groups in 90 % RH at different temperature.

### 6.3.4.4 Membrane electrode assembly fabrication

The electrodes with a gas diffusion layer and a catalyst layer were fabricated by following the same procedure as mentioned earlier in section 2.3.4.4 of chapter 2. After that the 5 wt% Nafion solution was coated on the catalyst layer by brushing. A membrane of SBPI (100 μm) was treated by immersing the membrane in 1 M $H_2SO_4$ for 24 h at room temperature, followed by washing in distilled water at room temperature for another 24 h, while Nafion 115 (127 μm, DuPont Co.) membrane was treated with boiling 5% $H_2O_2$ and 1M $H_2SO_4$ for 1 h to remove organic and metallic impurities respectively, and then washed in

distilled water for 24 h. The membrane and electrode assemblies (MEAs) were made by hot-pressing the pretreated electrode (9 cm$^2$) and the membrane, under the conditions of 120 °C, 130 atm for 3 min.

### 6.3.4.5 Polarization study

Figure 6.11 shows the fuel cell performance of SBPI and Nafion-115 membranes in terms of polarization plots of MEAs fabricated using 20% Pt/C for both anode and cathode in a single cell experiment, at 80 °C with 80% RH H$_2$/O$_2$ gas flow rate of 0.4 slpm (standard liters per minute).
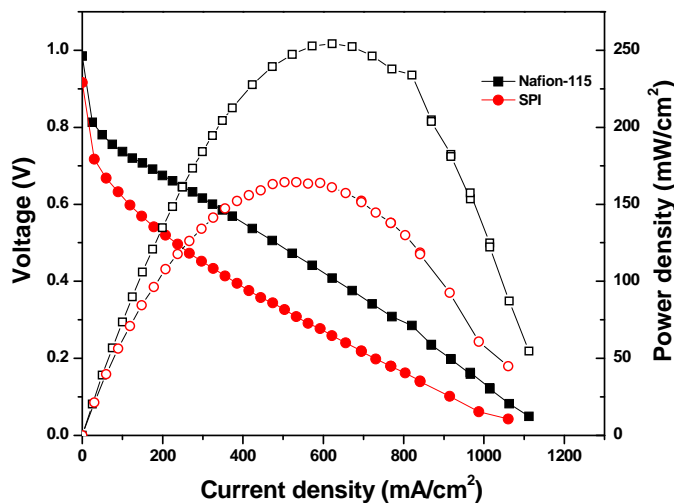


**Figure 6.11**   Polarization curves obtained with SBPI and Nafion-115 membrane fuel cell at 80 °C with 80% humidified H$_2$ and O$_2$ (flow rate 0.4 slpm). The cell was conditioned for 30 min at open-circuit potential and at 0.2 V for 15 min before measurements**.**

SBPI membrane shows lower performance than that of the Nafion-115 membrane. The open-circuit voltage (OCV) obtained with the SBPI membrane is 0.91 V at 80 °C, whereas for Nafion-115   it is 0.98 V. The SBPI membrane gives a maximum power density of 164 mW/cm$^2$ at 0.3 V, whereas the Nafion-115   membrane gives 254 mW/cm$^2$ at 0.4 V.  This lower fuel cell performance of SBPI membrane can be attributed to low proton conductivity of SBPI membrane.

## 6.4  Conclusions

- Two new diamines namely, 4-(2,4-diaminophenoxy) benzoic acid and 3-(3,5-diaminobenzoyl) benzenesulfonic acid were successfully synthesized by simple condensation and oxidation, acylation, sulfonation and reduction reactions in high purity and high yields.

- New series of polyimides having pendant benzoylsulfonic and phenoxycarboxyl acid groups were synthesized from a 4-(2,4-diaminophenoxy) benzoic acid and 3-(3,5-diaminobenzoyl) benzenesulfonic acid with NTDA using high temperature solution polycondensation in m-cresol.

- The presence of flexible phenyl ether and benzoyl functionalized groups in side chain in these polymers enhances the solvent solubility.

- SBPI shows high hydrolytic stability as compared to other copolyimides of DABBSA and DAPBA probably, due to flexibility of polymer and position of sulfonic acid groups in the polymers.

- Water uptake of copolyimides decreases as the carboxyl group content increases due to hydrophobic nature of phenyl carboxyl groups.

- SBPI shows high IEC value than the SCPI membranes, which led to decrease in both the proton conductivity and the water uptake content of the SCPI membranes.

- SCPIs show slightly low proton conductivities as compared to SBPI due to low IEC values of these polymers. It appears that carboxyl groups do not contribute much toward proton conductivity.

# References

1. D. Wilson, P. M. Hergenrother and H. D. Stenzenberger, Eds., *Polyimides*, Chapman and Hall, New York, 1990.

2. M. K. Ghosh and K. L. Mittal, Eds., *Polyimides: Fundamentals and Applications*, Marcel Dekker, New York, 1996.

3. Fang, J.; Guo, X.; Harada, S.; Watari, T.; Tanaka, K.; Kita, H.; Okamoto, K. I. *Macromolecules* **2002,** 35, (24), 9022-9028.

4. Genies, C.; Mercier, R.; Sillion, B.; Cornet, N.; Gebel, G.; Pineri, M. *Polymer* **2001,** 42, (2), 359-373.

5. Guo, X.; Fang, J.; Watari, T.; Tanaka, K.; Kita, H.; Okamoto, K. I. *Macromolecules* **2002,** 35, (17), 6707-6713.

6. Zhaoxia, H. U.; Yin, Y.; Chen, S.; Yamada, O.; Tanaka, K.; Kita, H.; Okamoto, K. I. *Journal of Polymer Science, Part A: Polymer Chemistry* **2006,** 44, (9), 2862-2872.

7. Miyatake, K.; Yasuda, T.; Hirai, M.; Nanasawa, M.; Watanabe, M. *Journal of Polymer Science, Part A: Polymer Chemistry* **2007,** 45, (1), 157-163.

8. Yin, Y.; Fang, J.; Watari, T.; Tanaka, K.; Kita, H.; Okamoto, K. I. *Journal of Materials Chemistry* **2004,** 14, (6), 1062-1070.

9. Yasuda, T.; Miyatake, K.; Hirai, M.; Nanasawa, M.; Watanabe, M. *Journal of Polymer Science, Part A: Polymer Chemistry* **2005,** 43, (19), 4439-4445.

10. Yin, Y.; Chen, S.; Guo, X.; Fang, J.; Tanaka, K.; Kita, H.; Okamoto, K. I. *High Performance Polymers* **2006,** 18, (5), 617-635.

11. Chen, X.; Yin, Y.; Tanaka, K.; Kita, H.; Okamoto, K. I. *High Performance Polymers* **2006,** 18, (5), 637-654.

12. Guo, X.; Fang, J.; Tanaka, K.; Kita, H.; Okamoto, K. I. *Journal of Polymer Science, Part A: Polymer Chemistry* **2004,** 42, (6), 1432-1440.

13. Yasuda, T.; Li, Y.; Miyatake, K.; Hirai, M.; Nanasawa, M.; Watanabe, M. *Journal of Polymer Science, Part A: Polymer Chemistry* **2006,** 44, (13), 3995-4005.

14. Asano, N.; Aoki, M.; Suzuki, S.; Miyatake, K.; Uchida, H.; Watanabe, M. *Journal of the American Chemical Society* **2006,** 128, (5), 1762-1769.

15. Souzy, R.; Ameduri, B. *Progress in Polymer Science* **2005,** *30*, 644-687.

16. Mauritz, K. A.; Moore, R. B. *Chemical Reviews* **2004,** 104, (10), 4535-4586.

17. Faure S, Mercier R, Aldebert P, Pineri M, Sillion B. French Pat. 9605707, 1996.

18. Lee, C.; Sundar, S.; Kwon, J.; Han, H. *Journal of Polymer Science, Part A: Polymer Chemistry* **2004,** 42, (14), 3612-3620.

19. Yasuda, T.; Miyatake, K.; Hirai, M.; Nanasawa, M.; Watanabe, M. *Journal of Polymer Science, Part A: Polymer Chemistry* **2005,** 43, (19), 4439-4445.

20. Guktepe, F.; Bozkurt, A.; Gunday, S. T. *Polymer International* **2008,** 57, (1), 133-138.

21.     Kreuer, K. D.; Fuchs, A.; Ise, M.; Spaeth, M.; Maier, J. *Electrochimica Acta* **1998,** 43, (10-11), 1281-1288.

22.     Yang, C.; Costamagna, P.; Srinivasan, S.; Benziger, J.; Bocarsly, A. B. *Journal of Power Sources* **2001,** 103, (1), 1-9.

23.     H. E. Fierz and H. Koechlin, *Helv. Chim. Acta* , **1**, 218 (1918).

24.     Sek, D.; Wanic, A.; Schab-Balcerzak, E. J. *Polymer* **1994**, 34, 2440-2442.

# Chapter 7

## Summary and Conclusions

## 7.1 Summary of the work

The primary objectives of this research were i) to synthesize new polybenzimidazoles containing pendant functional groups such as nitro, amino hydroxy and pendant benzimidazole groups, ii) to synthesize polyimides containing sulfonic acid groups in side chain, iii) to prepare blend of polymers to explore possible application of these polymers as polymer electrolytes for fuel cell. Accordingly, three new diacids, namely, 5-(4-nitrophenoxy) isophthalic acid (NEDA), 5-(4-aminophenoxy) isophthalic acid (AEDA) and 5-(1H-benzo[d]imidazol-2-yl) isophthalic acid (BIPA) and a series of new polybenzimidazoles containing functional groups were synthesized by condensing these diacids and mixture of these diacids and six other commercial diacids with 3,3',4,4,'-tetra amino biphenyl (TAB).

NEDA was successfully synthesized in high yield in two steps and easily purified by recrystallization in acetic acid. The series of nitro group containing polybenzimidazole and co-polybenzimidazoles derived from NEDA provided improved solubility, ductility, and acid uptake compared to the more rigid commercial PBI. The influence of copolymer composition and nitrophenoxy group on thermal and oxidative stability, acid uptake, and proton conductivity was studied. The nitro group containing polybenzimidazole and co-polybenzimidazoles show better proton conductivities as compared to commercial PBI. NPBI's become elastomeric at high temperature in the presence of phosphoric acid, which enhance proton conductivity and shows better fuel cell performance.

AEDA was also synthesized to prepare amino group containing polybenzimidazole and co-polybenzimidazoles. Amino groups form a acid base complex with the phosphoric acid and increase the phosphoric acid uptake in APBI's. AEDA was successfully synthesized in high yield in one step from NEDA just by reduction and purified as amino hydrochloride by recrystallization from conc. HCl. Incorporation of amino groups in polybenzimidazole improves the solubility, acid uptake and oxidative stability of the polymers. However, it reduces the mechanical properties of the polymer as compared to the commercial PBI. The proton conductivity of APBI's is slightly lower compared to PBI. The proton conductivity results indicate that free amino group in pendant aminophenoxy group does not contribute to proton conductivity. For good proton conductivity, proton formed should be labile. A

strongly bonded proton cannot be transported easily resulting in low proton conductivity. It appears that primary amine in these polymers form strong ionic bond with phosphoric acid and restricts mobility of protons, which explains low proton conductivity of APBI polymers compared to PBI.

A series of hydroxyl functional groups containing polybenzimidazole and co-polybenzimidazoles (HPBI's) was synthesized from commercial diacid, 5-hydroxy isophthalic acid (HIPA), and 3,3',4,4,'-tetra amino biphenyl (TAB). Homopolymer (HPBI) shows solubility in DMSO only, while, copolybenzimidazoles are the soluble in all aprotic solvents. The acidic and hydrophilic phenolic hydroxyl groups enhance both KOH and water uptake. Compared to PBI, all HPBI's show high water and KOH uptake values, which increase with increase in hydroxyl groups in the polymer. The phosphoric acid uptake of HPBI's is low as compared to PBI. The acid uptake increases as the content of HIPA in polymer decreases. This behavior of HPBI's toward phosphoric acid is due to the formation of cross-linking phosphate ester bonding in polymer which inhibits the excessive $H_3PO_4$ uptake. Incorporation of hydroxyl groups in polybenzimidazole improves the oxidative stability and proton conductivity of PBI.

Polybenzimidazoles containing pendant benzimidazole groups were prepared from BIPA. The incorporation of pendant benzimidazole groups into polybenzimidazole and co-polybenzimidazoles was accomplished by synthesizing a diacid with pendant benzimidazole moiety and synthesizing its polymer with TAB and other commercial diacids. The synthesis of 5-(1H-benzo[d]imidazol-2-yl) isophthalic acid (BIPA) proved to be more difficult than other diacids as it contains both basic and acidic groups in same moiety. However, 5-(1H-benzo[d]imidazol-2-yl) isophthalic acid (BIPA) was successfully synthesized in high yield in two steps and finely purified by recrystallization in formic acid after trying lots of solvents. Introducing pendant benzimidazole groups in polybenzimidazole improves the solubility, oxidative stability of PBI. BPBI's show more thermal stability than the conventional PBI. Thermal stability of copolymers increases as the content of BIPA increases. BPBI's show excessive acid uptake capacity and loose the mechanical integrity, so we had to doped them in low acid concentration to control the acid uptake, which results in low doping level and low

proton conductivity as compared to PBI. From the results of chapter 4 it shows that the synthesized benzimidazole group containing polybenzimidazoles can be used as polymer electrolyte membranes for operation at high temperature and also as polymeric material for other high temperature applications.

Blend membranes of amino group containing polybenzimidazole (APBI) with sulfonated polyether ether ketone (SPEEK) and commercial PBI with polyvinyl alcohol in varying ratio were prepared by solution casting technique and characterized by IR spectroscopy, SEM analysis, XRD analysis, thermal analysis, and mechanical properties. In SEM, APBI/SPEEK blends show good miscibility upto 50% SPEEK content, while, PBI-PVOH polymers form miscible blends in all ratios. APBI-SPEEK blends show better oxidative stability than APBI and SPEEK due to hydrogen bonding between –NH-, $NH_2$ of APBI and $SO_3H$ of SPEEK, while in PBI/PVOH blends oxidative stability decreases due to the presence of the water soluble aliphatic PVOH. In both blend systems introduction of SPEEK and PVOH lowers the thermal and mechanical properties of APBI and PBI. In APBI/SPEEK blends only APS-1 blend showed a high $H_3PO_4$ uptake and proton conductivity as compared to APS-2, APS-3 and APBI. In PBI-PVOH blends acid uptake and proton conductivity increases with increase in PVOH content in blends. Blend membranes shows better conductivity than PBI.

It has been proposed that the aggregation of side-chain sulfonic acid sites to form ion channels enhances the proton conductivity of Nafion membranes. In order to study the effect of carboxyl and sulfonic acid groups on properties of PI, two new diamines namely, 4-(2,4-diaminophenoxy) benzoic acid and 3-(3,5-diaminobenzoyl)benzene sulfonic acid were synthesized. A series of side chain sulfonated polyimide and copolyimides were synthesized in order to combine this advantage with the stability of polyimides. In the expectation to have good stability in water and good proton conductivity compared to membrane based on copolyimides of sulfonated and non-sulfonated diamines, we synthesized the membranes based on copolyimides of sulfonated and carboxylated diamines. By introducing carboxyl groups in sulfonated polyimides no improvement in water stability and proton conductivity was observed. Water uptake, water stability and proton conductivity decreases as carboxyl

group's content in polyimides increases may be due to hydrophobic nature of phenyl carboxyl group. From the results of proton conductivities it appears that carboxyl groups do not contribute much toward proton conductivity.

The investigation of high temperature polymers for fuel cell applications, as discussed in the preceding chapters, has allowed us to gain valuable insight into the properties necessary for a successful PEM.

## 7.2 Conclusions

➢ Three new m-substituted phenylene diacids having pendant nitrophenoxy, aminophenoxy and benzimidazole groups were synthesized in high yields and purity from commercially available compounds like 3-5 dimethylphenol and 3-5 dimethylbenzoic acid.

➢ Several novel homo and copolybenzimidazoles were synthesized and the structure property relationship was studied.

➢ The solubility, thermal properties and crystallinity of polymers are dependent on the nature of diacid monomers. It was observed that incorporation of pendant bulky functional groups along with pendant flexible connecting groups in polybenzimidazoles improved the solubility without affecting the thermal properties significantly. Here the solubility was found to be dependent on the nature of pendant groups.

➢ The thermal stability and glass transition temperatures were dependent on the diacid monomers. The introduction of alkyl groups decreased the glass transition temperatures to large extent.

➢ All homo and copolybenzimidazoles containing pendant bulky functional groups showed good phosphoric acid uptake, while hydroxyl group containing polymers shows limited phosphoric acid uptake.

➢ The oxidative stability studies on homo and copolybenzimidazoles showed that, in general oxidative stability increases with the incorporation of pendant bulky functional groups.

➢ The proton conductivity studies on homo and copolybenzimidazoles showed that, proton conductivity increases with the incorporation of pendant nitrophenoxy and hydroxyl groups, while incorporation of pendant aminophenoxy and benzimidazole groups does not enhance proton conductivity.

➢ APBI and PBI show miscibility in blends with SPEEK and PVOH upto 50% content of SPEEK and PVOH.

➢ Two new diamines namely, 4-(2,4-diaminophenoxy) benzoic acid and 3-(3,5-diaminobenzoyl) benzenesulfonic acid were successfully synthesized by simple condensation and oxidation, acylation, sulfonation and reduction reactions in high purity and high yields.

➢ New series of polyimides having pendant benzoylsulfonic and phenoxycarboxyl acid groups were synthesized from a 4-(2,4-diaminophenoxy) benzoic acid and 3-(3,5-diaminobenzoyl) benzenesulfonic acid with NTDA using high temperature solution polycondensation in m-cresol.

➢ In copolyimides carboxyl groups do not contribute much toward proton conductivity.

## 7.3 Future work

The study on pendant functional group containing polybenzimidazoles showed that the modification of chemical structure of PBI could improve key membrane properties of PBI. However, the role of functional groups in the proton conduction mechanism is not fully understood. Systematic investigations on 1) the diffusion coefficient of proton transport in membranes using NMR, 2) morphology of functional group containing polybenzimidazoles membranes, and 3) morphology effects on proton conductivity by comparative study of functional group containing polybenzimidazoles with PBI membrane, would provide useful information to understand the contribution of functional groups to proton conductivity. These polymers are expected to have interesting properties as membranes for separation technology for high temperature applications. A systematic study on gas separation and other separation technology is worth investigating.

# List of Publications

1.  Synthesis and characterization of novel polybenzimidazoles bearing pendant phenoxyamine groups. **Mahesh Kulkarni**, Ravindra Potrekar, R. A. Kulkarni, S. P. Vernekar, *Journal of Polymer Science Part A: Polymer Chemistry* **46** (17), 5776 (2008).

2.  Nitrophenoxy groups containing Polybenzimidazoles as polymer electrolytes for fuel cells: Synthesis and Characterization. **Mahesh Kulkarni**, Ravindra Potrekar, R. A. Kulkarni, S. P. Vernekar. Accepted, in *Journal of Applied Polymer Science.*

3.  Synthesis and characterization of polyimides and co-polyimides having pendant benzoic acid moiety. **Mahesh Kulkarni**, Kothawade, Sandeep Arabale, Girish, Wagh, Deepali Vijayamohanan, K.Vernekar, S. P. and Kulkarni, R. A. *Polymer* **46** (11), 3669 (2005).

4.  Hydroxyl group containing Polybenzimidazoles for Fuel Cells: Synthesis and Characterization. (*To be communicated*) **Mahesh Kulkarni**, Ravindra Potrekar, R. A. Kulkarni, S. P. Vernekar

5.  Blends of Polybenzimidazole and Polyvinyl Alcohol as Polymer Electrolytes for Fuel Cells (*To be communicated*) **Mahesh Kulkarni**, Ravindra Potrekar R. A. Kulkarni K. Vijayamohanan, S. P.  Vernekar

6.  Blends of Amino group containing Polybenzimidazole and Sulfonated-PEEK as Polymer Electrolytes for Fuel Cells (*To be communicated*) **Mahesh Kulkarni**, Ravindra Potrekar, R. A.  Kulkarni, S. P. Vernekar

7.  Synthesis and Properties of Polyimides and Co-polyimides having pendant Sulfonated benzophenone and benzoic acid moiety for Fuel Cells (*To be communicated*) **Mahesh Kulkarni**,   Ravindra Potrekar, R. A. Kulkarni, S. P. Vernekar

8.  Synthesis and Characterization of Polybenzimidazoles having pendant benzimidazole moiety for Fuel Cells (*To be communicated*) **Mahesh Kulkarni**, Ravindra Potrekar, R. A. Kulkarni, S. P. Vernekar

9.  Synthesis, characterization, and gas permeability of aromatic polyimides containing pendant phenoxy group. Sandeep Kothawade, **Mahesh Kulkarni**, Ulhas Kharul, Anandrao Patil, S. P. Vernekar *Journal of Applied PolymerScience* **108** (6), 3881 (2008).

10. Polybenzimidazoles Tethered with Phenyl Triazole Units as Polymer Electrolytes for Fuel Cell. Ravindra Potrekar, **Mahesh Kulkarni**, R. A. Kulkarni S. P. Vernekar Accepted, in *Journal of Polymer Science Part A: Polymer Chemistry*.

11. Enhanced supercapacitance of multiwalled carbon nanotubes functionalized with ruthenium oxide. Arabale Girish, Wagh Deepali, **Kulkarni Mahesh**, Mulla, I. S., Vernekar, S. P. Vijayamohanan, K. Rao, A. M. *Chemical Physics Letters* **376** (1-2), 207 (2003).

12. Oxidation of cellulose under controlled conditions. Varma, A. J. and **Mahesh Kulkarni**, *Polymer Degradation and Stability* **77** (1), 25 (2002).

# Patent

1. An improved process for the preparation of high surface area carbon useful for fuel cell and ultracapacitor. Patent No. *US 2005/0221981 A1*D. Wagh, G. Arabale, **M. Kulkarni**, S.P. Vernekar, K. Vijayamohanan
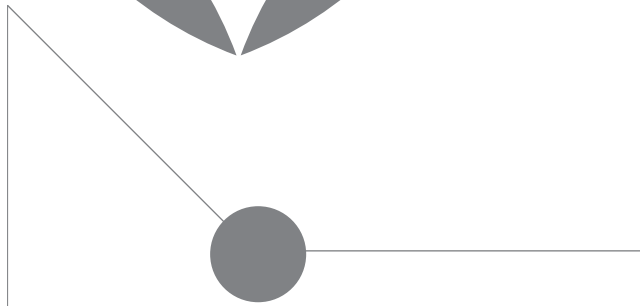
Synopsis

Electricity is the fastest growing form of energy. Although it is being used more efficiently, and despite progress having been made in switching to fuels other than oil, the electricity industry still faces a number of challenges, one of most important is environmental impact of electricity generation and use. The other principle contributor to urban pollution is road transport. Fuel cells will contribute to reducing the demands for fossil fuel and nuclear-derived energy both in power generation sector and road transport sector.

The proton exchange membrane fuel cell (PEMFC) is one of the most promising electrochemical power sources for electricity generation and electric vehicle applications. Fuel cells represent a clean and efficient conversion technology and it is alternate energy source for the vehicles to control vehicular pollution for clean environment. Today various kinds of fuel cells with different types of electrolytes are used for various applications. However today there has been increasing interest to develop polymer electrolyte fuel cells (PEFC) [3] due to its advantage as compare to other fuel cell systems particularly for vehicular applications. Though technology for such fuel cells is well established, its high cost is hurdle for implementation. One of major component, which decides cost of fuel cell, is the cost of polymer electrolytes. Presently Nafion [4,5] is used as polymer electrolyte which has very high cost about 700 US \$/m$^2$ . There is dire need to develop alternate cost effective efficient polymer electrolytes for fuel cells and hence there has been a consistent effort to develop comparatively less expensive alternate membrane material for PEFC having properties comparable to Nafion.

Sulfonated and Acid doped heterocyclic polymers are one class of polymeric membranes used for fuel cells. Various polymers Sulfonated to different extent have been tried as polymeric electrodes. These materials may be grouped mainly in three categories. 1) Fluorinated polymers such as Nafion or Sulfonated trifluoro vinyl styrene's. 2) Non-fluorinated polymers such as Sulfonated polystyrenes, polyphenylene oxides (PPO) [6], polyphenylene sulphides [7]-polyether ether ketone (PEEK) [8] block copolymers of styrene-ethylene-butylenes, [9]. 3) Heterocyclic polymers such as polybenzimidazoles [10] polyimides [11], polyquinoxalines [12] etc. Apart from these polymers, grafted polymers [13] are also reported.

A good polymer electrolyte is desired to have good thermal stability, high proton conductivity, good $N_2$ and $O_2$ barrier properties, good oxidative and chemical resistance, high current density and long service life with least change in efficiency with time. Cost is another important factor, which controls the application of a polymer electrolyte for fuel cell. Significant work is being carried out to replace expensive nafion membrane with cheap material. Sulfonated and Acid doped heterocyclic thermally polymers such as polybenzimidazoles and polyimides are considered as promising alternate polymers to nafion. These polymers being thermally stable can be used at higher temperature. However, much work has not been reported on these types of polymers. In present work we propose to undertake detailed study on these polymers as polymer electrolytes for fuel cells.

Acid doped polybenzimidazoles: polybenzimidazoles are good polymer electrolytes after acid doping as they are thermally very stable and have longer service life at high temperature. PBI are stable in stronger acidic medium, as they are basic polymers, N-H of benzimide ring form a complex with acid molecule and shows proton conductivity when doped with $H_3PO_4$ and $H_2SO_4$. Sulfonation using Oleum, $SO_3$ etc. is reported but it does not takes place on main backbone of polymer as it is rigid and hindered, grafting of methyl benzenesulfonate group on benzimidazole ring replacing hydrogen from N-H linkage is reported. We propose to synthesize PBI having functional groups in side chain and not grafting on N-H linkage by this we can doped it with phosphoric acid also which will definitely increase the proton conductivity and thermal properties of polymer.

Sulfonated polyimides as polymer electrolytes: polyimides are well known thermally stable polymers which are stable in acidic medium. These polymers have low oxygen/hydrogen permeability good hydrolytic stability and chemical resistance. Sulfonated polyimides have been patented as polymer electrolytes. However these polymers contain sulfonic acid groups in main chain attached to diamine moiety. Generally, as in nafion, sulfonic acid groups in side chain are preferred. We propose to synthesize polyimides containing sulfonic acid grouping side chain and study their proton conductivity. We propose to synthesis aromatic diamines linked to benzene Sulfonic acid via flexible group such as keto, SO2 etc. and synthesize polyimides and copolyimides with different dianhydrides.

***Objectives of the present thesis:***

- Synthesis a new diacid monomers having different functional groups such as Amino, Nitro and Benzimidazole etc.

- Synthesis and characterization of polybenzimidazole and series of copolybenzimidazoles from the new diacids having functional groups

- Synthesis a new diamine monomers having different functional groups such as Carboxyl and Sulfonic acid etc

- Synthesis and characterization of polyimide and series of copolyimides from the new diamines having functional groups

- Study the acid doping, proton conductivity and efficiency of membrane in fuel cell.

**Chapter 1** gives a comprehensive literature review on heterocyclic polymers, with special emphasis on polybenzimidazoles and Sulfonated polyimides and their Fuel cell application. It also includes the blends of heterocyclic polymer with other Sulfonated and commercial polymers used as PEM in fuel cells. This chapter also discusses the scope and objective of the thesis in detail.

**Chapter 2** presents a synthesis and characterization of two diacid monomers having Nitro and Amino functional groups. The diacids synthesized were i) 5-(4-nitrophenoxy) isophthalic acid ii) 5-(4-aminophenoxy) isophthalic acid hydrochloride. These diacids were characterized using NMR, IR and elemental analysis. New polybenzimidazole and series of copolybenzimidazoles from the new diacids having functional groups were synthesized and characterized by IR spectroscopy, inherent viscosity, elemental analysis, Solubility tests, X-ray diffraction studies, Differential scanning calorimetry and Thermogravimetric analysis, tensile properties study. These polymers show good oxidative stability in Fentons reagent. The fuel cell characterization such as acid doping study, proton conductivity measurements and actual fuel cell performance in single fuel cell stack were done.

**Chapter 3** presents a synthesis and characterization new polybenzimidazole and series of copolybenzimidazoles from the 5 hydroxy isophthalic acid and 3, 3'diaminobenzidine. The new hydroxyl group containing PBIs were characterized as above mention in chapter 1. As these polymers contain hydroxyl group there alkaline fuel cell study was done by doping it with 6M KOH.

**Chapter 4** presents a synthesis and characterization of diacid monomer having Benzimidazole functional groups. The diacid synthesized were i) 5-(1H-benzo[d]imidazol-2-yl) isophthalic acid. These diacid were characterized using NMR, IR and elemental analysis. New polybenzimidazole and series of copolybenzimidazoles from the new diacid having benzimidazole functional groups were synthesized and characterized by IR spectroscopy, inherent viscosity, elemental analysis, Solubility tests, X-ray diffraction studies, Differential scanning calorimetry and Thermogravimetric analysis, tensile properties study. The fuel cell characterization such as acid doping study, proton conductivity measurements and actual fuel cell performance in single fuel cell stack were done.

**Chapter 5** presents a preparation and characterization of i) Acid-Base blends of Amino group containing PBI and Sulfonated-PEEK and ii) Commercial PBI and Polyvinyl alcohol in different Wt%. The blends were characterized by SEM, IR, and DSC, TGA.
These blends show good mechanical properties. All fuel cell characterization was done as mentioned in other chapters.

**Chapter 6** presents a synthesis and characterization of two diamine monomers having Carboxyl and Sulfonic acid functional groups. The diamines synthesized were i) 4-(2, 4-diaminophenoxy) benzoic acid ii) 3-(3, 5-diaminobenzoyl) benzenesulfonic acid. These diamines were characterized using NMR, IR and elemental analysis. New polyimides and copolyimides from the new diamines having functional groups were synthesized and characterized by IR spectroscopy, inherent viscosity, elemental analysis, Solubility tests, X-ray diffraction studies, Differential scanning calorimetry and Thermogravimetric analysis, tensile properties study. These polymers show good oxidative stability in Fentons reagent. The fuel cell characterization such as water uptake study, proton conductivity measurements and actual fuel cell performance in single fuel cell stack were done.

**Chapter 7** summarizes the salient conclusions of the work.

**References:**

1.    E.A. Ticianelli, C.R. Deroucin, S. Srinivasan, J. Electroanal. Chem. 251 (1988) 275.

2.    P.G. Patil, J. Power Sources 37 (1992) 171.

3.    J. Haggin, Chem Eng. News 28 (1995) 28.

4.    W.G. Grot, Perfluorinated ion exchange polymers and theiruse in research and industry, Macromol. Symposia 82 (1994), pp. 161-172.

5.    D.J. Vaughan, Du Pont innovation 4 (1973)10.

6.    Chalk A.J, Hay A S. J. Polym Sci A 1968;7;691.

7.    Qi Z, Lefebvre MC, Pickup PG. J Electroanal Chem 1998;459;9.

8.    Kobayashi H, Tomita H, Moriyama H. J Am Chem Soc 1994;116:3153-4

9.    A. Makrini, J.L.Acosta Polymer 42 (2001) 9-15.

10.   J.S. Wainright, J.-T. Wang, D. Weng, R.F. Savinell and M.H.Litt, acid-doped.

11.   polybenzimidazoles: a new polymer electrolyte. J. Electrochem.soc 142 (1995),pp. L121-L123.

12.   Faure S, Pineri M, Aldebert P, Mercier R, Sillion B. PCT Int.Appl. WO 9742253A1 13 Nov 1997,51 pp.

13.   A.Steck, C.Stone, Montreal, Canada, 1997, pp. 792-807.

14.   G.G.Scherer, Polymer membrane for fuel cells. Ber. Bunsenges. Phys. Chem.94 (1990), pp. 1008-1014.